

MULTIPLE MAGMA BODIES: UNDERSTANDING THE PRE-ERUPTIVE ARCHITECTURE AND
MAGMATIC PROCESSES OF SUPERERUPTIONS BASED ON TEXTURAL, MINERALOGICAL, AND
GEOCHEMICAL FEATURES OF FIAMME FROM THE ORA IGNIMBRITE (PERMIAN, ITALY)

By

Genna R. Chiaro

Thesis

Submitted to the Faculty of the
Graduate School of Vanderbilt University
in partial fulfilment of the requirements
for the degree of

MASTER OF SCIENCE

in

Earth and Environmental Sciences

August 31, 2019

Nashville, Tennessee

Approved:

Guilherme A.R. Gualda, Ph.D.

Calvin F. Miller, Ph.D.

To all of the geology professors who believed in me and introduced me to my lifelong passion.

ACKNOWLEDGEMENTS

First and foremost, I would like to thank my advisor, Dr. Guilherme Gualda. Without his guidance and feedback, this thesis would not have been possible. Thanks for taking a chance on me and mentoring me for these first two years. I have learned so much from you already and am in awe of your deep understanding of thermodynamics. Secondly, I am extremely grateful for the time Dr. Calvin Miller has given to help me with this thesis. As always, you give extremely helpful advice. I'm thankful that I'm able to pop into your office to discuss data and work through ideas. I'm always rewarded with interesting ramblings and stories about the field, which are priceless.

I'd also like to acknowledge the PUMMUS and MESSY research groups that I belong to. Thank you for the knowledge I have gained discussing research among awesome colleagues. Also, thank you to my committee members, Guilherme Gualda, Lily Claiborne, and Simon Darroch for keeping me on track to succeed as a graduate student. Thank you David Furbish (aka Gandalf) for your infinite knowledge regarding earth processes. I loved taking your classes and am thankful that you autographed my copy of your book, Fluid Physics in Geology.

I'd like to extend a huge thank you to the professors I had in undergrad, specifically Tim Cope, Jim Mills, and Beth Pratt-Sitaula. I cherish the memories I had being in your classes and in the field with you all. And Beth, thanks for being a kickass female role model!

I must thank my predecessor and one of my best friends, Michelle Foley. You are an inspiration to me every day. Lastly, to the love of my life, my cat Pumba. You da best.

Funding for this project was provided by Vanderbilt University.

TABLE OF CONTENTS

	Page
DEDICATION	ii
ACKNOWLEDGEMENTS	iii
LIST OF TABLES	vi
LIST OF FIGURES	vii
Chapter	
I. INTRODUCTION	1
1.1 Overview	1
1.2 Geologic Background	4
II. METHODS	11
2.1 Field Work	11
2.1.1 Sampling Locations	13
2.1.1.1 Ora 2: Outflow Vitrophyre	13
2.1.1.2 Ora 5: Intracaldera Vitrophyre	16
2.2 Analytical Methods	18
2.2.1 Sample Preparation	18
2.2.2 Petrography	19
2.2.3 Crystal Content Analysis	19
2.2.4 Elemental Analysis	20
III. RESULTS.....	22
3.1 Categorization	22
3.2 Textural Analysis	23
3.2.1 Crystal Contents.....	23
3.2.2 Crystal Sizes	25
3.3 Intracaldera Fiamme	26
3.3.1 Very Coarse-Grained Crystal-Rich (VCCR) Fiamme	26
3.3.2 Fine-Grained (FG) Fiamme.....	27
3.4 Outflow Fiamme.....	28
3.4.1 Medium-Grained (MG) Fiamme	29
3.4.2 Fine-Grained Crystal-Poor (FGCP) Fiamme.....	30
3.5 Mineralogy	32

3.5.1 Quartz	33
3.5.2 Alkali Feldspar.....	36
3.5.3 Plagioclase	40
3.5.4 Biotite	43
3.5.5 Fayalite and Orthopyroxene	46
3.5.6 Accessory Minerals.....	48
3.6 Intracaldera Glass Textures and Major Element Compositions	51
3.6.1 Very Coarse-Grained Crystal-Rich (VCCR) Fiamme	51
3.6.2 Fine-Grained (FG) Fiamme.....	53
3.7 Outflow Glass Textures and Major Element Compositions.....	55
3.7.1 Medium-Grained (MG) Fiamme	55
3.7.2 Fine-Grained Crystal-Poor (FGCP) Fiamme.....	58
3.8 All Ora Fiamme Glass Major Element Compositions.....	62
 IV. DISCUSSION	64
4.1 Do Fiamme Major Element Compositions Represent Plausible Melt Compositions?.....	64
4.2 What Does the Presence of Multiple Fiamma Types Reveal About the Ora Eruption?	68
4.3 Magma Mingling vs. Magma Mixing	70
4.4 Can Magma Mixing Lead to a Rhyolite Continuum?	71
4.5 What Can Minerals Reveal About the Ora Supereruption?	71
4.7 The Pre-Eruptive Ora Magmatic System	73
 V. CONCLUSIONS.....	75
 Appendix	
A. CRYSTAL CONTENT ANALYSIS	77
B. MINERAL TEXTURES	85
C. FINE-GRAINED CRYSTAL-POOR FIAMME GLASS TYPES	96
D. USGS RGM-1 GLASS STANDARD	104
E. GLASS MAJOR ELEMENT COMPOSITIONS	105
F. NORMALIZED ALKALI FELDSPAR COMPOSITIONS	143
G. NORMALIZED PLAGIOCLASE COMPOSITIONS.....	146

H. BIOTITE COMPOSITIONS (TiO ₂ AND MG#)	150
I. NORMALIZED FAYALITE COMPOSITIONS	152
J. NORMALIZED OPX COMPOSITIONS	152
REFERENCES	154

LIST OF TABLES

Table	Page
1. Sampling Locations and Outcrops	13
2. Fiamma Type Categorization Scheme	23
3. Crystal Content Categorization	23
4. Crystal Content for Each Fiamma	24
5. Maximum Crystal Size Categorization.....	25
6. Maximum Crystal Size for Each Fiamma	25
7. Mineral Assemblage of Each Fiamma	32

LIST OF FIGURES

Figure	Page
1. The intracaldera deposit of the Ora Ignimbrite in Bolzano, Italy	3
2. Stratigraphic cross section of the AVG from NNW to SSE.....	5
3. A paleographic and paleotectonic reconstruction of Pangaea during the Early Permian.....	7
4. The base of the outflow vitrophyre at the Ora 2 sampling location	9
5. Multiple types of fiamme present at Castel Firmiano.....	10
6. Geological map of the Ora Formation and the AVG with sampling locations marked	12
7. The outflow vitrophyre at the Ora 2 sampling location	15
8. A closeup of the alteration zone above the vitrophyre at Ora 2.....	16
9. A very coarse-grained crystal-rich (VCCR) fiamme concentration zone at Ora 5.....	17
10. ORA-2A-035 and the images used for crystal content analysis.....	20
11. VCCR fiamme thin section images.....	27
12. FG fiamme thin section images	28
13. MG fiamme thin section images	30
14. FGCP thin section images	31
15. Quartz from the VCCR fiamme.....	34
16. Quartz from the MG fiamme	35
17. Alkali feldspar from the VCCR fiamme showing interlocking growth textures	37
18. Alkali feldspar from the MG fiamme showing interlocking growth textures.....	38
19. PPL images of alkali feldspar glomerocrysts in MG fiamme.....	39
20. BSE images of altered alkali feldspar from FGCP fiamme	39

21. Ternary diagram of alkali feldspar compositions	40
22. BSE images of sieve textured plagioclase in VCCR fiamme	41
23. BSE images of plagioclase with An-rich cores in MG fiamme	42
24. Ternary diagram of plagioclase compositions.....	43
25. BSE images of biotite in VCCR fiamme	44
26. BSE images of biotite in the MG fiamme	45
27. TiO ₂ vs. Mg# for biotite in the Ora Ignimbrite	46
28. BSE images of fayalite in FGCP fiamme.....	47
29. Ternary diagram of fayalite and orthopyroxene compositions.....	48
30. A BSE image of a biotite glomerocryst from a VCCR fiamma	49
31. Monazite, zircon, and apatite present in the MG fiamma groundmass of ORA-2A-031	49
32. BSE images of accessory minerals in a FGCP fiamma.....	50
33. BSE image of magnetite in ORA-2A-003.....	50
34. BSE image of fiamma glass in ORA-5B-402	51
35. Major element compositions of glass from the VCCR fiamme	52
36. BSE images of FG fiamme glass	53
37. Major element compositions of glass from the FG fiamme.....	54
38. BSE image of MG fiamma glass in ORA-2A-001	56
39. Devitrified glass surrounding quartz in ORA-2A-001.....	56
40. Major element compositions of glasses in the MG fiamme	57
41. Quartz grain rimmed with multiple glass types in ORA-2A-002	58
42. K ₂ O vs. SiO ₂ for ORA-2A-016 showing the multiple glass types present.....	59

43. Multiple glass types shown in ORA-2A-024	60
44. Asteroidal trichites present in ORA-2A-024	60
45. Major element compositions of glasses in the FGCP fiamme	61
46. Glass major element compositions of all the Ora Ignimbrite fiamme glass.....	63
47. Na ₂ O wt. % vs. K ₂ O wt. % for all fiamme glass to show possible alkali exchange alteration .	66
48. A/CNK vs. SiO ₂ for all of the Ora Ignimbrite fiamme	67
49. K ₂ O vs. SiO ₂ for glasses in fiamme from the intracaldera vitrophyre.....	69
50. K ₂ O vs. SiO ₂ for glasses in fiamme from the outflow vitrophyre	70
51. Multiple bodies of magma within a continuous crystal mush zone.....	74

CHAPTER I

INTRODUCTION

1.1 Overview

During a supereruption, magma reservoirs located in the shallow crust evacuate massive amounts ($>450 \text{ km}^3$) of viscous material from the subsurface (Sparks et al., 2005; Miller and Wark, 2008). Mineral fragments, glass shards, and highly vesiculated magma fragments—pumice – are explosively expelled, forming pyroclastic flows that emanate from volcanic vents. The resulting deposits from these catastrophic events are called ignimbrites. Fiamme develop in welded ignimbrites when pumice clasts undergo compaction and the vesiculated glass welds back together. Glass within fiamme may preserve melt compositions and the minerals inside fiamme record historical information from rim to core. By studying the fiamme from supereruptions, we can obtain textural, mineralogical, and geochemical information regarding the magma involved in supereruptions.

There are a few current models of how magma systems are organized in the shallow crust. The “mush model” (e.g. Hildreth, 2004) suggests that there is a melt-rich lens present at the top of the magma chamber comprised of highly fractionated, crystal-poor magma. This high-silica rhyolite magma leaves behind a crystal-rich residue, coined the crystal mush (e.g. Hildreth, 1981, 2004). Interstitial melt from the crystal mush percolates upwards and contributes to the crystal-poor lens situated at the top of the magma chamber. Surrounding the crystal mush is a

crystal-rich, melt-poor rigid sponge. Injections of magma can thermally sustain and rejuvenate this system with influxes of heat and gas.

Work involving fluid dynamics and melt extraction expanded on the mush model by calculating the optimal crystallinity for melt extraction from a crystalline mush (Bachmann and Bergantz, 2008). At 45-60% crystallinity, the separation of crystals from interstitial liquid (i.e. unmixing, crystal fractionation) is the most efficient. At higher crystal contents, melt extraction is extremely slow, inefficient, and can only occur due to compaction (Bachmann and Bergantz, 2008). Bachmann and Bergantz (2008) further expanded on the mush model by proposing that active convection within a magma system produces homogeneous, un-zoned ignimbrites whereas the lack of convection results in heterogeneous ignimbrites.

Recent work has suggested the possibility of multiple magma bodies within a large, crystal mush framework (Begué et al., 2014; Cashman and Giordano, 2014; Gualda and Ghiorso, 2013; Miller et al., 2011; Lipman, 2007). This type of magma system can be formed via lateral sill emplacement (Miller et al., 2011; Lipman, 2007). Miller (2011) suggests that magmatic systems can lie dormant in a rigid sponge state and be rapidly mobilized with intense periods of recharge via dike injections. These studies regarding the behavior and structure of large-scale magma systems have aided in our understanding of the subsurface reservoirs that feed supereruptions.

The Permian Ora Ignimbrite – the subject of this study – presents an opportunity for investigating the subsurface organization of a supereruption-sized magma system prior to eruption. Glacial incision has exposed intracaldera deposits that tower over 1,350 m above the city of Bolzano, Italy (Fig. 1). The presence of multiple populations of fiamme found throughout

the $>1,300$ km 3 (dense rock equivalent) deposit suggests that multiple bodies of magma contributed to this eruption (Willcock et al., 2013). Relatively fresh, intensely welded, glassy fiamme from two basal vitrophyre deposits provide a record of melt compositions present in the magma body prior to eruption. The intracaldera vitrophyre allows us to study the early-erupted products of the Ora ignimbrite while the late-erupted, outflow vitrophyre gives us an opportunity see how the erupted products changed during the eruption. By analyzing the varieties of fiamme erupted out of the Ora Caldera, we can illuminate pre-eruptive processes and the magmatic architecture of a supereruption-sized system.



Figure 1: View of the intracaldera deposit of the Ora Ignimbrite. Note the relief of 1,350 meters. Photo taken from near the Bolzano Airport (46°27'51.8"N 11°19'59.8"E).

1.2 Geologic Background

The Ora Ignimbrite and its volcanic predecessors are part of the Athesian Volcanic Group (AVG). Located in the southern Alps of northern Italy, the AVG erupted multiple deposits of rhyodacitic to rhyolitic ignimbrites and lava flows in the region, forming a nested caldera complex (Fig. 2) (Marocchi et al., 2008). A transition from primarily effusive eruptions to large ignimbrite eruptions higher in the stratigraphic sequence likely represents the successful priming of the crust, allowing for large amounts of molten material to accumulate in the subsurface.

The first caldera collapse is associated with the rhyodacitic Gargazonne Ignimbrite (276.5 ± 1.1 Ma) (Marocchi et al., 2008). After the first caldera collapse, a shift from rhyodacitic to rhyolitic volcanism is observed in the stratigraphic record (Fig. 2). This begins with the eruption of the rhyolitic Nalles Ignimbrite (276.7 ± 1.1 Ma) (Marocchi et al., 2008). The second caldera collapse occurred with the eruption of the Ora Ignimbrite (Marocchi et al., 2008). Figure 2 is an idealized cross section of the erupted units of the Athesian Volcanic Group and the 1st and 2nd caldera margins are clearly shown. Single zircon U-Pb dates show that this volcanic flareup lasted for around 10 million years from 285 to 274 Ma (Marocchi et al., 2008).

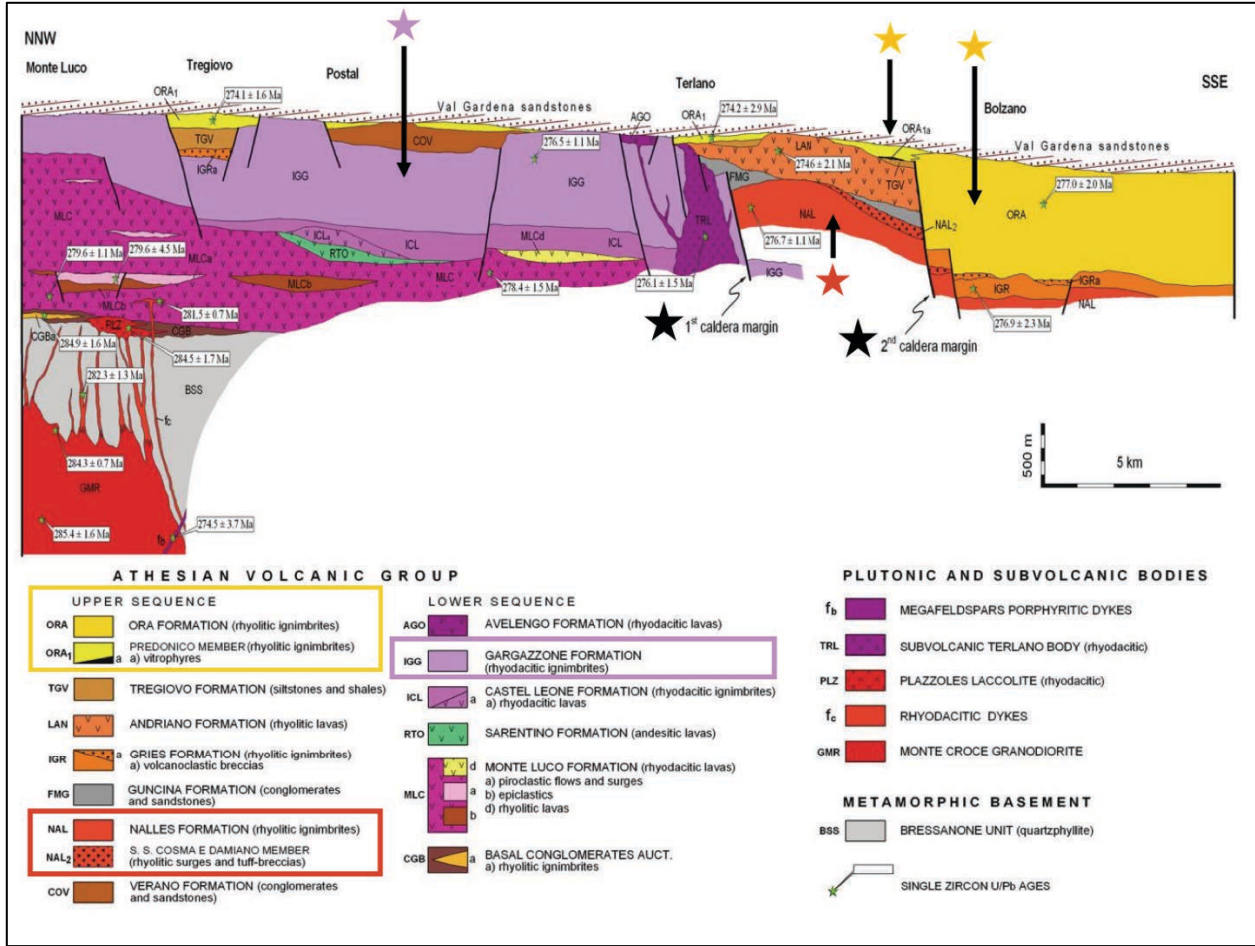


Figure 2: Stratigraphic cross section of the northwestern Athenian Volcanic Group from NNW to SSE with sample position and age data added (modified after Morelli et al., 2007). The Ora intracaldera and outflow deposits from this study are marked with yellow stars. The caldera margins are labelled and marked with black stars. The rhyodacitic Gargazzone Fm. is marked with a light purple star. The rhyolitic Nalles Fm. is marked with a red star. Section is not to scale. From Marocchi et al., 2008.

The Ora Ignimbrite is the last eruptive unit of the AVG. Single zircon U-Pb dating yields ages of 277 ± 2 Ma for the intracaldera fill and 274.1 ± 1.6 Ma for the outflow deposits (Marocchi et al., 2008). Marocchi et al. (2008) suggest that the age gap between the intracaldera and outflow deposits, while within error, may indicate that the outflow deposits occurred after the main intracaldera volcanism. However, the deposit does not show any obvious evidence of time breaks, suggesting that this may be a single eruptive event.

Back-arc extensional tectonics in the Permian, a consequence of the collapse of the Variscan orogenic belt and subsequent closure of the Paleo-Tethys ocean, likely influenced the onset of magmatism in the region (De Rita and Giordano, 1996). As the Paleo-Tethys subducted under Eurasia, the locus of an oceanic spreading center and a transform margin coincided to produce a stable transform-trench-ridge triple junction that was active during the end of the Carboniferous and into the Early Permian (Fig. 3) (Cassinis et al., 2012). Coupled subduction and transtensional shear resulted in basin formation and extension that allowed for the upwelling of the asthenosphere and the resulting elevation of the geothermal gradient. Cassinis et al. (2012) note the prominence of magmatic activity after the Permo-Carboniferous boundary and suggest that the variable compositions of the extrusive and intrusive rocks may be related to the subduction of the Paleo-Tethys oceanic plate. This unique geotectonic setting of back-arc extension resulting from combined subduction and transform faulting has produced other voluminous rhyolitic supereruptions in Earth history that have been referred to as slab-rollback ignimbrite flareups (Best et al., 2016).

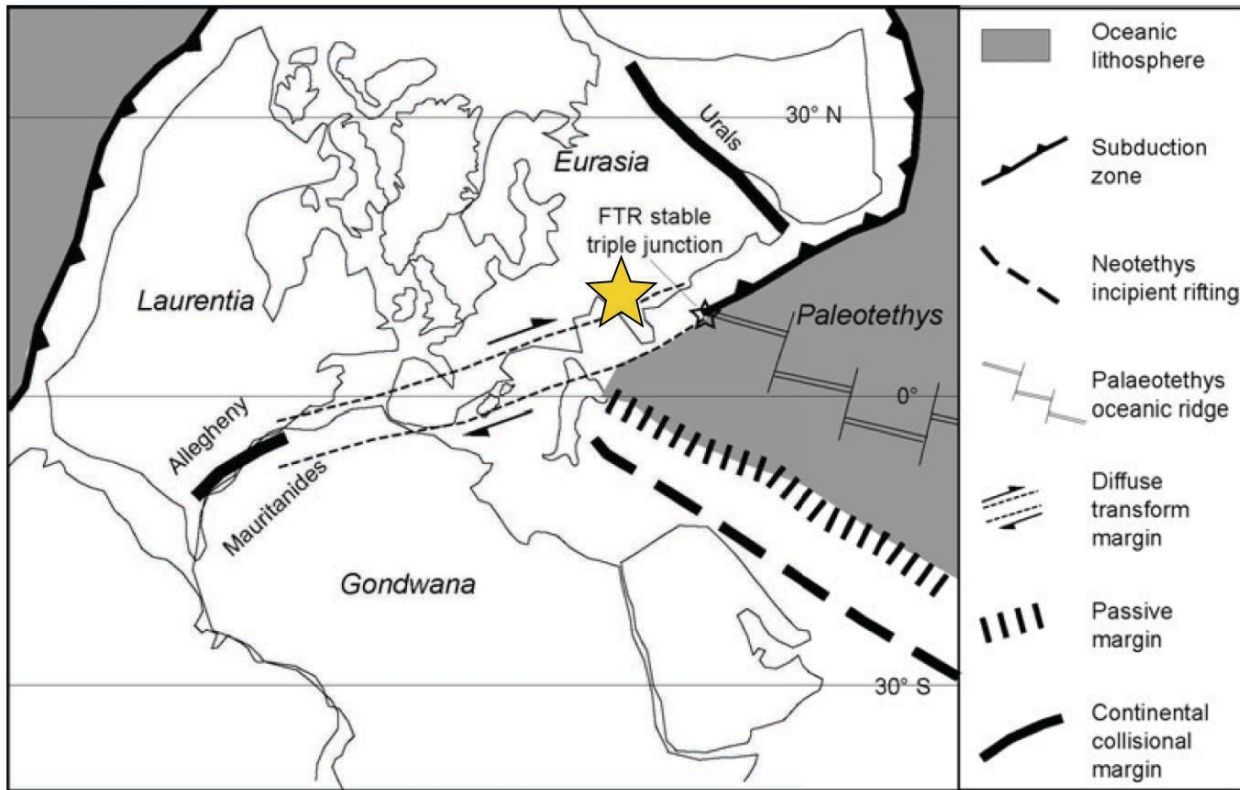


Figure 3: A paleogeographic and paleotectonic reconstruction of Pangaea during the Early Permian. The yellow star shows the approximate location of the Ora Caldera at the time of formation. The location of the transform-trench-ridge (FTR) triple junction between the Paleo-Tethys, Laurentia, and Gondwana is proximal to the site of the Ora supereruption. From Cassinis et al., 2012.

In the Mesozoic, the Ora Formation and its underlying volcanic units were not subject to the intense Alpine deformation that affected regions to the northwest of the Periadriatic line. Ring and Richter (1994) suggest that this region escaped alpine deformation due the rigid behavior of a large mass of rhyolitic lavas and ignimbrites that resulted from volcanism in the Permian.

The Ora Ignimbrite expelled $>1300 \text{ km}^3$ of material to form a crystal-rich welded deposit (Willcock et al., 2013). Glacial incision has exposed the intracaldera deposits, which have a maximum thickness of 1350 m, while the outflow deposits are less than 250 m thick (Willcock

et al., 2013). The Ora Ignimbrite is predominantly an intracaldera deposit and it is likely that there was an early caldera collapse, which allowed for the majority of the erupted material to be confined to the interior of the caldera (Willcock et al., 2013). The deposit is welded throughout and it is interpreted to have resulted from a low-energy fissure-fountaining eruption that produced hot, slow-moving, high-particle-concentration flows (Willcock et al., 2013). There are no early surge or fall deposits at the base of Ora, which suggests that the Ora System did not experience a Plinian precursor phase (Willcock et al., 2013).

The caldera collapse is interpreted to have occurred early, based on the large volume of the intracaldera fill and the fact that the outflow correlates with the middle and upper, late-erupted units of the intracaldera deposit (Willcock et al., 2013). Willcock et al. (2015) identify two discrete collapse calderas (northern and southern) and suggest that the eruption commenced in the southern caldera as less evolved, more biotite-rich material was erupted. As the Ora Eruption continued, the magma chamber beneath the caldera deflated and there was likely continuous slip along the caldera-bounding faults during the eruption sequence to accommodate the large volume of the intracaldera deposit. The eruption of the northern caldera resulted in more evolved deposits with less biotite, suggesting that the Ora Eruption may have tapped multiple magma chambers (Willcock et al., 2015).

The presence of vitrophyre in the Ora Ignimbrite is perplexing. In the intracaldera fill, basal vitrophyre occurs where the Ora Ignimbrite overlies the sedimentary Tregiovo Formation. However, in the northeastern outflow, vitrophyre occurs above a 2 m thick welded ignimbrite deposit that is interpreted to be part of the Ora Ignimbrite (Fig. 4). This deposit overlies volcaniclastic sediments and has reworked sedimentary grains inside it.



Figure 4: The base of the outflow vitrophyre at the Ora 2 sampling location. The vitrophyre overlies a 2 m thick welded, non-vitrophyric unit of the Ora Ignimbrite. This suggests that there was a time gap prior to the eruption of the vitrophyre, allowing for the basal unit to weld separately.

Willcock et al. (2015) note the presence of multiple fiamma types throughout the Ora Ignimbrite and hypothesized that the varieties of fiamme, deposit heterogeneity, and slight geochemical variations may be due to genetically related, subtly different magma bodies within a reservoir network. The research presented in this thesis aims to characterize fiamme from two Ora Ignimbrite vitrophyre units, an early-erupted intracaldera vitrophyre and a late-erupted outflow vitrophyre, in order to provide more insight on the multiple types of magmas involved in the eruption. By characterizing the multiple types of glass in each fiamma, the

mineralogy, and the crystal textures, we strive to understand more about the magma chamber architecture and pre-eruptive processes for large-scale magmatic systems such as the Ora System.

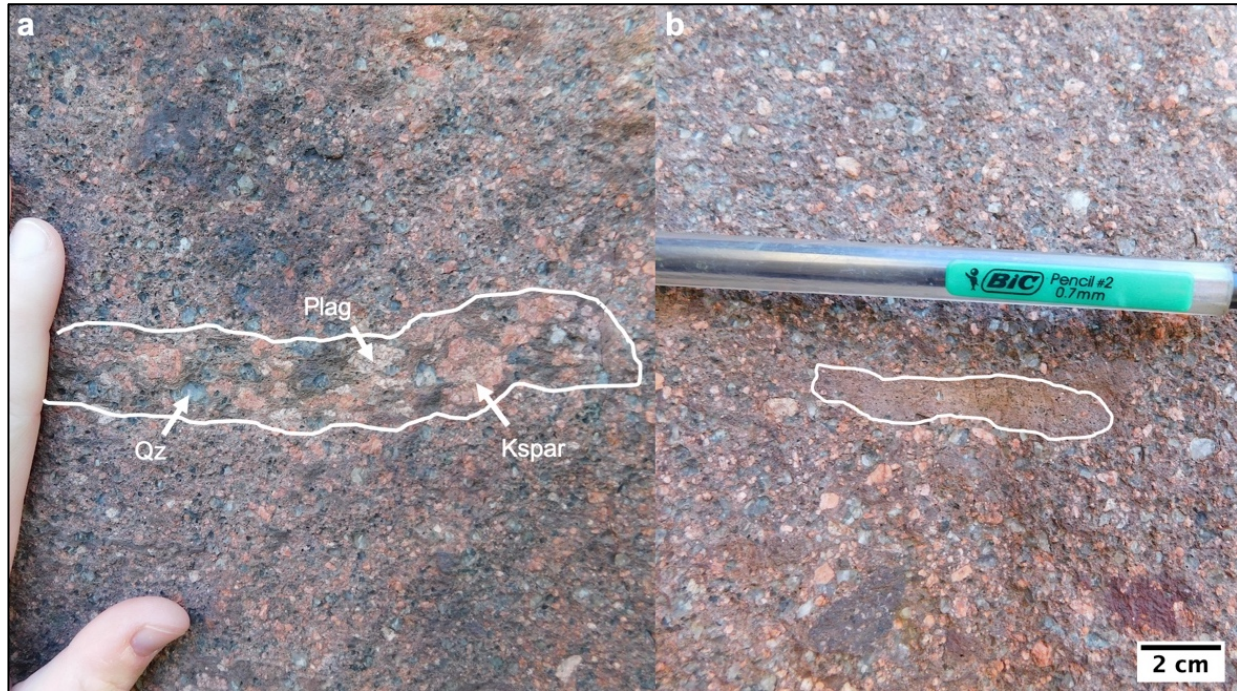


Figure 5: Multiple types of fiamme present at Castel Firmiano, an outcropping of the intracaldera Ora Ignimbrite. (A) Very coarse-grained crystal-rich (VCCR) fiamma. Note the large (~2 cm) alkali feldspar present. (B) Fine-grained crystal-poor (FGCP) fiamma.

CHAPTER II

METHODS

2.1 Field Work

Fieldwork commenced in October 2017. The main goals were: (1) to observe many different outcrops in order to gain an understanding of the variety present in the Ora Ignimbrite deposits, (2) to identify multiple fiamme populations at each outcrop, (3) to collect abundant, unaltered samples for geochemical analysis, and (4) to understand the volcanic history of the region. Figure 6 marks the locations of each outcrop that we visited and table 1 lists their coordinates. The two sampling locations from this study, the early-erupted intracaldera vitrophyre and the late-erupted outflow vitrophyre, will be discussed in the following sections.

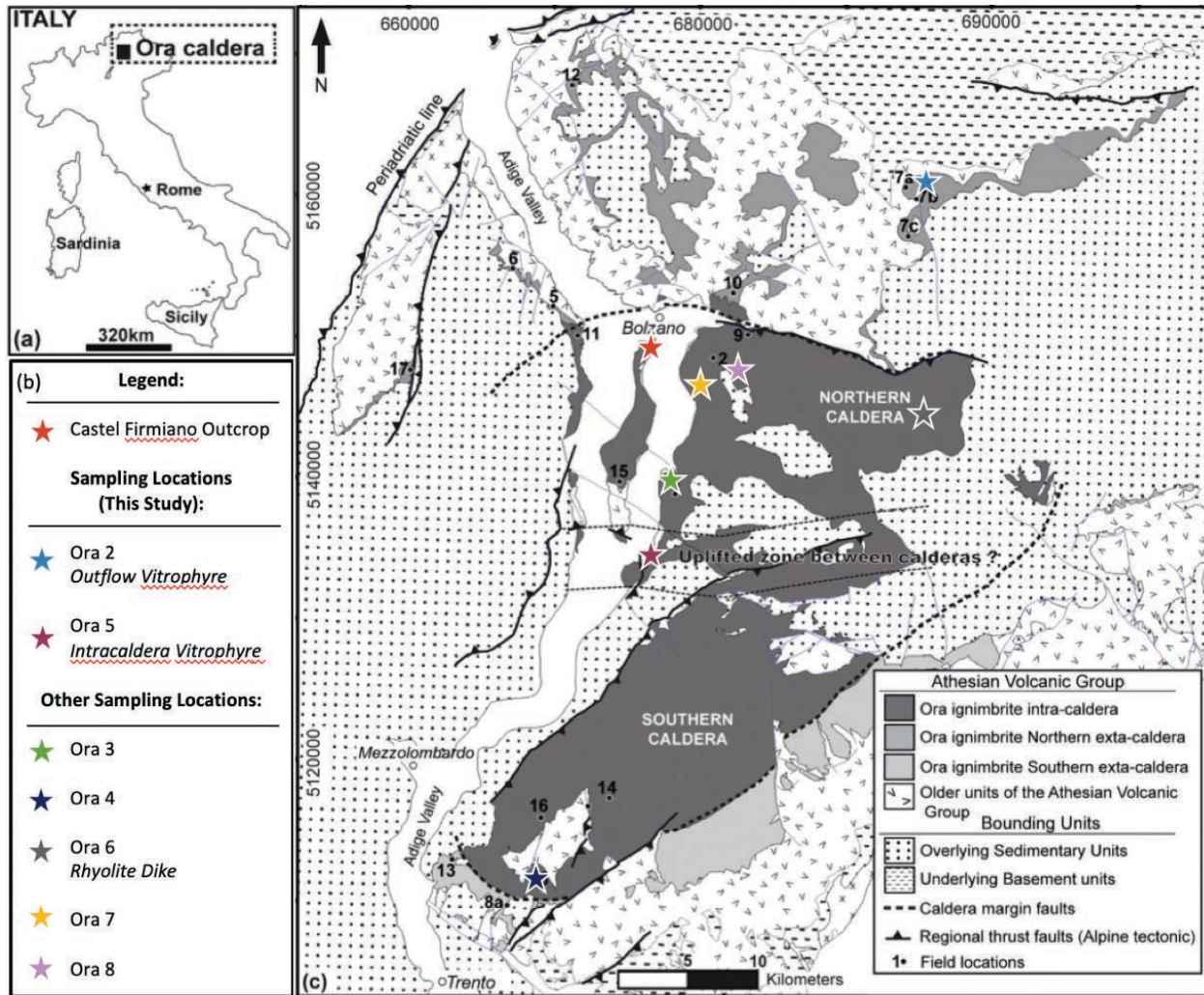


Figure 6: Geological map of the Ora Formation and the Athesian Volcanic Group, southern Alps, Italy. The sampling locations are marked with stars. The intracaldera deposits are dark grey and divided into two main calderas (northern and southern). The outflow deposits are lighter grey. Note that the intracaldera deposits (dark grey) represent the majority of the Ora Ignimbrite. (From Willcock et al., 2013; modified from Italian geological map and unpublished data of Bargossi, G.M., Morelli, C., and Piccin G.).

Table 1: The sample name, type, coordinates, and the number of samples taken from each outcrop visited during the 2017 field season. The outcrops marked with stars (Ora 2 and Ora 5) are the focus of this study.

Name	Type	Coordinates	# Samples
Castel	Intracaldera	46°28'48"N, 11°18'19"E	(No Sampling,
Firmiano			Museum Site)
Ora 2 ★	Outflow	46°34'44"N, 11°32'07"E	40 Fiamme
	Vitrophyre		1 Bulk Tuff
Ora 3	Intracaldera	46°23'54"N, 11°19'18"E	3 Fiamme
			1 Bulk Tuff
Ora 4	Intracaldera	46°08'48"N, 11°12'24"E	56 Fiamme
Ora 5 ★	Intracaldera	46°20'36"N, 11°18'29"E	22 Fiamme
	Vitrophyre		1 Bulk Tuff
Ora 6	Rhyolite Dike	46°25'36"N, 11°31'23"E	4 Bulk Rock
Ora 7	Intracaldera	46°27'01"N, 11°20'51"E	1 Bulk Tuff
Ora 8	Intracaldera	46°27'42"N, 11°22'42"E	1 Bulk Tuff

2.1.1 Sampling Locations

2.1.1.1 Ora 2: Outflow Vitrophyre

Ora 2 is the location of the late-erupted outflow vitrophyre. The Ora 2 outcrop occurs at a mine and provides great exposure for viewing the vitrophyre and the overlying alteration zone (Fig. 7). This outcrop is the thickest vitrophyric horizon of all the northern outflow deposits. Below the vitrophyre horizon is a 2 m unit of welded, non-vitrophyric Ora (Fig. 4). The non-vitrophyre base has reworked volcaniclastic sediments and is very lithic-rich. While

the other vitrophyre is a basal vitrophyre atop sedimentary strata, this vitrophyre overlies previously deposited Ora Ignimbrite. This appears to represent a time gap in the eruption sequence because (1) the basal unit does not show graded welding into the vitrophyre and (2) there is a change in lithic content from a lithic-rich base to the lithic-poor vitrophyre (Fig. 4).

The ignimbrite matrix of this outflow vitrophyre is coarse-grained and there are abundant fine-grained crystal-poor and crystal-rich fiamme. Above the vitrophyre lies an alteration zone that is approximately 1.5 m thick (Fig. 7, 8). Within this zone, fiamme are altered from black to red, orange, and white. Overlying the alteration zone is the coarse-grained, crystal-rich ignimbrite lithofacies. Continuous cooling joints through the vitrophyre and the overlying ignimbrite suggest that these units cooled together as one unit (Fig. 7). A total of 16 fine-grained crystal-poor fiamme, 24 medium-grained fiamme, and one bulk tuff sample were collected from the outflow vitrophyre.



Figure 7: The outflow vitrophyre at the sampling location Ora 2 ($46^{\circ}34'44''N$, $11^{\circ}32'07''E$). This outcrop is a mining locality, allowing for great exposure of the vitrophyre, alteration zone, and overlying ignimbrite. The continuous cooling joints from base to top of the outcrop suggest that this deposit cooled as one unit.



Figure 8: A closeup of the alteration zone above the vitrophyre. It is about 1.5 m thick. Note the different colored layers and how they are roughly parallel to the vitrophyre horizon.

2.1.1.2 Ora 5: Intracaldera Vitrophyre

Ora 5 is the location of an intracaldera basal vitrophyre horizon (Fig. 6). This vitrophyre is located on a relict basement ridge between the two (northern and southern) collapse calderas (Willcock et al., 2015) (Fig. 6). It overlies the sedimentary Tregiovo formation and is ~10 m thick. As a basal deposit, Ora 5 contains early-erupted material from the Ora Ignimbrite.

There is a fiamme concentration zone present at the sampling location with very coarse-grained, crystal-rich fiamme up to 10 cm in length (Fig. 9). The ignimbrite matrix is crystal-rich and has noticeably more biotite than the ignimbrite matrix from the outflow vitrophyre. A total

of 19 very coarse-grained crystal-rich fiamme and three fine-grained fiamme were collected from this sampling location.

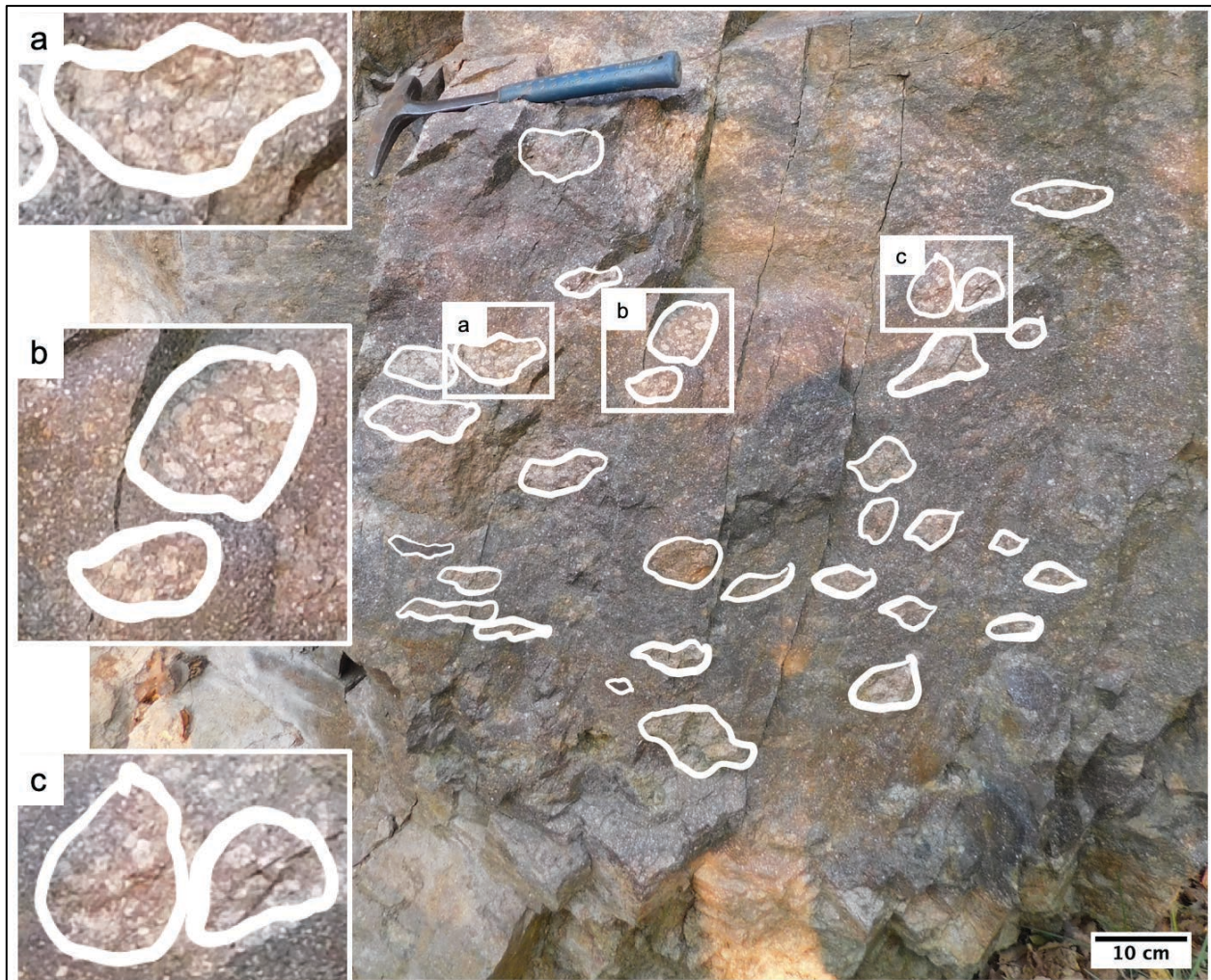


Figure 9: A very coarse-grained crystal-rich (VCCR) fiamme concentration zone present at the Ora 5 sampling location ($46^{\circ}20'36''N$, $11^{\circ}18'29''E$). The outlined features are individual VCCR fiamme. These fiamme can be up to 10 cm in length. Note the large mineral grains.

2.2 Analytical Methods

The analytical methods from this study are described in the following sections.

Methodology detailing sample preparation, petrography, crystal content analysis, and elemental analysis are documented. Objectives for the petrographic analysis are listed, the process of greyscale thresholding to obtain crystal contents is discussed, and the machines and the parameters used to obtain major element compositions are noted.

2.2.1 Sample Preparation

I created thin section billets using the Vanderbilt University rock saw. In order to effectively analyze the multiple fiamme types observed in the field, I chose to send off nine medium-grained and five fine-grained billets from the outflow vitrophyre (Ora 2), thirteen very coarse-grained billets and four fine-grained billets from the intracaldera vitrophyre (Ora 5) and four altered intracaldera billets from the southern intracaldera non-vitrophyre (Ora 4).

The production of thin sections was outsourced to R.A. Petrographic Thin Sections for mounting and polishing. Of the 35 thin sections, 16 were identified as critical for sufficiently demonstrating the variability within the fiamme population. These 16 thin sections were made from 14 individual fiamme. Due to limited samples, two thin sections were made from the same fiamma for ORA-5B-404A/B and ORA-5B-412A/B. The altered intracaldera thin sections (Ora 4) were too altered to obtain any textural or elemental information, so they were excluded from this study. Overall, ten thin sections from the outflow vitrophyre (Ora 2) and six thin sections from the intracaldera vitrophyre (Ora 5) were used.

2.2.2 Petrography

With a Zeiss Axioscope transmitted and reflected-light petrographic microscope, I gathered detailed petrological observations of each thin section. My petrographic analysis included: (1) identification of the minerals present; (2) measurement of the sizes of each mineral phase in the fiamme; (3) characterization using grain shapes; and (4) observation of fiamme glass textures. Photographs were taken in both plane-polarized and cross-polarized light. This petrographic analysis helped to identify regions of interest for SEM-EDS analysis.

2.2.3 Crystal Content Analysis

Whole-rock modal abundance of crystals in the Ora Ignimbrite has been previously estimated to range from 35-45% (Willcock et al., 2013). However, this estimate includes the crystal-rich ignimbrite matrix which may not represent magmatic crystal content. In order to determine the crystal content of the magma involved in the Ora supereruption, I needed to solely analyze the fiamme. I began by making scans of my thin sections in plane polarized light using an HP G010 scanner. Then, I utilized the software Adobe Photoshop Mix on an iPad and used an Apple Pencil to trace out the fiamme so that it would be separate from the ignimbrite matrix.

Using Adobe Illustrator, I created grayscale image traces of my fiamme. The grayscale images easily differentiate quartz and felspar (light grey) and biotite (dark grey) from fiamma groundmass (intermediate grey) (Fig. 10). In ImageJ, I used greyscale thresholding to obtain pixel counts for thresholded features (Fig. 10). By dividing the thresholded values from the total area of the fiamma, I obtained crystal content measurements.

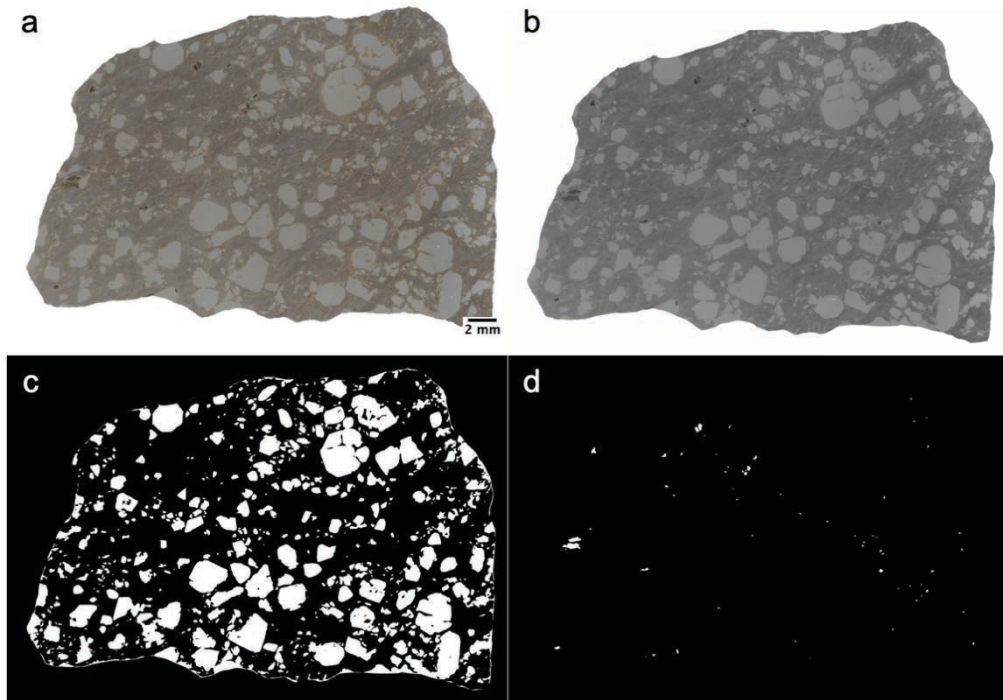


Figure 10: (a) ORA-2A-035 fiamma separated from the ignimbrite matrix. (b) The resulting greyscale image trace from Adobe Illustrator. (c) Thresholded quartz and feldspars of ORA-2A-035. They represent 29% of the fiamma. (d) Thresholded biotite of ORA-2A-035. They represent 0.26% of the fiamma.

2.2.4 Elemental Analysis

Mineral and glass major element compositions were obtained at Vanderbilt University using an Oxford X-max 50 mm² Energy Dispersive Spectrometer (EDS) attached to a Tescan Vega 3 LM Variable Pressure Scanning Electron Microscope (SEM). The thin sections were carbon-coated before being studied with the SEM. A working distance of 15 mm, accelerating voltage of 15 kV, and a beam intensity of 19 were used for imaging and analysis. The emission current was approximately 21×10^{-6} A and the specimen current was approximately 2×10^{-9} A. Backscattered images were acquired using a scan speed of 6. The dwell time was around 32×10^{-6} seconds.

The software Aztec from Oxford Instruments was used for EDS analysis. The EDS was optimized daily with Copper. USGS RGM-1 rhyolite glass was used as a secondary standard to check the quality of glass analyses. Elemental data regarding the secondary standard are located in Appendix D. The dead time was typically around 40%. The smallest analyzed area for glass analysis was $15 \times 15 \mu\text{m}$. This was used for EDS analysis of small regions of unaltered glass in the FG fiamma. The most frequently used size for glass analysis was $50 \times 50 \mu\text{m}$. The smallest analyzed area for mineral analysis was $10 \times 10 \mu\text{m}$. This size was used for EDS analysis of regions within a single feldspar and for accessory mineral analysis. The most frequently used size for EDS analysis of mineral grains was $150 \times 150 \mu\text{m}$.

EDS analysis was used to obtain glass and mineral major element compositions. The data are presented as weight percent of the oxides. Minerals that were identified on the microscope were verified using EDS analysis. The accessory minerals were also identified using EDS analysis.

CHAPTER III

RESULTS

3.1 Categorization

The samples were initially characterized by the textural features of the fiamme. Since it was difficult to group the samples based upon glass major element trends, I chose to group the samples based upon crystal content and maximum phenocryst size for a preliminary categorization scheme. The geochemical analyses of glass within the fiamme then verified that these four fiamma types represent all of the samples.

This study is limited to the analysis of samples from two outcrops: the outflow vitrophyre (Ora 2) and the intracaldera vitrophyre (Ora 5) (Fig. 6). I chose to focus on these two outcrops because the vitrophyre preserved the glass compositions while the non-vitrophyre was found to be extremely altered. Nonetheless, these sampling locations represent both early-erupted intracaldera deposits (Ora 5) and late-erupted outflow deposits (Ora 2), allowing us to see potential variations over the course of the eruption.

The early-erupted intracaldera deposits have two varieties of fiamme present: very coarse-grained crystal-rich (VCCR) and fine-grained (FG) fiamme. The late-erupted outflow deposits also have two varieties of fiamme present: medium-grained (MG) and fine-grained crystal-poor (FGCP) fiamme. For the rest of this thesis, these fiamme types will be referred to by their abbreviations.

Table 2: The four types of fiamma present in the Ora Ignimbrite.

FIAMMA TYPES:	DESCRIPTION:	LOCATION	CRYSTAL CONTENT:	MAX PHENOCRYST SIZE:	MAFICS:
TYPE 1:	Very Coarse-Grained Crystal-Rich (VCCR)	Intracaldera	~40-50%	>5 mm	~2-3%
TYPE 2:	Medium-Grained (MG)	Outflow	~20-40%	1-3 mm	<0.5%
TYPE 3:	Fine-Grained (FG)	Intracaldera	~20%	≤1 mm	<0.1%
TYPE 4:	Fine-Grained Crystal-Poor (FGCP)	Outflow	~10%	≤1 mm	≤0.15%

3.2 Textural Analysis

This section presents the crystal content, biotite content, and maximum phenocryst size for each fiamme. The corresponding descriptive terminology is shown for the crystal content and maximum phenocryst size. These data influenced the categorization shown in Table 2.

3.2.1 Crystal Contents

The following table shows the descriptive term that corresponds to the crystal content. If the crystal content ranges from 10-40%, like the MG and FG fiamme, no descriptive term is added to the fiamme type name. Otherwise, the samples are either crystal-rich (40-50%; VCCR) or crystal-poor (<10%; FGCP). Table 4 presents each sample with its location, type, crystal content, and biotite content.

Table 3: The crystal content and associated descriptive term for the Ora Ignimbrite fiamme. Note that if the sample is within the range of variable crystal content (10-40%), there is no descriptive term added.

Description:	Crystal Content:
Crystal-Rich (CR)	40-50%
Variable Crystal Content	10-40%
Crystal-Poor (CP)	<10%

Table 4: The location, type, crystal content, and biotite content of each sample. The colors for the crystal content boxes are gradational from the highest content (green) to intermediate content (yellow) to the lowest content (red).

ORA	Sample	Location	Type	Xtal Content	Biotite Content
5B	ORA-5B-402	Intracaldera	VCCR	46%	2.2%
	ORA-5B-404A	Intracaldera	VCCR	45%	2.3%
	ORA-5B-404B	Intracaldera	VCCR	45%	2.5%
2A	ORA-2A-001	Outflow	MG	21%	0.03%
	ORA-2A-031	Outflow	MG	21%	0.07%
	ORA-2A-032	Outflow	MG	39%	0.42%
	ORA-2A-035	Outflow	MG	29%	0.26%
	ORA-2A-040	Outflow	MG	26%	0.21%
5B	ORA-5B-412A	Intracaldera	FG	21%	0.01%
	ORA-5B-412B	Intracaldera	FG	23%	0.03%
	ORA-5B-414	Intracaldera	FG	21%	0.06%
2A	ORA-2A-002	Outflow	FGCP	10%	0.01%
	ORA-2A-016	Outflow	FGCP	10%	0.03%
	ORA-2A-023	Outflow	FGCP	10%	0.04%
	ORA-2A-003	Outflow	FGCP	8%	0.15%
	ORA-2A-024	Outflow	FGCP	12%	0.02%

3.2.2 Crystal Sizes

The following table shows the descriptive terms that correspond to the maximum crystal size found in each fiamma. Table 6 presents each fiamma from this study and its associated maximum crystal size.

Table 1: The descriptive term that corresponds to the maximum crystal size found in each Ora Ignimbrite fiamma (From Willcock et al., 2015).

Description:	Size:
Very Coarse-Grained	>5 mm
Coarse-Grained	3-5 mm
Medium-Grained	1-3 mm
Fine-Grained	≤1 mm

Table 2: The samples and the maximum crystal size present in each fiamma. Samples are grouped by fiamma type.

ORA	SAMPLE	TYPE	MAX CRYSTAL SIZE
5B	ORA-5B-402	VCCR	> 5 mm
	ORA-5B-404A	VCCR	> 5 mm
	ORA-5B-404B	VCCR	> 5 mm
2A	ORA-2A-001	MG	1-2 mm
	ORA-2A-031	MG	1-2 mm
	ORA-2A-032	MG	2-3 mm
	ORA-2A-035	MG	1-3 mm
	ORA-2A-040	MG	1-3 mm
5B	ORA-5B-412A	FG	< 1 mm
	ORA-5B-412B	FG	< 1 mm
	ORA-5B-414	FG	< 1 mm
2A	ORA-2A-002	FGCP	≤1 mm
	ORA-2A-016	FGCP	≤1 mm
	ORA-2A-023	FGCP	≤1 mm
	ORA-2A-003	FGCP	≤1 mm
	ORA-2A-024	FGCP	≤1 mm

3.3 Intracaldera Fiamme

This section gives an overview of the textural characteristics observed in the VCCR and FG fiamme. Textures and major element compositions are briefly described in order to provide diagnostic characteristics of each subtype.

3.3.1 Very Coarse-Grained Crystal-Rich (VCCR) Fiamme:

Macroscopically, the diagnostic features of the VCCR fiamme are (1) large (>5 mm) crystals, (2) high crystal content (~45%), and (3) abundance of biotite (2-2.5%) (Fig. 11). In thin section, quartz and plagioclase show resorption textures (Section 3.5). Interlocking growth textures are observed between multiple plagioclase and alkali feldspar grains (Section 3.5). Biotite is irregular (bent, resorbed) with multiple accessory mineral inclusions (Section 3.5).

The VCCR fiamme have homogeneous, high-silica rhyolite glass (Section 3.6). The glass compositions cluster tightly from 76.5-77.5 wt. % SiO₂ and show the least elemental variation among all the fiamma types (Section 3.8). Lastly, the VCCR fiamme have the most iron-rich biotite (Section 3.5).

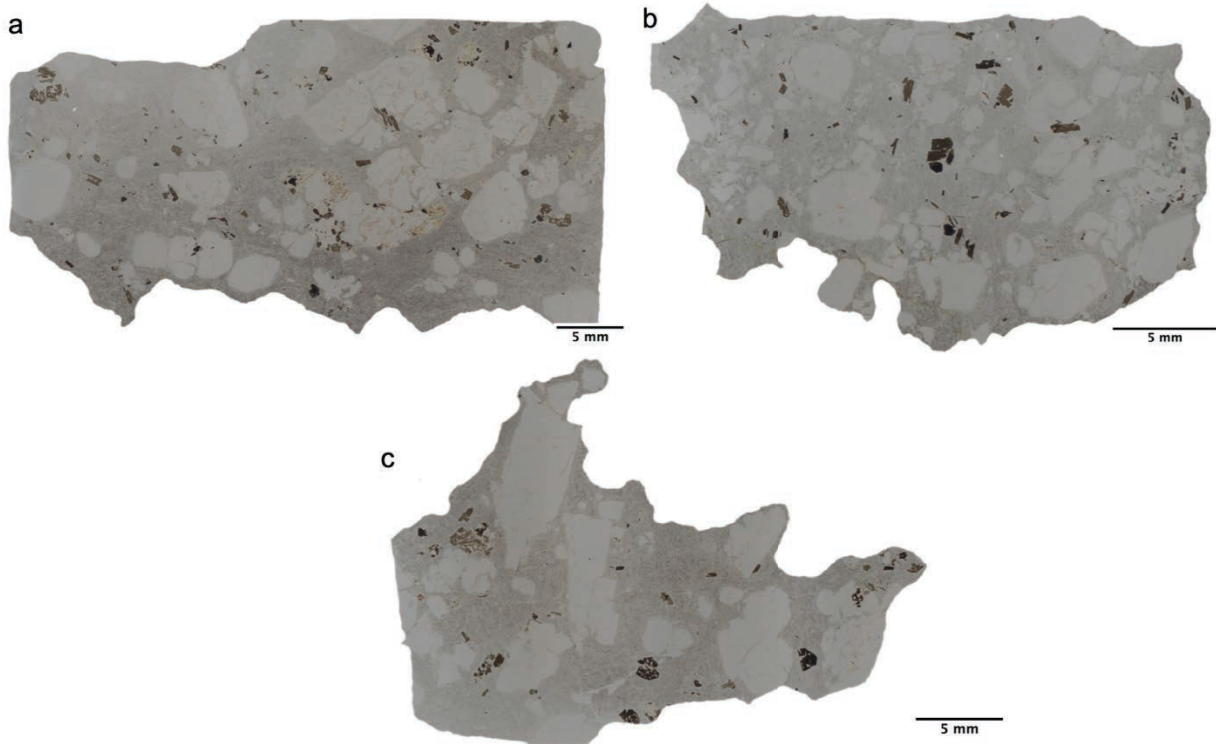


Figure 11: VCCR fiamme (A) ORA-5B-402 (B) ORA-5B-404A (C) ORA-5B-404B. Note the (1) presence of large phenocrysts (>5 mm), (2) the high crystal content (~45%), and (3) the abundance of biotite (2-2.5%).

3.3.2 Fine-Grained (FG) Fiamme:

The FG fiamme can be differentiated in hand sample by their (1) small (<1 mm) crystal sizes and (2) relatively low crystal content (~20%) (Fig. 12). In comparison to the outflow fiamme, the crystal content of the FG fiamme is marginally higher than the FGCP (~10%) fiamme and their crystals are smaller than the MG fiamme (1-3 mm) (Section 3.2). Biotite is rare (<0.10%) and the only accessory mineral found was one apatite in ORA-5B-414 (Section 3.2). There are abundant microlites present, imparting a speckled appearance in back-scattered electron images (Section 3.6).

Geochemically, the FG fiamme glass ranges from 72-78 wt. % SiO₂ (Section 3.6). Glass from ORA-5B-414 has the highest K₂O concentration (3.5-4.5 wt. % K₂O) in this study (Section 3.8). Biotite in the FG fiamme is more iron-rich than biotite from the MG and FGCP outflow fiamme (Section 3.5).

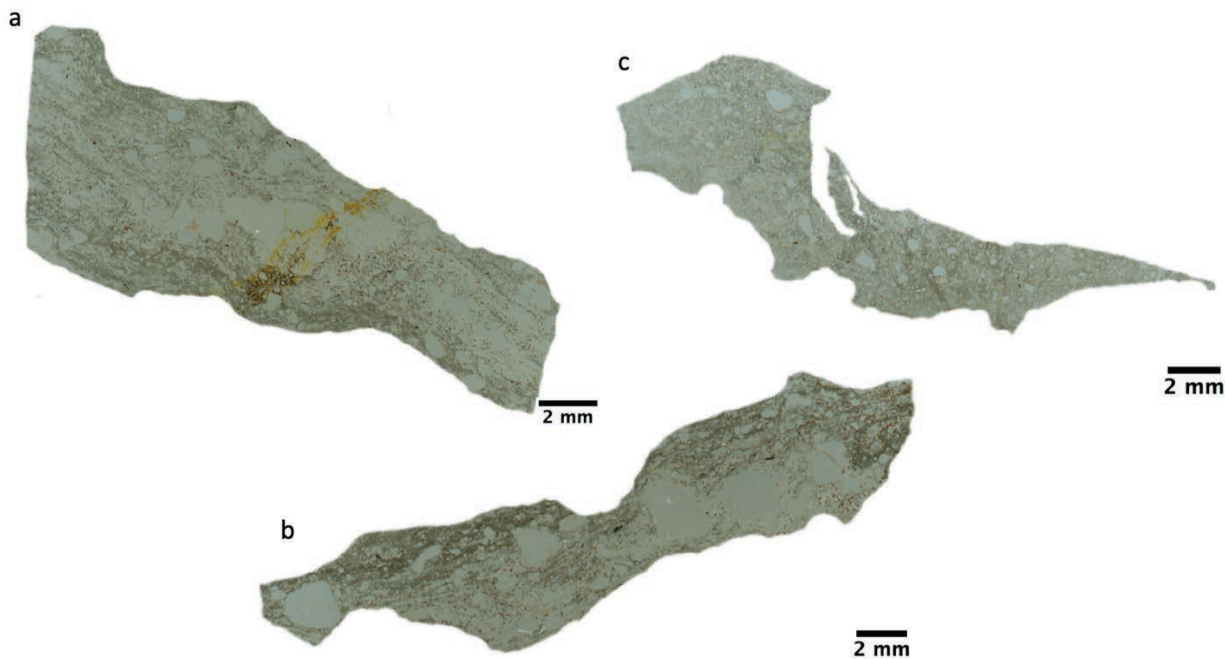


Figure 12: FG fiamme (A) ORA-5B-412A (B) ORA-5B-412B (C) ORA-5B-414. Note the (1) small (<1 mm) crystal sizes and (2) low crystal content (~20%).

3.4 Outflow Fiamme:

This section gives an overview of the textural characteristics observed in the MG and FGCP fiamme. Textures and major element compositions are briefly described in order to provide diagnostic characteristics of each subtype.

3.4.1 Medium-Grained (MG) Fiamme:

Macroscopically, the diagnostic features of the MG fiamme are (1) intermediate crystal content (20-40%), (2) intermediate crystal sizes (1-3 mm), and (3) the presence of clumped crystals (often rimmed in orange, devitrified glass) (Fig. 13). In comparison with the VCCR fiamme, quartz in the MG fiamme is more resorbed (Section 3.5). The MG fiamme also have interlocking growth textures between alkali feldspar and plagioclase grains (Section 3.5). Biotite in the MG fiamme is less abundant (<0.5%) than in the VCCR fiamme (Section 3.2). Lastly, the only occurrence of the accessory mineral xenotime was in the MG fiamma, ORA-2A-031 (Section 3.2).

The MG fiamme have homogeneous, high-silica rhyolite glass that ranges from 76-78 wt. % SiO₂ (Section 3.7). The MG glass is slightly more variable than the VCCR high-silica rhyolite glass and has less K₂O (2-3 wt. % (MG) vs. 3-3.5 wt. % (VCCR)) (Section 3.8). Plagioclase in the MG fiamme is more Ab-rich than the VCCR fiamme (Section 3.5). Unique to the MG fiamme are plagioclase crystals with An-rich cores (Section 3.5).

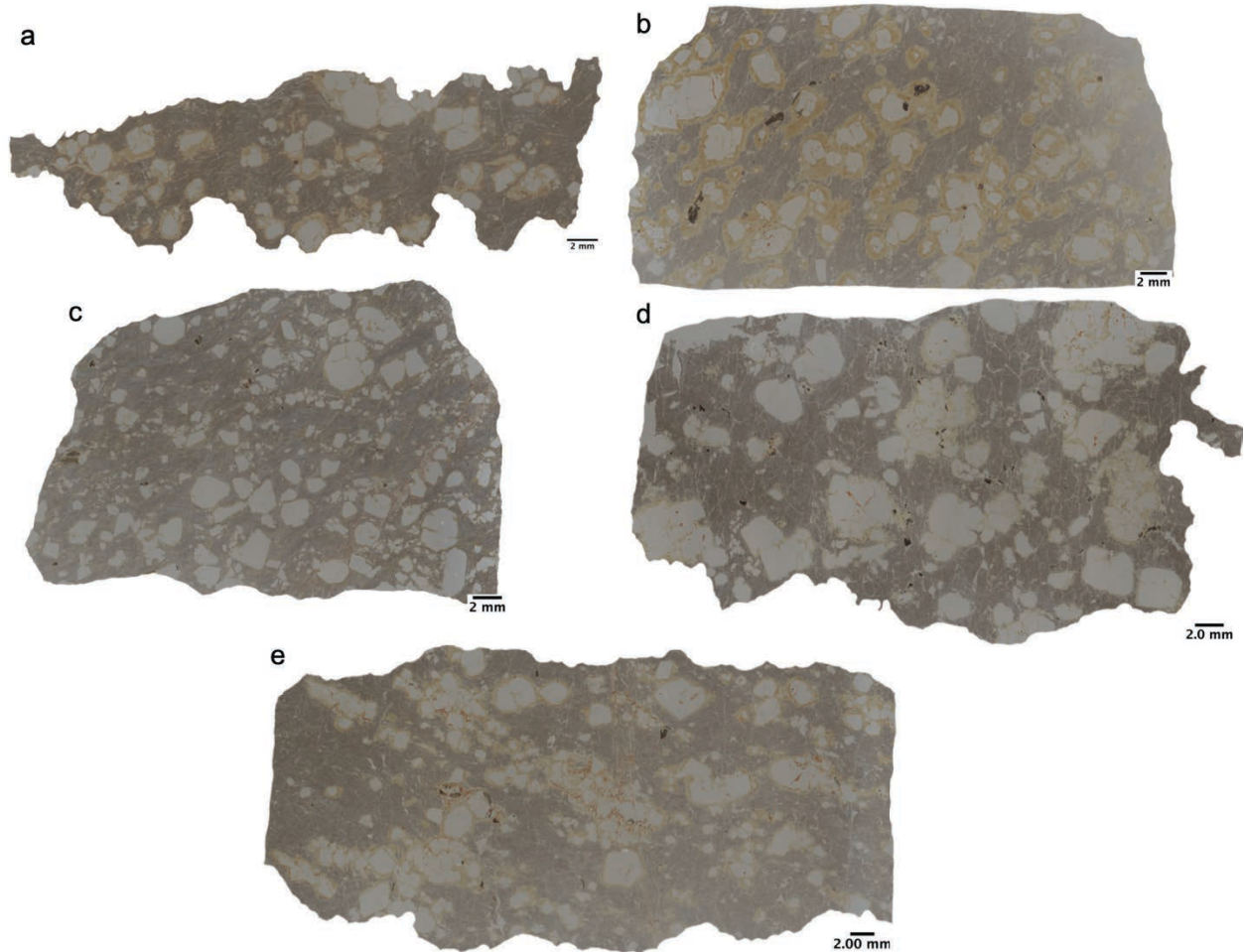


Figure 13: MG fiamme (A) ORA-2A-001 (B) ORA-2A-031 (C) ORA-2A-035 (D) ORA-2A-032 (E) ORA-2A-040. Note the (1) intermediate crystal content (20-40%), (2) intermediate crystal sizes (1-3 mm), and (3) clumped crystals (rimmed in orange, devitrified glass in all but ORA-2A-035).

3.4.2 Fine-Grained Crystal-Poor (FGCP) Fiamme:

The FGCP fiamme can be differentiated in hand sample based on their (1) crystal-poor (<10%) texture and (2) small (<1 mm) crystal sizes (Fig. 14). In thin section, quartz and feldspars are anhedral and fractured (Appendix B). Biotite is rare (<0.15%) (Table 4). Unique to the FGCP fiamme is the mineral fayalite (Section 3.2). In ORA-2A-024 and ORA-2A-003 there are multiple fayalite grains undergoing differential amounts of OPX replacement (Section 3.5). Another

characteristic of this subtype is the presence of multiple glass types in a single fiamma (Section 3.7). In ORA-2A-002, ORA-2A-016, and ORA-2A-024, these glass types can be distinguished texturally (Appendix C).

Geochemically, the FGCP fiamme have the most variable glass compositions (Section 3.8). The FGCP fiamme glass ranges from 64-80 wt. % SiO₂ (Section 3.7). Glass from ORA-2A-016 has the lowest K₂O concentration (0.5 wt. %); overall the FGCP fiamme glass has K₂O concentrations from 0.5-3.5 wt. %. Like the MG fiamme, the FGCP fiamme has very Ab-rich plagioclase (Section 3.5). Lastly, the FGCP biotite has less iron than biotite from the intracaldera fiamme (Section 3.5).

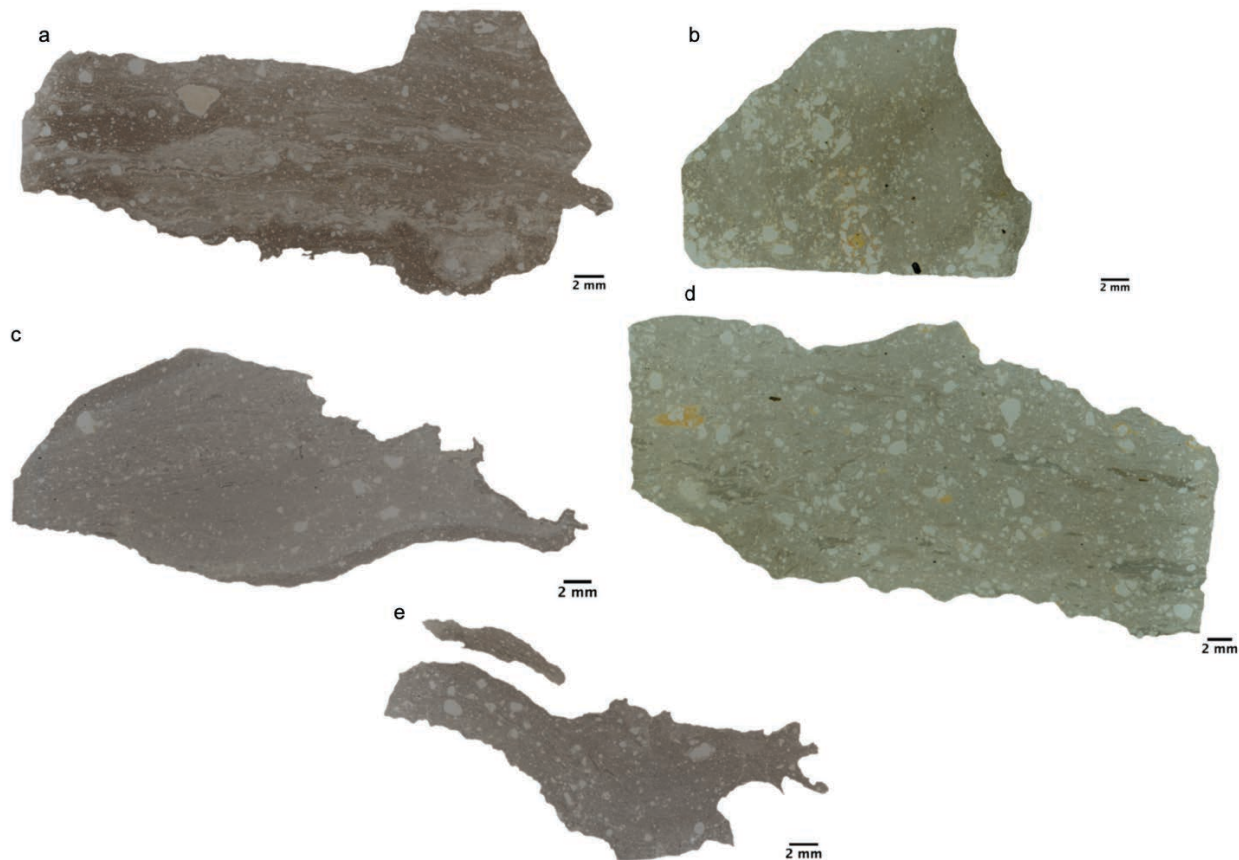


Figure 14: FGCP fiamme (A) ORA-2A-002 (B) ORA-2A-024 (C) ORA-2A-023 (D) ORA-2A-016 (E) ORA-2A-003. Note the (1) crystal-poor texture (<10%) and (2) small (<1 mm) crystal sizes.

3.5 Mineralogy

This section includes both mineral textures and mineral major element compositions.

Table 7 shows the minerals that are present in each fiamma. The major mineral phases are presented along with multiple photographs detailing their textures. Differences between the fiamma subtypes are emphasized. Supplemental images of various minerals and their textures are provided in Appendix B.

Table 7: The minerals present in each of the samples collected for this study. The abbreviations used are QZ = quartz, AFS = alkali feldspar, PLAG = plagioclase, BT = biotite, FAY = fayalite, OPX = orthopyroxene, ZR = zircon, AP = apatite, MNZ = monazite, XNT = xenotime.

SAMPLE	TYPE	LOCATION	QZ	AFS	PLAG	BT	FAY	OPX	ZR	AP	MNZ	XNT
ORA-5B-402	VCCR	Intracaldera	x	x	x	x			x	x	x	
ORA-5B-404A	VCCR	Intracaldera	x	x	x	x			x	x	x	
ORA-5B-404B	VCCR	Intracaldera	x	x	x	x			x	x	x	
ORA-5B-412A	FG	Intracaldera	x	x	x	x						
ORA-5B-412B	FG	Intracaldera	x	x	x	x						
ORA-5B-414	FG	Intracaldera	x	x	x	x					x	
ORA-2A-001	MG	Outflow	x	x			x					
ORA-2A-031	MG	Outflow	x	x	x	x			x	x	x	x
ORA-2A-032	MG	Outflow	x	x	x	x			x	x		
ORA-2A-035	MG	Outflow	x	x	x	x			x	x	x	
ORA-2A-040	MG	Outflow	x	x	x	x			x	x	x	
ORA-2A-002	FGCP	Outflow	x	x	x	x			x	x		
ORA-2A-016	FGCP	Outflow	x	x	x	x						
ORA-2A-023	FGCP	Outflow	x	x	x	x						
ORA-2A-003	FGCP	Outflow	x	x	x	x	x	x	x	x	x	
ORA-2A-024	FGCP	Outflow	x	x	x	x	x	x				x

3.5.1 Quartz

Quartz is present as 1-3 mm crystals in both the VCCR and MG fiamme. In the VCCR fiamme, the quartz is often found clumped with other quartz grains (Fig. 15). Melt inclusions are present in both the MG and VCCR fiamme, but they have been completely crystallized. Fractures often emanate from the melt inclusions, resulting in broken grains. Both the VCCR and MG quartz grains exhibit dissolution textures (Fig. 15, 16). However, quartz in the MG fiamme appears to be more resorbed than quartz from the VCCR fiamme (Fig. 16). In the FG and FGCP fiamme, the quartz grains are small (<1 mm) and anhedral. Photos of quartz from the FG and FGCP fiamme are located in Appendix B

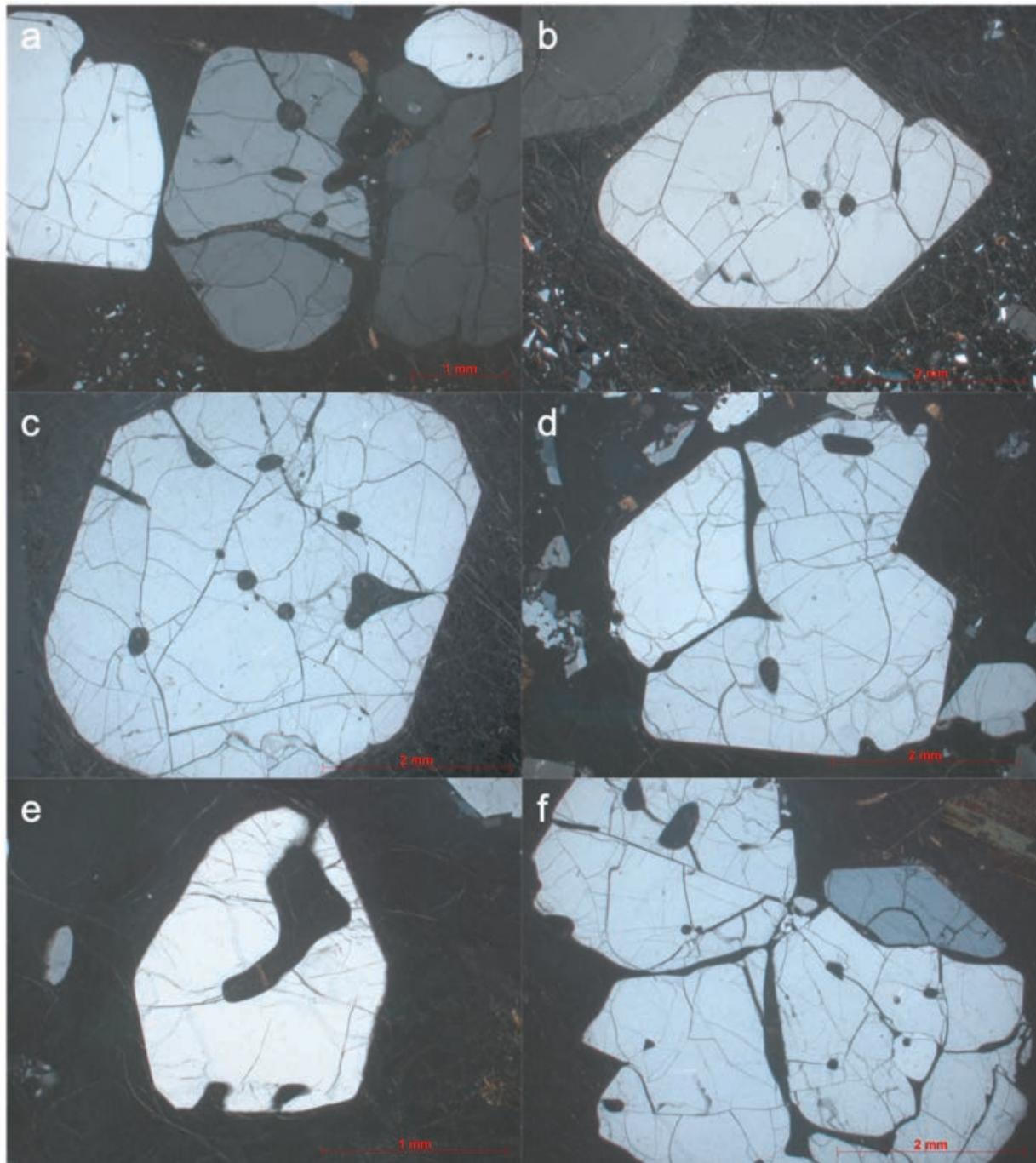


Figure 15: Quartz grains from VCCR fiamme exhibiting resorption textures in XPL. (A-C) ORA-5B-402. (D-E) ORA-5B-404A. (F) ORA-5B-404B. Note the presence of multiple quartz grains in close contact (a, f). Also, the resorbed grains in b and c appear to have once been euhedral.

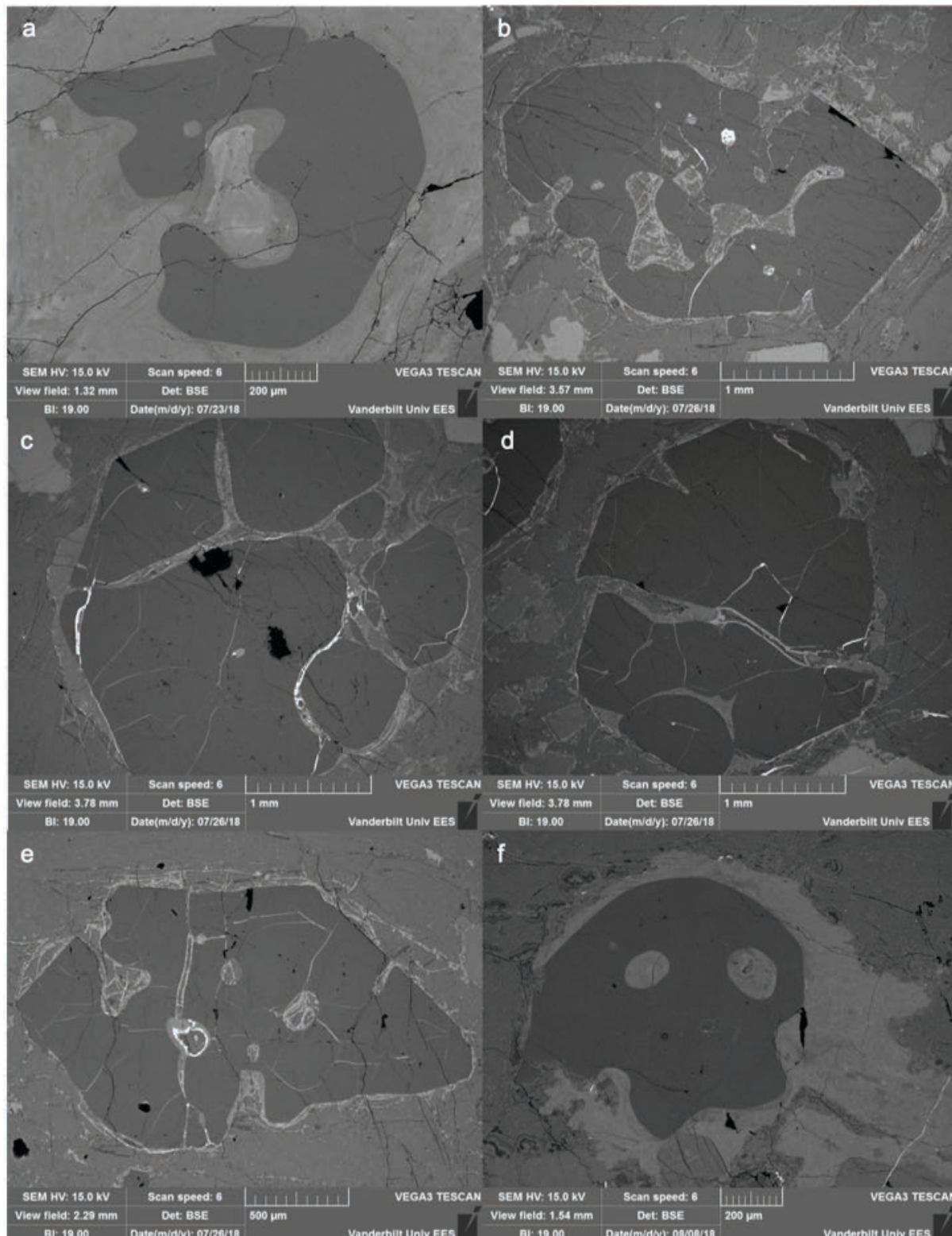


Figure 16: BSE images of quartz grains from MG fiamme exhibiting resorption textures (A) ORA-2A-031A. (B-E) ORA-2A-035. (F) ORA-2A-040. Note how these grains appear to be more resorbed than quartz from the VCCR fiamme.

3.5.2 Alkali Feldspar

Alkali feldspar in the VCCR fiamme is present as 0.5-5 mm grains. In the MG fiamme, alkali feldspar is smaller and its size ranges from 1-3 mm. Fractured alkali feldspar grains are found in both the VCCR and MG fiamme (Appendix B). In the VCCR and MG fiamme many alkali feldspar grains exhibit interlocking growth textures with plagioclase (Fig. 17, 18). More photographs of these textures are located in Appendix B. Unique to the MG fiamme are clumped glomerocrysts of fractured alkali feldspar grains and they are rimmed in orange, devitrified glass (Fig. 19).

In the FG and FGCP fiamme, alkali feldspar is fractured and <1 mm (Appendix B). In one FGCP fiamma, ORA-2A-002, there is a large (>1 mm) altered alkali feldspar (Fig. 20). In back-scattered images, this altered feldspar is surrounded by a lighter colored material. This material has the composition of a feldspar, but it is very potassium-rich (Or ~95-100). This same material is surrounding the smaller alkali feldspar in figure 20. The elemental compositions of all the alkali feldspar range from Or 50-Or 75 (Fig. 21). All of the normalized alkali feldspar compositions are located in Appendix F.

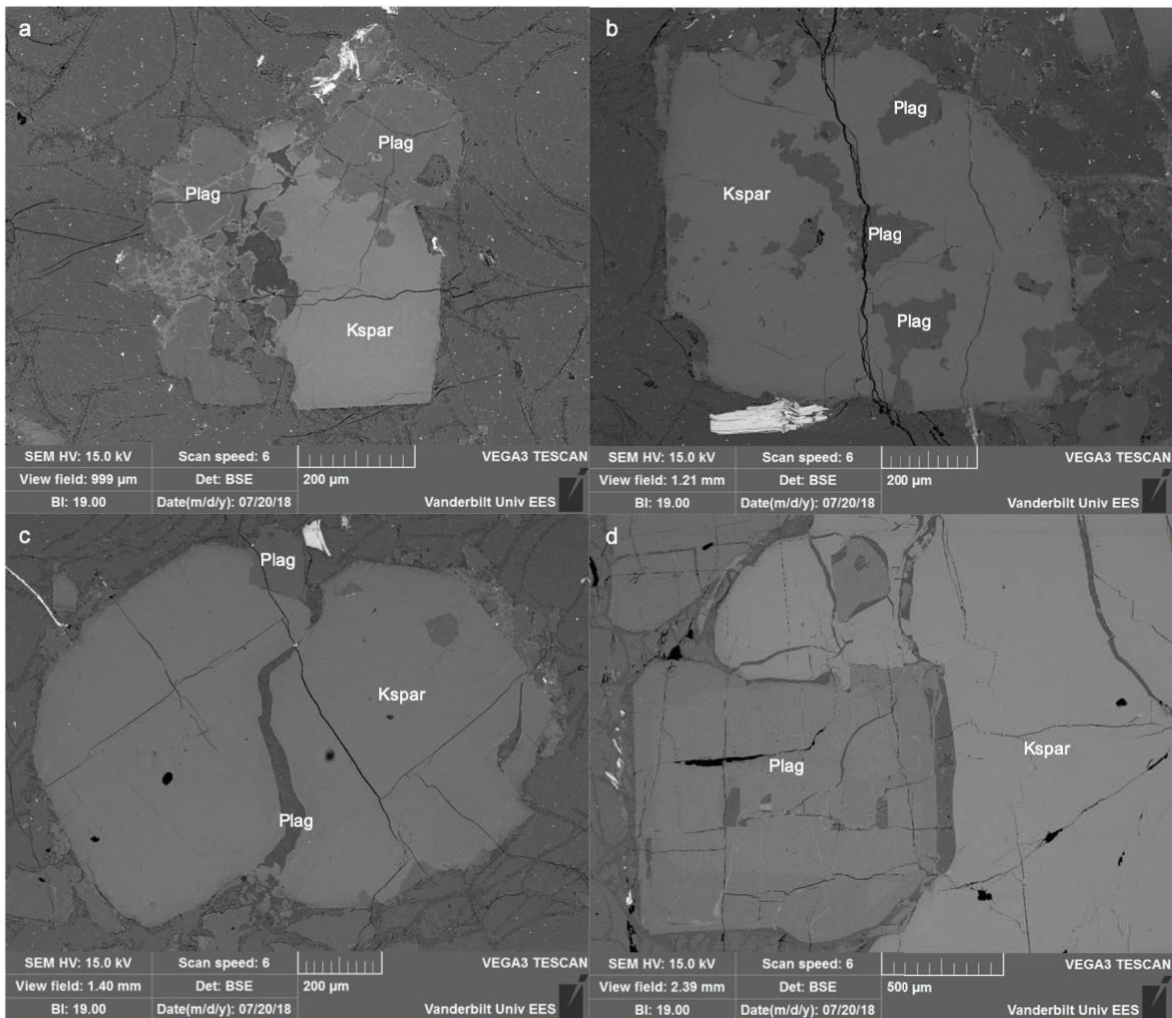


Figure 17: BSE images of alkali feldspar in VCCR fiamma showing an interlocking growth texture with plagioclase. (A-C) ORA-5B-404A. (D) ORA-5B-404B.

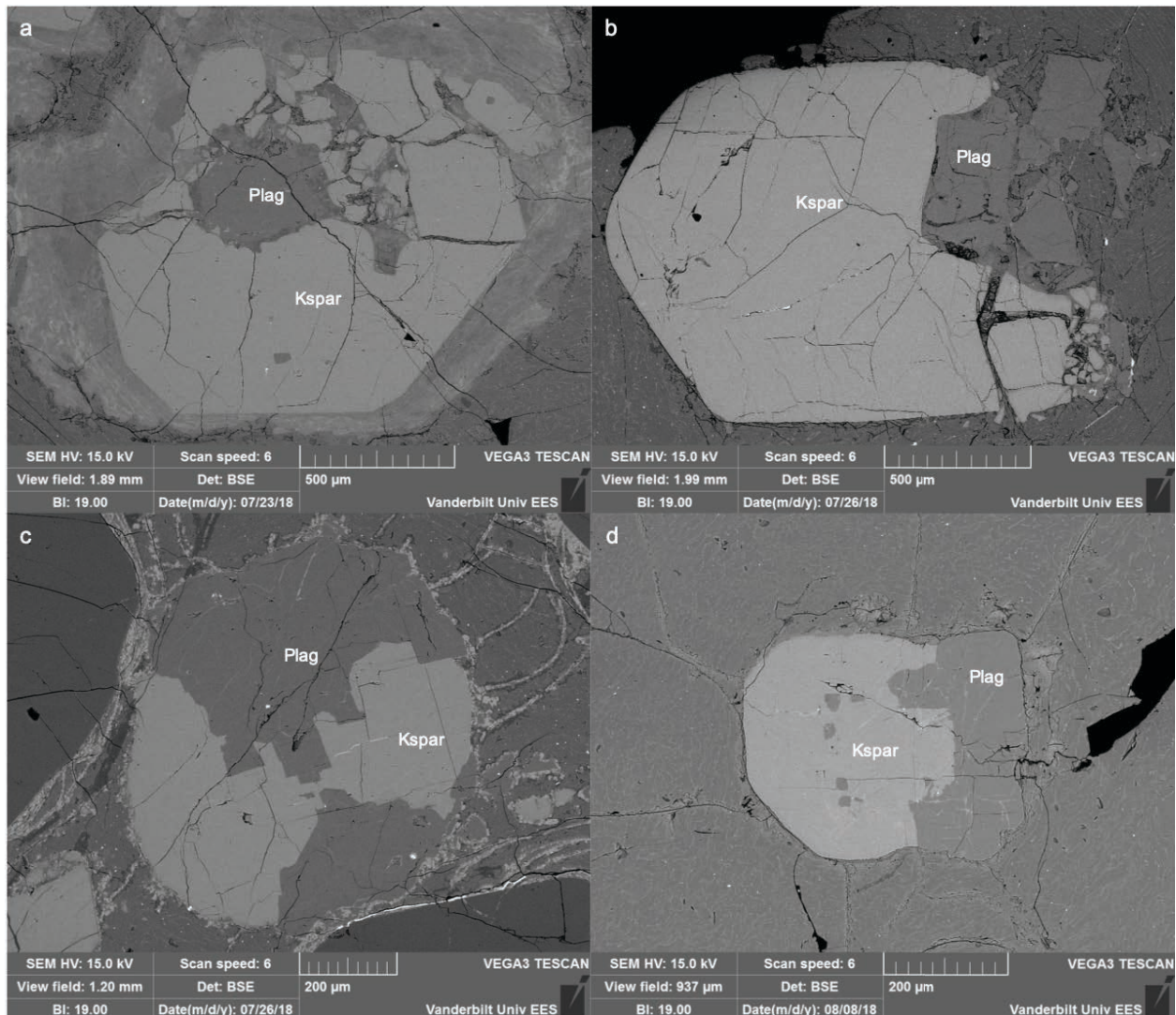


Figure 18: BSE images of alkali feldspar exhibiting an interlocking growth texture with plagioclase in MG fiamme. (A) ORA-2A-031. (B) ORA-2A-032. (C) ORA-2A-035. (D) ORA-2A-040.

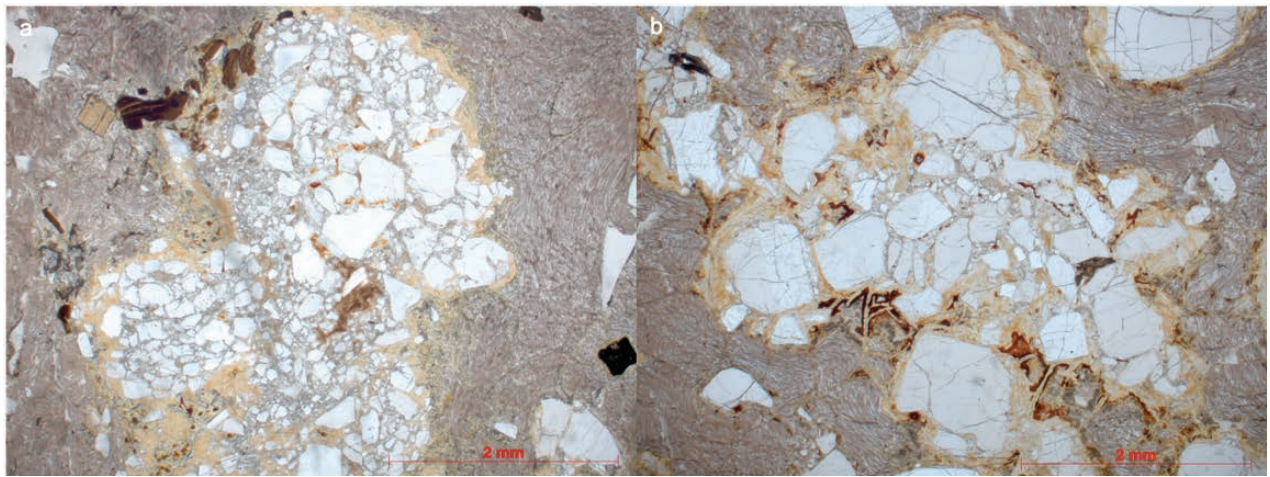


Figure 19: PPL images of highly-fractured alkali feldspar glomerocrysts rimmed in orange, devitrified glass. These are from MG fiamme. (A) ORA-2A-032 (B) ORA-2A-040.

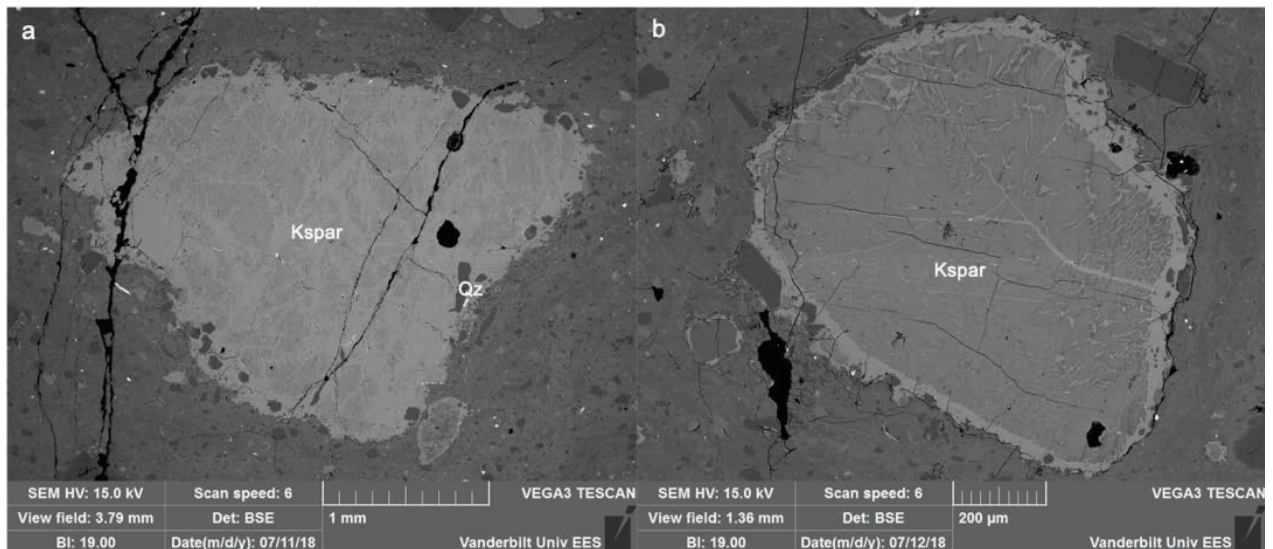


Figure 20: BSE images of alkali feldspar showing varying degrees of alteration in the FGCP fiamme, ORA-2A-002. Note the lighter colored material that is present in both grains. This material has a feldspar composition of Or ~95-100.

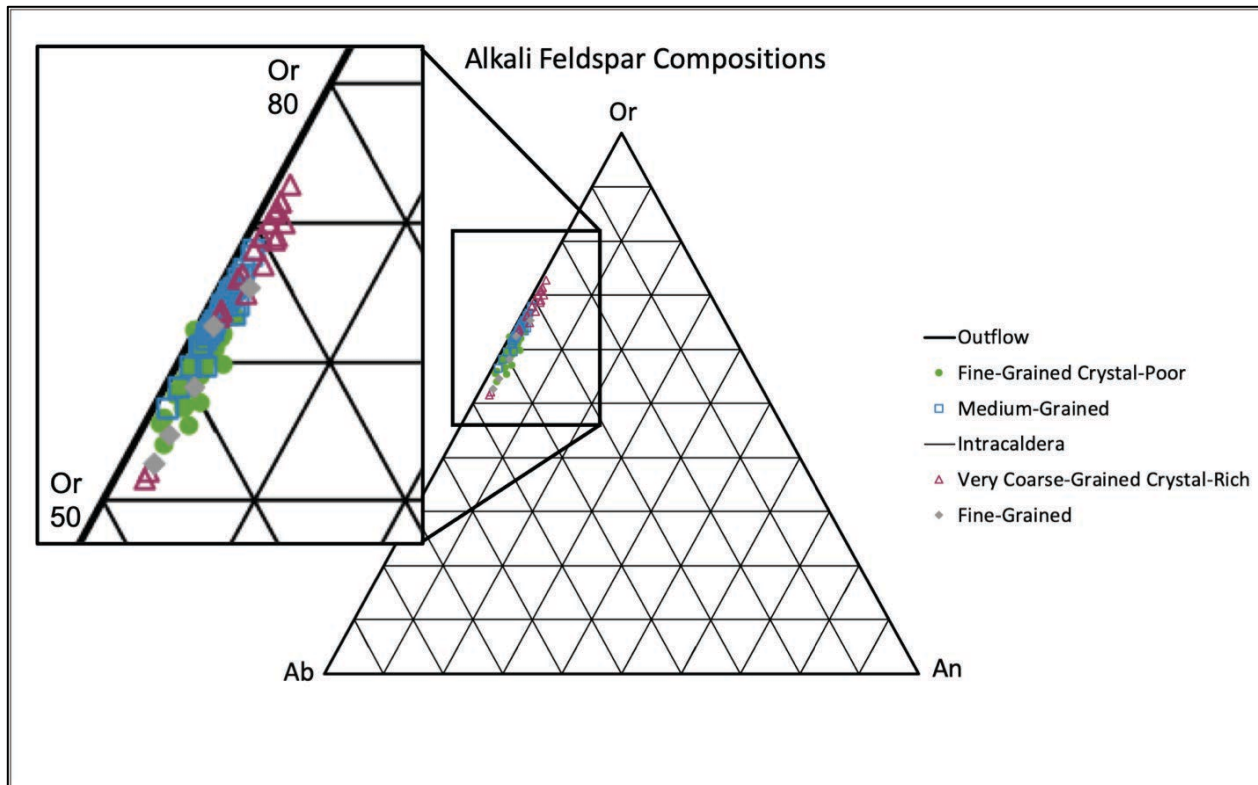


Figure 21: Ternary diagram of alkali feldspar compositions. The symbology is based on fiamma type. Note how all of the alkali feldspar compositions cluster between Or 50-Or 75.

3.5.3 Plagioclase

Plagioclase in the VCCR fiamme is present as 0.5-10 mm grains. In the MG fiamme, plagioclase is smaller and its size ranges from 1-3 mm. ORA-2A-001 (MG) is the only fiamma in this study that doesn't have plagioclase. Fractured plagioclase is found in both the VCCR and MG fiamme (Fig. 22 & 23; Appendix B). In the VCCR fiamme, only ORA-5B-402 has sieve textured plagioclase (Fig. 22). In the MG fiamme, there was only one sieve textured plagioclase found (Appendix B). As mentioned in the previous section, plagioclase exhibits an interlocking growth texture with alkali feldspar. The sieve textured plagioclase in ORA-5B-402 appears to have grown interlockingly with alkali feldspar (Fig. 22a, c). Unique to the MG fiamme is the presence of An-rich plagioclase cores (Fig. 23). Sometimes the plagioclase crystals with An-rich

cores are rimmed in the orange, devitrified glass that is found in ORA-2A-001, ORA-2A-031, and ORA-2A-040 (Fig. 23c,d). In ORA-2A-032, one plagioclase crystal was found with zircon, ilmenite, and apatite inclusions (Fig. 23a).

In the FG and FGCP fiamme, plagioclase is small (<1 mm), fractured, and anhedral (Appendix B). Plagioclase is found as microlites only in the FGCP fiamme. Compositinally, the VCCR plagioclase cluster around An20-An30 whereas the MG plagioclase cluster around An10-An20 (Fig. 24). Both the FGCP and FG fiamme contain plagioclase with a variety of compositions. All of the normalized plagioclase compositions are found in Appendix G.

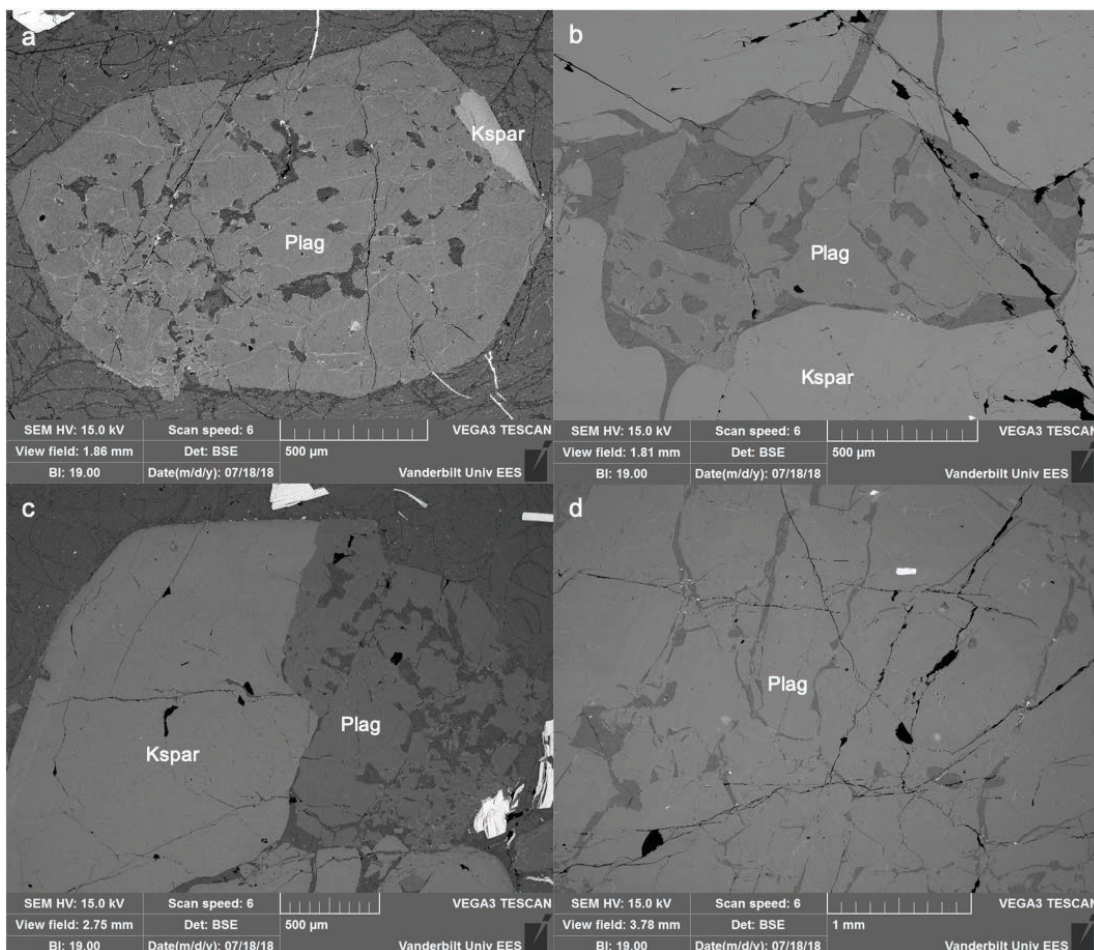


Figure 22: BSE images of sieve textured plagioclase in the VCCR fiamme, ORA-5B-402. Note the interlocking growth texture between plagioclase and alkali feldspar in a and c.

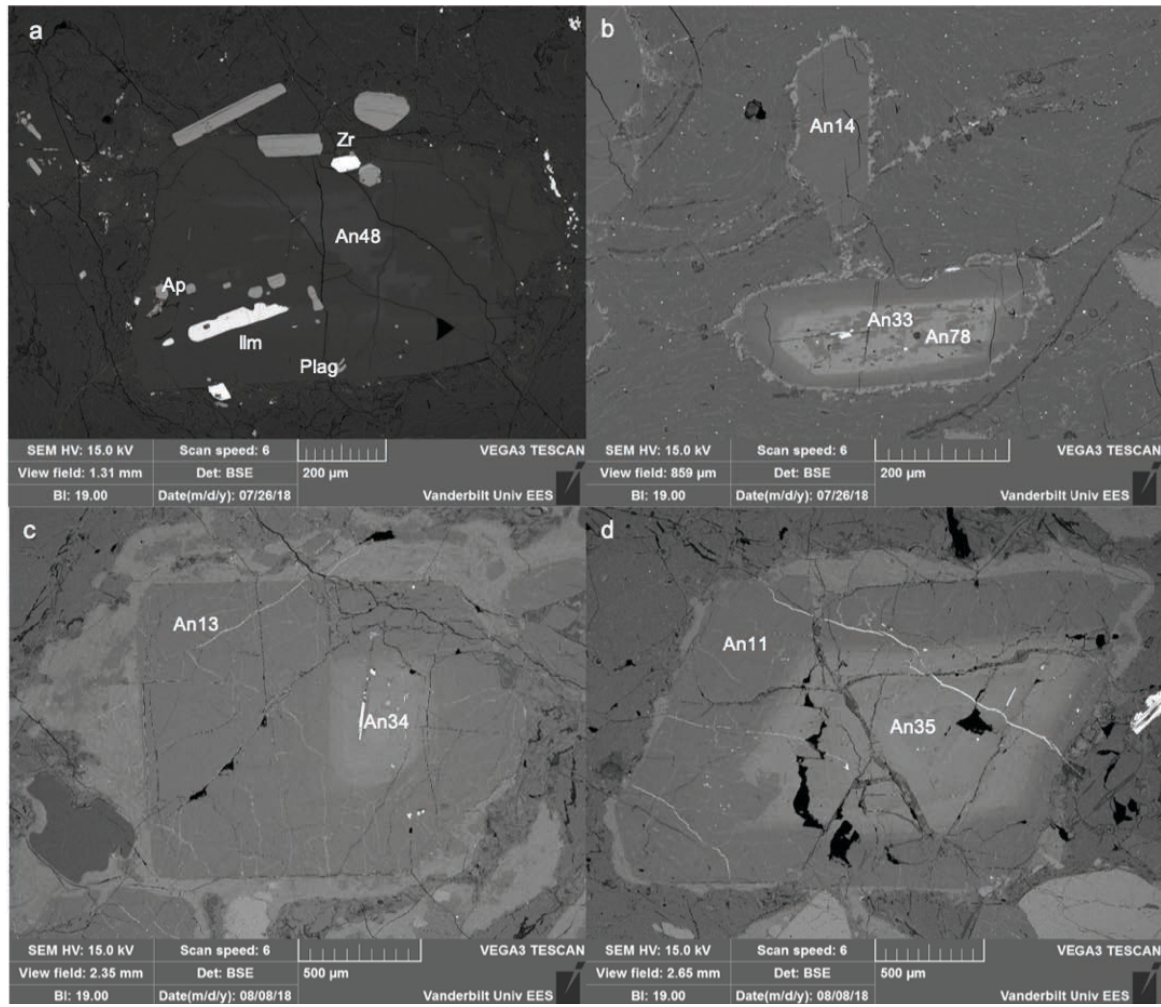


Figure 23: BSE images of plagioclase with An-rich cores in MG fiamme. (A) The plagioclase in ORA-2A-032 has ilmenite, zircon, and apatite inclusions. (B) The plagioclase in ORA-2A-035 has a core with a composition of An33. Also, the highest An content is found here (An78). (C-D) The plagioclase in ORA-2A-040 is fractured and rimmed in a lighter colored material.

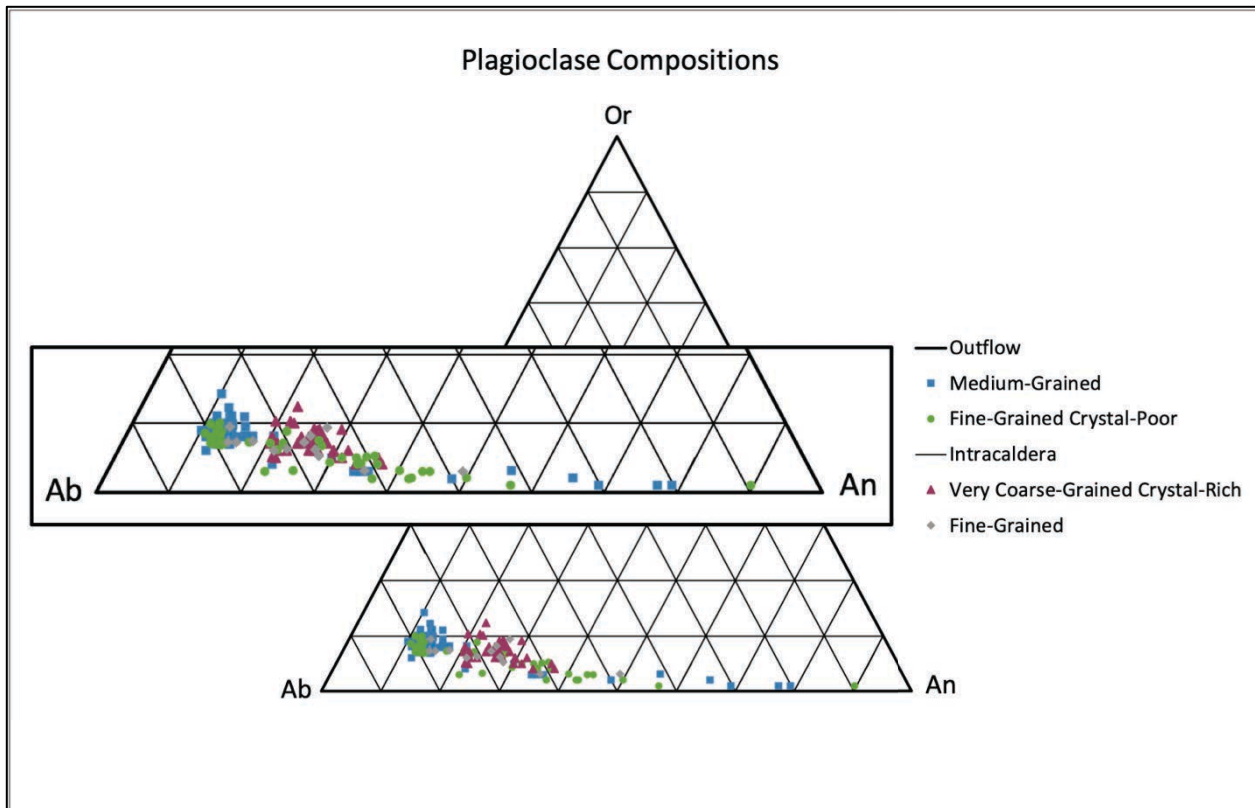


Figure 24: Ternary diagram of plagioclase compositions. The symbology is based upon fiamme type. Note that the MG and FGCP fiamme have the most Ab-rich plagioclase compared to the VCCR fiamme. Also note the An-rich plagioclase present in the MG and FGCP fiamme.

3.5.4 Biotite

Biotite in the VCCR fiamme is present as 0.5-1.5 mm crystals. In the MG fiamme, biotite is present as 0.5-2 mm grains. Biotite is irregular and bent in both the VCCR and MG fiamme. Unique to the VCCR biotite is the presence of dissolution textures (Fig. 25d). In both VCCR and MG biotite are small (<0.1 mm) accessory mineral inclusions of zircon, monazite, and apatite (Fig. 25 & 26). Compared to the other fiamme types, the VCCR fiamme have the highest biotite content, ranging from 2-3% (Table 4). Biotite in the MG fiamme is less abundant and makes up <0.5% of the crystal content (Table 4).

Biotite is rare in both the FG and FGCP fiamme and occurs as small (<0.1 mm), thin, elongated grains (Appendix B). There are no accessory minerals found in biotite from the FG and FGCP fiamme. Compositinally, biotite from the outflow has more iron than biotite from the intracaldera (Fig. 27). Most of the MG biotite clusters in the same region, except that the biotite from ORA-2A-032 contains more Ti (Fig. 27). The FGCP biotite was limited to one sample, ORA-2A-023, because of the lack of biotite available for analysis. Similarly, the FG biotite was limited to one sample, ORA-5B-414. The VCCR biotite tends to cluster in the same region and has more Ti than most of the outflow biotite, but less Fe (Fig. 27). All TiO_2 compositions and Mg#'s for biotite are located in Appendix H.

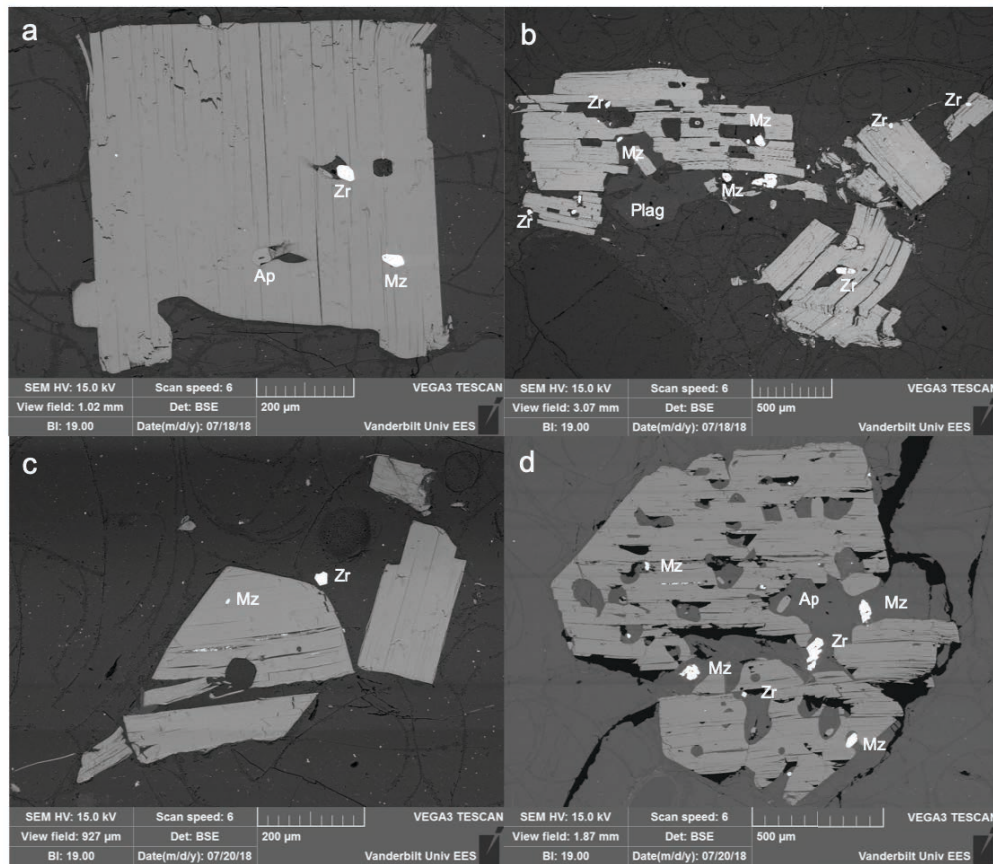


Figure 25: BSE images of biotite in the VCCR fiamme and its inclusions of zircon, monazite, and apatite. (A-B) ORA-5B-402. (C) ORA-5B-404A. (D) ORA-5B-404B. Note the dissolution present.

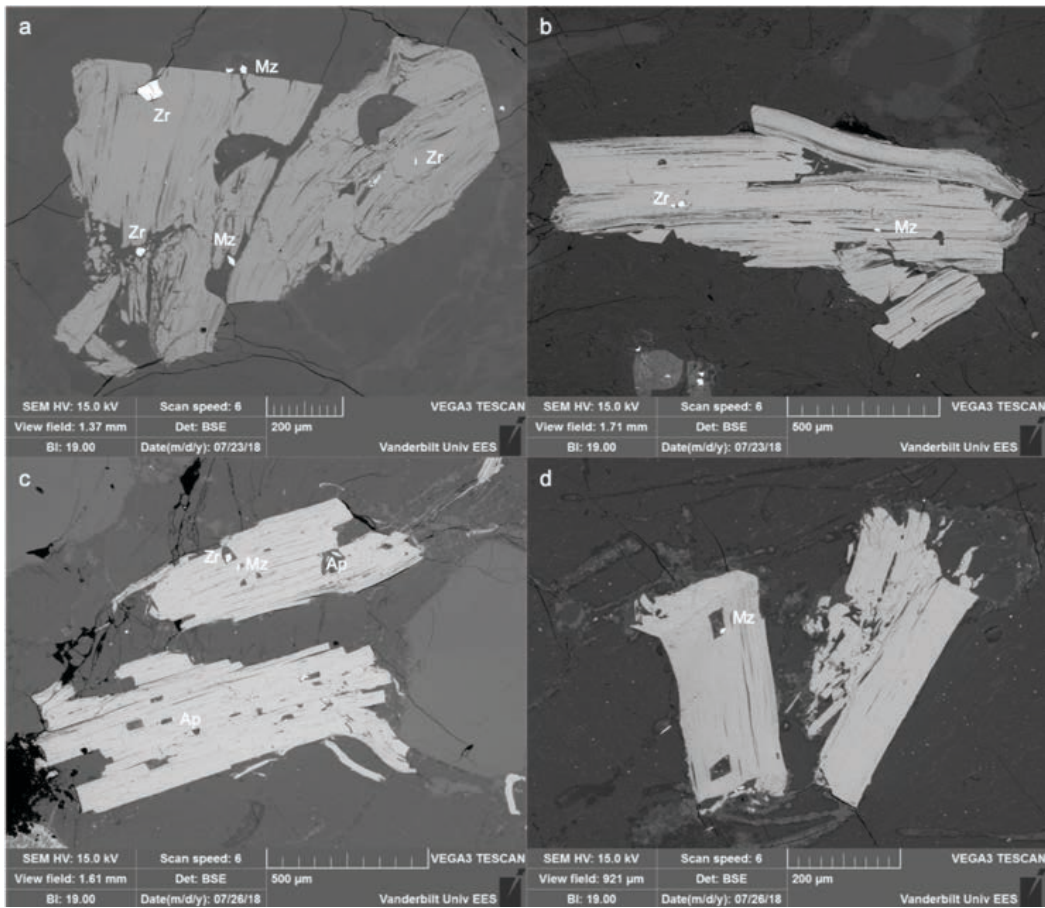


Figure 26: BSE images of biotite in the MG fiamme and its inclusions of zircon, monazite, and apatite. (A-B) ORA-2A-031 (C-D) ORA-2A-035.

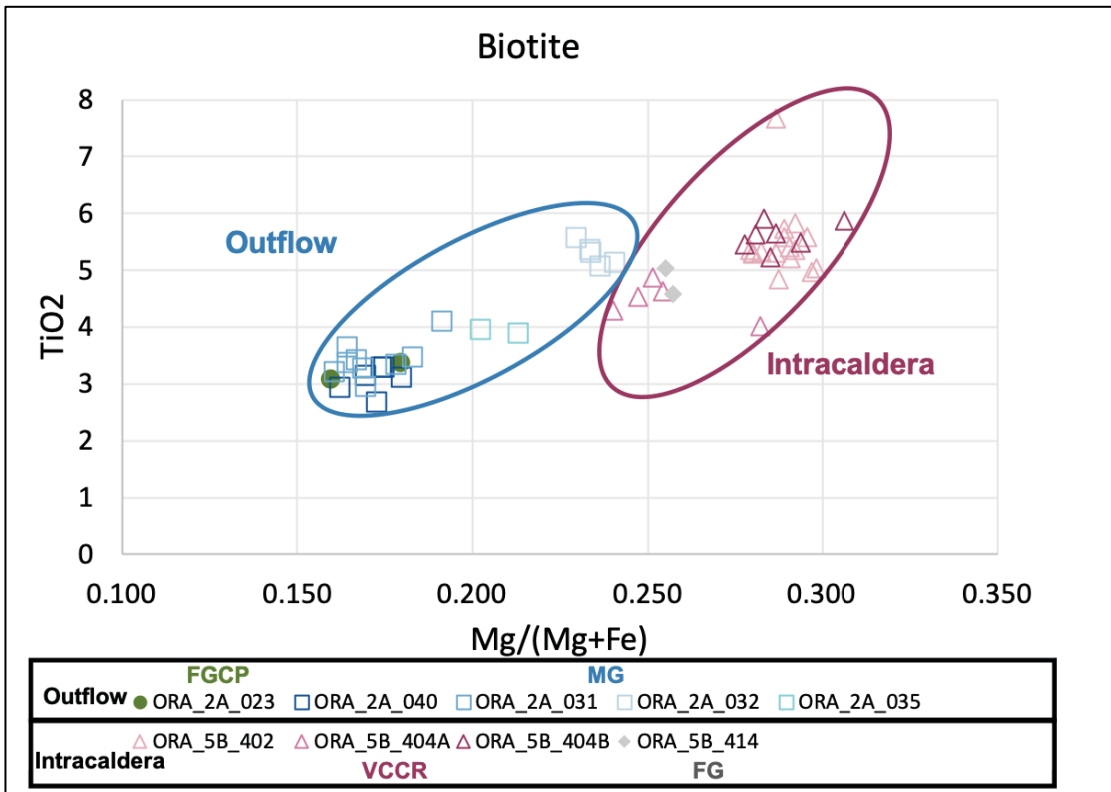


Figure 27: TiO₂ vs. Mg# for biotite in the Ora Ignimbrite. Mg# = Mg/(Mg + Fe). The biotite encircled in blue are from the outflow (Ora 2) and the biotite within the pink ellipsis are from the intracaldera deposit (Ora 5). Note that biotite from the late-erupted outflow is more enriched in iron than the early-erupted intracaldera biotite.

3.5.5 Fayalite and Orthopyroxene

Multiple fayalite grains are found in two FGCP fiamme: ORA-2A-024 and ORA-2A-003.

Each grain exhibits varying degrees of OPX replacement (Fig. 28). These grains are all anhedral and <1 mm. Geochemically, fayalite is the iron-rich endmember of olivine. Accordingly, all of the fayalite compositions lie within Fa88-Fa98 (Fig. 29). The OPX replacing fayalite is an iron-rich orthopyroxene, ferrosilite. The orthopyroxene compositions are within Fs93-Fs96 (Fig. 29).

All normalized fayalite compositions are located in Appendix I. All normalized OPX compositions are located in Appendix J.

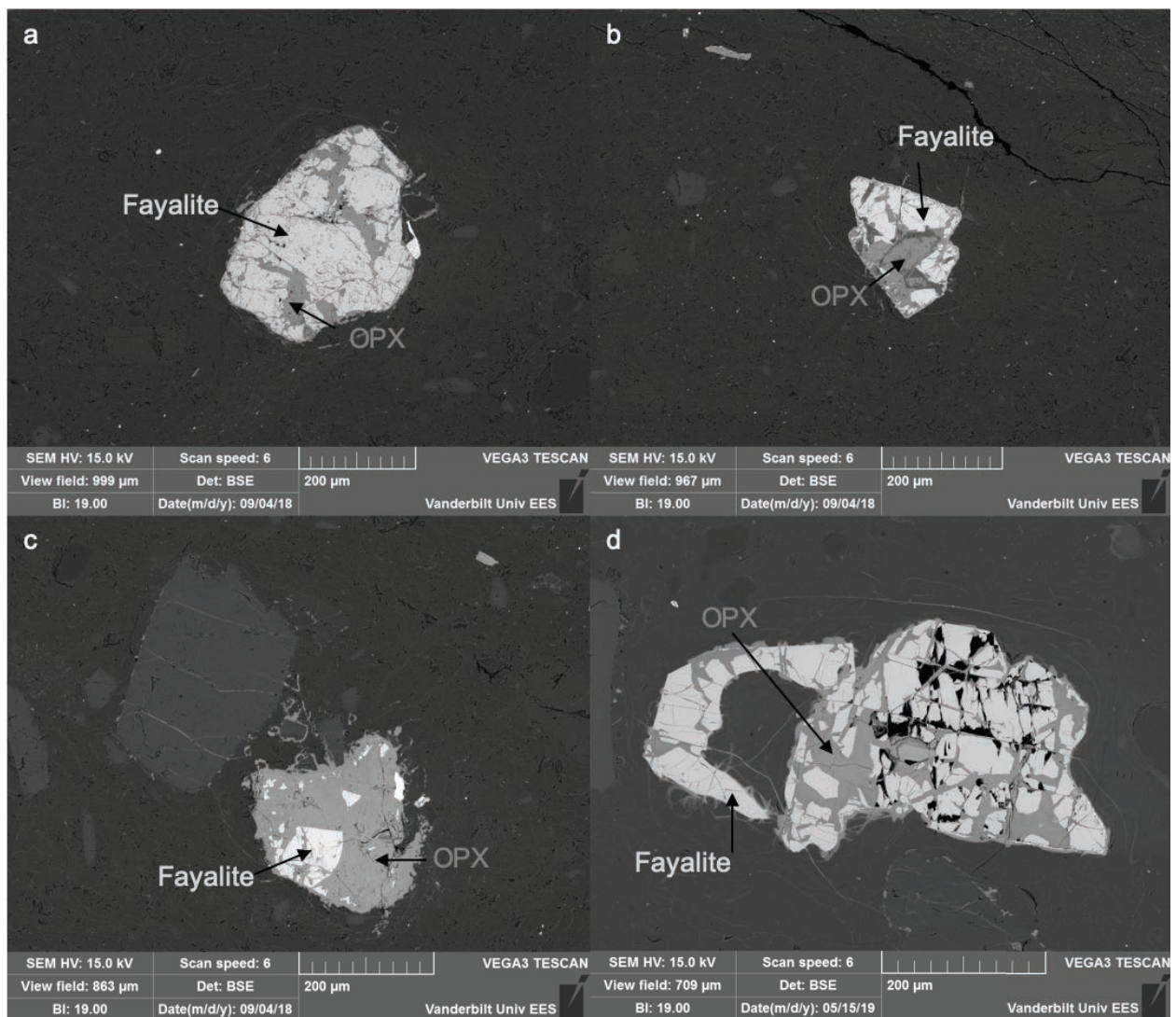


Figure 28: BSE images of fayalite in FGCP fiamme undergoing varying degrees of orthopyroxene replacement. (A-C) ORA-2A-024. (D) ORA-2A-003. Note the irregular shape of the grains.

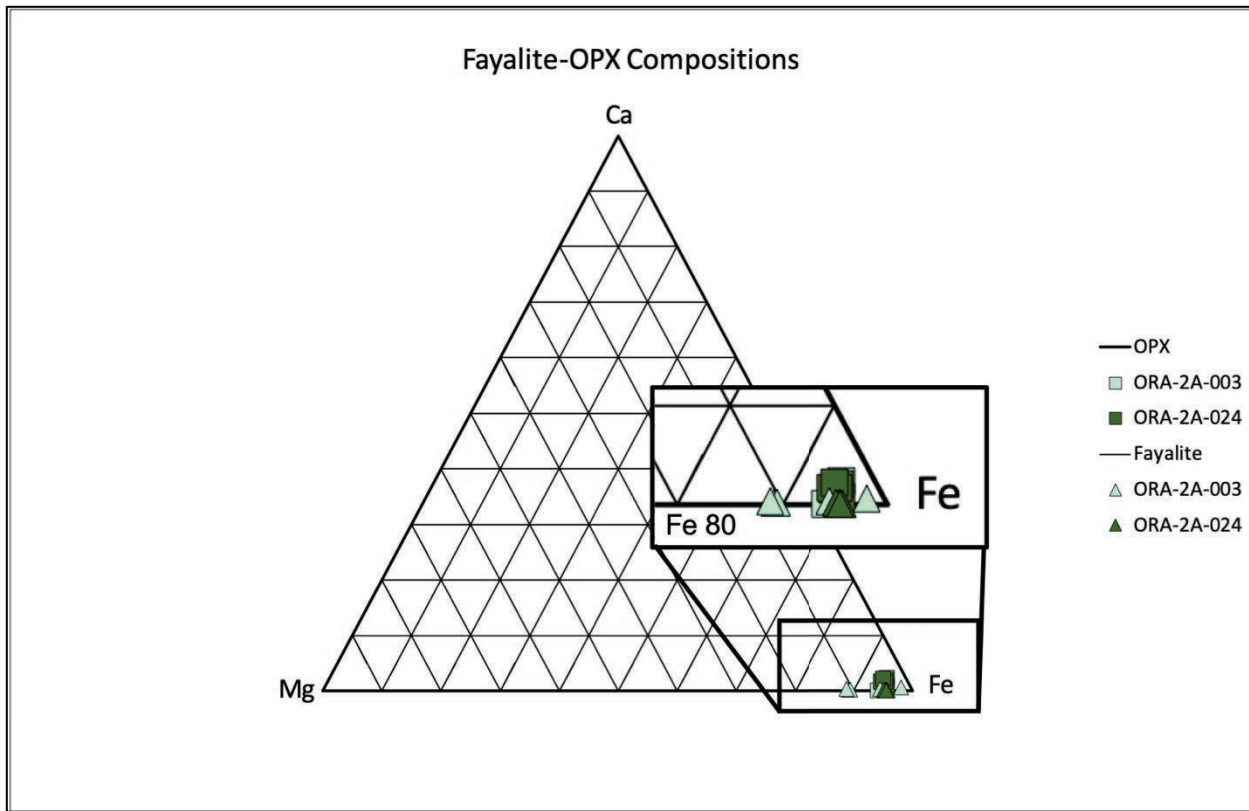


Figure 29: Ternary diagram of fayalite and orthopyroxene compositions. The fayalite compositions lie within Fa88-Fa98 while the orthopyroxene compositions lie within Fs93-Fs96.

3.5.6 Accessory Minerals

The accessory minerals in the VCCR fiamme are most often found as inclusions in biotite (Fig. 25). Monazite, zircon, and apatite are found as small (<0.1 mm) subhedral grains. Figure 30 shows a biotite glomerocryst with associated zircon, monazite, and apatite. This was the only instance of accessories found where they were not inclusions in biotite.

In the MG fiamme, the accessory minerals are all <0.1 mm and are found as either mineral inclusions in biotite or in the fiamme groundmass. Monazite, apatite, and zircon are the most common accessory phases, but xenotime was observed in one sample, ORA-2A-031. Ilmenite was found in only one fiamma as an inclusion in plagioclase (Fig. 23a).

The accessory minerals in the FGCP fiamme are zircon, apatite, and monazite. They are all small, <0.5 mm, and euhedral to subhedral (Fig. 32). Magnetite was only found in ORA-2A-003 (Fig. 33). Lastly, only one accessory mineral – a small (<0.05 mm) apatite – was found in the FG fiamme (Appendix B).

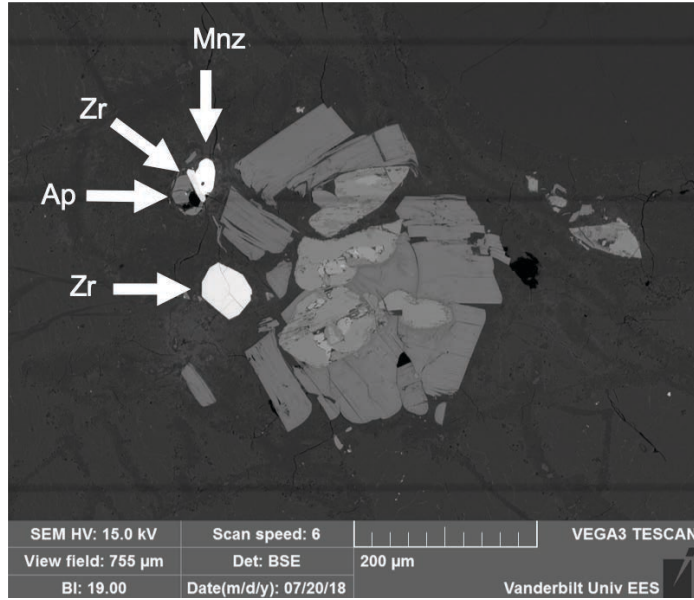


Figure 30: A BSE image of a biotite glomerocryst with zircon, monazite, and apatite accessory minerals in a VCCR fiamma.

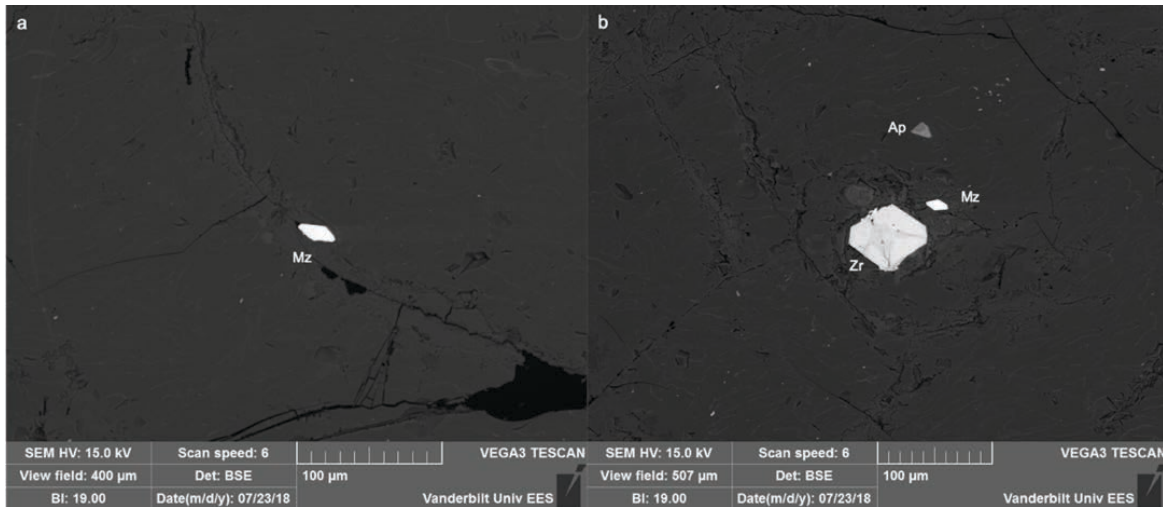


Figure 31: Monazite, zircon, and apatite present in the MG fiamma groundmass of ORA-2A-031.

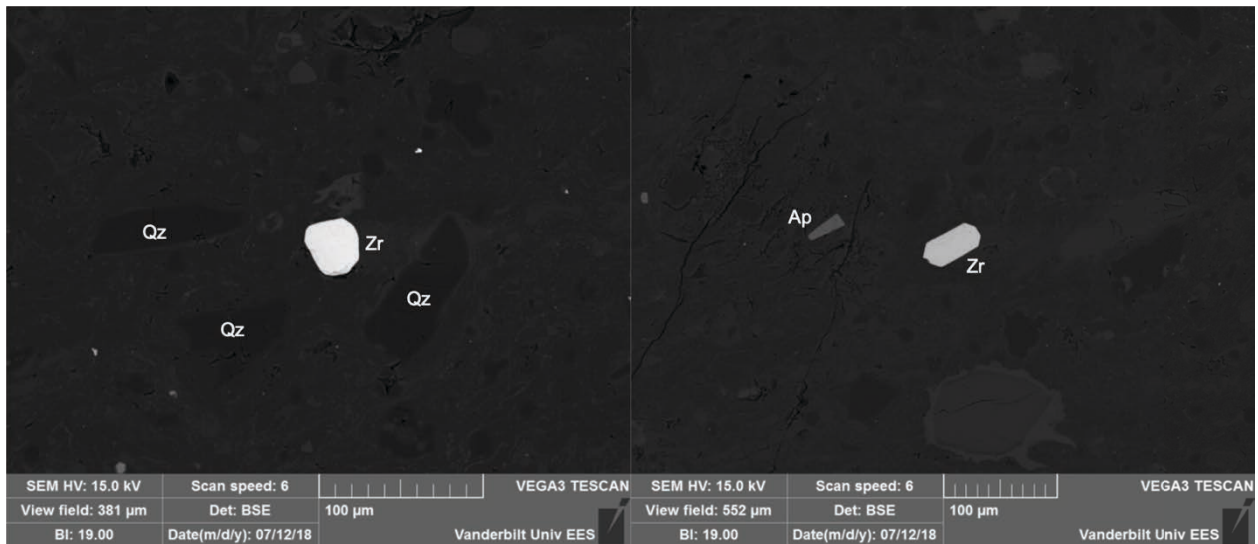


Figure 32: BSE images of accessory minerals in a FGCP fiamma. (A) Zircon in ORA-2A-002. (B) A euhedral zircon and apatite in ORA-2A-002.

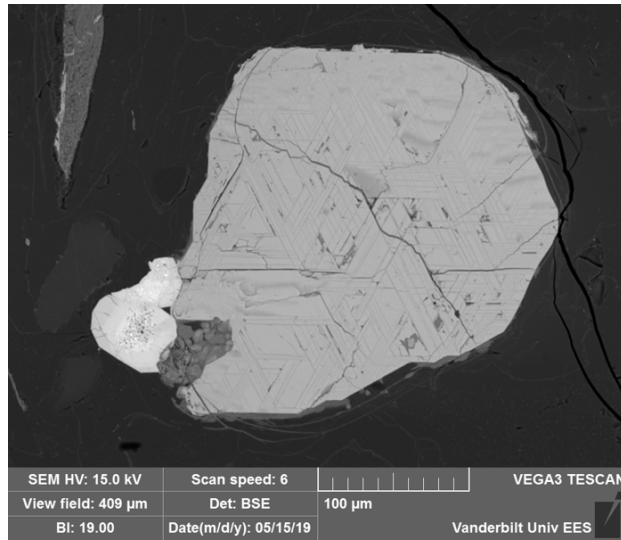


Figure 33: BSE image of magnetite in ORA-2A-003. This magnetite is exsolving ilmenite, forming lines that intersect at 60° and 120°. A zircon is attached to bottom left of the magnetite along with a cluster of apatite grains.

3.6 Intracaldera Glass Textures and Major Element Compositions

This section describes the fiamme glass textures and major element compositions of the intracaldera fiamme. All glass major element data collected from SEM-EDS analysis are included in Appendix E.

3.6.1 Very Coarse-Grained Crystal-Rich (VCCR) Fiamme

The VCCR fiamme glass has perlitic fractures (Fig. 34). The fiamme glass major element compositions are the most homogeneous of all the glass analyzed in this study. The silica content clusters from 76.5-77.5 wt. % SiO₂ and the potassium ranges from 3-3.5 wt. % K₂O (Fig. 35). The only noticeable variation is that ORA-5B-402 has less Na₂O (4.25 wt. %) than the other two samples (4.75 wt. %) and it is slightly more enriched in CaO.

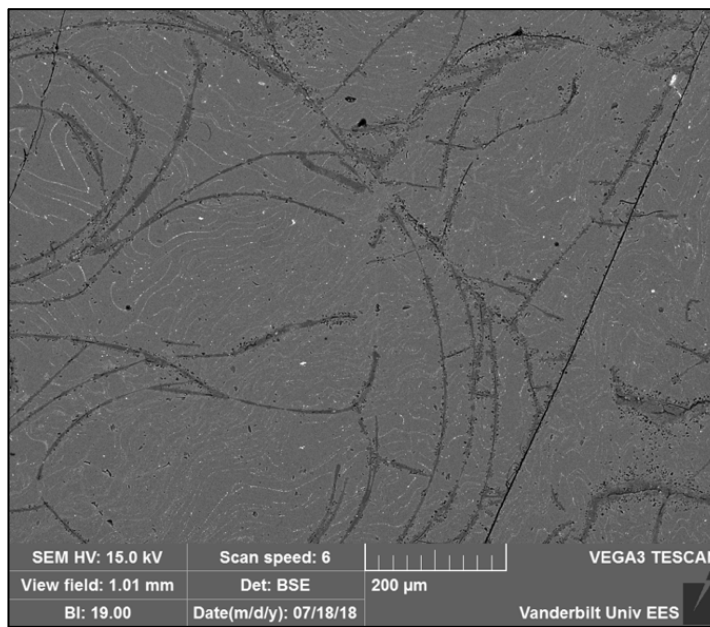


Figure 34: BSE image of fiamma glass in ORA-5B-402. Perlitic fracturing is shown.

Very Coarse-Grained Crystal-Rich Fiamme Glass

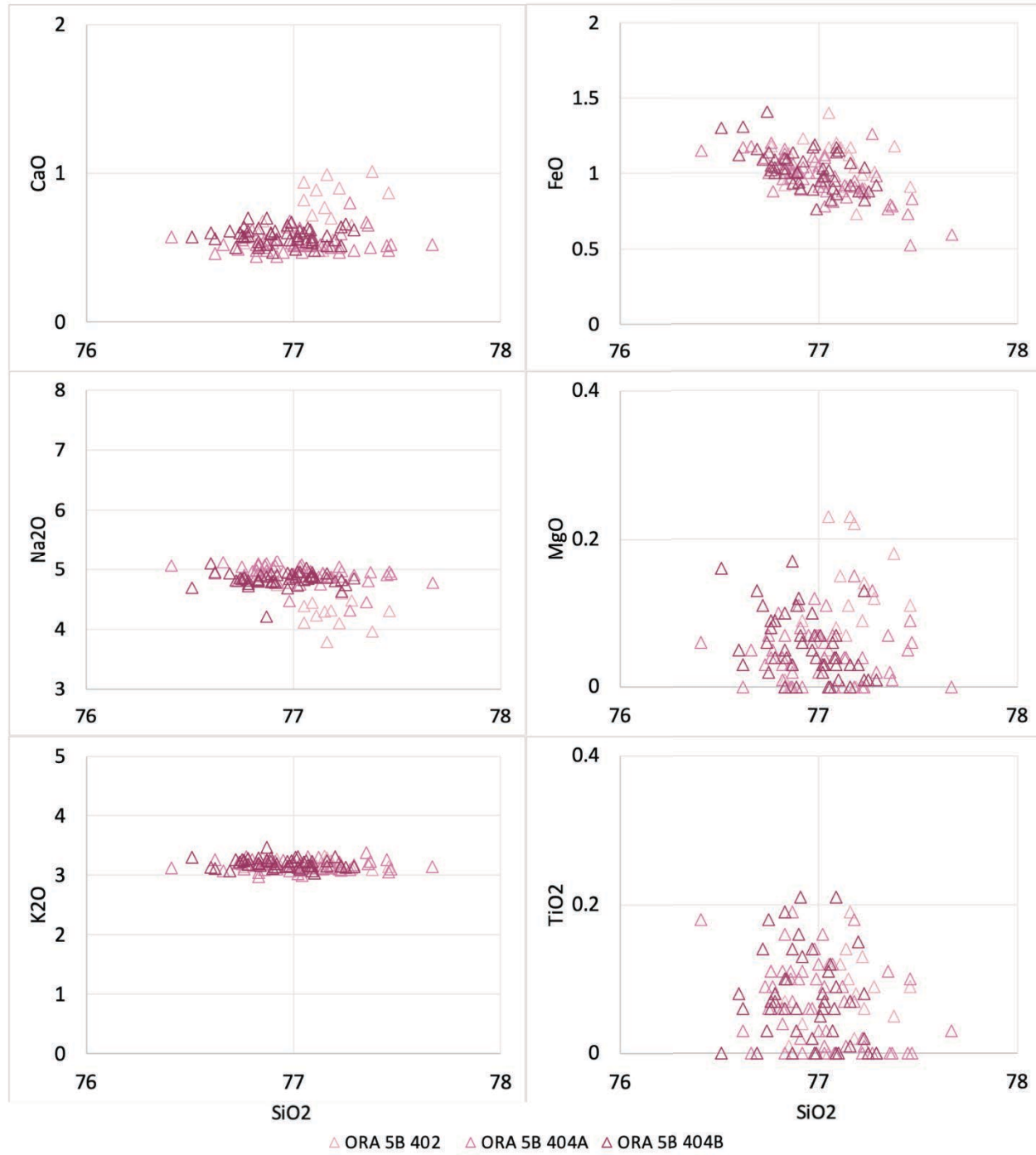


Figure 35: Major element compositions of glass from the VCCR fiamme. The glass is homogeneous and clusters between 76.5-77.5 wt% SiO_2 with potassium concentrations from 3-3.5 wt. % K_2O .

3.6.2 Fine-Grained (FG) Fiamme

The FG fiamme glass has a speckled appearance in back-scattered electron images due to the presence of microlites in the fiamme groundmass (Fig. 36). The microlites are small ($\sim 1\text{-}2 \mu\text{m}$) and are spaced $\sim 20 \mu\text{m}$ apart. By using small spot sizes of $15 \times 15 \mu\text{m}$, we were able to obtain glass analyses without any microlite inclusions.

In thin section, fractures and red speckled material suggest that ORA-5B-412A and ORA-5B-412B may be slightly altered. However, ORA-5B-414 lacks those features and appears to be the least altered in thin section (Fig. 12).

ORA-5B-414 has a continuum of glass compositions from 72-78 wt. % SiO_2 (Fig. 37). It also has the highest K_2O concentration out of all the fiamme glass analyzed (3-4.5 wt. % K_2O) (Fig. 46). The glass from the other two fiamme shows more limited compositional variation, ranging from 75-78 wt. % SiO_2 (Fig. 37). It also has less K_2O ($\sim 3\text{-}4$ wt. % K_2O) than ORA-5B-414 (Fig. 37).

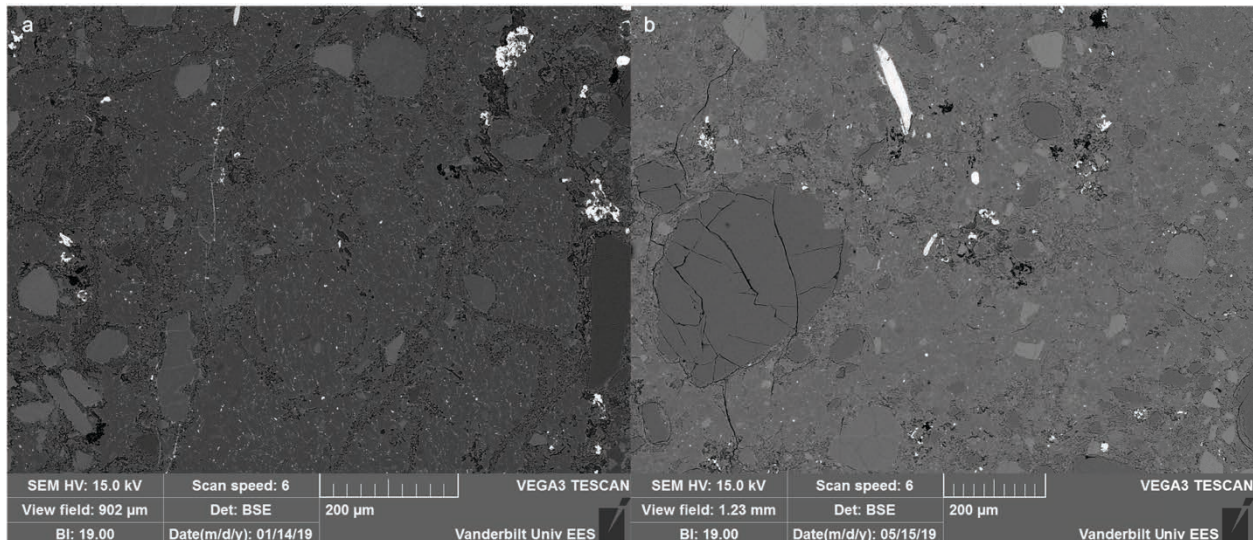


Figure 36: BSE images of FG fiamme glass (A) ORA-5B-412A. (B) ORA-5B-414. Note the speckled appearance of the glass.

Fine-Grained Fiamme Glass

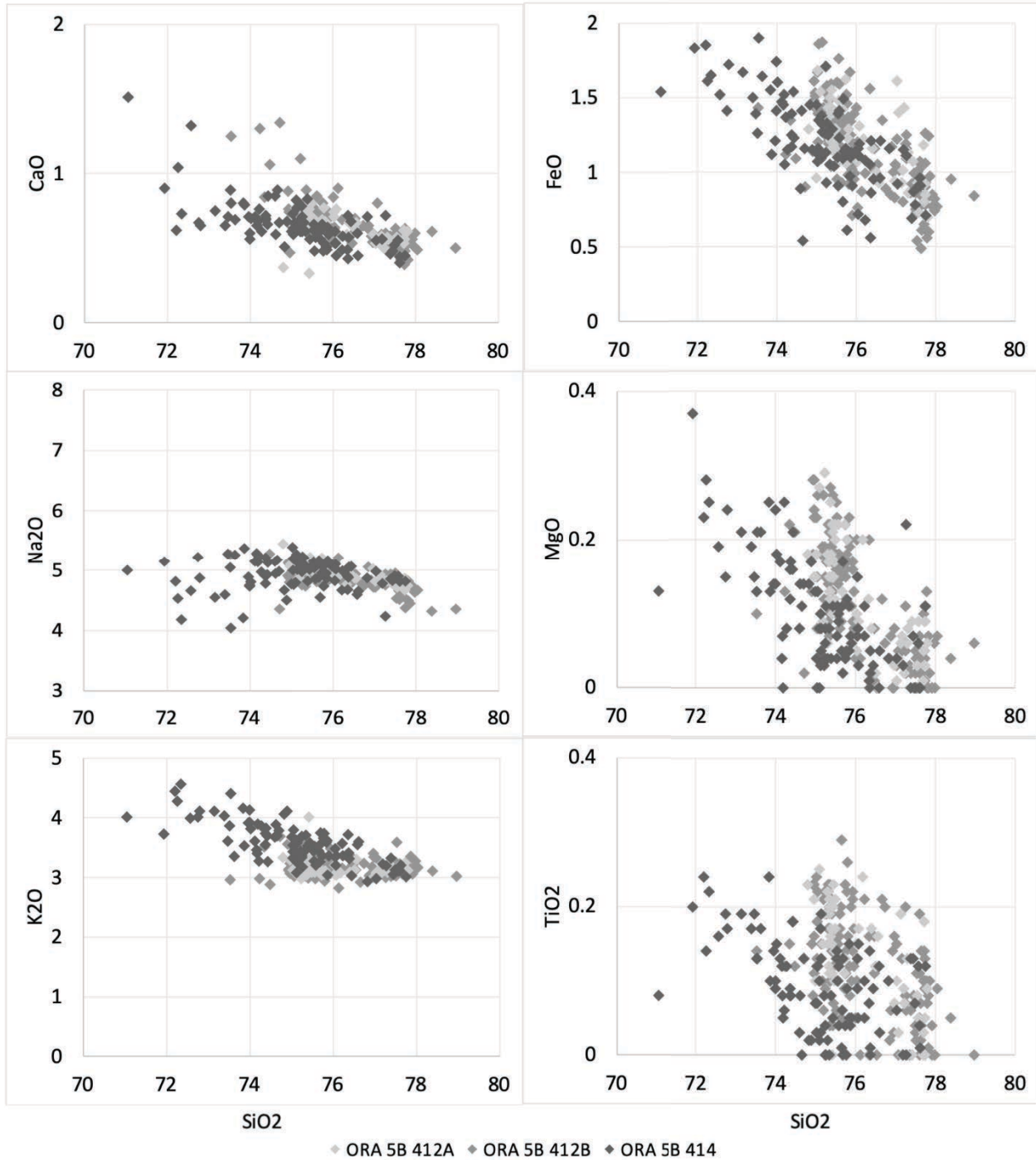


Figure 37: Major element compositions of glass from FG fiamme. This glass is more heterogeneous and ranges from 71-79 wt. % SiO_2 with potassium concentrations from 2.75-4.5 wt. % K_2O .

3.7 Outflow Glass Textures and Major Element Compositions

This section describes the fiamme glass textures and major element compositions of the outflow fiamme. Supplemental images of glass textures are included in Appendix C. All glass major element data collected from SEM-EDS analysis are included in Appendix E.

3.7.1 Medium-Grained (MG) Fiamme

The MG fiamme glass is texturally similar to the glass from the VCCR fiamme. However, the MG fiamme glass lacks the perlitic fracturing that is present in the VCCR fiamme (Fig. 38). The MG fiamme have relatively homogeneous glass compositions; their silica content ranges from 76-78 wt. % SiO₂ and their potassium ranges from 2-3 wt. % K₂O (Fig. 40).

A unique feature in some of the MG fiamme is the presence of orange, devitrified glass surrounding larger (1-3 mm) minerals. In samples ORA-2A-001, ORA-2A-031, and ORA-2A-040, the glass surrounding larger minerals appears orange in PPL and under XPL it exhibits a radiating, recrystallized texture (Fig. 39). This distinctive texture only surrounds crystals and clusters of fractured crystals (Fig. 19). Often, the minerals enveloped in the devitrified glass display unique textures: the quartz crystals are resorbed (Fig. 16a, 16f, 39), alkali feldspar and plagioclase show interlocking growth (Fig. 18a), and some plagioclase crystals have calcic cores (Fig. 23c, 23d).

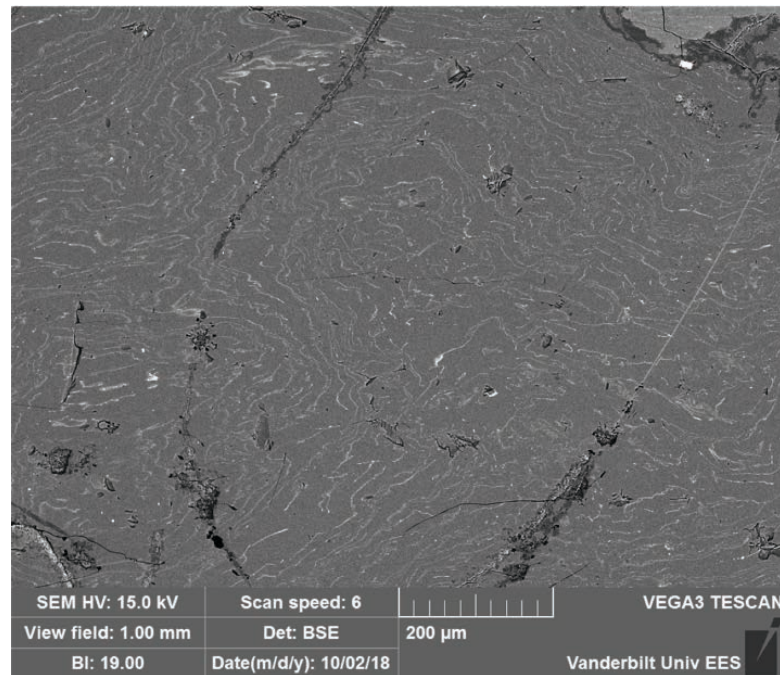


Figure 38: BSE image of MG fiamma glass in ORA-2A-001. There is no perlitic fracturing present.

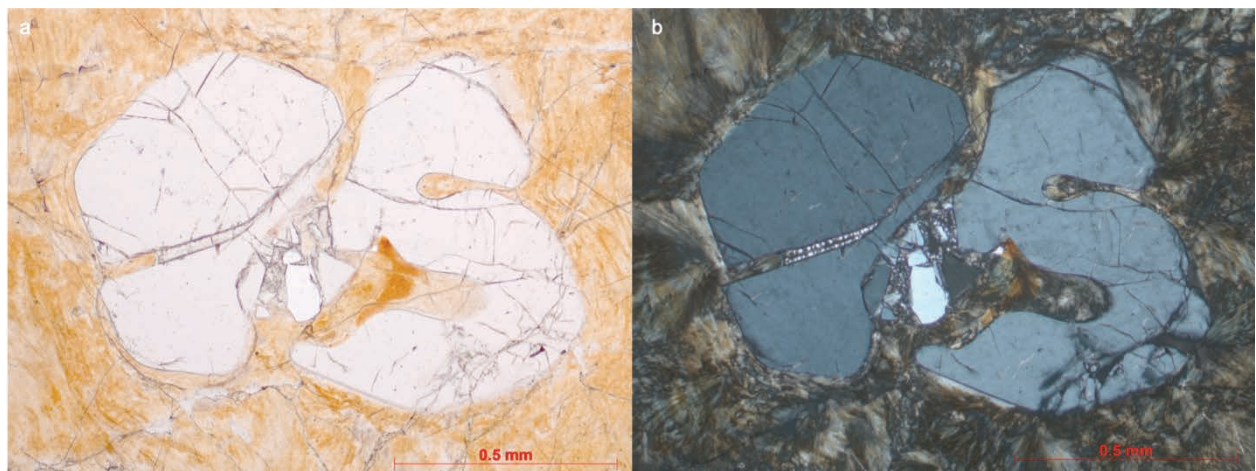


Figure 39: Devitrified glass surrounding quartz in ORA-2A-001 (A) PPL. (B) XPL. Note the radiating morphology.

Medium-Grained Fiamme Glass

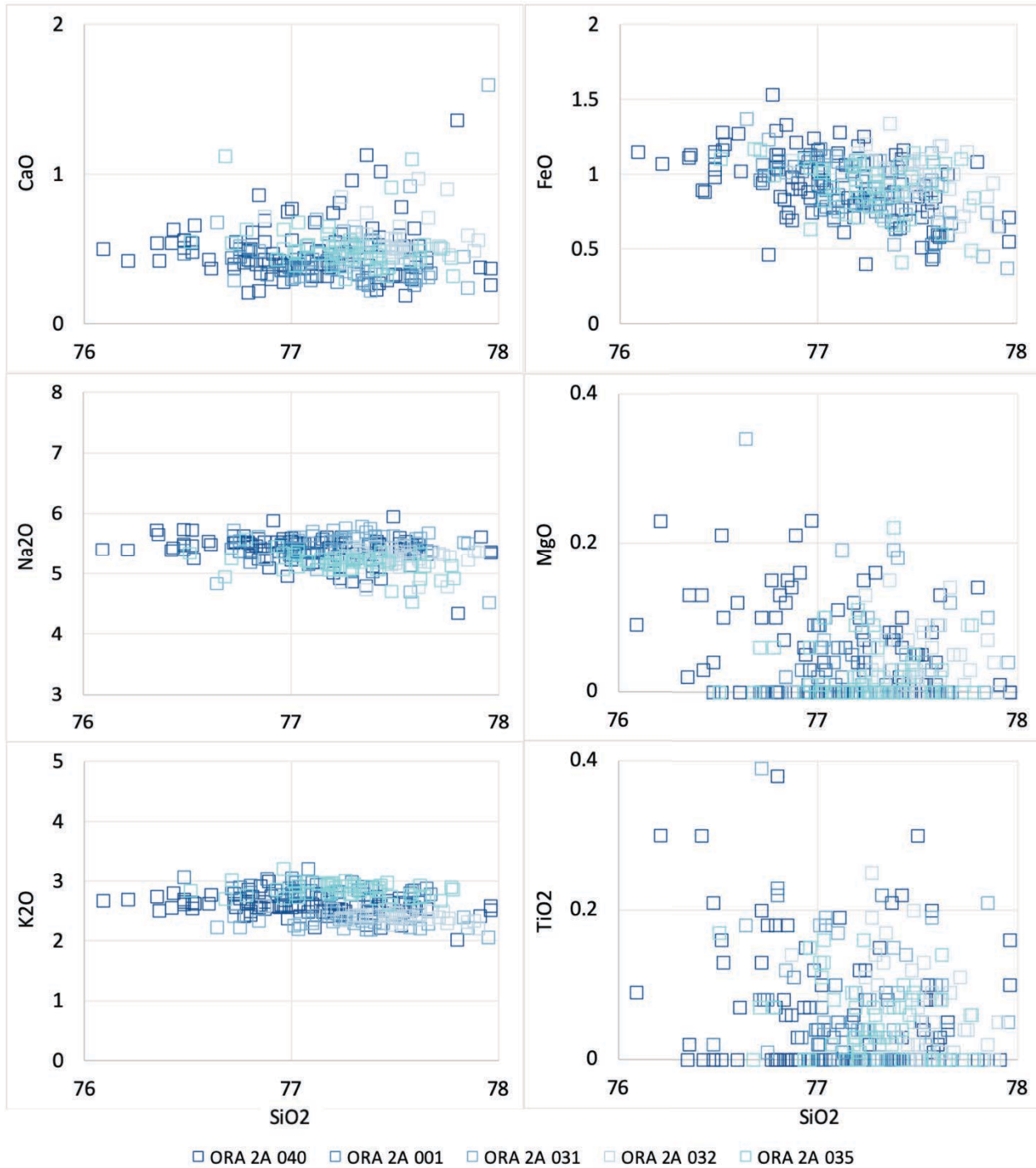


Figure 40: Major element compositions of glasses in MG fiamme. The glass is fairly homogeneous and ranges from 76-78 wt. % SiO_2 with potassium concentrations from 2-3 wt. % K_2O .

3.7.2 Fine-Grained Crystal-Poor (FGCP) Fiamme

The FGCP fiamme glass has a wide variety of textures. Often, there are multiple glass types found in a single fiamma. Like FG fiamme, glass from the FGCP fiamme often has a speckled appearance in back-scattered electron images. In ORA-2A-002, ORA-2A-016, and ORA-2A-024, glass types can be texturally distinguished (Fig. 41, 42, & 43). Multiple glass types from these three fiamme are discussed in detail in Appendix C.

Unique to the FGCP fiamme is the presence of asteroidal trichites (Skinner, 1983). Asteroidal trichites are a unique morphology of microlites that can be used as a distinguishing characteristic for identifying glass types (Skinner, 1983). The different sizes and abundances of the trichites affect the appearance of the glass in PPL (Fig. 44a, 44b). Asteroidal trichites are present in both ORA-2A-024 and ORA-2A-003.

Geochemically, the FGCP fiamme have the most variable glass compositions (Fig. 46). The FGCP fiamme glass ranges from 64-80 wt. % SiO₂. K₂O shows the most variation between the glasses. Glass from ORA-2A-016 has the lowest K₂O concentration (0.5 wt. %); overall the FGCP fiamme glass has 0.5-3.5 wt. % K₂O (Fig. 45).

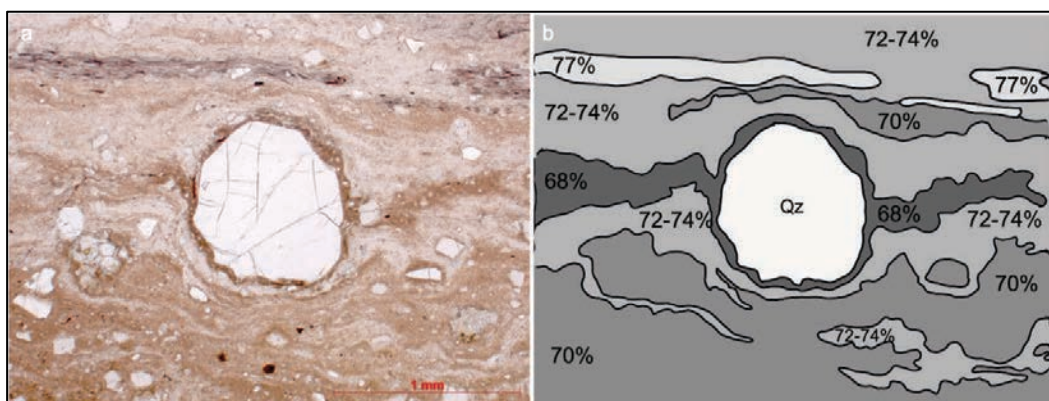


Figure 41: Quartz grain rimmed with multiple glass types in ORA-2A-002. In (B) the percentages represent the SiO₂ wt. % of the melt.

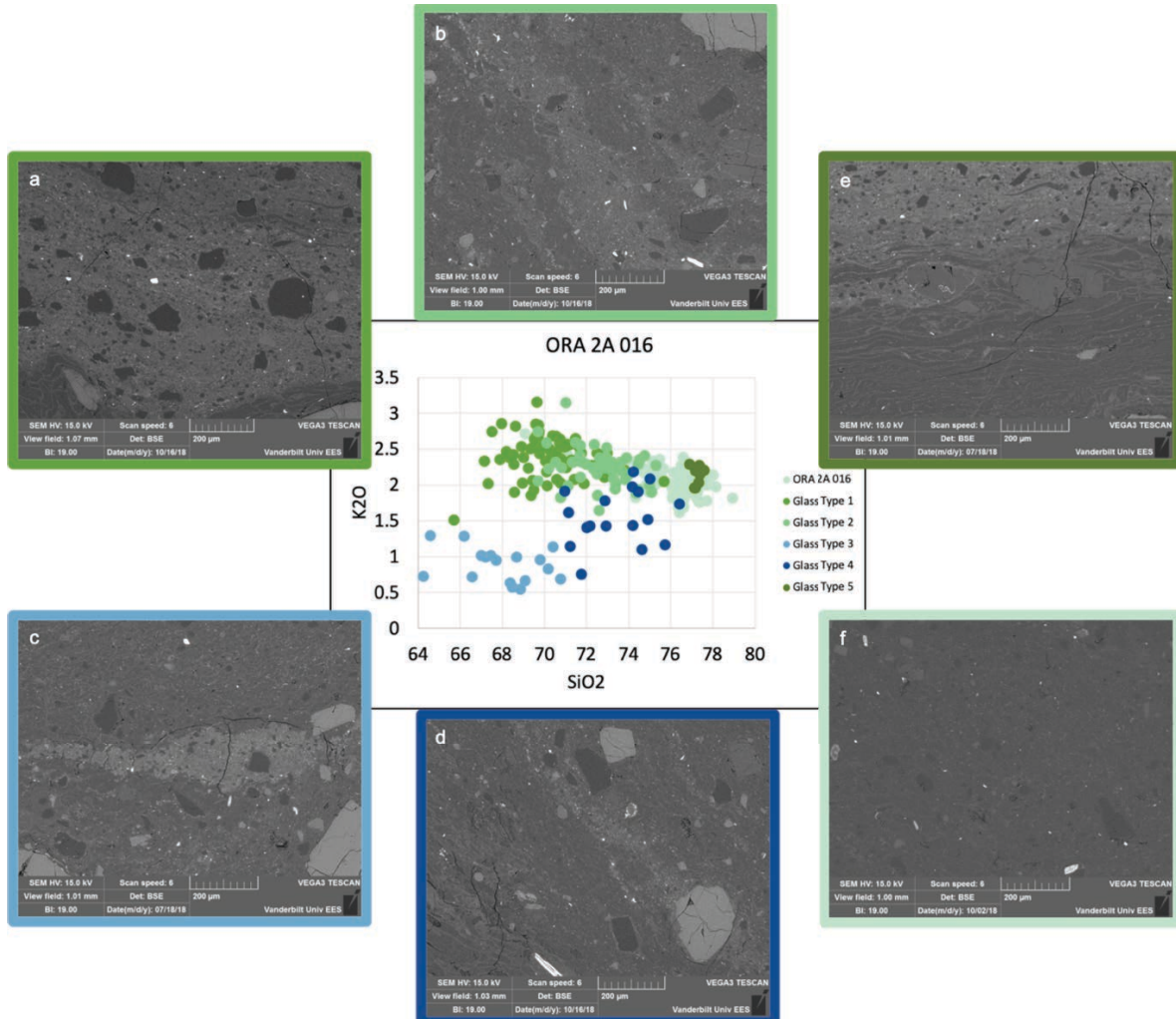


Figure 42: K₂O vs SiO₂ for ORA-2A-016. The colored border on each of the photographs matches the color of the symbols used for each glass type. (A) Type 1 (~67-74 wt. % SiO₂). (B) Type 2 (~70-75 wt. % SiO₂). (C) Type 3 (64-71 wt. % SiO₂). (D) Type 4 (71-77 wt. % SiO₂). (E) Type 5 (bottom half of the image) (77-78 wt. % SiO₂). (F) ORA-2A-016 glass with no textural differentiation (69-79 wt. % SiO₂).

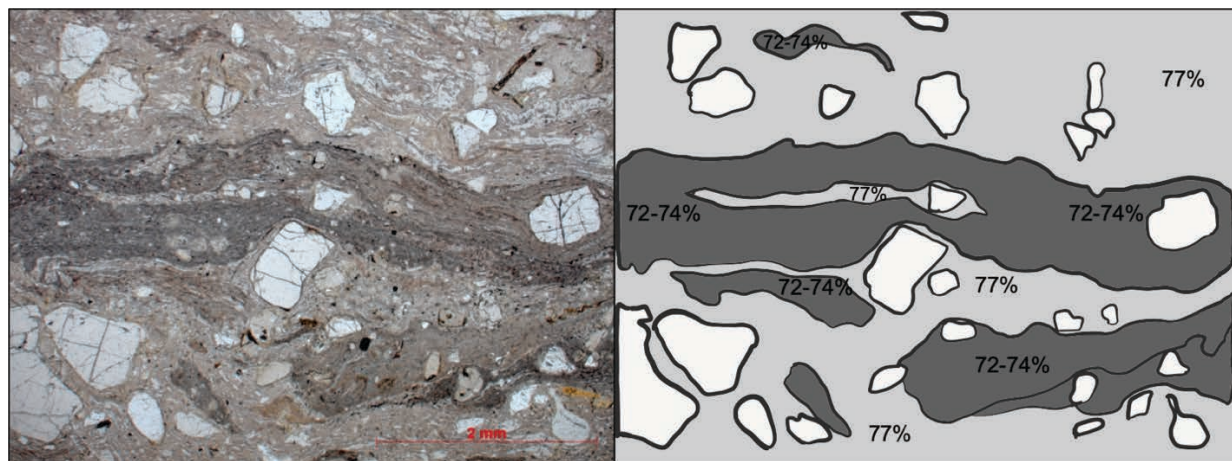


Figure 43: (A) Glass type 1 of ORA-2A-024 exhibiting a darker color in PPL. (B) Glass type 1 is the darker grey (~72-74 wt. % SiO₂) and glass type 2 is the lighter grey (~77 wt. % SiO₂).

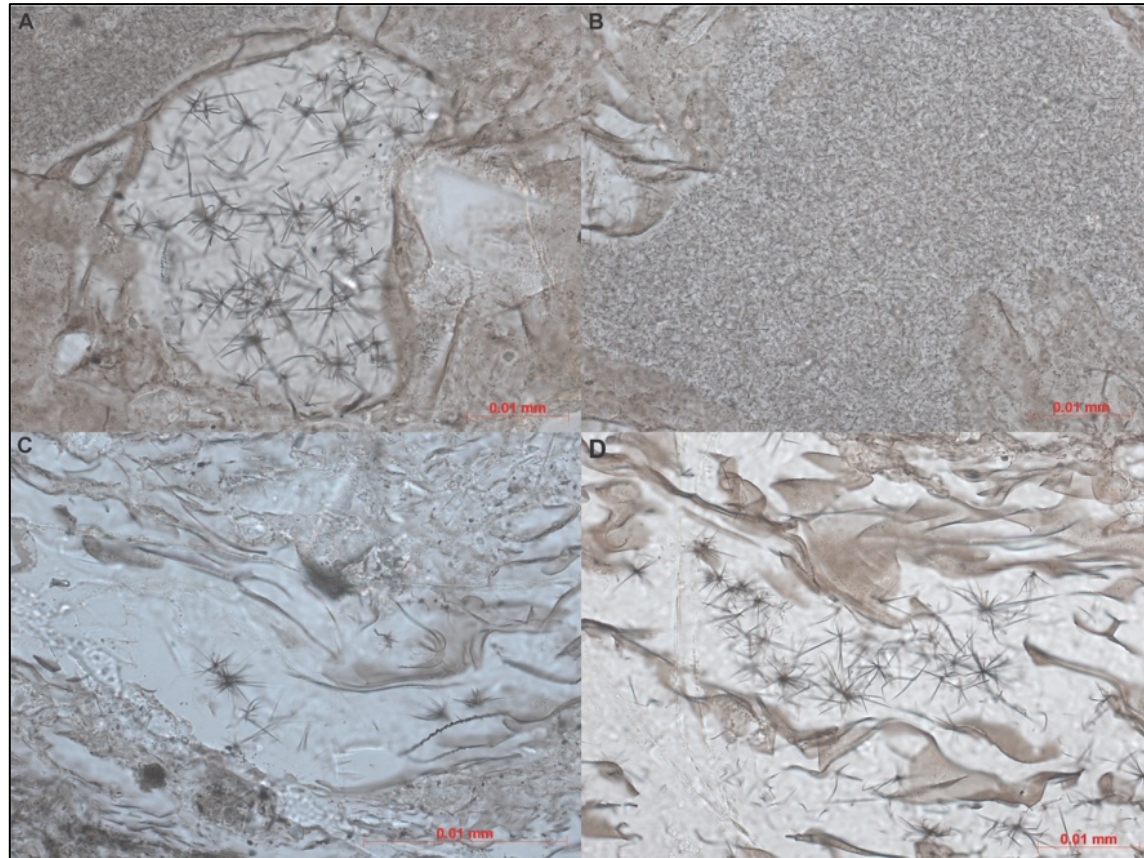


Figure 44: Asteroidal trichites present in ORA-2A-024. (A) A parcel of glass with abundant trichites. (B) Neighboring glass to (A) which contains many more small sized trichites. This results in a darker appearance of the glass in PPL. (C) Sparse trichites. (D) Spidery asteroidal trichites.

Fine-Grained Crystal-Poor Fiamme Glass

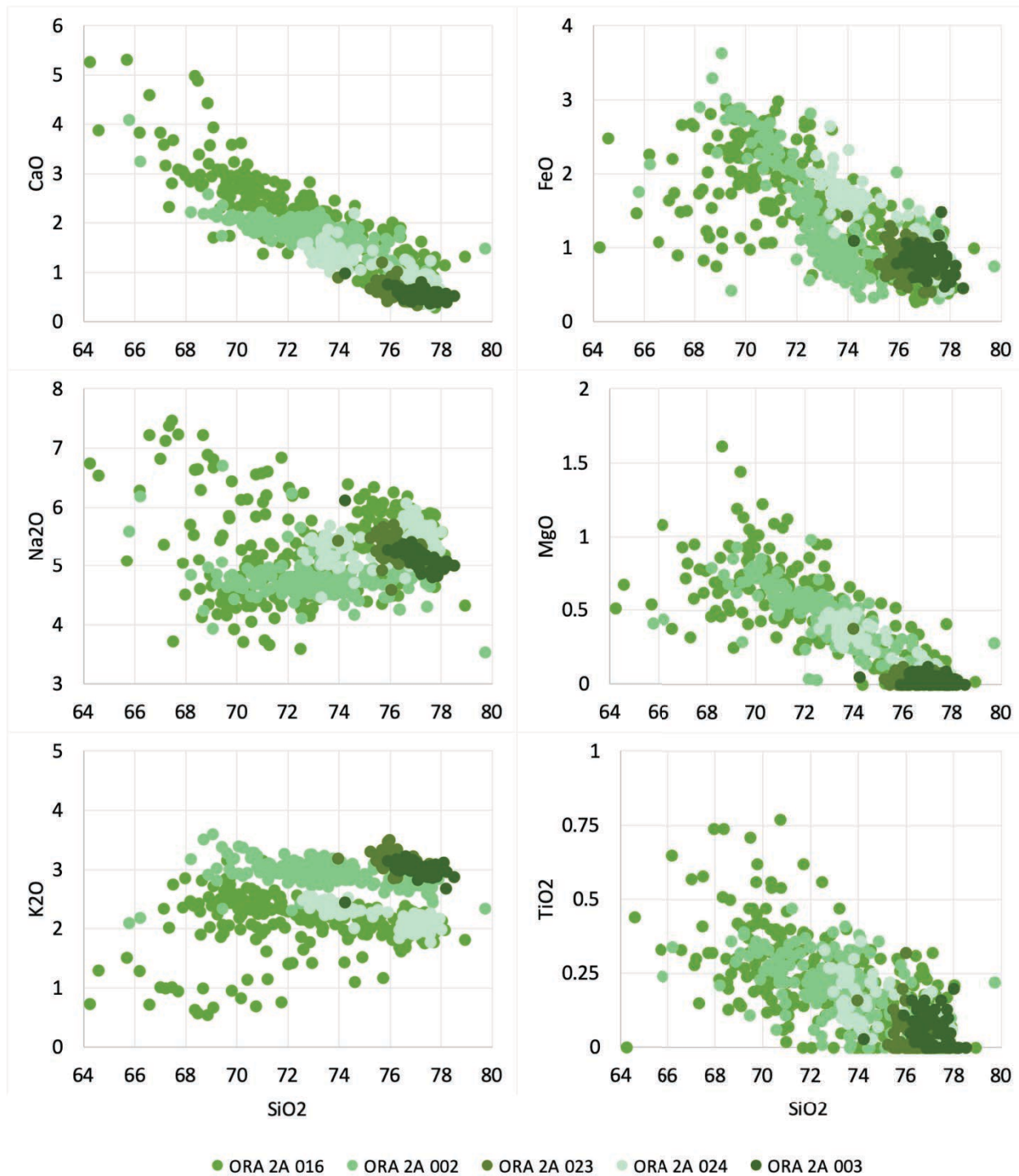


Figure 45: Major element compositions of glasses in FGCP fiamme. This glass is very heterogeneous. The silica content ranges from 64-80 wt. % SiO₂ and the potassium ranges from 0.5-3.5 wt. % K₂O.

3.8 All Ora Fiamme Glass Major Element Compositions

Figure 46 illustrates the elemental differences among all of the fiamme types. By plotting all of the fiamme glass major element compositions on one graph, the diversity that is present between the fiamme types becomes evident.

Lower CaO concentrations distinguish the FG fiamme glass (0.5-1.5 wt. % CaO) from the FGCP fiamme glass (0.5-5 wt. % CaO) (Fig. 46). The SiO₂ varies much more in the FGCP fiamme glass (64-80 wt. % SiO₂) than in the FG fiamme glass (71-79 wt. % SiO₂). Also, the higher K₂O concentrations for the FG fiamme glass (2.75-4.5 wt. % K₂O) in comparison to the lower K₂O content of the FGCP fiamme glass (0.5-3.5 wt. % K₂O) help illustrate key differences between the FG and FGCP fiamme glass.

The differences between the intracaldera VCCR fiamme glass and the outflow MG fiamme glass are more subtle, but can be observed in the figure below. While both fiamme types are constrained between 76-78 wt. % SiO₂, slight variations in K₂O and Na₂O are seen (Fig. 46). Overall, the VCCR fiamme glass tends to cluster more tightly (76.5-77.5 wt. % SiO₂) at higher K₂O concentrations (3-3.5 wt. % K₂O) and have lower Na₂O concentrations (3.75-5 wt. % Na₂O) (Fig. 46). The MG fiamme glass is more spread out (76-78 wt. % SiO₂) with lower K₂O concentrations (2-3 wt. % K₂O) and have higher Na₂O concentrations (4.5-6 wt. % Na₂O) (Fig. 46).

All Ora Fiamme Glass

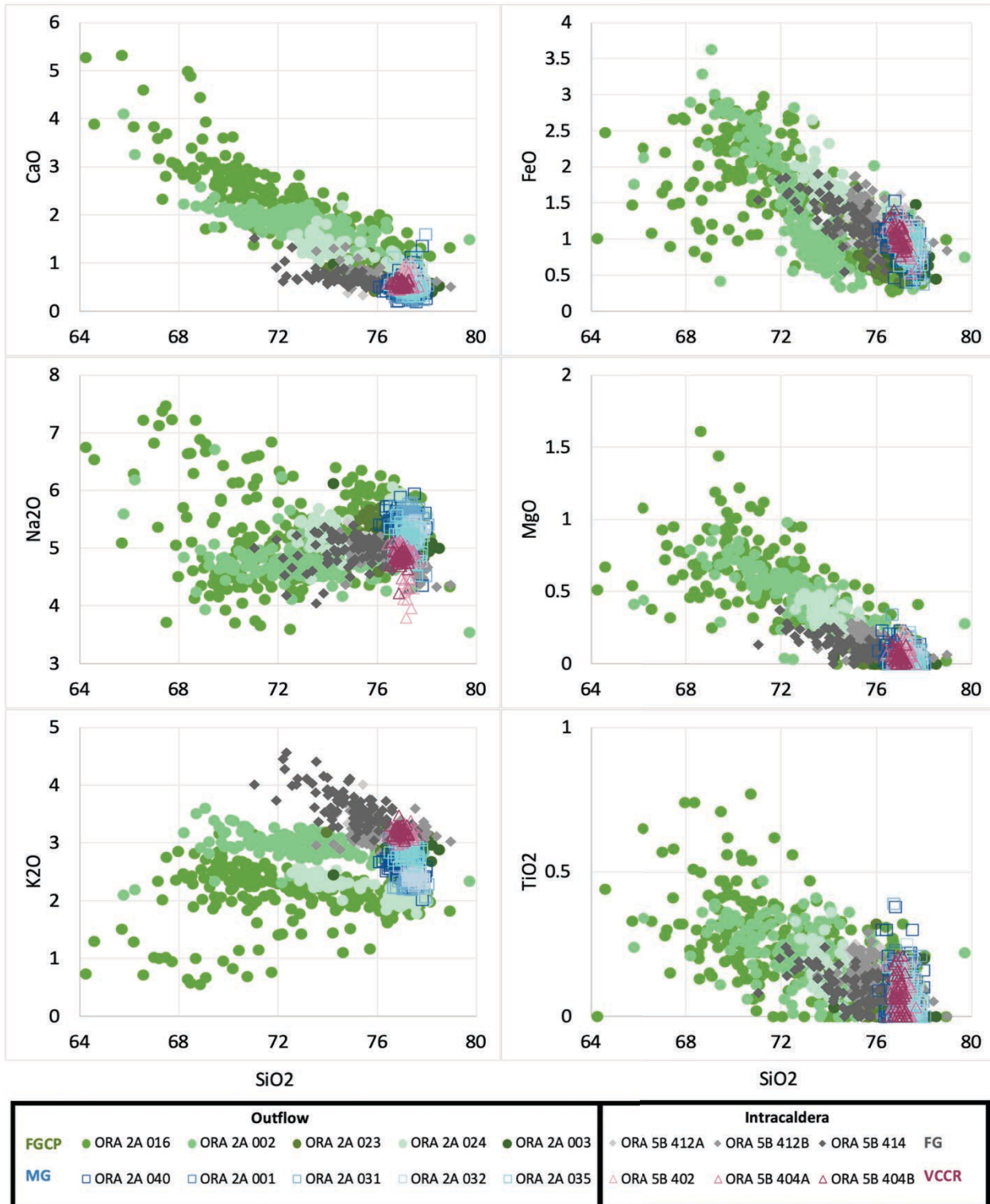


Figure 46: All Ora fiamme glass major element compositions. Note the how the most variation occurs with K₂O compositions (0.5-4.5 wt. %).

CHAPTER IV

DISCUSSION

4.1 Do Fiamme Major Element Compositions Represent Plausible Melt Compositions?

Due to the age of the Ora Ignimbrite (277 ± 2 Ma for the intracaldera fill and 274.1 ± 1.6 Ma for the outflow deposits), it is remarkable to have preserved glass for geochemical analysis (Marocchi et al., 2008). As discussed in the geologic background, the Ora Ignimbrite deposits did not experience ductile deformation for the past 280 million years, likely due to the rigid behavior of a large mass of rhyolitic lavas and ignimbrites that resulted from extensive volcanism in the Permian (Ring and Richter, 1994). Deformation of welded ignimbrites causes fracturing, allowing for fluids to travel along those conduits. These fluids can alter glass, resulting in compositions that do not accurately represent the original melt. Based on our thin sections of fiamme from both the vitrophyre and the densely welded non-vitrophyre, only the vitrophyre horizons remained impermeable to fluid flow, thus preserving fiamme glass. For this reason, we have limited this study to two outcrops: the early-erupted intracaldera vitrophyre (Ora 5) and the late-erupted outflow vitrophyre (Ora 2).

Clustering shown by the MG fiamme (blue squares) and VCCR fiamme (pink triangles) are representative of preserved, unaltered glass compositions (Fig. 47). The large number of SEM analyses coupled with the minor variability of Na₂O and K₂O concentrations for these fiamma types bolsters the interpretation that these samples accurately represent original glass compositions. This is because the possibility that every glass analysis underwent the same

amount of alteration is extremely unlikely. In contrast, the FG fiamme (grey diamonds) and FGCP fiamme (green circles) have large compositional variability. While some of this variability may be due to magmatic processes, alteration may be responsible as well.

Alteration due to alkali-exchange occurs during secondary hydration of glass and it imparts characteristically low Na/high K concentrations (alkali exchange, with Na loss on an atomic basis approximately balanced by K gain; e.g., Lipman, 1965; Scott, 1971). Pamukcu et al. (2015) showed that Rhyolite-MELTS geobarometry was only successful with glass from the Peach Spring Tuff that had relatively high Na and low K concentrations, suggesting that glass with low Na/high K had undergone 1:1 alkali exchange.

When plotted as Na_2O vs. K_2O , glasses from the Ora Ignimbrite fiamme display two possible alteration trends: a typical 1:1 alkali exchange (Na^+ depletion/ K^+ enrichment) trend and a reverse 1:1 alkali exchange (K^+ depletion/ Na^+ enrichment) trend (Fig. 47). The remaining glass compositions that do not evolve along the 1:1 exchange slope can be explained by either (1) magmatic processes, (2) alkali loss (leaching), or (3) another type of alteration (Fig. 47).

Glass from ORA-5B-414 has the highest K_2O concentration of all the fiamme (>4 wt. %), suggesting that potential alkali exchange occurred (Fig. 47). While it is feasible to have a rhyolite with 4-4.5 wt. % K_2O and 4-5 wt. % Na_2O , this Na^+ depletion/ K^+ enrichment trend suggests that the more K^+ enriched glasses of ORA-5B-414 may be altered.

ORA-2A-016 appears to have undergone a reverse alkali exchange alteration with K^+ depletion/ Na^+ enrichment (Fig. 47). This type of alteration is very likely to have occurred in order to produce the high Na_2O (6-7 wt. %) and low K_2O (0.5-1 wt. %) concentrations observed in ORA-2A-016 (Fig. 47). Based on this preliminary analysis, we speculate that unaltered glasses

from the Ora Ignimbrite fiamme have Na_2O concentrations ranging from 4-6 wt. % and K_2O concentrations ranging from 2-4 wt. %. Any outliers may not represent true magmatic compositions.

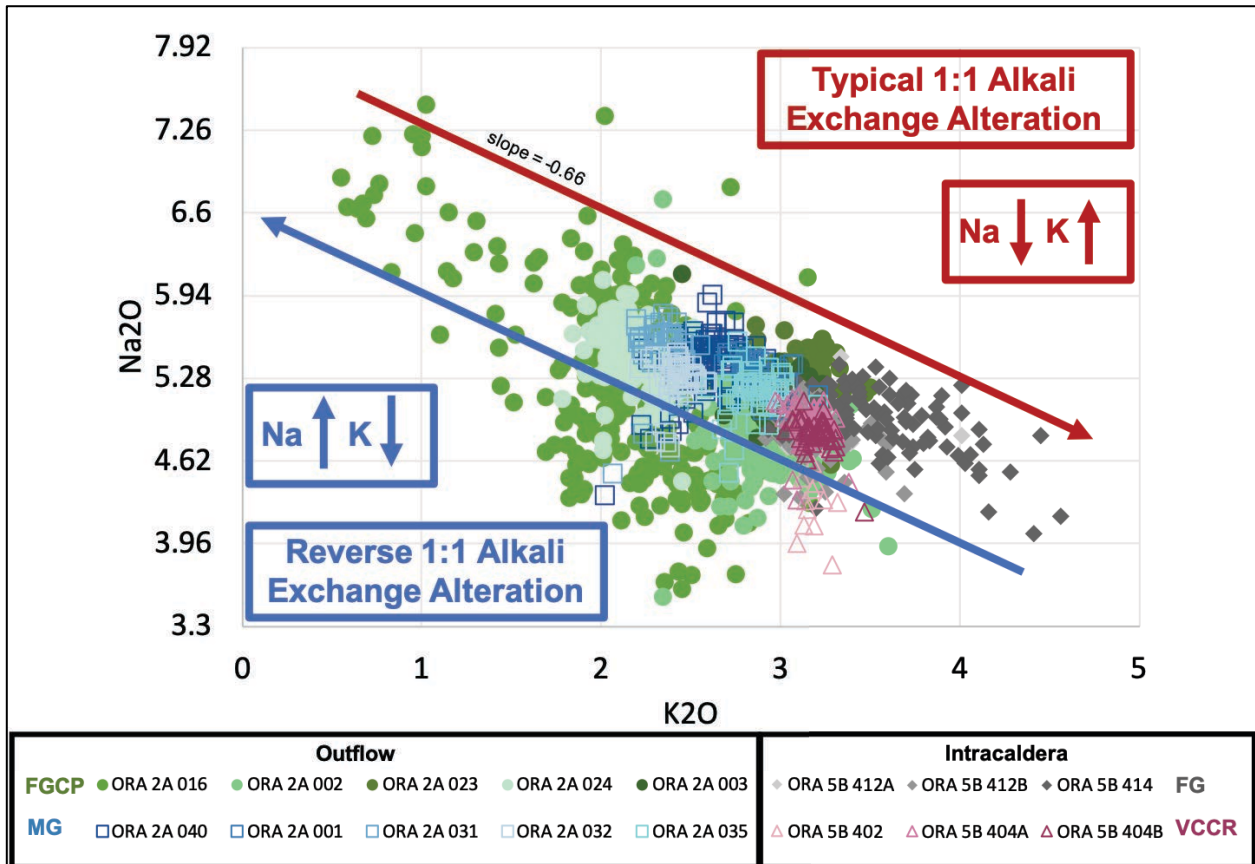


Figure 47: Na_2O wt. % vs. K_2O wt. % for all Ora fiamme glass. The slope of the red arrow indicates a typical 1:1 alkali exchange alteration trend while the slope of the blue arrow shows a reverse 1:1 alkali exchange alteration trend. The slope of $\text{Na}_2\text{O}/\text{K}_2\text{O}$ (atomic weight) is -0.66. ORA-5B-414 may have undergone typical alkali exchange alteration while ORA-2A-016 may have experienced reverse alkali exchange alteration.

Pamukcu et al. (2015) also discuss the A/CNK ratios of the Peach Spring Tuff glasses, stating that the glass compositions returning rhyolite-MELTS geobarometry pressures tended to have A/CNK ratios close to 1, whereas many of the altered (low Na/high K) glasses had A/CNK ratios greater than ~1.05. The A/CNK values that provided pressures ranged from 0.99-1.07

(Pamukcu et al., 2015). However, the Peach Spring Tuff is metaluminous whereas the majority of the Ora Ignimbrite fiamme glasses appear to be slightly peraluminous, with A/CNK ratios ranging from 0.98-1.1 (Fig. 48).

In figure 48, as the SiO₂ content decreases, the A/CNK ratio rises. Since the opposite trend is expected for unaltered glass, this represents the alteration process of leaching. Leaching differs from alkali exchange because calcium, sodium, and potassium ions are depleted from the glass, thus raising the A/CNK ratio.

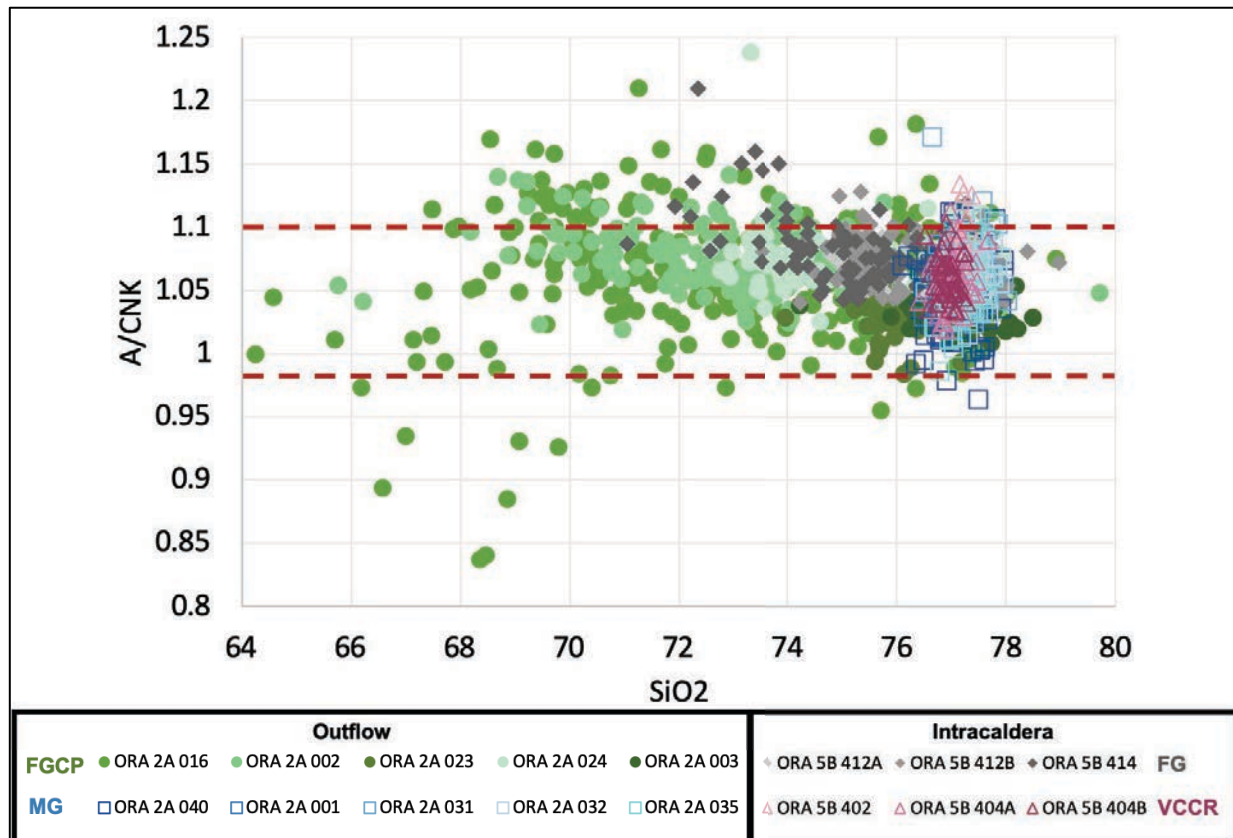


Figure 48: A/CNK vs. SiO₂ for all of the Ora Ignimbrite samples. Glasses within the red dashed lines (0.98-1.1 A/CNK) are suggested to be unaltered. Note the variability present in the FGCP outflow fiamme (ORA-2A-016 and ORA-2A-002).

4.2 What Does the Presence of Multiple Fiamma Types Reveal About the Ora Eruption?

There are four distinct fiamma types found in the Ora Ignimbrite: very coarse-grained crystal-rich (VCCR) fiamme, fine-grained (FG) fiamme, medium-grained (MG) fiamme, and fine-grained crystal-poor (FGCP) fiamme. Glass from each fiamma type has unique compositional signatures (Fig. 46). As shown in figure 46, each fiamma type displays a different trend. This geochemical diversity strongly suggests that there were multiple magma bodies, each evolving independently of the others.

The pieces of evidence suggesting that multiple magma bodies were present throughout the eruption of the Ora Ignimbrite include: (1) the multiple fiamma types present, (2) the variations in elemental compositions within and between fiamma types, and (3) the identification of multiple glass types in a single fiamma. Both the early-erupted intracaldera vitrophyre and late-erupted outflow vitrophyre had homogeneous high-silica rhyolite fiamme (VCCR and MG) and heterogeneous, fine-grained fiamme (FG and FGCP), suggesting that at least two different magma bodies were tapped during the early and late-eruptive sequences (Fig. 49, 50). The geochemical distinction between the VCCR and MG glasses may indicate that the magmas that erupted to form the fiamme were sourced from different magma bodies or zones within the magmatic system. This same case could be made for FG and FGCP fiamme; they likely originated from different melt-rich magma bodies in the system.

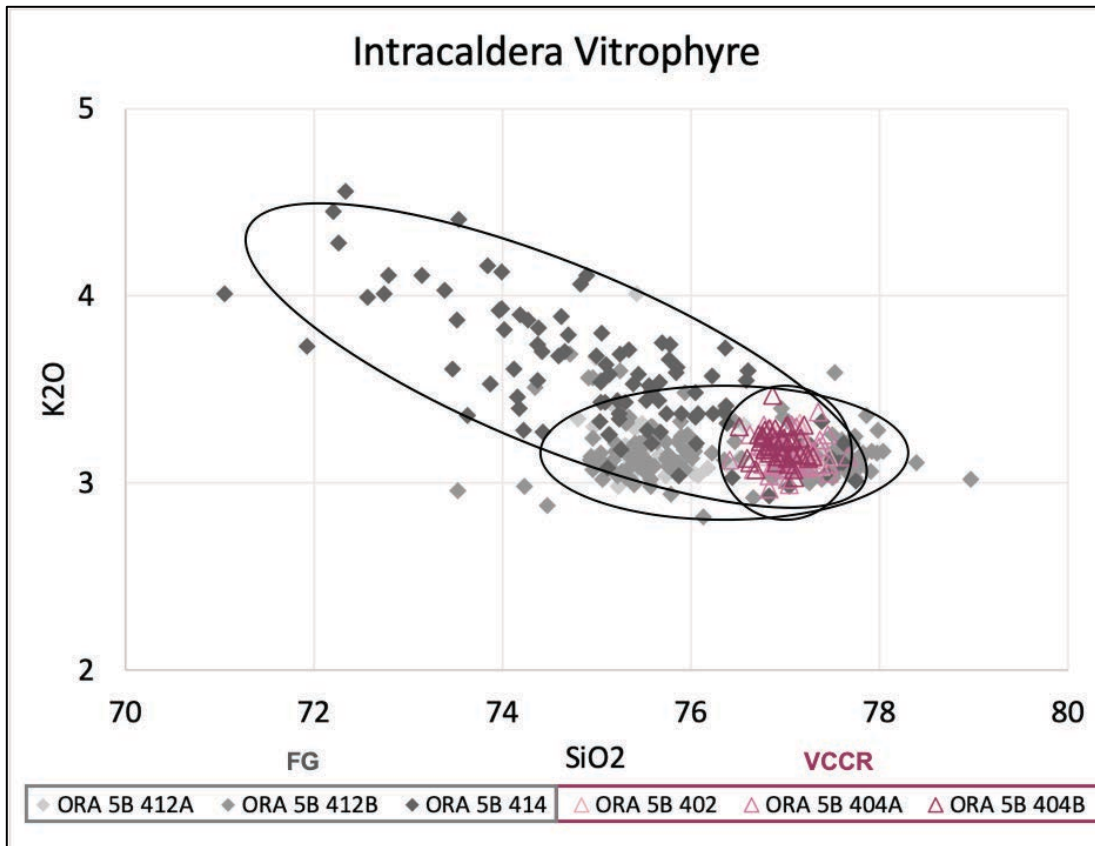


Figure 49: K₂O vs. SiO₂ for glasses in fiamme from the intracaldera vitrophyre. The circled regions suggest discrete magma bodies were present that experienced different histories.

Due to the evidence of multiple glass types in single fiamme and the unique elemental signature of each FGCP fiamma, I infer that each of the FGCP fiamme was sourced from a discrete melt-rich magma body. The multiple glass types found in single fiamma suggest that different magmas interacted with each other prior to eruption. ORA-2A-002, ORA-2A-016, and ORA-2A-024 each experienced influxes of different melt types and retained magma mingling textures upon eruption. Since each FGCP fiamma essentially recorded a separate magmatic history, I cannot be sure of the exact number of magma bodies present. However, the presence of multiple different mixing trends suggests that a multitude of magma bodies mixed and mingled to form the outflow of the Ora Ignimbrite (Fig. 50).

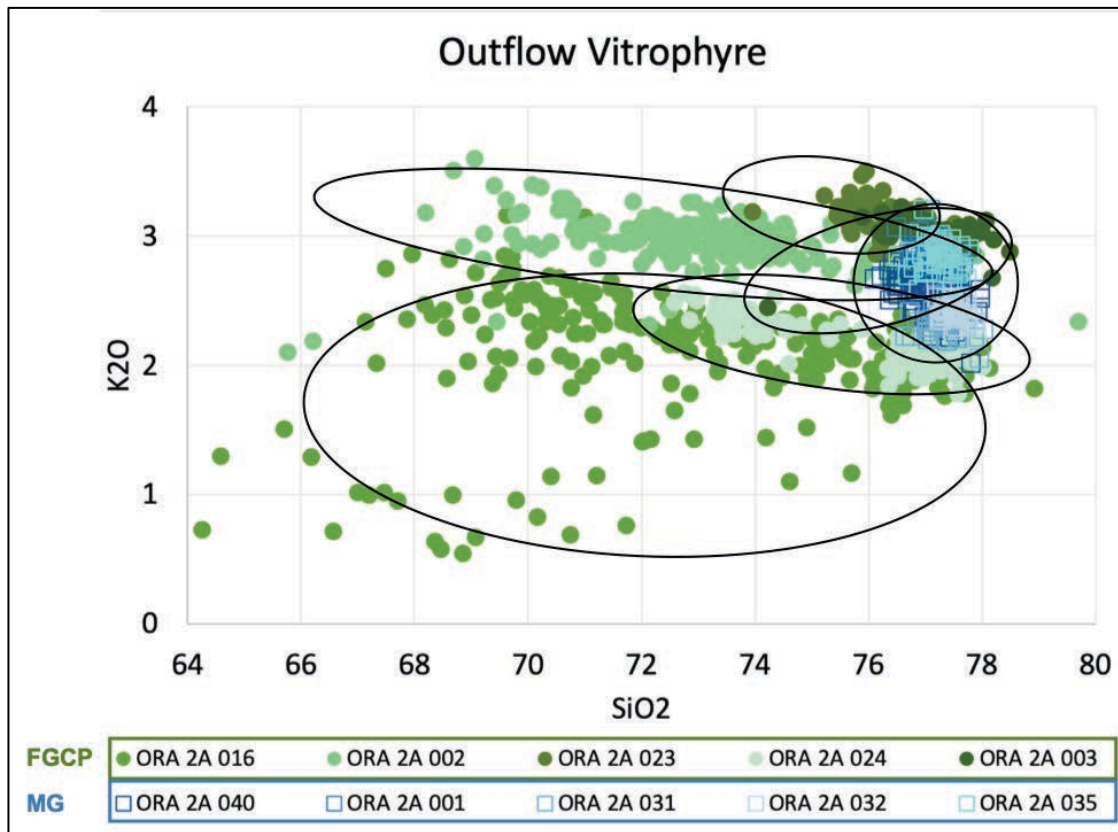


Figure 50: K₂O vs. SiO₂ for fiamme from the outflow vitrophyre. The circled regions suggest discrete magma bodies that each evolved separately and experienced influxes of different magmas.

4.3 Magma Mingling vs. Magma Mixing

Magma mingling is the physical interaction between two distinct magmas whereas magma mixing is the geochemical process which occurs by interdiffusion of elements between melts of different compositions. When there is mingling but minimal mixing, a bimodal distribution of elemental concentrations in glass should result. ORA-2A-002 has a clear mixing line spanning from 68-78 wt. % SiO₂. The glass textures illuminate the process of magma mingling with melts of differing compositions in close contact with one another (Fig. 41, 42, 43). The compositions suggests that the possible end members of melt-- a high-silica rhyolite and a

dacite-- were in contact for enough time to produce the geochemical mixing lines observed in figure 45.

4.4 Can Magma Mixing Lead to a Rhyolite Continuum?

The fine-grained fiamme (FGCP and FG subtypes) both show a continuum of glass compositions. While glass from the FGCP fiamme range from 64-80 wt.% SiO₂, glass from the FG samples range from 71-80 wt.% SiO₂ (Fig. 37, 45). As discussed previously, some of these trends can be attributed to alteration. However, not all of the variation is due to alteration, and magmatic processes, such as magma mixing, are likely to have produced some of these unique geochemical signatures.

The high-silica rhyolites found in ORA-2A-002 and ORA-2A-016 are likely to be the most evolved end member. Interestingly, they both appear to have similar textural characteristics; the glass is dark grey and with a wave-like texture in PPL (Appendix C). The lower silica end members (~67-72 wt. % SiO₂) for both ORA-2A-002 and ORA-2A-016 have similar textural characteristics as well (Appendix C).

4.5 What Can Minerals Reveal About the Ora Supereruption?

The VCCR fiamme have a variety of mineral textures that suggest that the minerals experienced a rejuvenation event. Figure 15 shows multiple large (>2mm) quartz crystals with resorption textures. Resorption is also present in sieve textured plagioclase grains (Fig. 22). Perhaps the most telling feature that suggests that these crystals may not have grown from the high-silica rhyolite melt that they are in contact with is the abundance of interlocking growth

textures between plagioclase and alkali feldspar (Fig. 17). The presence of these textures suggests that (1) this system may have mostly crystallized at one point in time and (2) these mineral grains may be sourced from either the rigid sponge or crystal mush.

Similar to the VCCR minerals, the MG minerals exhibit resorption textures. Quartz grains are more resorbed than the VCCR quartz grains (Fig. 16) and interlocking growth textures between alkali feldspar and plagioclase are abundant (Fig. 18). This texture suggests that the minerals originally grew in a system that was largely crystallized. The highly fractured alkali feldspar glomerocrysts also suggest that this eruption may have remobilized prior crystallized material (Fig. 19)

In MG fiamme, plagioclase with An-rich cores are observed (Fig. 23). The outer rims of the plagioclase crystals all have low An contents (An11-An14) whereas the cores range from An33-An45. There is one instance of an extremely An-rich analysis with An78. These An-rich cores record individual histories of each plagioclase grain and suggest that they began growth in a more mafic melt. Due to the abrupt change from core to rim, these plagioclase crystals were likely transported into a more silicic magma body via injection. Since the crystals have more Ab-rich rims, it is interpreted that they continued to crystallize in the system until they were erupted out.

It is possible that the Ora Ignimbrite either tapped (1) two or more discrete mush zones or (2) two or more heterogeneous regions within a continuous mush zone over the course of the eruption. The mineral compositions and textures that suggest that the early-erupted VCCR fiamme were sourced from a different location than the late-erupted MG fiamme are (1) the biotite content from the VCCR fiamme (2-3%) differs from the MG fiamme (<0.5%) (Table 4), (2)

the biotite from the VCCR and has less iron ($Mg\# = 0.24$ - 0.31) compared to the biotite from the MG fiamme ($Mg\# = 0.15$ - 0.25) (Fig. 27), and (3) the plagioclase from the VCCR fiamme cluster from An20-An30 whereas the plagioclase from the MG fiamme cluster from An10-An20 (Fig. 24).

4.7 The Pre-Eruptive Ora Magmatic System

Recent work on supereruption-sized eruptions has suggested that the diversity of eruptive products can be attributed to the presence of multiple magma bodies within a large, crystal mush framework (Begué et al., 2014; Lipman, 2007; Miller et al., 2011). This type of magma system can be formed by the incremental emplacement of sills (Miller et al., 2011; Lipman, 2007). The presence of multiple magma bodies, each evolving separately due to progressive fractionation, offers a model to explain the multiple types of fiamme found in the Ora Ignimbrite (Fig. 51).

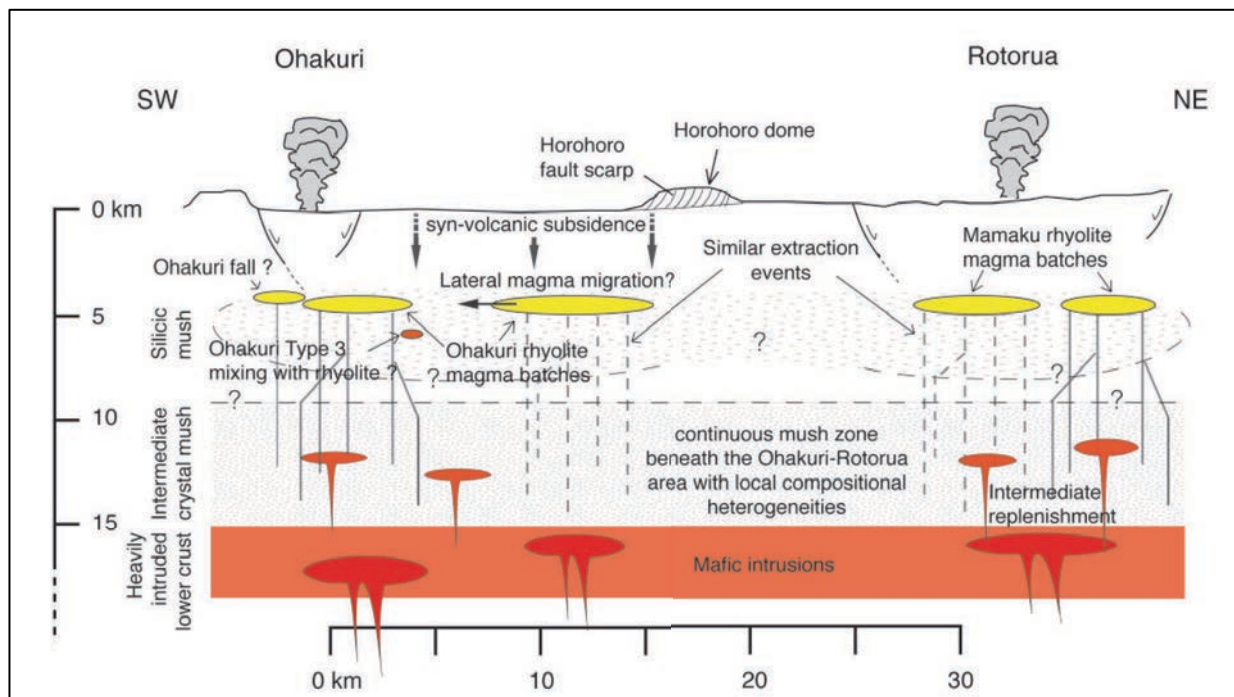


Figure 51: Multiple bodies of magma within a continuous crystal mush zone (from Begué et al., 2014). Note their sill-like geometries.

The mingling textures with multiple glass types present in a single FGCP fiamme suggest that different magmas interacted prior to eruption. It is unknown whether they came into contact in a melt-rich magma body or during ascent. Regardless, the evidence that multiple magma bodies contributed to form FGCP fiamme is substantial.

As mentioned previously, it is entirely possible that the Ora eruption tapped two or more different sources over the course of its eruption. The variation in biotite content, the major element compositions of biotite and plagioclase grains, and the slight differences in glass major element compositions between the outflow and intracaldera fiamme provide evidence for either (1) two or more distinct mush zones or (2) heterogeneity within a continuous mush zone.

CHAPTER V

CONCLUSIONS

The investigation of fiamme from two vitrophyre horizons allowed us to observe both the early and late-erupted products of the Ora Ignimbrite. Four types of fiamme were categorized based upon crystal content and maximum phenocryst size. In the early-erupted intracaldera vitrophyre, the very coarse-grained crystal-rich (VCCR) fiamme and the fine-grained (FG) fiamme were distinguished. The late-erupted outflow vitrophyre included medium-grained (MG) fiamme and fine-grained crystal-poor (FGCP) fiamme. Most of the fiamme glass analyzed represents original melt compositions. Samples were identified that may have been altered due to their low Na₂O concentrations, high A/CNK ratios, and large variations in elemental compositions.

Mineral textures suggest that the Ora Ignimbrite may have remobilized material that was once mostly crystallized. Interlocking growth textures observed between plagioclase and alkali feldspar suggest that these grains may have originated from either the crystal mush or rigid sponge. Other dissolution textures such as resorbed quartz grains and sieve textured plagioclase further suggest that the crystals found in the VCCR and MG fiamme had experienced a rejuvenation event prior to eruption.

Our evidence from this study suggests that multiple melt-rich magma bodies were present in the pre-eruptive Ora magmatic system. The geochemical diversity of the FGCP fiamme suggests that each fiamma was sourced from a discrete melt-rich magma body.

Differential amounts of magma mingling and mixing occurred within these melt-rich magma bodies to form the rhyolitic continua observed.

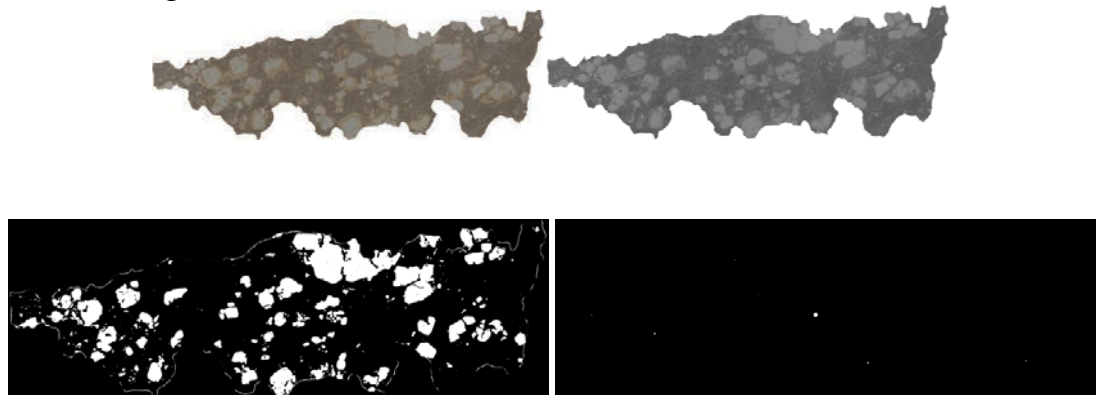
There is a possibility that the Ora eruption tapped either (1) two or more distinct mush zones or (2) heterogeneous zones within a continuous crystal mush. Differences in biotite content, biotite and plagioclase major element compositions, and fiamme glass major element compositions suggest that the early-erupted VCCR fiamme originated from a different source than the late-erupted MG fiamme.

This investigation of the Ora Ignimbrite illuminates the magmatic processes that occurred during the final episode of this ignimbrite flareup. This study helps to further our understanding of the architecture of large silicic magma systems.

APPENDIX

A. Crystal Content Analysis

ORA-2A-001: *insignificant amount of mafics* <0.1%

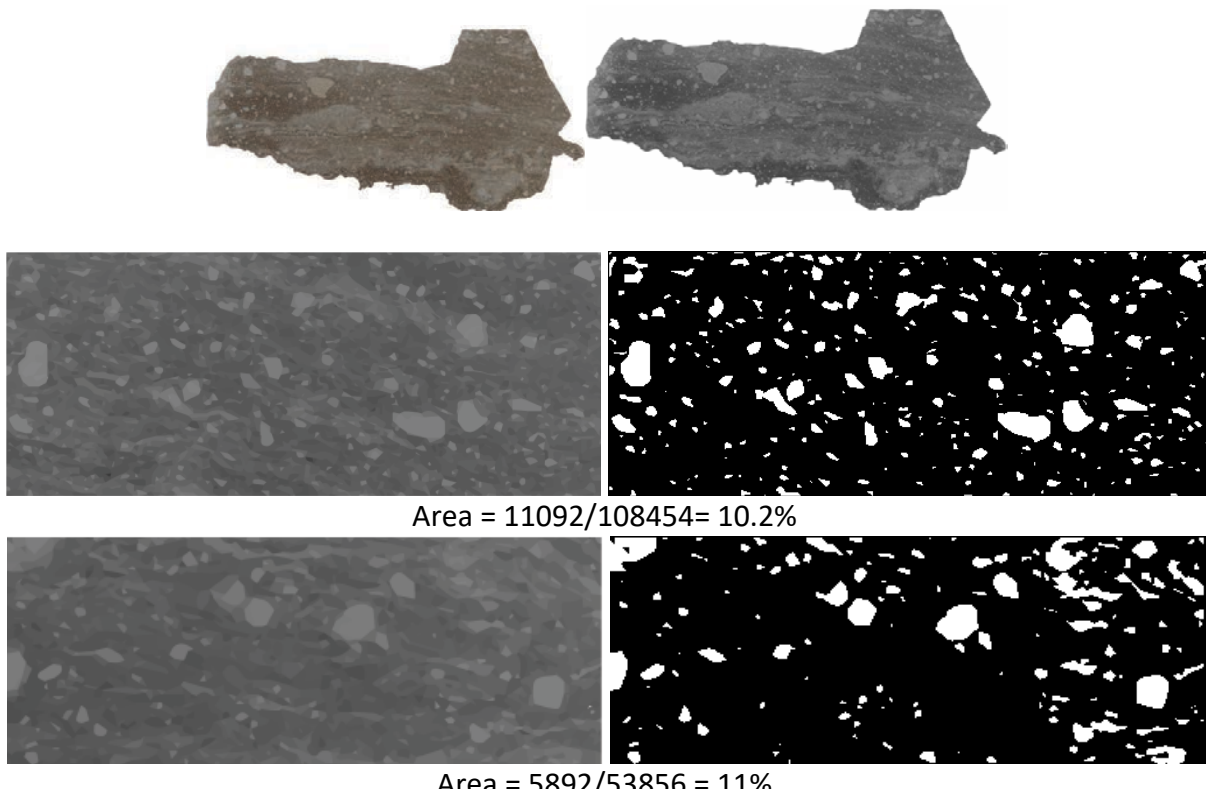


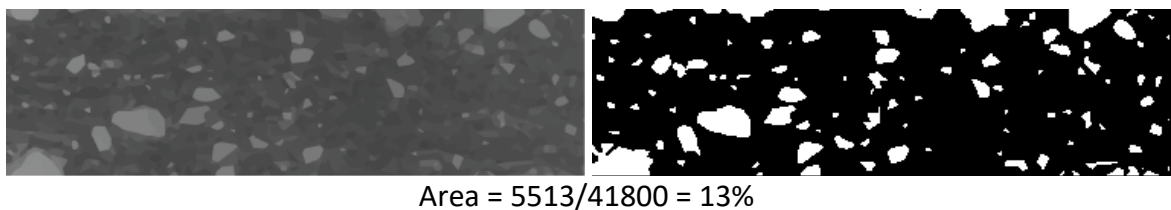
$$\text{Light minerals} = 25.30/118.54 = 21\%$$

$$\text{Dark minerals} = 0.04/118.54 = .03\%$$

$$\text{Total Crystal Content} = 21\%$$

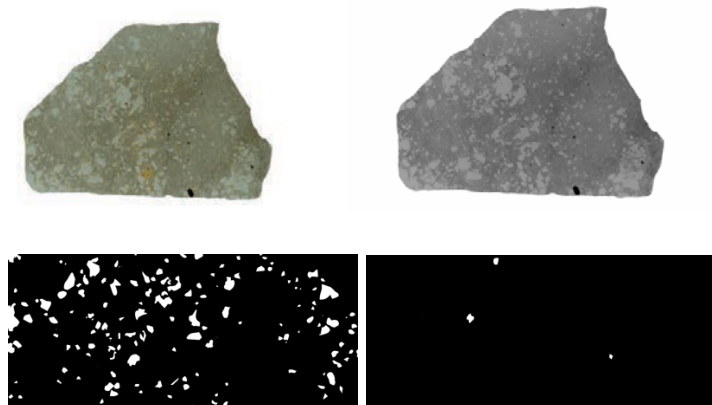
ORA-2A-002: *no mafic minerals*





$$\text{Area} = 5513/41800 = 13\%$$

ORA-2A-003:

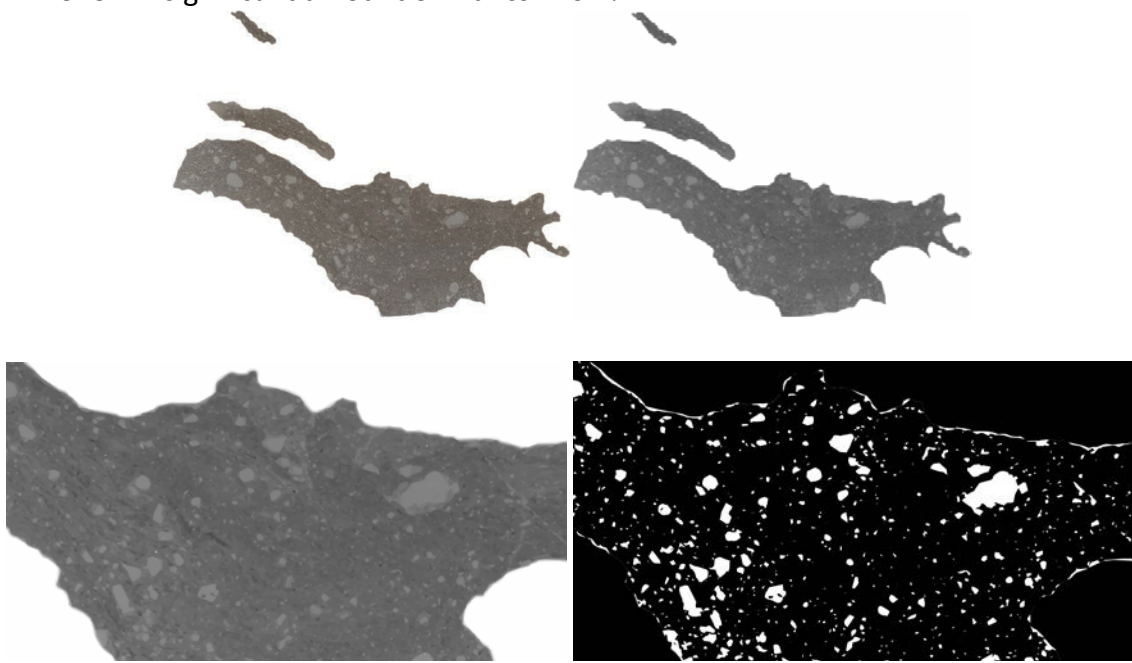


$$\text{Light minerals} = 2.85/37.93 = 7.5\%$$

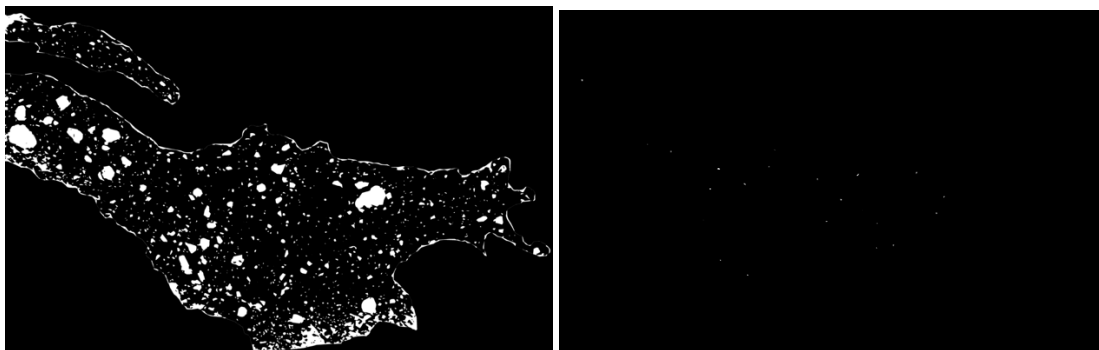
$$\text{Dark minerals} = 0.057/37.93 = 0.15\%$$

$$\text{Total Crystal Content} = 7.7\%$$

ORA-2A-016: *insignificant amount of mafics* <0.1%

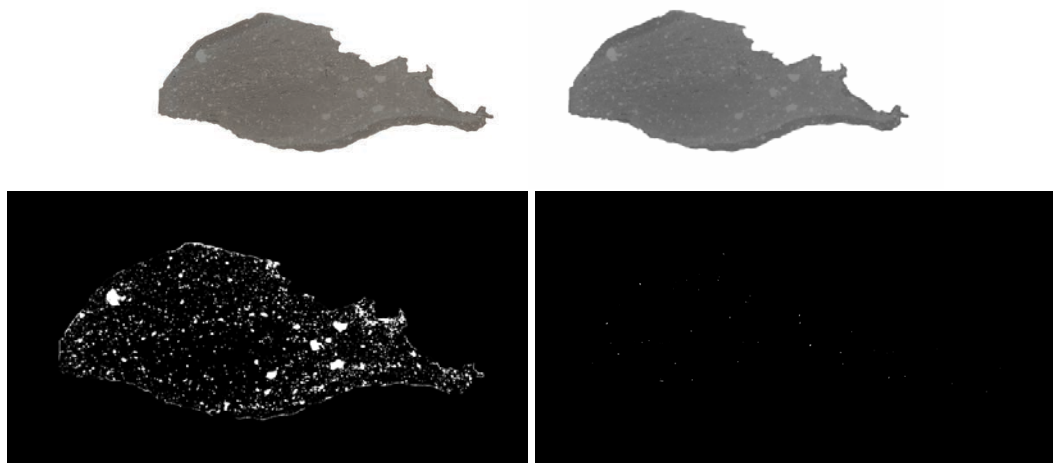


$$\text{Light minerals} = 4.51/45.56 = 9.9\%$$



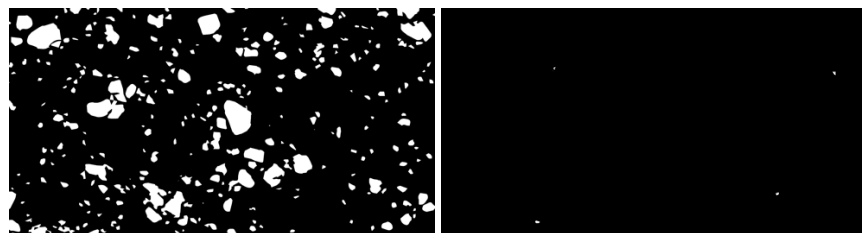
Light minerals = $9.67/74.30 = 13\%$
Dark minerals = $0.02/74.30 = 0.03\%$
Total Crystal Content = 13.03%

ORA-2A-023: *insignificant amount of mafics* <0.1%



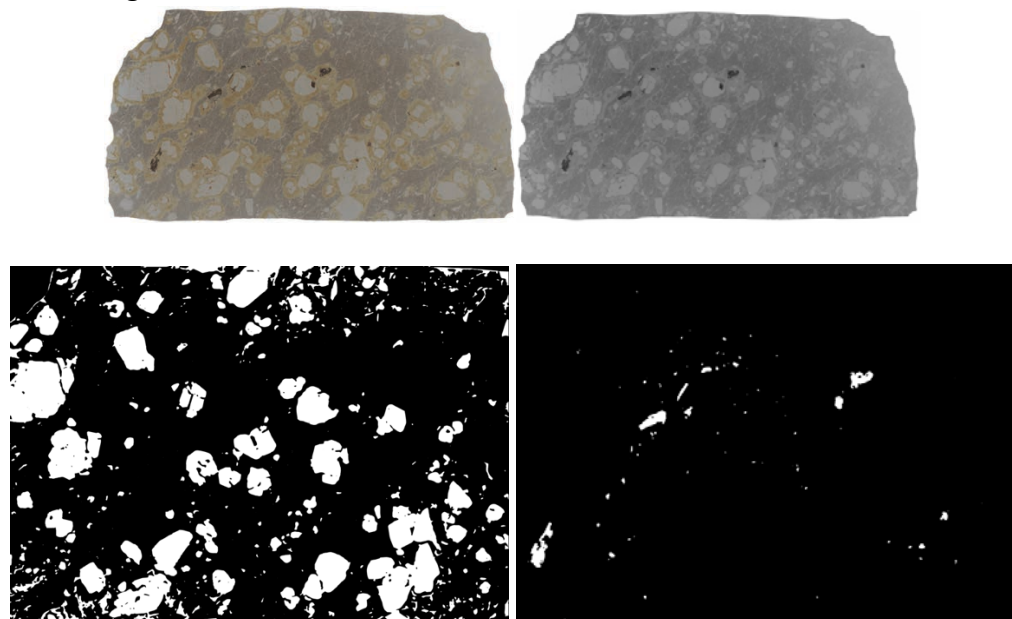
ORA-2A-024: *insignificant amount of mafics* <0.1%





Light minerals = $8.8/71.47 = 12.3\%$
Dark Minerals = $0.017/71.47 = 0.02\%$
Total Crystal Content = 12.32%

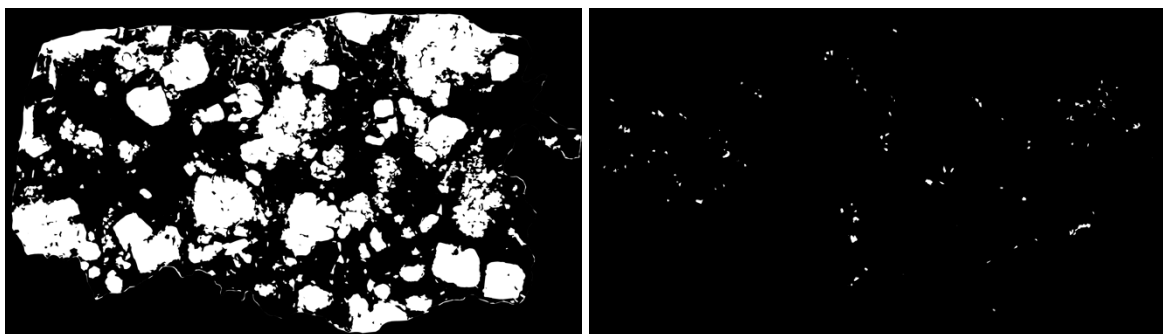
ORA-2A-031: *insignificant amount of mafics* <0.1%



Light minerals = $42.44 / 202.59 = 20.9\%$
Dark minerals = $1.54/202.59 = 0.07\%$
Total Crystal Content = 20.97%

ORA-2A-032:



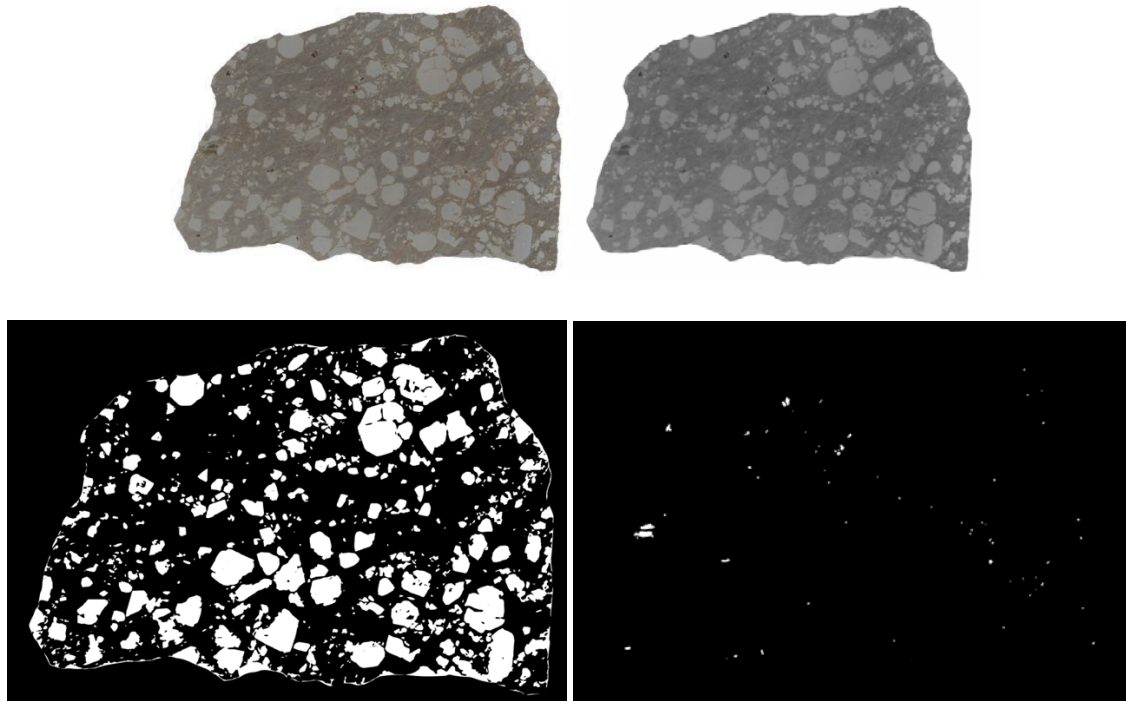


Light minerals = 123.08/319.98 = 38.5%

Dark minerals = 1.36/319.98 = 0.42%

Total Crystal Content = 38.92%

ORA-2A-035:

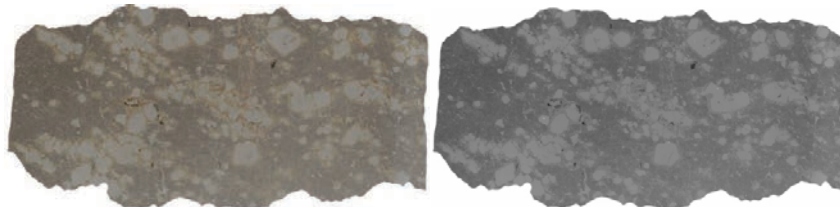


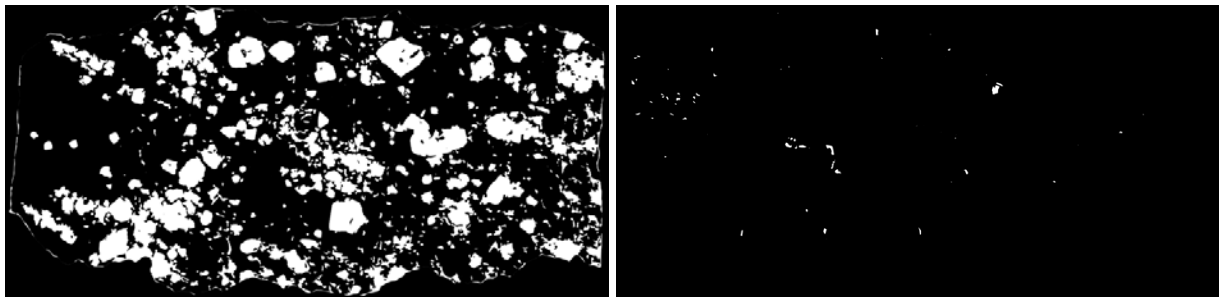
Light minerals = 69.67/241.13 = 28.89%

Dark minerals = 0.63/241.13 = 0.26%

Total Crystal Content = 29.15%

ORA-2A-040:



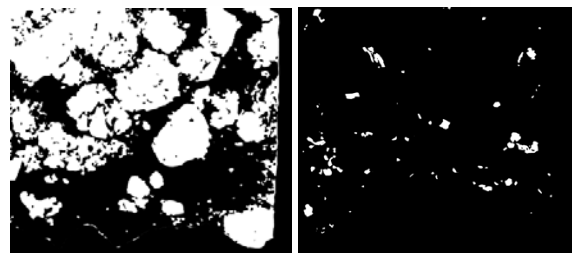
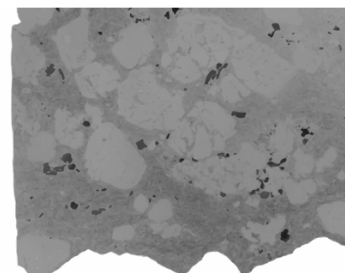


Light minerals = $77.53/299.32 = 25.9\%$

Dark minerals = $0.62/299.32 = 0.21\%$

Total Crystal Content = 26.1%

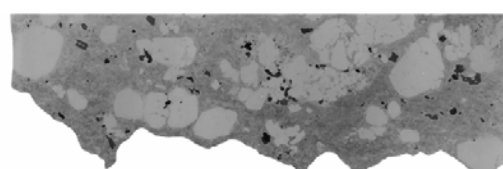
ORA-5B-402:

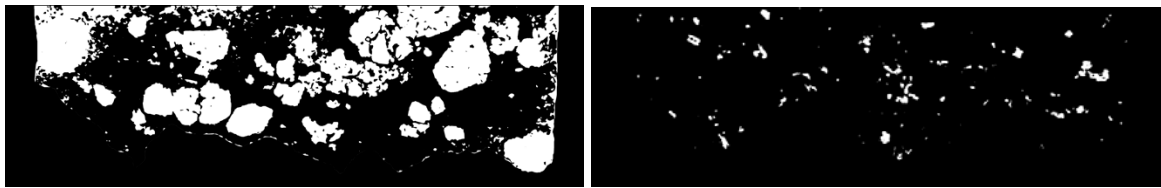


Light minerals = $71.75/144.32 = 49.7\%$

Dark minerals = $3.22/144.32 = 2.2\%$

Total Crystal Content = 51.9%





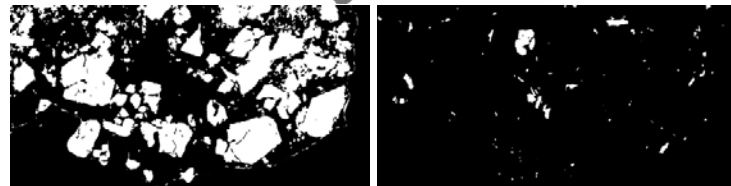
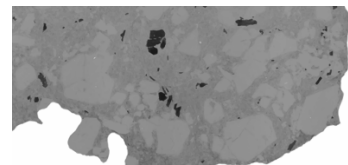
Light minerals = $68.83/178.61 = 38.5\%$

Dark minerals = $4.52/178.61 = 2.5\%$

Total Crystal Content = 41%

Average of the two is 46%

ORA-5B-404A:

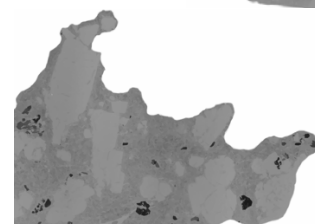
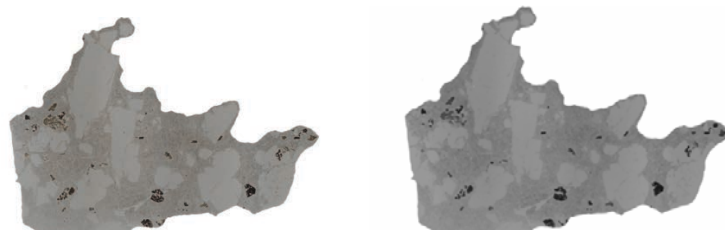


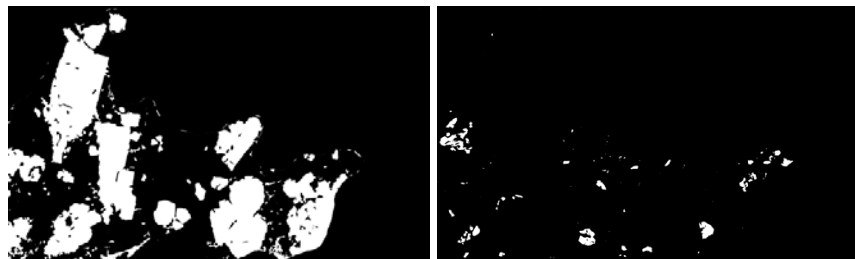
Light minerals = $81.95/193.76 = 42.3\%$

Dark minerals = $4.37/193.76 = 2.3\%$

Total Crystal Content = 44.6%

ORA-5B-404B:



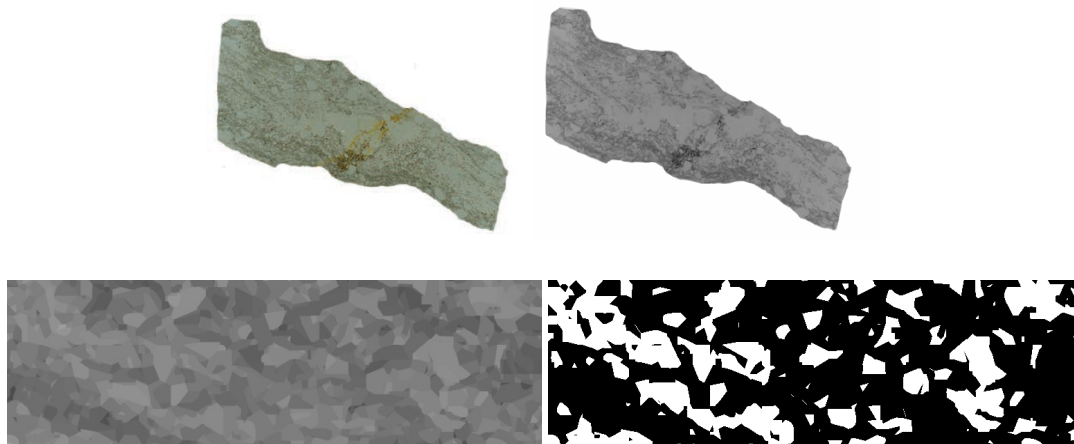


$$\text{Light minerals} = 67.81/160.94 = 42.13\%$$

$$\text{Dark minerals} = 4.04/160.94 = 2.5\%$$

$$\text{Total Crystal Content} = 44.6\%$$

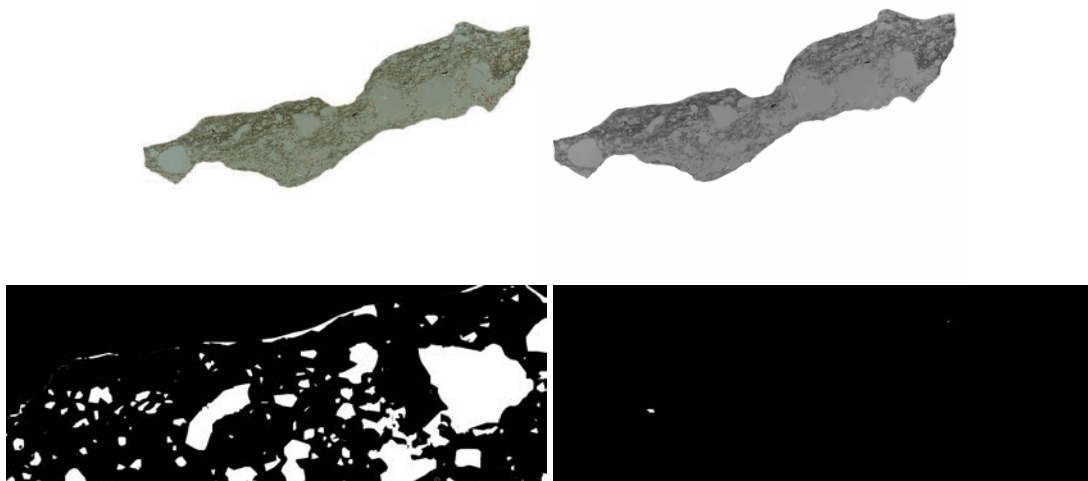
ORA-5B-412A: *insignificant amount of mafics* <0.1%



$$\text{Light minerals} = 0.443/2.071 = 21.4\%$$

$$\text{Mafic minerals} = 0$$

ORA-5B-412B:

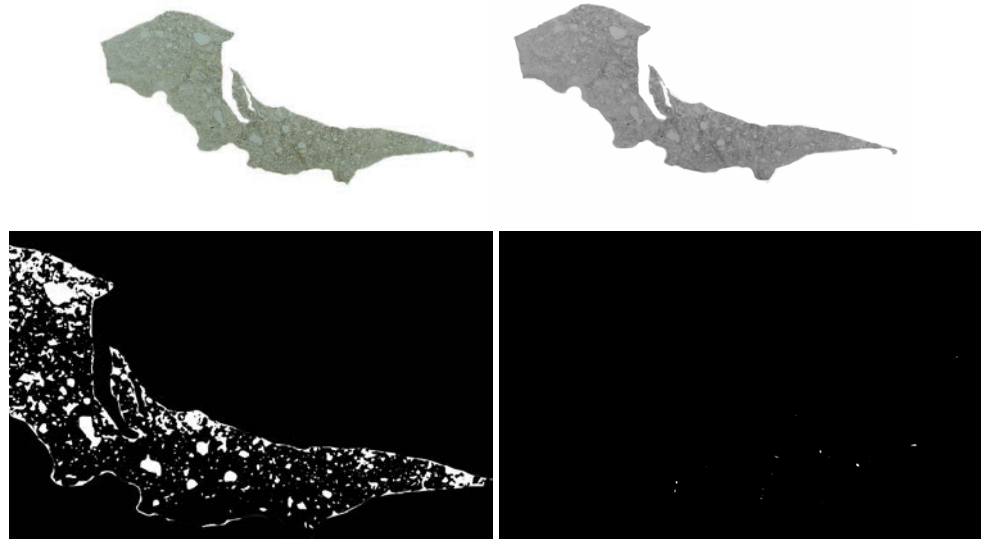


$$\text{Light minerals} = 1.63/7.17 = 23\%$$

$$\text{Dark minerals} = 0.002/7.172 = 0.03\%$$

Total Crystal Content = 23.03%

ORA-5B-414:



$$\text{Light minerals} = 3.4/16.1 = 21.3\%$$
$$\text{Dark minerals} = 0.01/16.14 = 0.06\%$$
$$\text{Total Crystal Content} = 21.3\%$$

B. Mineral Textures

Quartz

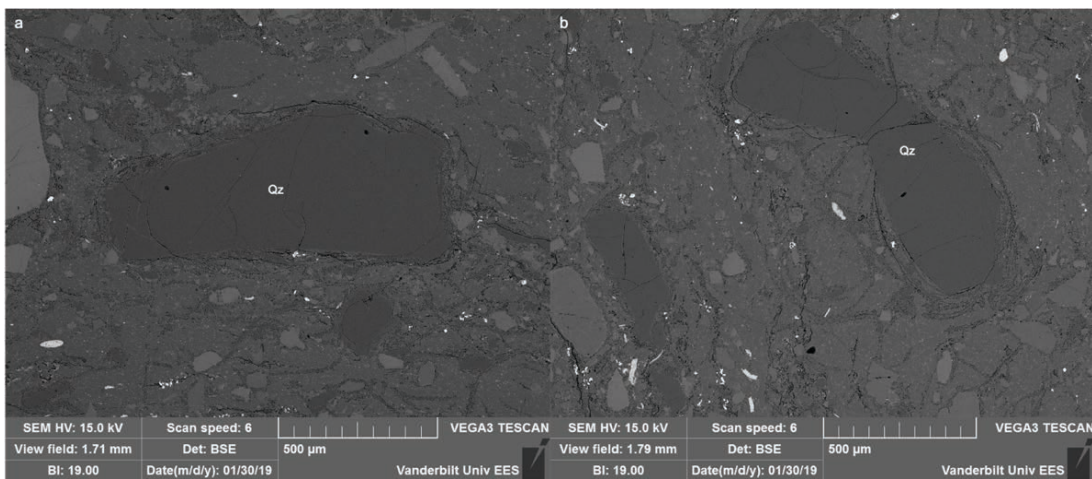


Figure 1: BSE images of small (≤ 1 mm), anhedral quartz in the FG fiamma, ORA-5B-412B.

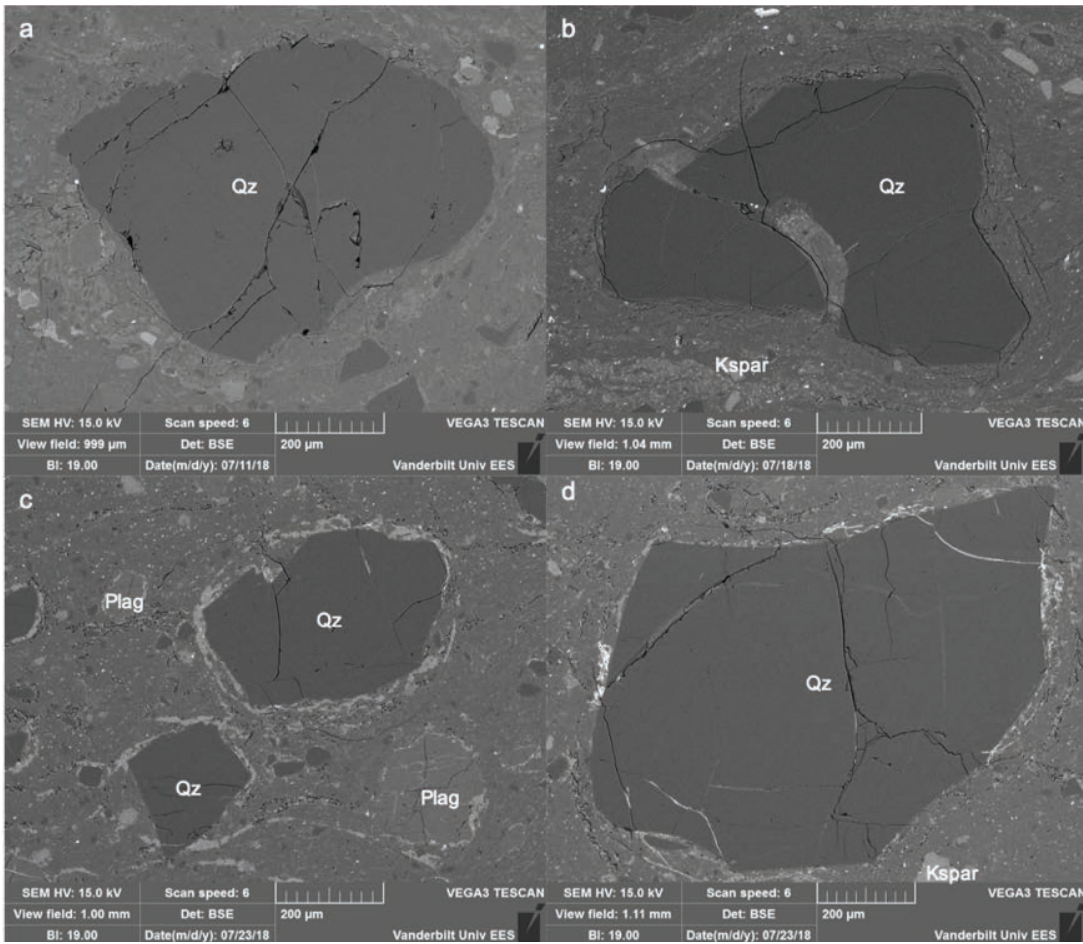


Figure 2: BSE images of small (<1 mm), anhedral quartz in FGCP fiamme (A) ORA-2A-002. (B) Quartz from ORA-2A-016 is slightly resorbed. (C-D) ORA-2A-023.

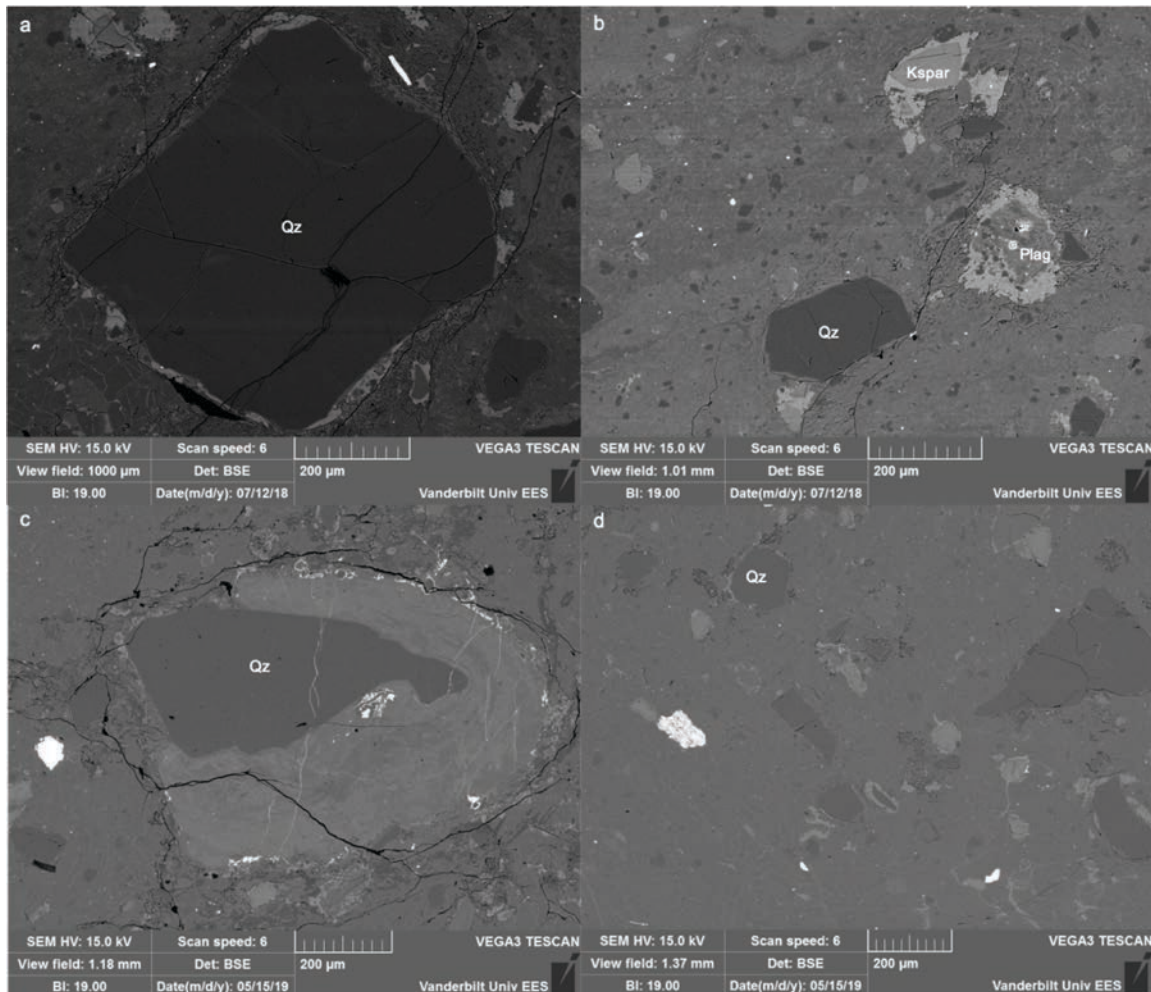


Figure 3: BSE images of small (<1 mm), anhedral quartz in FGCP fiamme (A-B) ORA-2A-002. (C-D) ORA-2A-003.

Alkali Feldspar

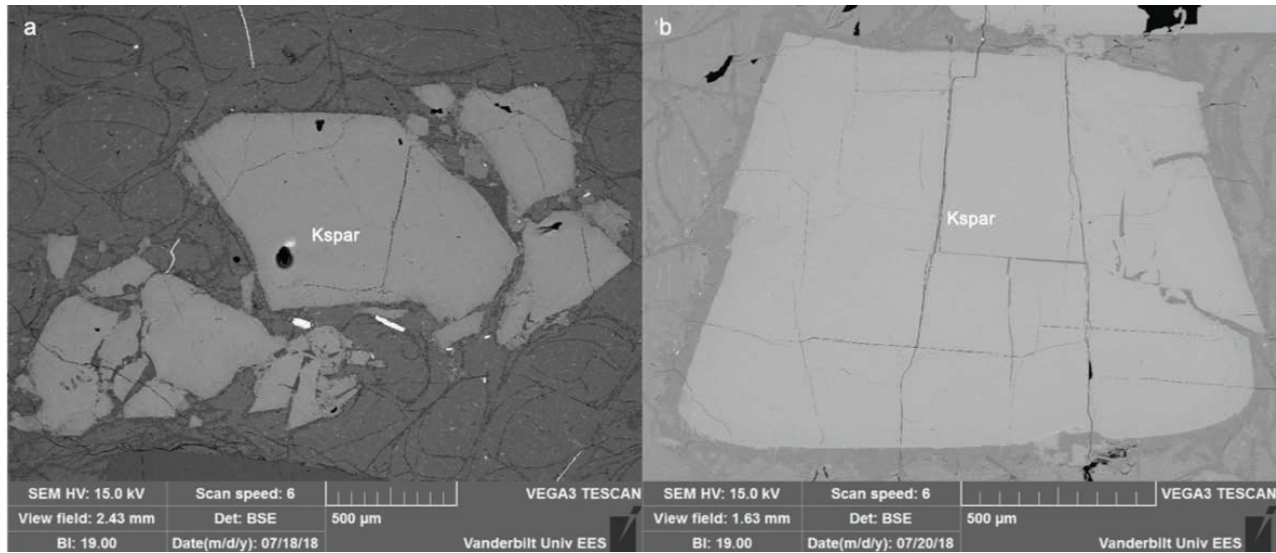


Figure 4: BSE images of alkali feldspar in VCCR fiamme (A) Alkali feldspar from ORA-5B-402 is broken into multiple pieces (B) Alkali feldspar from ORA-5B-404B shows fractures at $\sim 90^\circ$.

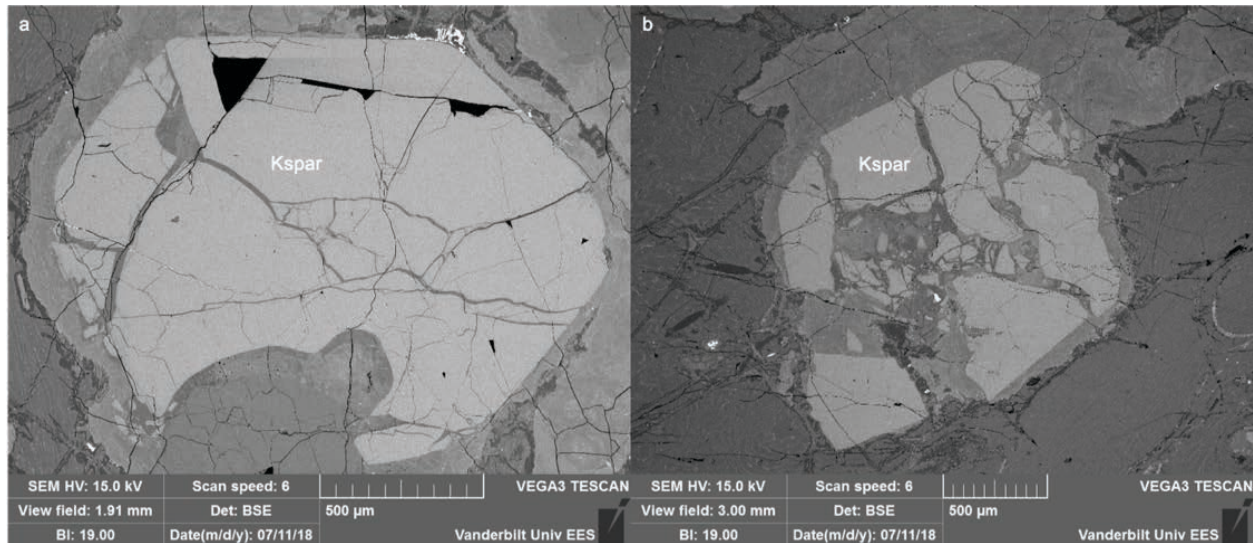


Figure 5: BSE images of highly fractured alkali feldspar rimmed in devitrified glass. These are from the MG fiamma, ORA-2A-001.

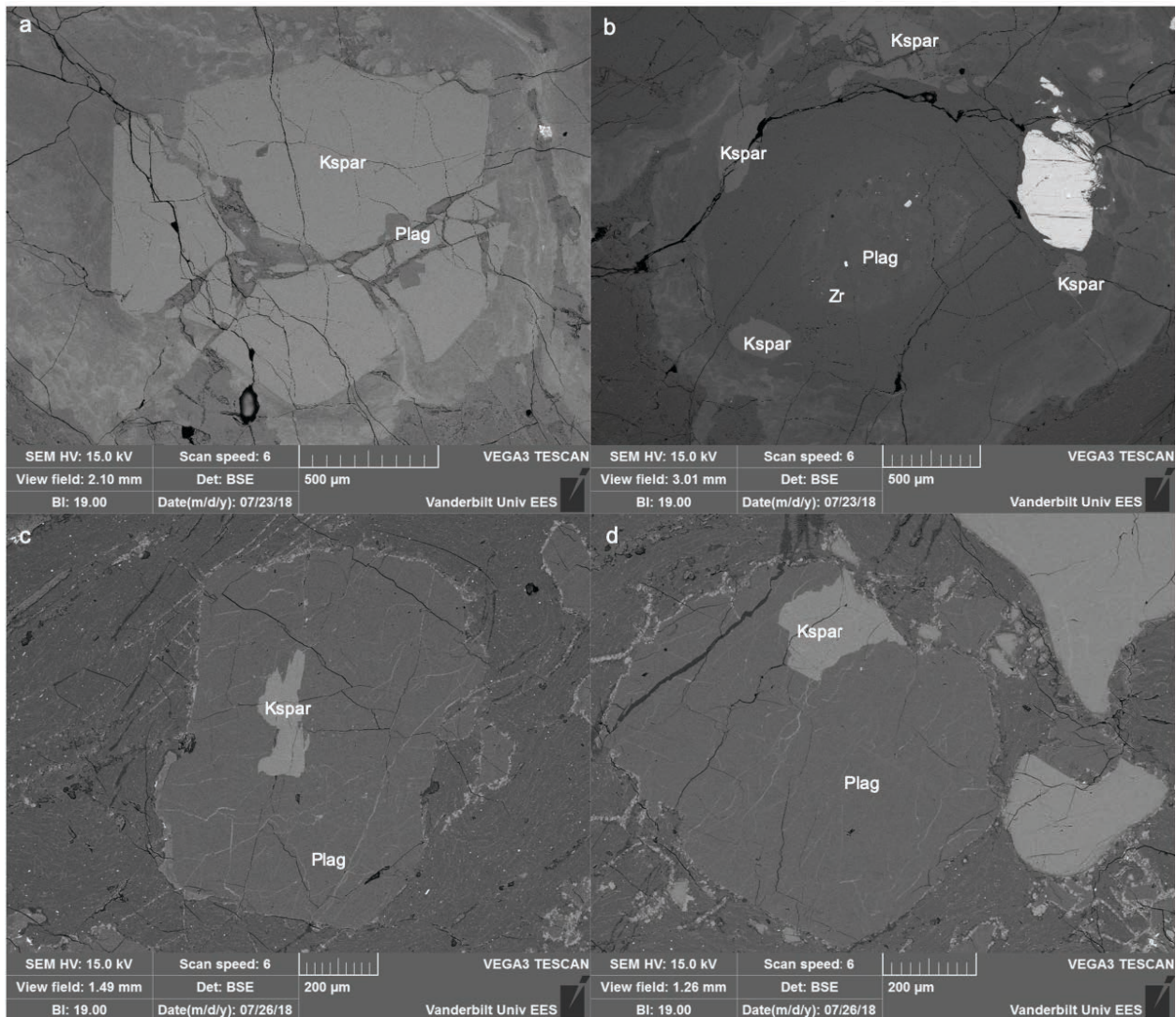


Figure 6: BSE images of alkali feldspar exhibiting an interlocking growth texture with plagioclase in MG fiamme. (A) ORA-2A-031. (B) ORA-2A-031. (C-D) ORA-2A-035.

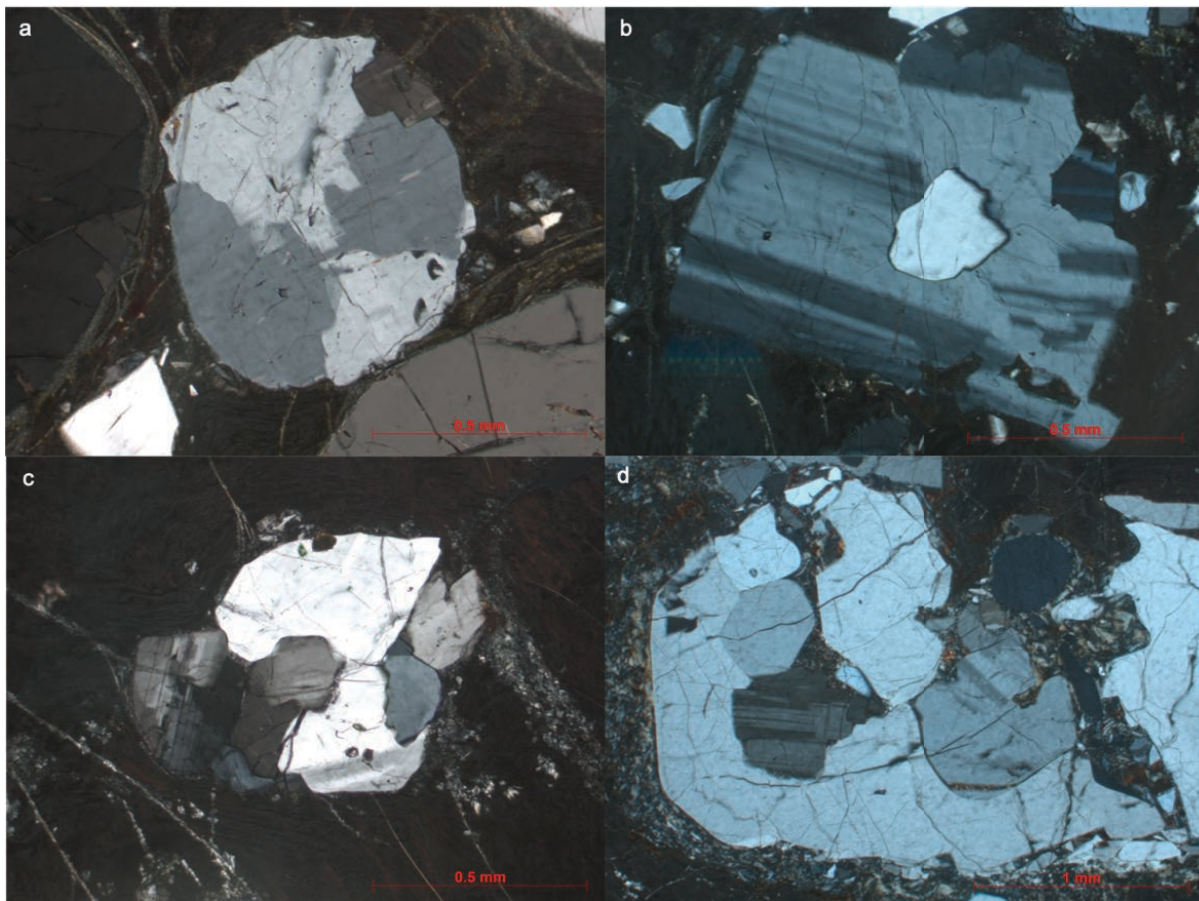


Figure 7: XPL images of alkali feldspar exhibiting interlocking growth texture with plagioclase in MG fiamme. (A-B) ORA-2A-035 (C-D) ORA-2A-032.

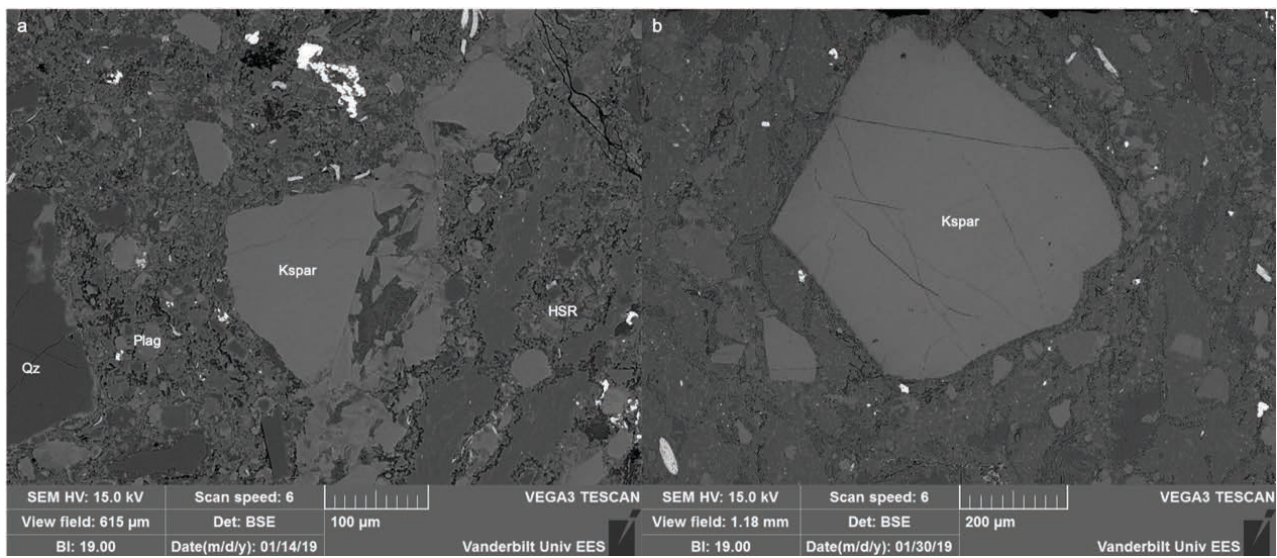


Figure 8: BSE images of alkali feldspar in FG fiamme. (A) A fractured alkali feldspar in ORA-5B-412A. (B) ORA-5B-412B. Note their small (<1 mm) size.

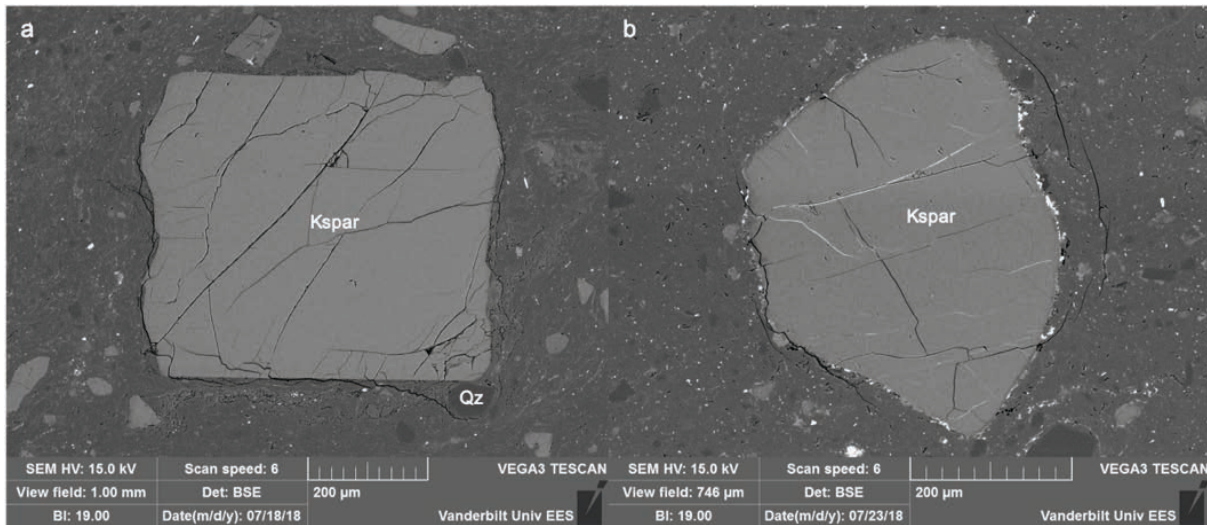


Figure 9: BSE images of fractured alkali feldspar in FGCP fiamme. (A) ORA-2A-016 (B) ORA-2A-023. Note their small (<1 mm) size.

Plagioclase

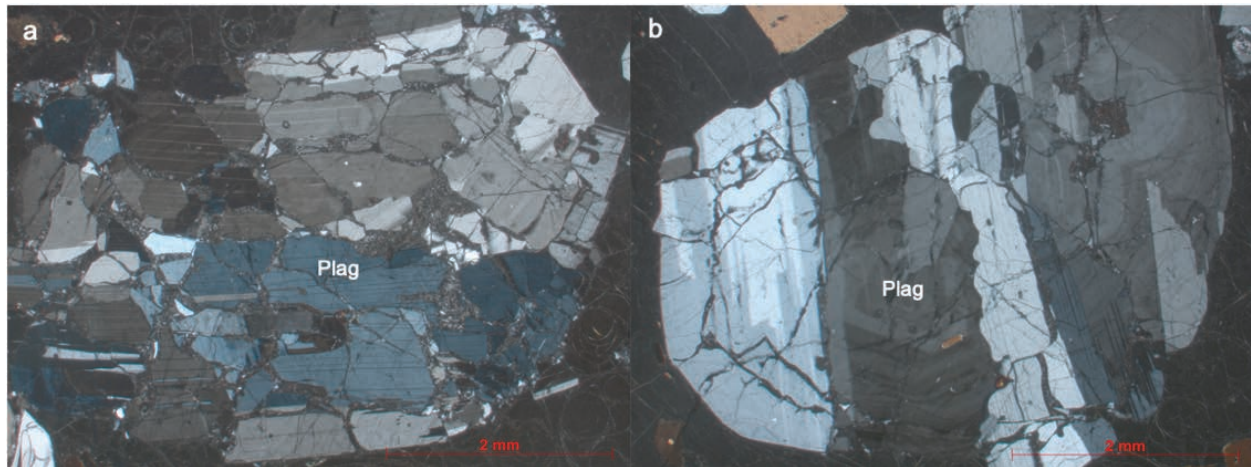


Figure 10: Plagioclase under XPL from ORA-5B-402. These grains are fractured. (B) Plagioclase shows clear zonation.

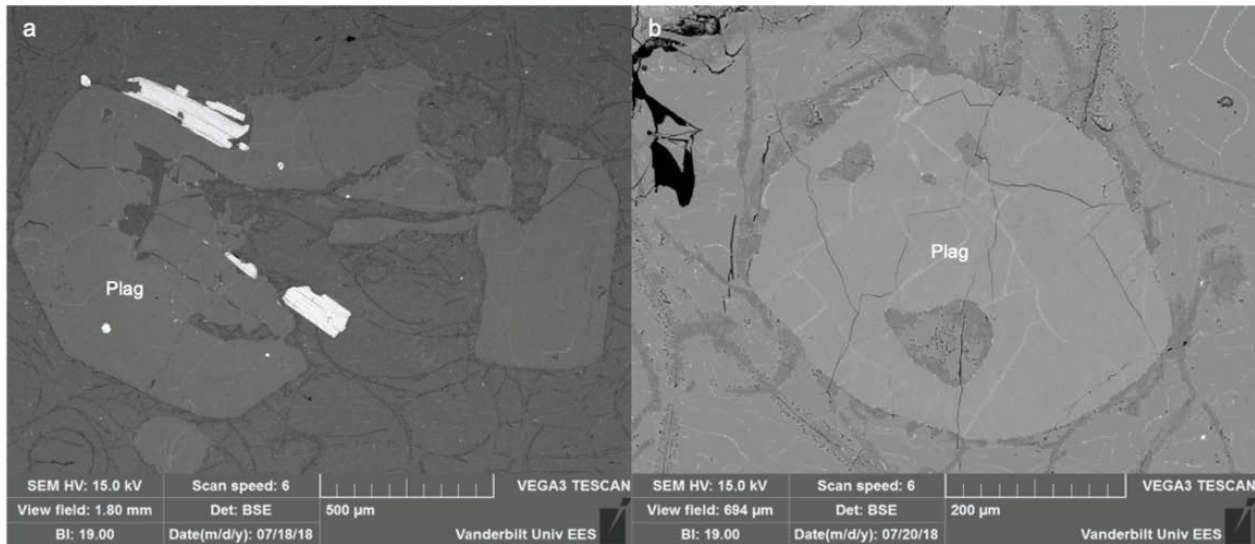


Figure 11: Plagioclase BSE images. Note the dissolution present. (A) ORA-5B-402 (B) ORA-5B-404B.

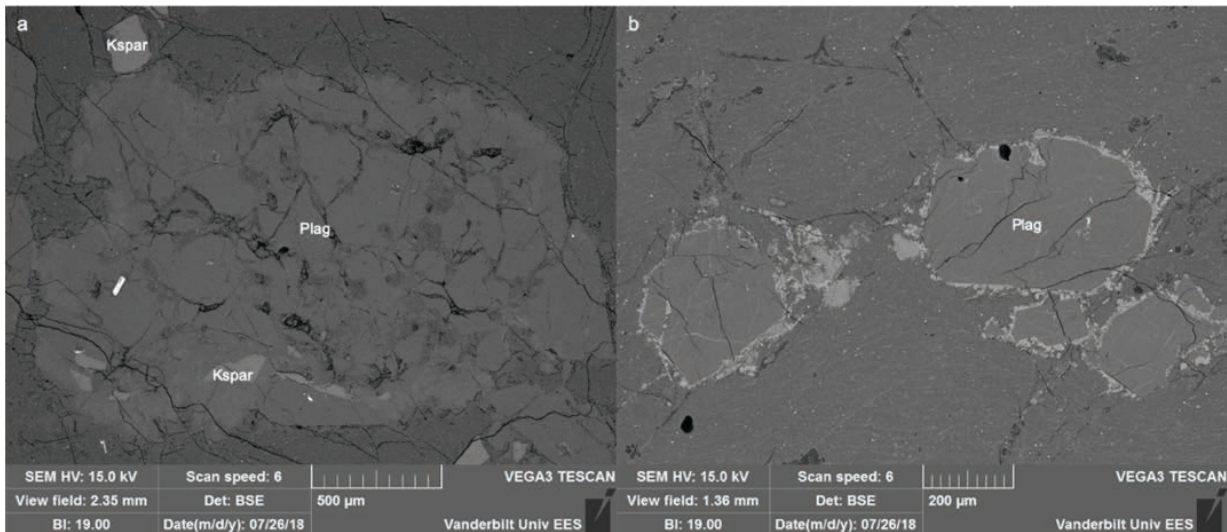


Figure 12: BSE images of plagioclase. (A) Plagioclase in ORA-2A-032 is sieve textured and fractured with minor alkali feldspar intergrowths. (B) Plagioclase in ORA-2A-035 is rimmed in a lighter colored material.

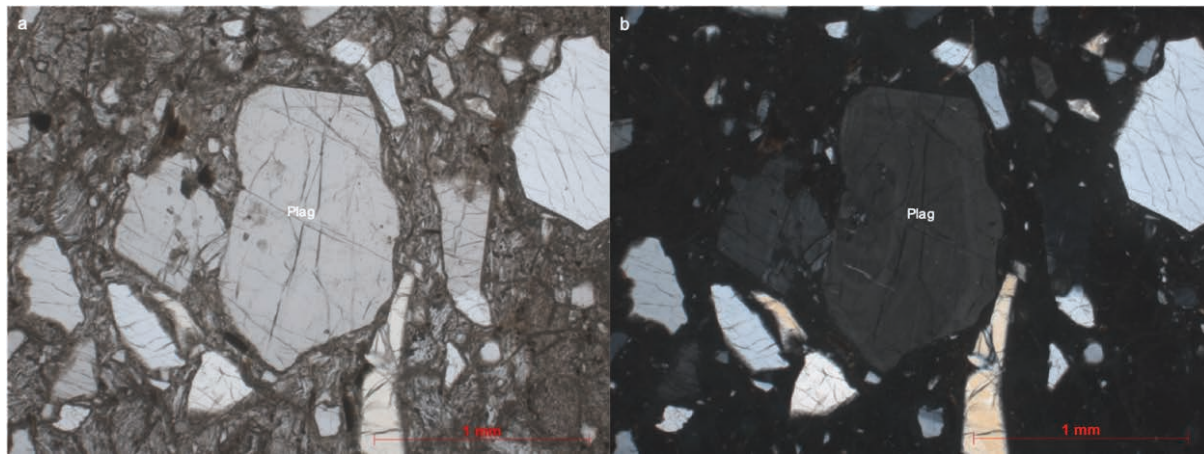


Figure 13: Small (<1 mm), fractured, anhedral plagioclase in PPL and XPL (A-B) ORA-5B-412B.

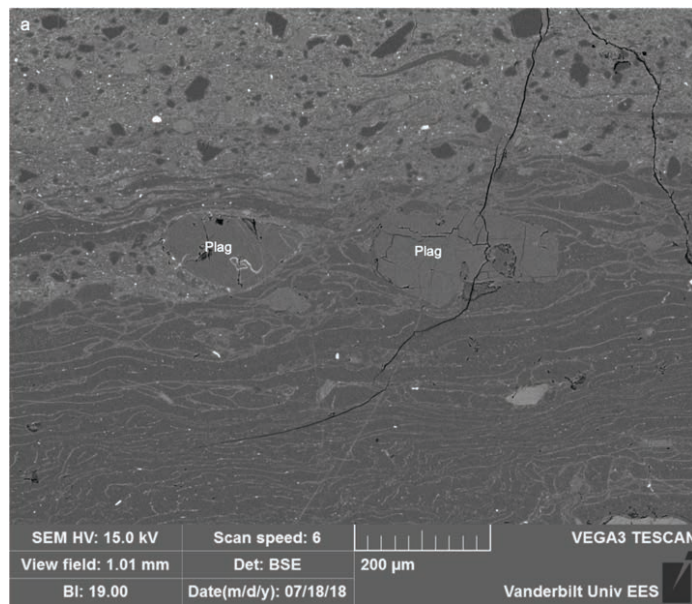


Figure 14: BSE image of small (<1 mm) anhedral plagioclase in ORA-2A-016.

Biotite

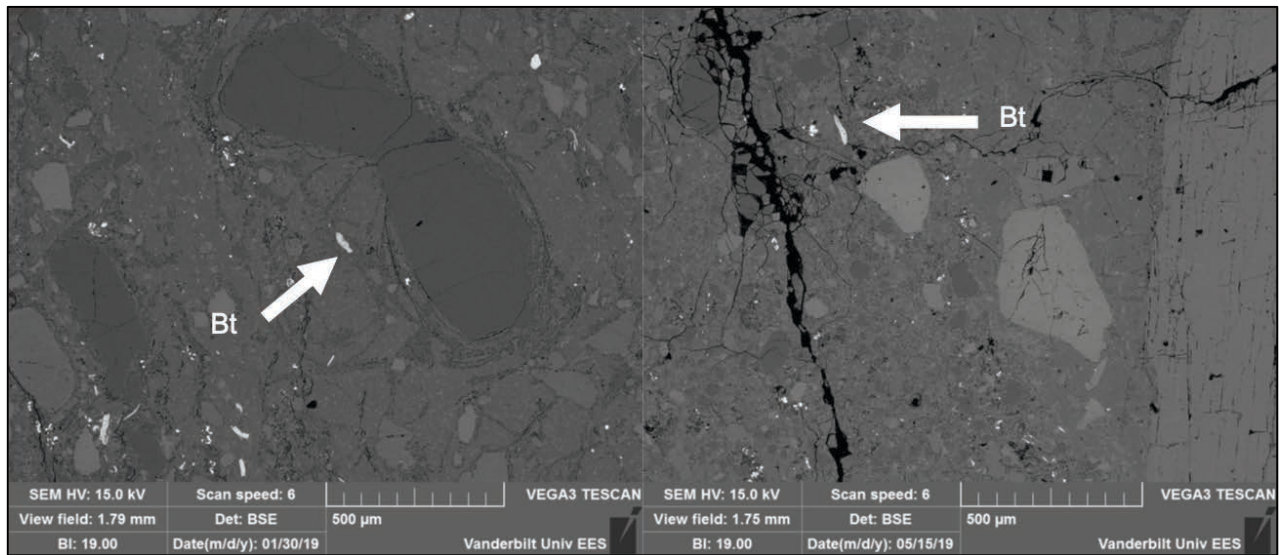


Figure 15: BSE images of biotite in FG fiamme. (A) ORA-5B-412B (B) ORA-5B-414.

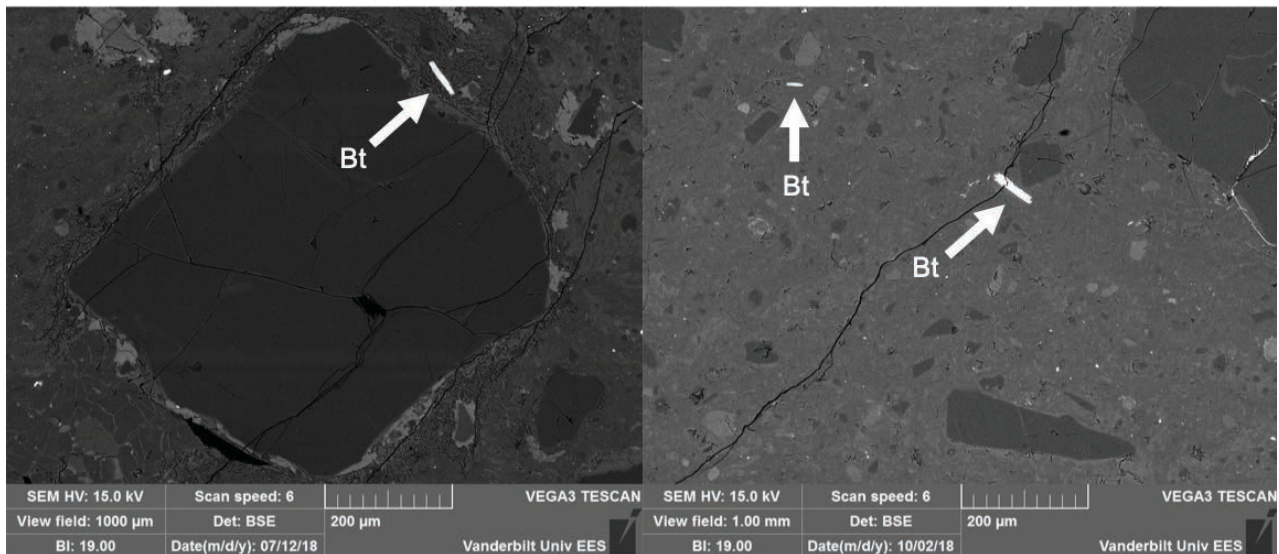


Figure 16: BSE images of small, elongated biotite in ORA-2A-002.

Fayalite

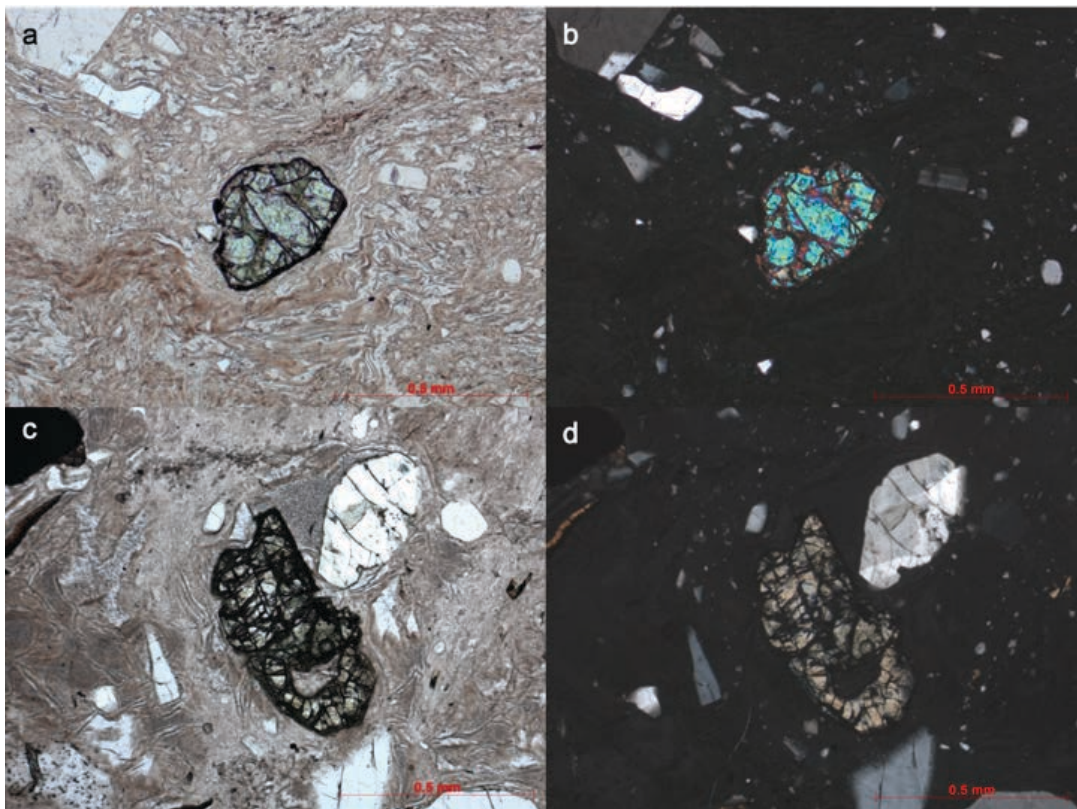


Figure 17: Fayalite with OPX replacement in PPL and XPL (A-B) ORA-2A-024 (B-C) ORA-2A-003.

Accessory Minerals:

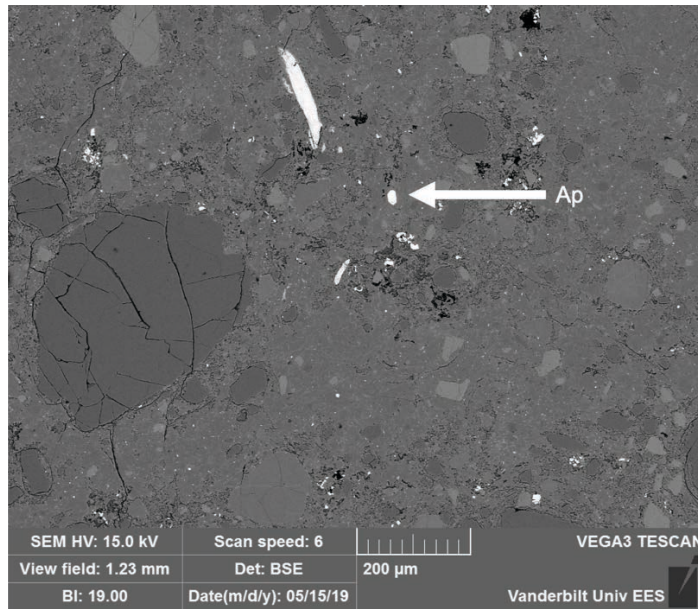


Figure 18: A BSE image of apatite (Ap) in ORA-5B-414.

C. Fine-Grained Crystal-Poor Fiamme Glass Types

ORA-2A-002

ORA-2A-002 has three separate glass populations: type 1, type 2, and undifferentiated ORA-2A-002. Glass type 1 and 2 have been differentiated based upon textural evidence and elemental compositions (Fig. 1, 2, 3). The remaining glass, labelled as ORA-2A-002 on figure 1, lacked any of the diagnostic textural features of the two glass types so it is grouped into a broad, undifferentiated category.

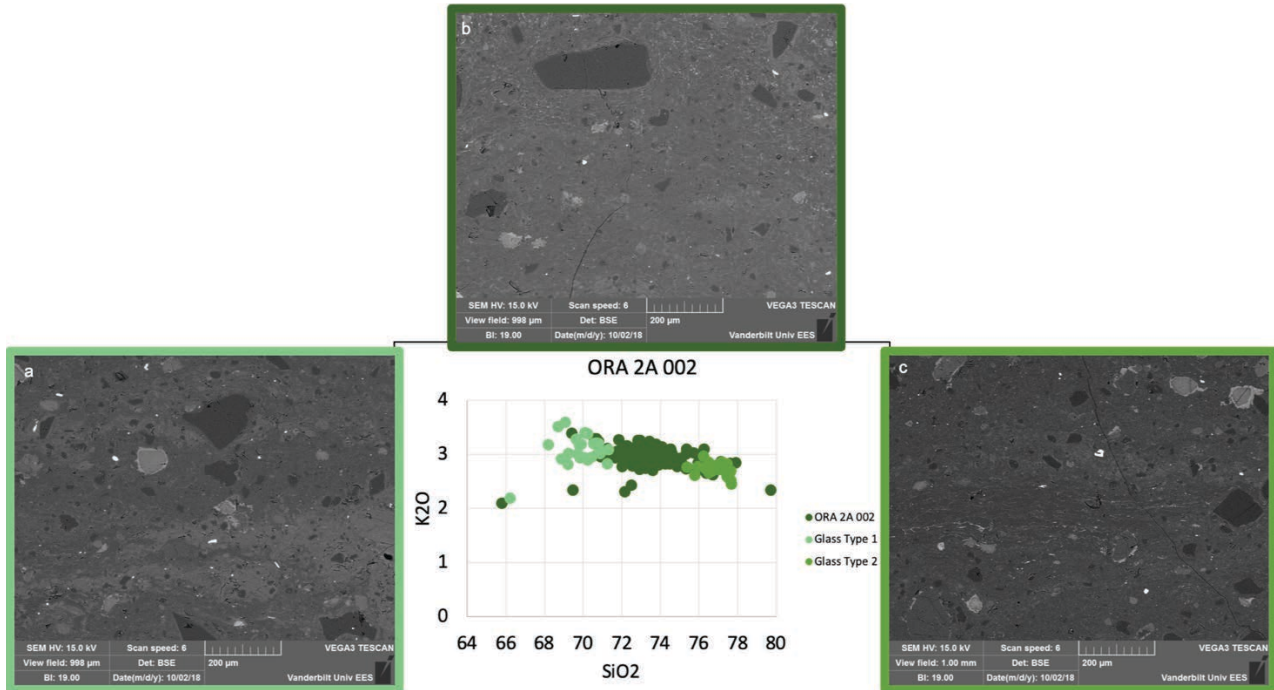


Figure 1: K₂O vs. SiO₂ for ORA-2A-002. The colored border on each of the photographs matches each glass type to its geochemical composition. (A) Type 1 ranges from ~68-72 wt. % SiO₂. (B) ORA-2A-002 is glass which cannot be texturally differentiated into either Type 1 or Type 2. It ranges from ~69-80 wt. % SiO₂. (C) Type 2 is constrained from 75-78 wt. % SiO₂.

The type 1 glass for ORA-2A-002 is the darkest in plane polarized light and tends to rim large crystals (Fig. 1, 2a). It also occurs along the border of the fiamma (Fig. 2b). The silica content ranges from ~68-72 wt. % SiO₂ and the K₂O ranges from ~2.75-3.5 wt. % K₂O. Enclosed within type 1 glass, there is abundant quartz even though the silica content is only ~70 wt.% SiO₂. All of the minerals, other than quartz, appear to have undergone partial dissolution (Appendix B) and are often rimmed with a lighter colored material that is around 67 wt.% SiO₂ and 16 wt.% K₂O.

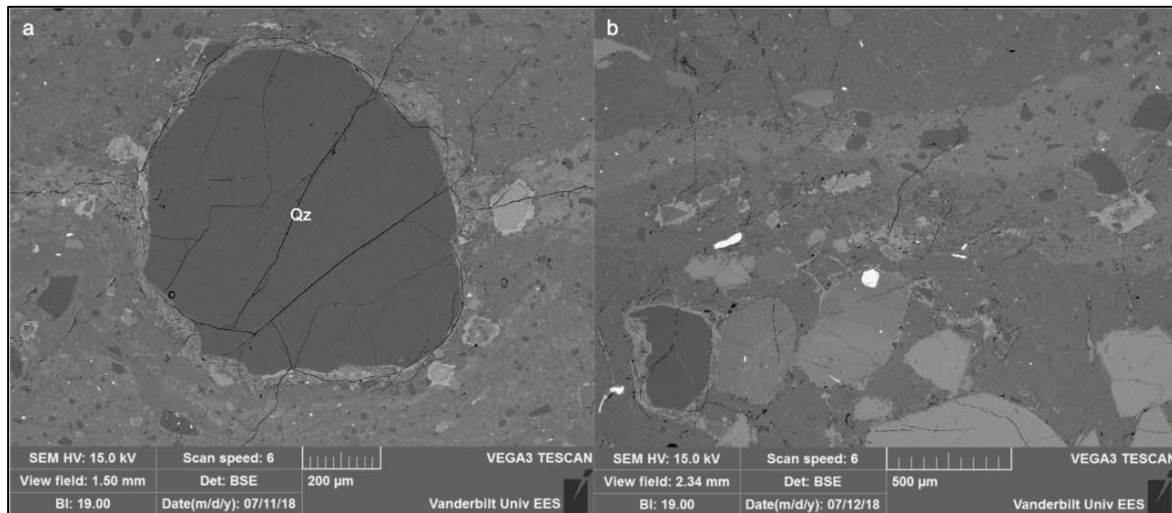


Figure 2: Type 1 glass for ORA-2A-002. This glass is the lightest grey in BSE images and has a silica content

The type 2 glass for ORA-2A-002 has a distinctive appearance. In plane-polarized light, it appears dark grey and wave-like textured (Fig. 3). In cross-polarized light, it is entirely extinct. This glass always has a high-silica rhyolite composition (~76-78 wt.% SiO₂). Compared to glass type 1, type 2 has a lower potassium content, ranging from 2.5-3 wt. % K₂O.

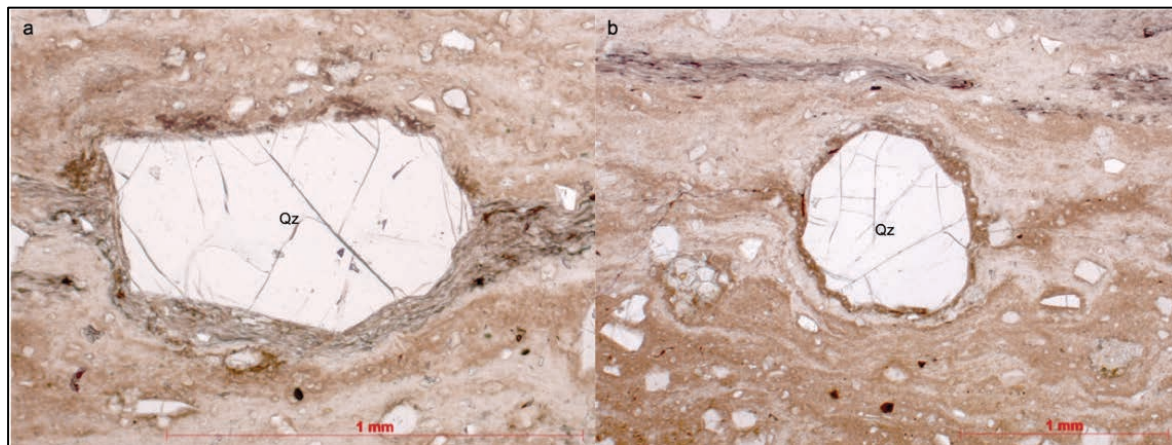


Figure 3: Type 2 glass for ORA-2A-002 in PPL.

ORA-2A-016

ORA-2A-016 has five discrete types of glass that can be differentiated based upon both textural observations and geochemical data. The remaining glass, labelled as ORA-2A-016 on figure 42 (Main Text), lacked any of the diagnostic textural features of the five glass types so it is grouped into a broad, undifferentiated category.

The type 1 glass ranges from ~67-74 wt. % SiO₂ and has a potassium content of ~1.75-3.25 wt. % K₂O (Fig. 42 (Main Text)). The large spread in silica content may be due to accidental incorporation of microlites during glass analysis.

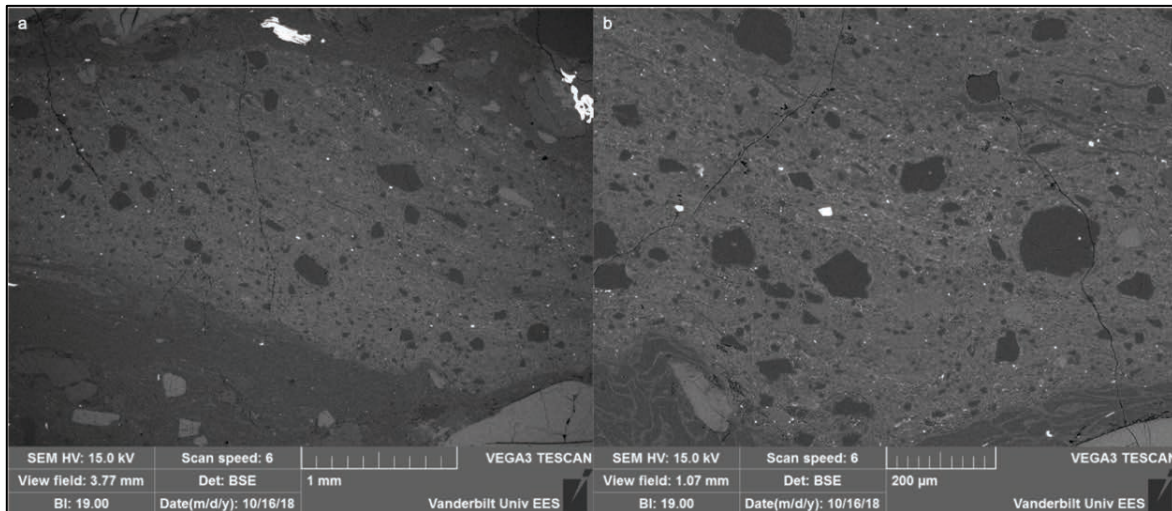


Figure 4: Type 1 glass for ORA-2A-016. Note the bimodal size distribution of quartz crystals.

ORA-2A-016's type 2 glass has a silica concentration from ~70-75 wt. % SiO₂ and a potassium content of ~1.5-3 wt. % K₂O (Fig. 42 (Main Text)). There are abundant microlites present, giving it a speckled appearance in BSE images (Fig. 5). These speckles are most likely microlites of either biotite or Fe-Ti oxides due to their light color in backscattered images.

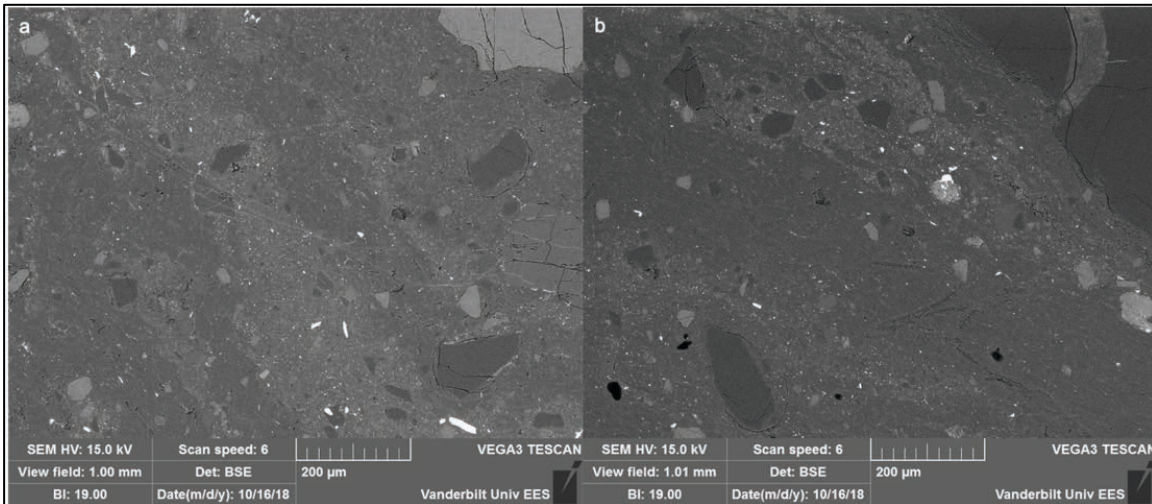


Figure 5: Type 2 glass for ORA-2A-016. It has a distinctive speckled appearance.

Glass type 3 appears as a single light grey bleb within the fiamma (Fig. 6). It ranges from 64-71 wt. % SiO₂ and has the lowest potassium content (0.5-1.25 wt. % K₂O) of any glass in the Ora Ignimbrite.

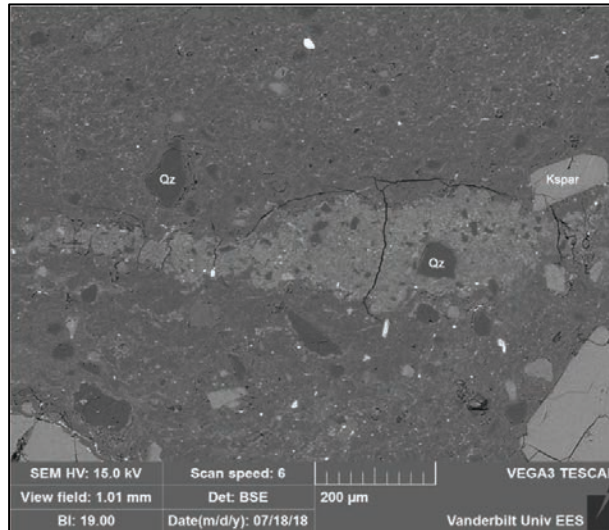


Figure 6: Type 3 glass for ORA-2A-016. This glass appears as a single bleb in the fiamma.

Glass type 4 is speckled and lighter in color, much like glass type 2 (Fig. 7). Like glass type 2, these speckles are most likely microlites of either biotite or Fe-Ti oxides due to their

light color in backscattered images. Differentiation between glass type 4 and glass type 2 is based on K₂O content; glass type 4 has a lower potassium content ranging from 0.75-2.25 wt. % K₂O whereas glass type 2 has higher potassium concentrations, ranging from ~1.5-3 wt. % K₂O (Fig. 42 (Main Text)). The silica content for glass type 4 ranges from 71-77 wt. % SiO₂.

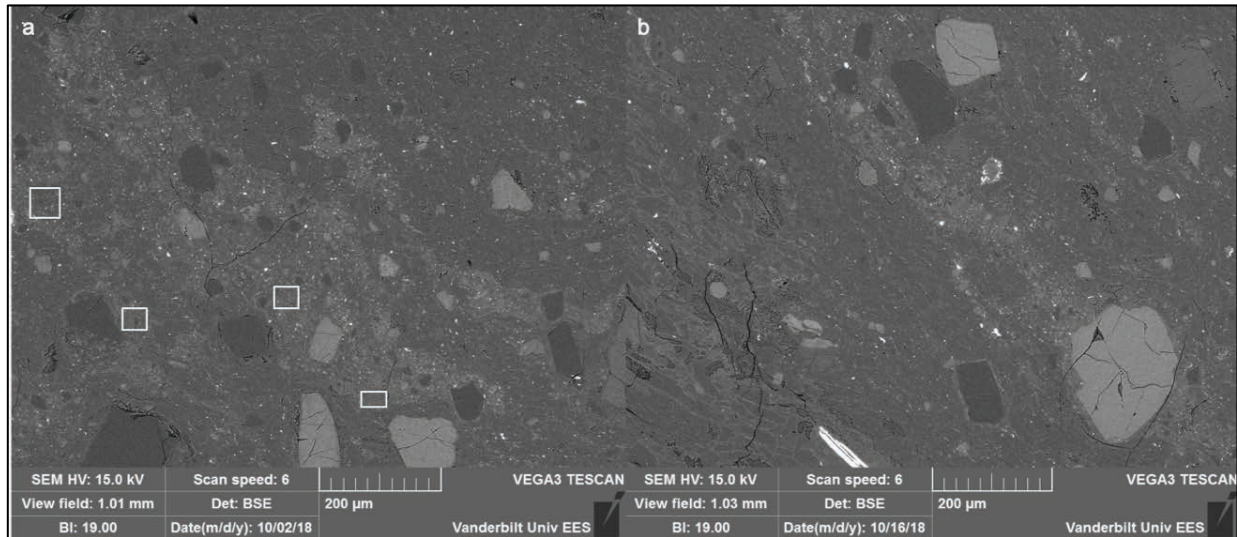


Figure 7: Type 4 glass for ORA-2A-016. (A) The white boxes represent glass type 4. (B) The entire thread of speckled glass is glass type 4.

Glass type 5 appears dark grey and wavy in PPL and is characteristically microlite-free (Fig. 8). It has a high-silica rhyolite signature (77-78 wt. % SiO₂) and has potassium concentrations ranging from 1.75-2.5 wt. % K₂O. Its appearance in PPL and its microlite-free nature is texturally similar to glass type 2 in ORA-2A-002 (Fig. 3).

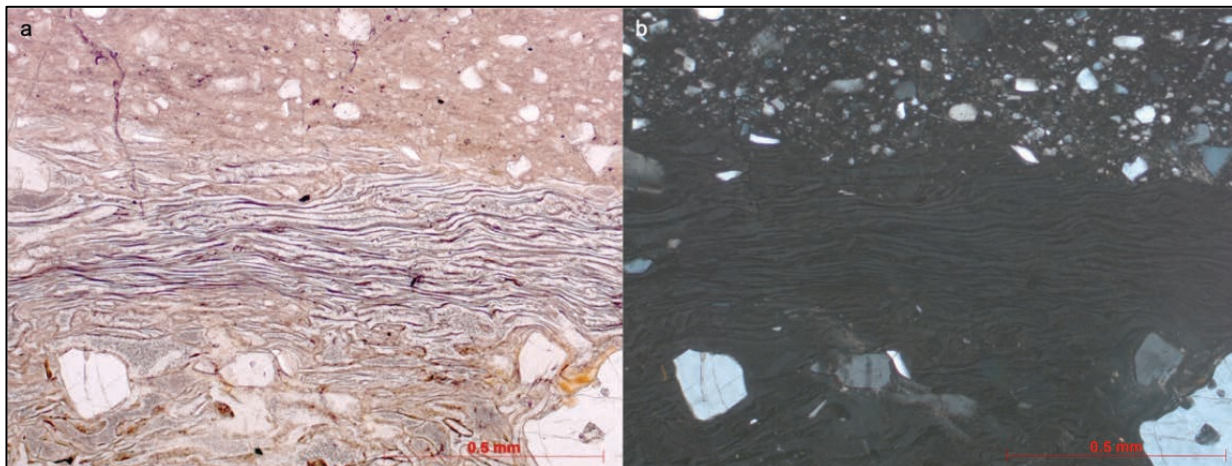


Figure 8: Type 5 glass for ORA-2A-016. (A) The dark grey, wavy texture of this glass in PPL. (B) Complete extinction shows the lack of microlites in XPL.

ORA-2A-024

The two types of glass in ORA-2A-024 are easily distinguished. The glass type 1 exhibits a darker color in PPL and appears as wavy blebs within the fiamma (Fig. 9, 10). In backscattered electron images, the type 1 glass has abundant microlites and exhibits a distinctive, speckled appearance (Fig. 9, 10). Glass type 1 is rhyolitic and ranges from 72-76 wt.% SiO₂. Its potassium concentration is from 2-3.5 wt. % K₂O (Fig. 9).

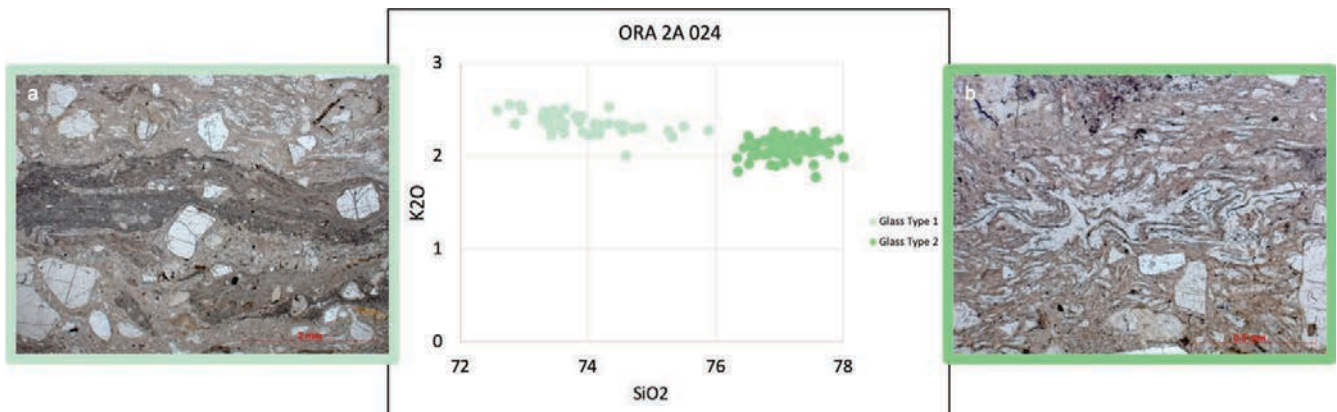


Figure 9: K₂O vs. SiO₂ for ORA-2A-024. The colored border on each of the photographs matches each glass type with its textural expression. (A) Type 1 (~72-76 wt. % SiO₂). (B) Type 2 (76-78 wt. % SiO₂).

Glass type 2 in ORA-2A-024 is texturally similar to the other high-silica rhyolite melts in the FGCP fiamme. It has a high-silica rhyolite silica concentration (76-78 wt. % SiO₂) and its potassium ranges from 1.75-2.25 wt. % K₂O (Fig. 9).

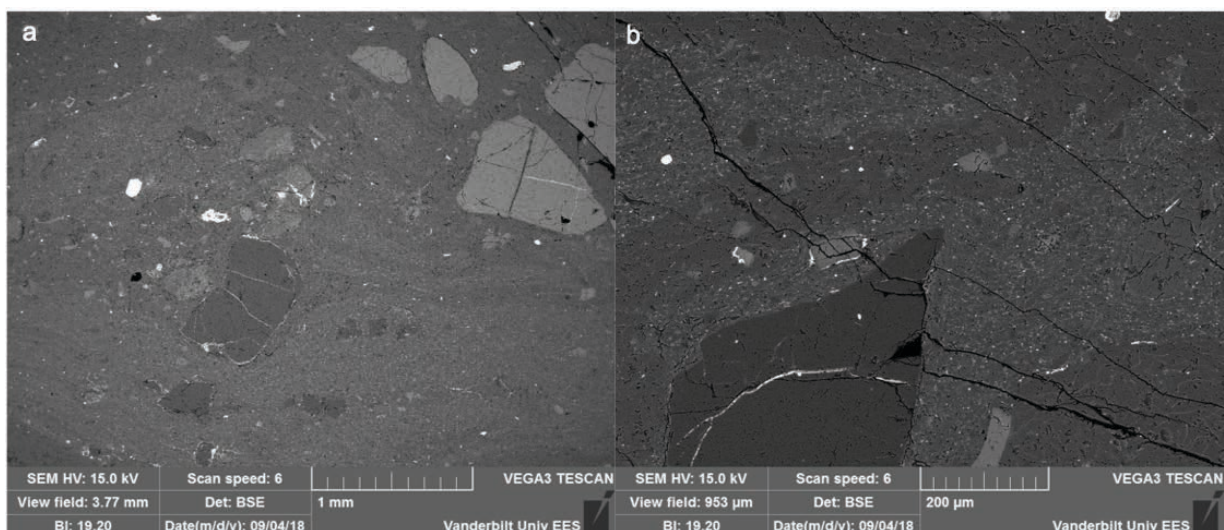


Figure 10: ORA-2A-024 illustrating the textural differences between glass Type 1 and glass type 2. Glass type 1 is the lighter, more microlite-rich subtype.

D. Glass Standard: USGS RGM-1

RGM-1	Na	Mg	Al	Si	K	Ca	Ti	Mn	Fe	Total
Average	4.12	0.26	14.07	74.05	4.31	1.21	0.31	0.04	1.63	100
1	4.25	0.26	13.96	74.08	4.37	1.16	0.3	0	1.63	100
2	4.23	0.25	13.87	73.96	4.28	1.3	0.44	0	1.68	100
3	4.07	0.24	14.14	74.14	4.27	1.28	0.25	0.04	1.57	100
4	4.18	0.3	14.2	74.1	4.22	1.17	0.35	0	1.49	100
5	4.13	0.24	14.25	74.05	4.36	1.14	0.21	0.17	1.46	100
6	4.2	0.25	14.17	73.99	4.34	1.13	0.36	0.08	1.49	100
7	4.02	0.31	14.12	74.09	4.34	1.2	0.3	0	1.62	100
8	4.07	0.3	13.94	73.97	4.34	1.26	0.35	0.05	1.73	100
9	4.03	0.23	14	74.01	4.29	1.19	0.3	0	1.95	100
10	4	0.28	14.05	74.14	4.26	1.27	0.28	0.06	1.67	100

E. Glass Major Element Compositions

ORA-2A-001:

Sample	Type	SiO ₂	TiO ₂	Al ₂ O ₃	MgO	FeO	MnO	CaO	Na ₂ O	K ₂ O	Total
ORA_2A_001	HSR	76.48	0.02	13.45	0	1.12	0	0.47	5.4	3.07	100
ORA_2A_001	HSR	76.71	0.08	13.25	0	0.96	0.14	0.44	5.42	2.88	99.87
ORA_2A_001	HSR	76.75	0.08	13.26	0	0.99	0.08	0.45	5.36	2.9	99.87
ORA_2A_001	HSR	76.8	0.22	13.25	0	1.09	0.05	0.48	5.19	2.93	100
ORA_2A_001	HSR	76.8	0.23	13.27	0	1.03	0.11	0.42	5.34	2.81	100
ORA_2A_001	HSR	76.88	0.11	13.36	0	1.05	0	0.33	5.23	3.04	100
ORA_2A_001	HSR	76.92	0.03	13.26	0.03	1.02	0.01	0.42	5.46	2.84	100
ORA_2A_001	HSR	76.95	0	13.23	0.01	1.08	0.09	0.36	5.5	2.77	100
ORA_2A_001	HSR	76.99	0.04	13.28	0	1.11	0	0.38	5.31	2.88	100
ORA_2A_001	HSR	77	0.04	13.08	0.02	0.92	0	0.36	5.39	3.05	99.85
ORA_2A_001	HSR	77	0.02	13.21	0.09	1.12	0	0.3	5.45	2.8	100
ORA_2A_001	HSR	77.01	0.02	13.17	0	1.17	0.03	0.37	5.42	2.82	100
ORA_2A_001	HSR	77.01	0	13.34	0.09	0.76	0.32	0.37	5.3	2.83	100
ORA_2A_001	HSR	77.02	0.07	13.07	0.06	0.83	0.06	0.39	5.36	2.98	99.85
ORA_2A_001	HSR	77.04	0	13.11	0.03	0.89	0.23	0.38	5.41	2.91	100
ORA_2A_001	HSR	77.04	0.18	13.31	0.03	0.78	0.09	0.37	5.35	2.84	100
ORA_2A_001	HSR	77.08	0.03	13.18	0.04	0.69	0.08	0.37	5.15	3.21	99.84
ORA_2A_001	HSR	77.09	0.1	13.08	0.01	1.12	0.11	0.29	5.36	2.84	100
ORA_2A_001	HSR	77.1	0.05	13.25	0.06	0.86	0	0.38	5.33	2.98	100
ORA_2A_001	HSR	77.12	0.04	13.13	0.02	0.78	0.16	0.48	5.33	2.94	100
ORA_2A_001	HSR	77.17	0.05	13.14	0.05	1.02	0.07	0.42	5.4	2.68	100
ORA_2A_001	HSR	77.19	0	13.36	0	0.81	0.06	0.4	5.4	2.79	100
ORA_2A_001	HSR	77.22	0	13.29	0.08	0.95	0.05	0.28	5.3	2.82	100
ORA_2A_001	HSR	77.23	0	13.14	0.04	1.07	0	0.4	5.31	2.82	100
ORA_2A_001	HSR	77.29	0	13.33	0	0.75	0	0.46	5.03	2.99	99.84
ORA_2A_001	HSR	77.32	0.22	13.15	0	0.87	0	0.33	5.25	2.85	100
ORA_2A_001	HSR	77.34	0.09	13.18	0.01	0.87	0	0.29	5.3	2.91	100
ORA_2A_001	HSR	77.35	0.08	13.27	0	0.84	0.06	0.27	5.35	2.78	100
ORA_2A_001	HSR	77.37	0	13.11	0.07	1.01	0.01	0.26	5.49	2.7	100
ORA_2A_001	HSR	77.37	0	13.41	0.03	0.68	0	0.35	5.46	2.71	100
ORA_2A_001	HSR	77.39	0	13.31	0	0.63	0.02	0.56	5.03	2.9	99.83
ORA_2A_001	HSR	77.57	0	13.25	0	0.53	0.15	0.34	5.36	2.8	100
ORA_2A_001	HSR	77.58	0	13.39	0	0.45	0	0.32	5.43	2.84	100
ORA_2A_001	HSR	77.59	0.1	13.22	0.01	0.54	0	0.26	5.43	2.85	100
ORA_2A_001	HSR	77.65	0.04	13.11	0	0.59	0	0.41	5.32	2.88	100
ORA_2A_001	HSR	77.67	0	13.17	0	0.67	0	0.34	5.37	2.78	100

ORA-2A-002:

Sample	Type	SiO ₂	TiO ₂	Al ₂ O ₃	MgO	FeO	MnO	CaO	Na ₂ O	K ₂ O	Total
ORA_2A_002	Glass (Type 1)	68.18	0.21	16.96	0.79	2.9	0.14	2.23	4.84	3.18	99.84
ORA_2A_002	Glass (Type 1)	68.68	0.36	16.83	0.74	3.29	0.16	2.19	4.24	3.51	100
ORA_2A_002	Glass (Type 1)	69.05	0.32	16.34	0.85	3.63	0.08	2.19	3.94	3.6	100
ORA_2A_002	Glass (Type 1)	69.61	0.34	16.45	0.7	2.76	0.04	2.07	4.64	3.28	99.89
ORA_2A_002	Glass (Type 1)	69.79	0.32	16.27	0.72	2.89	0	2.17	4.67	3.17	100
ORA_2A_002	Glass (Type 1)	70.06	0.26	16.39	0.72	2.21	0.21	2.12	4.64	3.4	100
ORA_2A_002	Glass (Type 1)	70.21	0.33	15.95	0.79	2.42	0.08	2.06	4.62	3.38	99.84
ORA_2A_002	Glass (Type 1)	70.53	0.3	16.38	0.71	2.27	0.02	2.12	4.48	3.2	100
ORA_2A_002	Glass (Type 1)	70.68	0.24	16.27	0.64	2.06	0.07	1.98	4.86	3.21	100
ORA_2A_002	Glass (Type 1)	70.76	0.27	16.12	0.54	2.22	0	2.06	4.83	3.19	100
ORA_2A_002	Glass (Type 1)	70.77	0.32	15.96	0.68	2.44	0.04	2.12	4.46	3.2	100

Sample	Type	SiO ₂	TiO ₂	Al ₂ O ₃	MgO	FeO	MnO	CaO	Na ₂ O	K ₂ O	Total
ORA_2A_002	Glass (Type 2)	66.2	0.34	19.25	0.44	2.13	0	3.26	6.19	2.19	100
ORA_2A_002	Glass (Type 2)	68.86	0.29	17.3	0.68	2.29	0.1	2.59	4.97	2.92	100
ORA_2A_002	Glass (Type 2)	69.2	0.39	17.14	0.62	2.73	0.03	2.23	4.85	2.82	100
ORA_2A_002	Glass (Type 2)	69.21	0.38	16.62	0.93	3.01	0	2.13	4.7	3.02	100
ORA_2A_002	Glass (Type 2)	69.71	0.36	16.36	0.77	2.89	0.03	2.06	4.82	3.01	100
ORA_2A_002	Glass (Type 2)	69.82	0.33	16.35	0.79	2.77	0.07	2.09	4.84	2.94	100
ORA_2A_002	Glass (Type 2)	69.87	0.23	16.43	0.8	2.71	0.2	2.12	4.44	3.19	100
ORA_2A_002	Glass (Type 2)	70.06	0.35	16.3	0.6	2.75	0.1	2.13	4.76	2.94	100
ORA_2A_002	Glass (Type 2)	70.22	0.28	16.26	0.85	2.74	0.07	1.98	4.7	2.9	100
ORA_2A_002	Glass (Type 2)	70.4	0.26	16.03	0.68	2.67	0.21	1.86	4.95	2.95	100
ORA_2A_002	Glass (Type 2)	70.82	0.26	15.85	0.68	2.57	0.03	1.83	4.89	3.07	100
ORA_2A_002	Glass (Type 2)	70.87	0.32	15.9	0.76	2.52	0	1.91	4.69	3.02	100
ORA_2A_002	Glass (Type 2)	71.22	0.47	15.94	0.65	2.12	0.05	2.11	4.6	2.83	100
ORA_2A_002	Glass (Type 2)	71.3	0.22	16.05	0.56	2.27	0.03	1.87	4.61	3.09	100

Sample	Type	SiO ₂	TiO ₂	Al ₂ O ₃	MgO	FeO	MnO	CaO	Na ₂ O	K ₂ O	Total
ORA_2A_002	HSR (Type 3)	75.37	0.13	14.35	0.3	0.64	0	1.71	4.73	2.77	100
ORA_2A_002	HSR (Type 3)	75.76	0.28	14.41	0.27	0.6	0.11	1.48	4.46	2.62	100
ORA_2A_002	HSR (Type 3)	75.92	0.25	13.62	0.14	1.35	0.07	0.95	4.92	2.78	100
ORA_2A_002	HSR (Type 3)	76.2	0.22	13.87	0.16	0.53	0.08	1.16	4.81	2.97	100
ORA_2A_002	HSR (Type 3)	76.33	0.09	13.18	0.12	1.59	0.12	0.83	5	2.74	100
ORA_2A_002	HSR (Type 3)	76.48	0.1	13.62	0.14	0.86	0	0.95	5	2.86	100
ORA_2A_002	HSR (Type 3)	76.5	0.15	13.73	0.09	0.76	0.02	0.82	5.25	2.67	100
ORA_2A_002	HSR (Type 3)	76.68	0.09	13.56	0.12	1.11	0	0.8	4.93	2.7	100
ORA_2A_002	HSR (Type 3)	76.74	0	13.5	0.06	1.11	0.01	0.77	5	2.8	100
ORA_2A_002	HSR (Type 3)	76.9	0.13	13.4	0.03	0.83	0.08	0.87	5.03	2.73	100
ORA_2A_002	HSR (Type 3)	77	0.12	13.2	0	1.09	0	0.86	4.91	2.82	100
ORA_2A_002	HSR (Type 3)	77.09	0	13.55	0.08	0.51	0.11	0.82	5.03	2.81	100
ORA_2A_002	HSR (Type 3)	77.13	0.05	13.22	0.04	0.9	0.23	0.72	4.98	2.73	100
ORA_2A_002	HSR (Type 3)	77.17	0	13.05	0.1	1.17	0.1	0.75	4.92	2.75	100
ORA_2A_002	HSR (Type 3)	77.18	0.09	13.07	0.01	0.93	0	0.93	4.93	2.86	100
ORA_2A_002	HSR (Type 3)	77.18	0	13.37	0.03	0.97	0	0.64	5.05	2.75	100
ORA_2A_002	HSR (Type 3)	77.26	0	13.36	0	0.76	0.14	0.69	5.07	2.74	100
ORA_2A_002	HSR (Type 3)	77.27	0	13.4	0	0.87	0	0.65	5.06	2.75	100
ORA_2A_002	HSR (Type 3)	77.38	0	13.03	0.02	1.02	0	1.03	4.7	2.82	100
ORA_2A_002	HSR (Type 3)	77.38	0	13.05	0	1.1	0.15	0.76	4.8	2.76	100
ORA_2A_002	HSR (Type 3)	77.39	0.08	12.88	0.06	1.29	0	0.65	4.97	2.7	100
ORA_2A_002	HSR (Type 3)	77.42	0	13.22	0.08	0.85	0.07	0.98	4.78	2.6	100
ORA_2A_002	HSR (Type 3)	77.43	0	13.01	0.04	1.38	0.02	1.01	4.31	2.8	100
ORA_2A_002	HSR (Type 3)	77.43	0.07	12.99	0.04	1.01	0.03	0.54	5.05	2.83	100
ORA_2A_002	HSR (Type 3)	77.52	0.12	12.82	0	1.25	0	0.87	4.84	2.57	100
ORA_2A_002	HSR (Type 3)	77.52	0	13.37	0	0.85	0	0.62	5.05	2.6	100
ORA_2A_002	HSR (Type 3)	77.54	0	13.21	0.08	1.02	0	0.81	4.65	2.69	100
ORA_2A_002	HSR (Type 3)	77.64	0	13.12	0.08	0.83	0.12	0.9	4.79	2.52	100
ORA_2A_002	HSR (Type 3)	77.64	0.06	12.97	0.06	0.85	0	0.7	5.02	2.7	100
ORA_2A_002	HSR (Type 3)	77.65	0.04	12.77	0.07	1.13	0.17	0.67	5.07	2.45	100

Sample	Type	SiO ₂	TiO ₂	Al ₂ O ₃	MgO	FeO	MnO	CaO	Na ₂ O	K ₂ O	Total
ORA_2A_002	Glass	65.76	0.24	19.97	0.41	1.76	0.07	4.1	5.6	2.1	100
ORA_2A_002	Glass	69.4	0.31	16.43	0.69	2.85	0	1.75	5.07	3.39	99.88
ORA_2A_002	Glass	69.44	0.11	18.3	0.29	0.42	0	2.37	6.71	2.34	100
ORA_2A_002	Glass	70.56	0.06	16.03	0.64	2.5	0.21	1.85	4.86	3.29	100
ORA_2A_002	Glass	70.79	0.18	15.84	0.66	2.63	0	1.89	4.85	3.04	99.89
ORA_2A_002	Glass	70.79	0.28	16.12	0.66	1.84	0.08	2.02	4.82	3.24	99.85
ORA_2A_002	Glass	70.89	0.22	16.23	0.47	2.35	0	2.16	4.71	2.96	100
ORA_2A_002	Glass	70.94	0.11	16.01	0.5	2.18	0.24	2.06	4.92	3.03	100
ORA_2A_002	Glass	70.95	0.15	15.52	0.58	2.69	0.04	2.23	4.77	3.07	100
ORA_2A_002	Glass	71.09	0.35	15.78	0.68	2.45	0	1.99	4.56	3.09	100
ORA_2A_002	Glass	71.12	0.28	16.11	0.55	2.15	0	1.88	4.88	3.02	100
ORA_2A_002	Glass	71.24	0.31	15.68	0.61	2.34	0.04	1.72	4.97	3.11	100
ORA_2A_002	Glass	71.36	0.36	15.78	0.55	2.52	0	1.64	4.83	2.95	100
ORA_2A_002	Glass	71.56	0.32	15.73	0.59	2.06	0.11	2.02	4.66	2.95	100
ORA_2A_002	Glass	71.66	0.28	15.86	0.56	1.82	0.06	1.84	4.97	2.94	100
ORA_2A_002	Glass	71.75	0.18	15.46	0.49	2.14	0.2	1.72	5	3.06	100
ORA_2A_002	Glass	71.76	0.37	15.6	0.63	2.13	0	2.02	4.52	2.96	100
ORA_2A_002	Glass	71.84	0.22	15.39	0.49	2.27	0.02	1.71	4.78	3.27	100
ORA_2A_002	Glass	71.86	0.17	15.7	0.57	2.03	0.02	2.06	4.64	2.95	100
ORA_2A_002	Glass	71.95	0.34	15.73	0.51	1.77	0.08	1.87	4.79	2.97	100
ORA_2A_002	Glass	71.96	0.24	15.83	0.62	1.48	0.04	1.95	4.81	3.08	100
ORA_2A_002	Glass	71.99	0.34	16.28	0.24	0.84	0.11	1.91	5.51	2.78	100
ORA_2A_002	Glass	72.05	0.21	15.72	0.63	1.7	0.01	1.79	4.76	3.14	100
ORA_2A_002	Glass	72.09	0.25	15.7	0.54	1.55	0	1.95	4.82	3.09	100
ORA_2A_002	Glass	72.1	0.19	15.48	0.63	1.99	0	2.13	4.64	2.84	100
ORA_2A_002	Glass	72.13	0.06	16.54	0.04	1.11	0	1.57	6.24	2.31	100
ORA_2A_002	Glass	72.2	0.2	15.65	0.57	1.98	0.05	1.79	4.56	3.02	100
ORA_2A_002	Glass	72.24	0.15	15.41	0.98	1.74	0.09	1.86	4.38	3.16	100
ORA_2A_002	Glass	72.25	0.24	15.6	0.35	1.55	0.28	2.06	4.77	2.91	100
ORA_2A_002	Glass	72.32	0.22	15.9	0.52	1.27	0	2.09	4.63	3.05	100
ORA_2A_002	Glass	72.38	0.23	15.47	0.59	1.55	0.08	2.1	4.52	3.08	100
ORA_2A_002	Glass	72.44	0.04	15.8	0.54	1.33	0	2.13	4.61	3.12	100
ORA_2A_002	Glass	72.44	0.17	16.08	0.45	1.15	0.08	1.99	4.78	2.86	100
ORA_2A_002	Glass	72.45	0.09	15.48	0.51	1.59	0.04	1.85	4.97	3.02	100
ORA_2A_002	Glass	72.46	0.27	15.25	0.55	1.86	0.04	1.78	4.85	2.94	100
ORA_2A_002	Glass	72.47	0.18	15.58	0.41	1.65	0.04	1.89	4.77	3.01	100
ORA_2A_002	Glass	72.48	0.34	15.45	0.5	1.42	0.13	1.94	4.67	3.06	100
ORA_2A_002	Glass	72.48	0.01	16.78	0.03	0.56	0.04	2	5.66	2.43	100
ORA_2A_002	Glass	72.48	0.26	15.39	0.51	1.76	0.04	1.66	5.01	2.89	100
ORA_2A_002	Glass	72.53	0.26	14.77	0.71	2.82	0	2.03	4.11	2.79	100

ORA_2A_002	Glass	72.56	0.21	15.88	0.51	1.08	0.11	1.94	4.66	3.05	100
ORA_2A_002	Glass	72.62	0.2	15.78	0.54	0.95	0.2	1.99	4.65	3.08	100
ORA_2A_002	Glass	72.67	0.11	15.86	0.36	1.51	0	1.63	4.92	2.93	100
ORA_2A_002	Glass	72.68	0.31	15.44	0.61	1.17	0.15	2.13	4.56	2.95	100
ORA_2A_002	Glass	72.72	0.21	15.82	0.38	1.35	0.07	1.73	4.88	2.84	100
ORA_2A_002	Glass	72.76	0.21	15.71	0.4	0.95	0.05	1.87	4.91	3	99.86
ORA_2A_002	Glass	72.78	0.24	15.33	0.43	1.59	0.01	1.72	4.81	3.1	100
ORA_2A_002	Glass	72.8	0.26	15.63	0.5	1.02	0	1.97	4.74	3.08	100
ORA_2A_002	Glass	72.8	0.19	15.65	0.36	1.32	0	1.96	4.66	3.05	100
ORA_2A_002	Glass	72.83	0.25	15.69	0.49	0.8	0.05	1.99	4.53	3.26	99.89
ORA_2A_002	Glass	72.87	0.2	15.68	0.44	1.16	0.14	1.81	4.64	3.05	100
ORA_2A_002	Glass	72.9	0.22	15.82	0.32	0.79	0.11	1.85	5.26	2.73	100
ORA_2A_002	Glass	72.91	0.18	15.69	0.58	1.35	0.05	1.58	4.61	3.04	100
ORA_2A_002	Glass	72.93	0.39	15.67	0.35	0.87	0.14	1.89	4.67	3.09	100
ORA_2A_002	Glass	72.93	0.12	15.71	0.5	1.09	0.07	1.7	4.83	3.05	100
ORA_2A_002	Glass	72.93	0.25	15.3	0.53	1.04	0.16	1.87	4.65	3.26	100
ORA_2A_002	Glass	72.96	0.25	15.28	0.53	1.23	0.15	1.95	4.72	2.93	100
ORA_2A_002	Glass	72.99	0.34	15.54	0.41	0.76	0.07	2.16	4.53	3.06	99.88
ORA_2A_002	Glass	73.13	0.18	15.29	0.53	1	0.08	2.11	4.49	3.2	100
ORA_2A_002	Glass	73.15	0.25	15.59	0.41	0.95	0	2.11	4.69	2.84	100
ORA_2A_002	Glass	73.2	0.31	15.21	0.47	0.98	0	1.93	4.81	3.08	100
ORA_2A_002	Glass	73.2	0.14	15.5	0.38	1.1	0	1.8	4.75	3.13	100
ORA_2A_002	Glass	73.2	0.16	15.69	0.39	0.64	0.04	2.07	4.77	3.03	100
ORA_2A_002	Glass	73.22	0.23	15.03	0.47	1.43	0	2.22	4.64	2.75	100
ORA_2A_002	Glass	73.22	0.12	15.64	0.26	0.78	0.18	1.81	5.02	2.97	100
ORA_2A_002	Glass	73.24	0.27	15.15	0.32	1.24	0.12	1.53	5.11	3.01	100
ORA_2A_002	Glass	73.24	0.17	15.35	0.5	1.17	0	1.92	4.71	2.94	100
ORA_2A_002	Glass	73.25	0.13	15.52	0.46	0.86	0	1.72	5	3.06	100
ORA_2A_002	Glass	73.4	0.24	15.15	0.45	1.11	0	1.91	4.5	3.24	100
ORA_2A_002	Glass	73.42	0.26	15.32	0.51	0.74	0	2.08	4.66	3.01	100
ORA_2A_002	Glass	73.43	0.3	15.48	0.39	0.82	0	1.89	4.8	2.9	100
ORA_2A_002	Glass	73.45	0.41	15.47	0.48	0.87	0	1.86	4.6	2.86	100
ORA_2A_002	Glass	73.48	0.11	15.61	0.36	0.69	0	1.77	5.11	2.87	100
ORA_2A_002	Glass	73.48	0.27	15.42	0.39	0.87	0	2.03	4.69	2.84	100
ORA_2A_002	Glass	73.49	0.18	15.41	0.36	0.78	0.05	1.82	4.82	3.08	100
ORA_2A_002	Glass	73.56	0.28	15.42	0.31	0.6	0.28	1.92	4.77	2.86	100
ORA_2A_002	Glass	73.57	0.27	15.15	0.45	0.98	0.13	1.94	4.53	2.98	100
ORA_2A_002	Glass	73.57	0.2	15.12	0.42	1.63	0	1.83	4.52	2.71	100
ORA_2A_002	Glass	73.6	0.04	15.57	0.28	0.81	0	1.59	5.26	2.84	100
ORA_2A_002	Glass	73.6	0.33	15.24	0.57	0.69	0	1.82	4.68	3.07	100
ORA_2A_002	Glass	73.61	0.17	15.12	0.42	0.81	0.29	1.86	4.73	2.99	100
ORA_2A_002	Glass	73.61	0.17	15.18	0.4	1.12	0	1.96	4.55	3.03	100
ORA_2A_002	Glass	73.63	0	15.15	0.46	1.07	0.07	1.82	4.73	3.07	100

ORA_2A_002	Glass	73.68	0.01	15.38	0.46	1.01	0.14	1.8	4.65	2.86	100
ORA_2A_002	Glass	73.71	0.23	15.31	0.5	1.03	0	1.67	4.63	2.91	100
ORA_2A_002	Glass	73.73	0.09	15.52	0.45	0.64	0.06	1.83	4.54	3.14	100
ORA_2A_002	Glass	73.74	0.12	15.11	0.52	0.89	0.04	1.77	4.63	3.19	100
ORA_2A_002	Glass	73.74	0.33	15.08	0.39	1.12	0	1.79	4.57	2.98	100
ORA_2A_002	Glass	73.75	0.25	15.09	0.42	0.79	0.1	1.91	4.74	2.94	100
ORA_2A_002	Glass	73.79	0.14	15.35	0.41	0.84	0.09	1.86	4.51	3	100
ORA_2A_002	Glass	73.8	0.13	15.15	0.25	1.03	0.29	1.69	4.75	2.92	100
ORA_2A_002	Glass	73.84	0.32	15.34	0.4	0.85	0.09	1.56	4.65	2.95	100
ORA_2A_002	Glass	73.85	0.12	15.24	0.39	0.9	0	1.72	4.73	3.05	100
ORA_2A_002	Glass	73.88	0.11	15.24	0.38	0.73	0.12	1.58	5.02	2.94	100
ORA_2A_002	Glass	73.89	0.21	15.51	0.43	0.53	0	1.75	4.63	3.04	100
ORA_2A_002	Glass	73.9	0.15	15.5	0.35	0.71	0	1.71	4.72	2.96	100
ORA_2A_002	Glass	73.9	0.12	15.61	0.35	0.59	0.06	1.75	4.79	2.81	100
ORA_2A_002	Glass	73.97	0.25	15.19	0.25	0.62	0.09	1.7	4.87	3.06	100
ORA_2A_002	Glass	73.98	0.14	15	0.4	0.87	0.06	1.79	4.66	3.09	100
ORA_2A_002	Glass	73.99	0.05	15.17	0.28	0.97	0	1.75	4.83	2.96	100
ORA_2A_002	Glass	73.99	0.15	15.29	0.28	0.68	0.08	1.61	4.78	3.13	100
ORA_2A_002	Glass	74.01	0.15	14.84	0.42	0.9	0.01	1.82	4.77	3.07	100
ORA_2A_002	Glass	74.01	0.21	15.22	0.24	0.79	0.07	1.81	4.74	2.9	100
ORA_2A_002	Glass	74.03	0.15	15.46	0.33	0.57	0.05	1.86	4.6	2.95	100
ORA_2A_002	Glass	74.03	0.38	15.04	0.26	0.93	0	1.79	4.68	2.89	100
ORA_2A_002	Glass	74.04	0.06	15.27	0.31	0.7	0	1.87	4.78	2.98	100
ORA_2A_002	Glass	74.04	0.13	15	0.36	0.7	0.1	1.8	4.79	3.08	100
ORA_2A_002	Glass	74.06	0.08	15.24	0.37	0.62	0.05	1.72	4.73	3.14	100
ORA_2A_002	Glass	74.07	0.37	14.97	0.38	0.76	0.29	1.58	4.72	2.86	100
ORA_2A_002	Glass	74.07	0.23	14.98	0.34	0.68	0	1.91	4.73	3.06	100
ORA_2A_002	Glass	74.1	0.23	15.23	0.34	0.57	0	1.87	4.76	2.9	100
ORA_2A_002	Glass	74.11	0.15	15.11	0.32	0.77	0.16	1.92	4.56	2.89	100
ORA_2A_002	Glass	74.13	0.08	15.26	0.37	0.85	0.11	1.18	5.17	2.84	100
ORA_2A_002	Glass	74.16	0.07	15.35	0.37	0.72	0	1.76	4.63	2.94	100
ORA_2A_002	Glass	74.16	0.16	15	0.46	0.9	0.04	1.8	4.53	2.94	100
ORA_2A_002	Glass	74.18	0.17	14.88	0.52	0.9	0.15	1.82	4.34	2.93	99.88
ORA_2A_002	Glass	74.2	0.34	14.8	0.39	1.01	0	1.67	4.54	3.05	100
ORA_2A_002	Glass	74.23	0.05	15.07	0.17	1.26	0	1.54	4.84	2.83	100
ORA_2A_002	Glass	74.29	0.23	15.29	0.39	0.42	0	1.68	4.74	2.96	100
ORA_2A_002	Glass	74.32	0.14	15.33	0.2	0.58	0.06	1.65	4.8	2.92	100
ORA_2A_002	Glass	74.38	0.15	14.85	0.37	1.16	0.05	1.55	4.65	2.84	100
ORA_2A_002	Glass	74.39	0	15.07	0.3	0.78	0.1	1.78	4.73	2.85	100
ORA_2A_002	Glass	74.44	0.1	15.14	0.31	0.8	0.01	1.68	4.58	2.93	100
ORA_2A_002	Glass	74.45	0.14	14.91	0.27	0.78	0.06	1.67	4.6	3.02	99.9
ORA_2A_002	Glass	74.45	0	15.19	0.4	0.77	0	1.82	4.55	2.83	100
ORA_2A_002	Glass	74.46	0.02	15.09	0.33	0.53	0.23	1.49	4.89	2.96	100

ORA_2A_002	Glass	74.46	0.14	15.28	0.14	0.34	0	1.79	4.77	3.08	100
ORA_2A_002	Glass	74.47	0.32	14.95	0.36	0.51	0	1.79	4.51	3.09	100
ORA_2A_002	Glass	74.52	0.16	14.64	0.35	1.06	0	1.7	4.48	3.1	100
ORA_2A_002	Glass	74.58	0.21	14.87	0.34	0.62	0.04	1.78	4.53	3.03	100
ORA_2A_002	Glass	74.58	0.04	14.36	0.55	1.5	0	1.94	4.17	2.87	100
ORA_2A_002	Glass	74.6	0.22	14.93	0.34	0.63	0.03	1.61	4.72	2.94	100
ORA_2A_002	Glass	74.75	0.11	14.64	0.43	0.92	0.03	1.88	4.41	2.83	100
ORA_2A_002	Glass	74.85	0.36	14.74	0.29	0.59	0	1.66	4.73	2.78	100
ORA_2A_002	Glass	74.98	0.15	15.02	0.22	0.33	0	1.52	4.84	2.93	100
ORA_2A_002	Glass	75.02	0.18	14.41	0.31	0.9	0	1.54	4.72	2.92	100
ORA_2A_002	Glass	75.1	0	14.83	0.13	0.9	0.03	1.27	4.92	2.83	100
ORA_2A_002	Glass	75.3	0.12	14.79	0.3	0.52	0	1.57	4.67	2.74	100
ORA_2A_002	Glass	75.32	0.11	14.61	0.21	0.41	0.16	1.22	4.96	3.01	100
ORA_2A_002	Glass	75.34	0.05	14.8	0.14	0.38	0	1.45	4.74	3.1	100
ORA_2A_002	Glass	75.7	0	14.06	0.24	0.86	0.09	1.33	4.68	3.03	100
ORA_2A_002	Glass	75.83	0.08	14.25	0.11	0.69	0.16	1.69	4.46	2.72	100
ORA_2A_002	Glass	75.9	0.07	13.32	0	2.02	0	0.89	5.11	2.71	100
ORA_2A_002	Glass	75.93	0.18	14.02	0.31	0.58	0.03	1.63	4.47	2.85	100
ORA_2A_002	Glass	76.23	0.04	13.85	0.14	0.68	0	1.11	4.84	3.1	100
ORA_2A_002	Glass	76.35	0.12	13.6	0.26	0.88	0.16	1.72	4.26	2.66	100
ORA_2A_002	Glass	70.67	0.22	15.87	0.59	2.64	0.11	1.8	4.68	3.29	99.89
ORA_2A_002	HSR	76.04	0.04	13.77	0.13	1.05	0.09	1.24	4.74	2.89	100
ORA_2A_002	HSR	76.36	0	13.65	0.31	0.79	0.08	1.85	4.26	2.71	100
ORA_2A_002	HSR	76.7	0	13.71	0.1	0.94	0.05	1.24	4.62	2.63	100
ORA_2A_002	HSR	76.83	0.12	13.37	0.02	1.36	0.04	0.75	4.79	2.71	100
ORA_2A_002	HSR	77.11	0.02	13.27	0	0.78	0	0.68	5.13	2.87	99.87
ORA_2A_002	HSR	77.53	0.12	13.36	0.05	0.31	0.05	0.87	4.98	2.72	100
ORA_2A_002	HSR	77.6	0.03	13.31	0.05	0.38	0.03	0.71	5.03	2.84	100
ORA_2A_002	HSR	77.88	0.1	12.78	0.01	0.72	0.08	0.66	4.91	2.85	100
ORA_2A_002	HSR	79.7	0.22	11.6	0.28	0.75	0.09	1.49	3.54	2.34	100

ORA-2A-003:

Sample	Type	SiO2	TiO2	Al2O3	MgO	FeO	MnO	CaO	Na2O	K2O	Total
ORA_2A_003	Glass	74.22	0.03	15.06	0.05	1.09	0	0.98	6.12	2.45	100
ORA_2A_003	Glass	75.89	0.11	13.88	0	0.79	0	0.76	5.28	3.15	99.87
ORA_2A_003	HSR	76.18	0.05	13.76	0	0.89	0.12	0.74	5.23	3.03	100
ORA_2A_003	HSR	76.23	0.16	13.6	0.08	0.8	0.01	0.7	5.24	3.18	100
ORA_2A_003	HSR	76.27	0.09	13.55	0.04	1.06	0.08	0.6	5.32	3	100
ORA_2A_003	HSR	76.35	0.02	13.64	0.09	0.85	0	0.68	5.25	3.12	100
ORA_2A_003	HSR	76.36	0.06	13.61	0.07	0.96	0.08	0.58	5.3	2.99	100
ORA_2A_003	HSR	76.44	0.13	13.51	0.03	1.01	0	0.52	5.24	3.13	100
ORA_2A_003	HSR	76.49	0.09	13.48	0.04	0.86	0.08	0.47	5.38	3.11	100
ORA_2A_003	HSR	76.51	0.14	13.52	0	0.92	0	0.53	5.33	3.05	100
ORA_2A_003	HSR	76.54	0.02	13.61	0.06	0.6	0.07	0.64	5.3	3.16	100
ORA_2A_003	HSR	76.58	0.06	13.45	0.06	0.79	0.07	0.58	5.18	3.08	99.85
ORA_2A_003	HSR	76.58	0.04	13.42	0.09	0.82	0.03	0.57	5.24	3.23	100
ORA_2A_003	HSR	76.63	0.09	13.53	0	0.61	0.05	0.6	5.19	3.19	99.88
ORA_2A_003	HSR	76.7	0.04	13.46	0.05	0.98	0.03	0.5	5.22	3.01	100
ORA_2A_003	HSR	76.75	0.16	13.4	0.01	0.64	0.12	0.54	5.27	3.1	100
ORA_2A_003	HSR	76.76	0.13	13.28	0.09	1.06	0.05	0.46	5.06	3	99.88
ORA_2A_003	HSR	76.76	0.07	13.42	0.06	0.74	0	0.44	5.27	3.13	99.89
ORA_2A_003	HSR	76.77	0.13	13.4	0.03	0.64	0.09	0.64	5.31	2.99	100
ORA_2A_003	HSR	76.82	0	13.66	0	0.61	0.08	0.41	5.42	2.99	100
ORA_2A_003	HSR	76.85	0	13.13	0.01	1.07	0.04	0.53	5.06	3.17	99.87
ORA_2A_003	HSR	76.9	0.03	13.5	0.02	0.67	0.02	0.54	5.21	3.12	100
ORA_2A_003	HSR	76.95	0.01	13.13	0.02	0.88	0	0.67	5.2	2.99	99.84
ORA_2A_003	HSR	76.98	0	13.29	0.12	0.84	0.02	0.6	5.02	3.01	99.88
ORA_2A_003	HSR	76.99	0.12	13.23	0.04	0.77	0	0.64	5.16	3.04	100
ORA_2A_003	HSR	77	0	13.52	0.06	0.67	0.01	0.47	5.14	3.12	100
ORA_2A_003	HSR	77.01	0.09	13.17	0.05	0.95	0.02	0.49	5.13	3.09	100
ORA_2A_003	HSR	77.05	0.08	13.34	0.07	0.81	0	0.54	5.08	3.03	100
ORA_2A_003	HSR	77.06	0.11	13.4	0	0.55	0.09	0.65	5.3	2.83	100
ORA_2A_003	HSR	77.12	0.01	13.35	0.04	0.87	0	0.63	4.95	3.03	100
ORA_2A_003	HSR	77.2	0	13.1	0.02	0.97	0.04	0.81	4.86	3	100
ORA_2A_003	HSR	77.2	0.13	13.19	0.06	0.79	0	0.46	5.24	2.94	100
ORA_2A_003	HSR	77.22	0	12.98	0.02	0.99	0.03	0.53	5.19	3.05	100
ORA_2A_003	HSR	77.29	0.08	13.13	0.06	0.73	0.05	0.58	5.16	2.92	100
ORA_2A_003	HSR	77.33	0.05	13.07	0	0.68	0.04	0.69	5.11	3.02	100
ORA_2A_003	HSR	77.35	0.06	13.03	0.01	0.79	0.04	0.56	5.13	2.89	99.85
ORA_2A_003	HSR	77.35	0	12.94	0.06	0.77	0.12	0.5	5.2	3.05	100
ORA_2A_003	HSR	77.46	0.16	12.78	0	1	0.08	0.49	5.16	2.88	100
ORA_2A_003	HSR	77.53	0.07	12.9	0.05	1.17	0	0.38	4.89	3.02	100
ORA_2A_003	HSR	77.61	0.09	12.93	0.05	0.78	0	0.57	4.9	3.07	100
ORA_2A_003	HSR	77.62	0.04	12.78	0	0.92	0	0.42	5.12	2.98	99.88
ORA_2A_003	HSR	77.64	0.05	12.57	0.06	1.48	0	0.51	4.81	2.87	100
ORA_2A_003	HSR	77.65	0	12.87	0.01	0.86	0.02	0.54	5.06	2.87	99.89

ORA_2A_003	HSR	77.66	0.01	12.81	0.05	1.01	0	0.49	4.92	3.06	100
ORA_2A_003	HSR	77.67	0.05	13.01	0.02	0.77	0.13	0.4	5.04	2.91	100
ORA_2A_003	HSR	77.69	0.02	12.72	0	0.87	0.04	0.44	5.16	2.95	99.88
ORA_2A_003	HSR	77.7	0.13	12.74	0.08	0.76	0	0.41	5.11	2.93	99.86
ORA_2A_003	HSR	77.72	0.04	12.83	0.09	0.77	0.03	0.5	4.94	2.93	99.86
ORA_2A_003	HSR	77.72	0.01	12.73	0.06	0.8	0.03	0.61	5	3.04	100
ORA_2A_003	HSR	77.74	0.04	12.86	0	0.83	0.07	0.6	4.95	2.91	100
ORA_2A_003	HSR	77.76	0.1	12.71	0.07	0.81	0.07	0.43	4.99	3.05	100
ORA_2A_003	HSR	77.77	0	12.96	0.02	0.48	0.2	0.45	5.03	3.09	100
ORA_2A_003	HSR	77.8	0	12.67	0.01	0.85	0.14	0.41	4.96	3.02	99.87
ORA_2A_003	HSR	77.82	0.02	12.93	0	0.63	0	0.46	5.09	2.89	99.84
ORA_2A_003	HSR	77.84	0.05	12.92	0	0.52	0.11	0.4	5.02	3	99.87
ORA_2A_003	HSR	77.84	0	12.85	0	0.86	0	0.61	4.83	3.01	100
ORA_2A_003	HSR	77.84	0.05	12.71	0	0.89	0.01	0.53	4.84	3.03	99.9
ORA_2A_003	HSR	77.99	0.2	12.63	0	0.54	0	0.45	5.05	3.03	99.88
ORA_2A_003	HSR	78.07	0	12.7	0.04	0.64	0	0.49	4.94	3.12	100
ORA_2A_003	HSR	78.17	0	12.82	0	0.63	0.13	0.58	4.99	2.68	100
ORA_2A_003	HSR	78.2	0	12.56	0.03	0.76	0	0.4	5.09	2.97	100
ORA_2A_003	HSR	78.49	0	12.66	0	0.45	0	0.53	5	2.88	100

ORA-2A-016:

Sample	Type	SiO ₂	TiO ₂	Al ₂ O ₃	MgO	FeO	MnO	CaO	Na ₂ O	K ₂ O	Total
ORA_2A_016	Glass Type 1	65.69	0.33	19.9	0.54	1.47	0.14	5.32	5.09	1.51	100
ORA_2A_016	Glass Type 1	67.13	0.28	18.1	0.72	2.2	0.02	3.59	5.37	2.34	99.75
ORA_2A_016	Glass Type 1	67.32	0.15	19.49	0.32	0.9	0.08	2.33	7.38	2.02	100
ORA_2A_016	Glass Type 1	67.48	0.58	17.62	0.95	2.66	0.09	3.69	3.72	2.75	99.54
ORA_2A_016	Glass Type 1	67.86	0.32	18.05	0.62	2.68	0	3.06	5.05	2.36	100
ORA_2A_016	Glass Type 1	67.95	0.74	17.54	0.77	2.65	0	2.98	4.51	2.86	100
ORA_2A_016	Glass Type 1	68.17	0.23	18.11	0.46	1.73	0.29	2.84	5.71	2.47	100
ORA_2A_016	Glass Type 1	68.3	0.51	17.88	0.69	1.79	0	2.9	5.54	2.39	100
ORA_2A_016	Glass Type 1	68.51	0.22	17.27	0.7	2.02	0.36	3.39	5.11	2.43	100
ORA_2A_016	Glass Type 1	68.54	0.2	18.13	0.86	2.34	0.03	2.99	4.61	2.29	100
ORA_2A_016	Glass Type 1	68.56	0.13	18.57	0.46	1.14	0.18	2.75	6.3	1.9	100
ORA_2A_016	Glass Type 1	68.61	0.5	16.64	1.61	2.81	0.12	2.77	4.13	2.82	100
ORA_2A_016	Glass Type 1	68.88	0.3	17.26	0.94	2.52	0	3.21	4.35	2.54	100
ORA_2A_016	Glass Type 1	68.93	0.42	17.97	0.5	1.73	0	3.58	4.84	2.03	100
ORA_2A_016	Glass Type 1	68.99	0.15	17.18	0.93	2.33	0.42	2.95	4.66	2.39	100
ORA_2A_016	Glass Type 1	69.23	0.27	16.82	1.19	2.92	0.06	3.09	4.18	2.24	100
ORA_2A_016	Glass Type 1	69.33	0.24	17.08	0.73	2.22	0.13	2.31	5.45	2.51	100
ORA_2A_016	Glass Type 1	69.36	0.37	17.17	1.44	2.36	0	3.05	4.39	1.86	100
ORA_2A_016	Glass Type 1	69.43	0.47	17.15	0.74	2.04	0.03	3.09	4.51	2.52	100
ORA_2A_016	Glass Type 1	69.43	0.32	17.81	0.49	1.73	0	2.62	5.53	2.07	100
ORA_2A_016	Glass Type 1	69.47	0.71	16.59	1.13	2.86	0	2.71	4.6	1.93	100
ORA_2A_016	Glass Type 1	69.49	0.41	17.09	0.67	2.31	0.18	2.71	4.51	2.64	100
ORA_2A_016	Glass Type 1	69.57	0.47	16.16	0.74	2.74	0.05	2.95	4.46	2.85	100
ORA_2A_016	Glass Type 1	69.59	0.36	16.81	0.93	2.54	0.07	2.85	4.16	2.69	100
ORA_2A_016	Glass Type 1	69.62	0.19	16.94	0.84	2.39	0	2.57	4.29	3.16	100
ORA_2A_016	Glass Type 1	69.71	0.56	16.42	0.81	2.41	0	2.64	4.6	2.84	100
ORA_2A_016	Glass Type 1	69.71	0.42	17.16	1.05	1.86	0.14	2.56	4.39	2.71	100
ORA_2A_016	Glass Type 1	69.72	0.25	16.56	0.87	2.55	0.31	2.54	4.69	2.51	100
ORA_2A_016	Glass Type 1	69.73	0.45	16.66	0.77	1.86	0.2	2.93	4.37	2.75	99.73
ORA_2A_016	Glass Type 1	69.75	0.62	16.93	0.65	1.97	0	2.96	4.68	2.44	100
ORA_2A_016	Glass Type 1	69.87	0.2	16.91	1.01	2.21	0.04	3.24	3.93	2.59	100
ORA_2A_016	Glass Type 1	69.94	0.31	16.62	0.93	2.5	0.02	2.71	4.29	2.55	99.89
ORA_2A_016	Glass Type 1	70.03	0.42	16.85	0.76	1.94	0.11	2.97	4.58	2.34	100
ORA_2A_016	Glass Type 1	70.09	0.26	16.55	1.01	2.49	0.08	2.85	4.49	2.19	100
ORA_2A_016	Glass Type 1	70.12	0.47	16.74	0.8	2.29	0	2.76	4.82	1.99	100
ORA_2A_016	Glass Type 1	70.17	0.25	16.84	0.73	1.81	0	2.73	4.69	2.52	99.75
ORA_2A_016	Glass Type 1	70.25	0.21	16.21	1.22	2.51	0	3.04	3.71	2.5	99.65
ORA_2A_016	Glass Type 1	70.31	0.33	16.51	0.83	2.06	0.11	2.43	4.97	2.34	99.89
ORA_2A_016	Glass Type 1	70.32	0.4	16.38	0.82	2.03	0.07	3.01	4.52	2.44	100
ORA_2A_016	Glass Type 1	70.34	0.56	16.66	0.54	1.83	0.14	2.96	4.48	2.47	100
ORA_2A_016	Glass Type 1	70.37	0.16	16.84	0.76	1.92	0.26	2.84	4.44	2.42	100
ORA_2A_016	Glass Type 1	70.37	0.32	16.07	0.84	2.6	0	2.83	4.32	2.42	99.76

ORA_2A_016	Glass Type 1	70.37	0.54	16.73	0.68	1.84	0	2.55	4.59	2.69	100
ORA_2A_016	Glass Type 1	70.43	0.23	16.31	0.81	2.29	0	2.37	5.1	2.46	100
ORA_2A_016	Glass Type 1	70.48	0.13	16.22	0.77	2.44	0.2	2.75	4.56	2.45	100
ORA_2A_016	Glass Type 1	70.55	0.38	16.18	0.92	2.62	0	2.84	4.05	2.46	100
ORA_2A_016	Glass Type 1	70.55	0.22	16.81	0.69	2.09	0	2.63	4.32	2.68	100
ORA_2A_016	Glass Type 1	70.56	0.13	16.11	0.7	2.41	0.45	2.47	5.1	2.08	100
ORA_2A_016	Glass Type 1	70.69	0.34	15.82	0.67	2.72	0.06	2.15	4.83	2.59	99.87
ORA_2A_016	Glass Type 1	70.72	0.77	15.6	1.09	2.33	0.02	2.4	4.44	2.64	100
ORA_2A_016	Glass Type 1	70.76	0.37	16.56	0.69	1.52	0.06	2.8	5.19	2.03	100
ORA_2A_016	Glass Type 1	70.78	0.23	15.98	0.76	2.3	0	2.69	4.89	2.37	100
ORA_2A_016	Glass Type 1	70.84	0.06	16.56	0.72	2.07	0.04	2.72	4.74	2.25	100
ORA_2A_016	Glass Type 1	70.93	0.34	15.5	0.78	2.73	0.18	2.61	4.41	2.53	100
ORA_2A_016	Glass Type 1	70.99	0.46	16.55	0.7	1.5	0.01	2.35	4.9	2.54	100
ORA_2A_016	Glass Type 1	71.04	0.14	16.01	0.86	2.52	0.17	2.22	4.79	2.25	100
ORA_2A_016	Glass Type 1	71.07	0.11	16.33	0.58	2.21	0	2.32	4.8	2.57	100
ORA_2A_016	Glass Type 1	71.15	0.4	15.43	0.71	2.86	0	2.58	4.31	2.56	100
ORA_2A_016	Glass Type 1	71.26	0.17	15.34	1.12	2.98	0.02	2.26	3.66	2.35	100
ORA_2A_016	Glass Type 1	71.34	0.3	16.17	0.67	1.65	0.08	2.53	4.94	2.32	100
ORA_2A_016	Glass Type 1	71.42	0.33	16.58	0.51	1.35	0	2.39	5.34	2.08	100
ORA_2A_016	Glass Type 1	71.46	0.23	15.63	0.77	2.29	0	2.85	4.11	2.65	100
ORA_2A_016	Glass Type 1	71.62	0.33	15.95	0.61	2	0	2.51	4.43	2.54	100
ORA_2A_016	Glass Type 1	71.7	0.62	15.79	0.6	1.82	0.06	2.32	4.66	2.44	100
ORA_2A_016	Glass Type 1	71.73	0.21	15.64	0.61	2.26	0.01	2.78	4.32	2.45	100
ORA_2A_016	Glass Type 1	71.87	0.38	15.97	0.29	1.45	0.21	2.78	5.03	2.02	100
ORA_2A_016	Glass Type 1	72.2	0.2	15.56	0.69	2.15	0.05	2.3	4.55	2.28	100
ORA_2A_016	Glass Type 1	72.47	0.56	15.06	0.95	2.46	0	2.46	3.6	2.45	100
ORA_2A_016	Glass Type 1	72.5	0.32	15.95	0.66	1.7	0	2.39	4.27	2.21	100
ORA_2A_016	Glass Type 1	72.57	0.25	15.23	0.59	2.33	0	2.43	4.27	2.33	100
ORA_2A_016	Glass Type 1	72.62	0.37	15.06	0.55	2	0.22	2.56	4.45	2.16	100
ORA_2A_016	Glass Type 1	72.84	0.3	14.96	0.95	2.13	0	2.56	4.15	2.11	100
ORA_2A_016	Glass Type 1	72.96	0	15.26	0.67	1.88	0.13	2.37	4.28	2.45	100
ORA_2A_016	Glass Type 1	73.8	0.27	14.31	0.66	1.76	0.01	2.46	4.51	2.21	100

Sample	Type	SiO2	TiO2	Al2O3	MgO	FeO	MnO	CaO	Na2O	K2O	Total
ORA_2A_016	Glass Type 2	69.69	0.29	16.84	0.65	2.22	0	1.74	5.82	2.75	100
ORA_2A_016	Glass Type 2	70.09	0.26	16.12	0.8	2.78	0.14	2.33	4.74	2.59	99.86
ORA_2A_016	Glass Type 2	71.66	0	15.74	0.59	2.11	0.12	2.58	4.86	2.34	100
ORA_2A_016	Glass Type 2	72.3	0.24	14.89	0.71	2.64	0	2.17	4.82	2.23	100

ORA_2A_016	Glass Type 2	72.61	0.11	15.45	0.42	1.54	0.15	1.73	5.6	2.38	100
ORA_2A_016	Glass Type 2	69.67	0.28	16.97	0.41	2.25	0.13	2.38	5.86	2.06	100
ORA_2A_016	Glass Type 2	70.18	0.12	17.2	0.43	1.88	0	2.69	5.28	2.23	100
ORA_2A_016	Glass Type 2	70.53	0.4	15.86	0.66	2.55	0.32	2.01	5.36	2.32	100
ORA_2A_016	Glass Type 2	70.75	0.39	16.65	0.45	1.59	0.29	2.21	5.85	1.83	100
ORA_2A_016	Glass Type 2	70.81	0.29	17.04	0.32	1.61	0	2.62	5.06	2.25	100
ORA_2A_016	Glass Type 2	71	0.22	16.6	0.47	1.07	0.02	1.38	6.09	3.15	100
ORA_2A_016	Glass Type 2	71.11	0.15	16.75	0.42	1.51	0.48	1.7	5.89	1.99	100
ORA_2A_016	Glass Type 2	71.3	0.15	16.21	0.47	2.17	0	1.98	5.39	2.32	100
ORA_2A_016	Glass Type 2	71.46	0.33	16.28	0.76	1.8	0.01	2.29	4.47	2.6	100
ORA_2A_016	Glass Type 2	71.66	0.38	16.09	0.56	1.84	0.4	1.62	5.04	2.41	100
ORA_2A_016	Glass Type 2	71.69	0.39	16	0.8	1.99	0.06	2.26	4.7	2.11	100
ORA_2A_016	Glass Type 2	71.69	0.14	15.72	0.62	2.24	0	2.06	4.99	2.55	100
ORA_2A_016	Glass Type 2	71.79	0.24	15.58	0.45	1.88	0.11	2.49	5.14	2.32	100
ORA_2A_016	Glass Type 2	71.98	0.34	15.31	0.7	2.47	0	1.4	5.22	2.29	99.72
ORA_2A_016	Glass Type 2	72.3	0.09	15.17	0.43	2.71	0	1.64	5.4	2.25	100
ORA_2A_016	Glass Type 2	72.35	0.17	15.55	0.32	1.91	0	1.96	5.17	2.57	100
ORA_2A_016	Glass Type 2	72.48	0.19	15.1	0.69	2.23	0	2	5.15	2.16	100
ORA_2A_016	Glass Type 2	72.51	0.18	15.13	0.53	2.67	0.18	2.36	4.59	1.86	100
ORA_2A_016	Glass Type 2	72.52	0.21	15.67	0.32	1.74	0	2	5.28	2.26	100
ORA_2A_016	Glass Type 2	72.58	0.15	16.35	0.28	0.63	0.18	1.91	6.25	1.65	100
ORA_2A_016	Glass Type 2	72.65	0.18	15.48	0.56	1.54	0.17	2.1	5.03	2.3	100
ORA_2A_016	Glass Type 2	72.78	0.3	15.29	0.8	1.55	0.21	2.1	4.72	2.26	100
ORA_2A_016	Glass Type 2	72.84	0.38	14.54	0.71	1.98	0	2.83	4.48	2.24	100
ORA_2A_016	Glass Type 2	72.91	0.23	15.01	0.5	1.72	0.21	1.38	5.78	2.27	100
ORA_2A_016	Glass Type 2	72.92	0.14	15.46	0.67	1.43	0.08	2.43	4.49	2.39	100
ORA_2A_016	Glass Type 2	72.94	0.34	14.96	0.31	1.62	0.22	2.17	4.93	2.52	100
ORA_2A_016	Glass Type 2	73.17	0.17	15.71	0.56	1.51	0	2.24	4.44	2.21	100
ORA_2A_016	Glass Type 2	73.19	0.47	15.18	0.3	1.38	0.05	1.95	5.17	2.32	100
ORA_2A_016	Glass Type 2	73.27	0.05	15.43	0.39	1.57	0.18	2.03	4.98	2.09	100
ORA_2A_016	Glass Type 2	73.34	0.16	14.92	0.21	1.8	0.2	1.9	5.51	1.95	100
ORA_2A_016	Glass Type 2	73.37	0.22	14.47	0.26	2.6	0.1	2.25	4.71	2.02	100
ORA_2A_016	Glass Type 2	73.49	0.4	14.71	0.58	1.45	0	2.24	4.89	2.24	100
ORA_2A_016	Glass Type 2	73.61	0.28	14.9	0.38	1.51	0	1.59	5.41	2.32	100
ORA_2A_016	Glass Type 2	73.65	0.05	15.3	0.5	1.63	0.09	2.07	4.52	2.2	100
ORA_2A_016	Glass Type 2	73.84	0	15.7	0.26	0.66	0.08	2.17	5.2	2.08	100
ORA_2A_016	Glass Type 2	73.87	0.1	14.8	0.39	1.46	0.07	2.14	4.78	2.38	100
ORA_2A_016	Glass Type 2	73.97	0	14.59	0.35	1.67	0.17	1.76	5.33	2.15	100
ORA_2A_016	Glass Type 2	74.33	0	15.22	0.17	1.39	0	1.59	5.41	1.89	100
ORA_2A_016	Glass Type 2	74.43	0.04	14.5	0.21	1.41	0.09	2.14	5.25	1.94	100
ORA_2A_016	Glass Type 2	74.45	0.26	14.48	0.21	1.27	0.18	1.2	5.64	2.29	100
ORA_2A_016	Glass Type 2	74.51	0.33	14.22	0.42	1.64	0	1.79	4.72	2.36	100
ORA_2A_016	Glass Type 2	74.75	0.05	14.53	0.3	0.95	0.15	1.52	5.34	2.41	100

ORA_2A_016	Glass Type 2	74.98	0.09	14.78	0.26	0.95	0.06	1.46	5.42	2	100
ORA_2A_016	Glass Type 2	75.08	0.16	14.22	0.55	1.74	0	1.95	4.4	1.9	100
ORA_2A_016	Glass Type 2	75.28	0.12	14.31	0.2	0.6	0.18	1	6.04	2.28	100

Sample	Type	SiO2	TiO2	Al2O3	MgO	FeO	MnO	CaO	Na2O	K2O	Total
ORA_2A_016	Glass Type 3	64.24	0	21.47	0.51	1.01	0.02	5.27	6.75	0.73	100
ORA_2A_016	Glass Type 3	64.57	0.44	20.11	0.67	2.48	0	3.89	6.54	1.3	100
ORA_2A_016	Glass Type 3	66.17	0.65	18.23	1.08	2.26	0.2	3.84	6.29	1.29	100
ORA_2A_016	Glass Type 3	66.56	0.33	18.79	0.38	1.08	0.31	4.6	7.22	0.72	100
ORA_2A_016	Glass Type 3	66.99	0.57	18.05	0.93	1.64	0.13	3.84	6.82	1.02	100
ORA_2A_016	Glass Type 3	67.19	0.3	18.46	0.82	1.74	0.2	3.17	7.13	1	100
ORA_2A_016	Glass Type 3	67.45	0.41	18.77	0.58	1.48	0	2.81	7.47	1.02	100
ORA_2A_016	Glass Type 3	67.7	0.32	18.42	0.78	1.5	0	3.09	7.23	0.95	100
ORA_2A_016	Glass Type 3	68.35	0.74	17.32	0.5	0.83	0	4.99	6.64	0.64	100
ORA_2A_016	Glass Type 3	68.45	0.3	17.19	0.62	1.23	0.09	4.89	6.65	0.58	100
ORA_2A_016	Glass Type 3	68.66	0.25	17.84	0.65	1.54	0.04	2.8	7.22	1	100
ORA_2A_016	Glass Type 3	68.84	0.28	17.71	0.54	0.75	0	4.44	6.89	0.55	100
ORA_2A_016	Glass Type 3	69.07	0.41	17.57	0.67	0.99	0.01	3.94	6.68	0.67	100
ORA_2A_016	Glass Type 3	69.78	0.31	16.84	0.95	1.13	0	3.6	6.44	0.96	100
ORA_2A_016	Glass Type 3	70.16	0.18	17.31	0.61	0.98	0.18	3.63	6.13	0.83	100
ORA_2A_016	Glass Type 3	70.4	0.28	16.7	0.78	1.31	0.05	3.2	6.14	1.14	100
ORA_2A_016	Glass Type 3	70.74	0.54	16.63	0.73	1.06	0.09	2.96	6.56	0.69	100

Sample	Type	SiO2	TiO2	Al2O3	MgO	FeO	MnO	CaO	Na2O	K2O	Total
ORA_2A_016	Glass Type 4	70.96	0.02	16.66	0.5	1.6	0	1.77	6.58	1.92	100
ORA_2A_016	Glass Type 4	71.14	0.14	16.63	0.44	1.9	0.01	1.91	6.21	1.62	100
ORA_2A_016	Glass Type 4	71.2	0.16	16.31	0.59	1.97	0	2.01	6.61	1.15	100
ORA_2A_016	Glass Type 4	71.73	0.33	16.15	0.24	1.47	0.18	2.31	6.84	0.76	100
ORA_2A_016	Glass Type 4	72	0.28	16.03	0.61	1.71	0.15	2.01	5.8	1.41	100
ORA_2A_016	Glass Type 4	72.03	0	16.26	0.28	1.52	0	2.15	6.34	1.42	100
ORA_2A_016	Glass Type 4	72.16	0.3	15.62	0.86	1.37	0	2.07	6.2	1.43	100
ORA_2A_016	Glass Type 4	72.85	0.24	15.45	0.46	1.57	0.06	2.2	5.39	1.78	100
ORA_2A_016	Glass Type 4	72.92	0.3	15.51	0.54	1.45	0	2.31	5.53	1.43	100
ORA_2A_016	Glass Type 4	74.17	0	15.21	0.2	1.23	0	1.88	5.33	1.98	100
ORA_2A_016	Glass Type 4	74.19	0.29	14.45	0.6	1.93	0.05	1.83	5.22	1.44	100
ORA_2A_016	Glass Type 4	74.2	0.11	14.76	0.41	1.59	0.25	1.72	4.78	2.19	100
ORA_2A_016	Glass Type 4	74.45	0.24	14.76	0.38	1.35	0	1.97	4.93	1.91	100
ORA_2A_016	Glass Type 4	74.61	0	14.93	0.34	0.96	0.07	2.36	5.63	1.1	100
ORA_2A_016	Glass Type 4	74.9	0.15	14.22	0.3	1.42	0.12	1.74	5.63	1.52	100
ORA_2A_016	Glass Type 4	74.99	0.15	14.58	0.14	0.69	0.33	0.8	6.23	2.09	100

ORA_2A_016	Glass Type 4	75.7	0.29	14.03	0.24	0.57	0.04	1.88	6.08	1.17	100
ORA_2A_016	Glass Type 4	76.39	0.31	13.44	0.1	1.42	0.13	1.72	4.75	1.74	100

Sample	Type	SiO2	TiO2	Al2O3	MgO	FeO	MnO	CaO	Na2O	K2O	Total
ORA_2A_016	Glass Type 5	76.88	0.06	13.34	0.01	1.12	0.05	0.47	5.77	2.29	100
ORA_2A_016	Glass Type 5	77.1	0.32	13.31	0.18	0.51	0.34	0.96	5.31	1.96	100
ORA_2A_016	Glass Type 5	77.15	0	13.43	0.02	1.02	0	0.67	5.51	2.2	100
ORA_2A_016	Glass Type 5	77.17	0.04	13.4	0	0.98	0.03	0.75	5.66	1.96	100
ORA_2A_016	Glass Type 5	77.31	0.02	13.21	0	0.77	0.08	1.37	5.21	2.04	100
ORA_2A_016	Glass Type 5	77.33	0	13.09	0.1	0.88	0	0.57	5.74	2.28	100
ORA_2A_016	Glass Type 5	77.36	0	13.08	0.1	0.85	0	0.59	5.87	2.15	100
ORA_2A_016	Glass Type 5	77.57	0	13.04	0	0.84	0	1.08	5.26	2.21	100

Sample	Type	SiO2	TiO2	Al2O3	MgO	FeO	MnO	CaO	Na2O	K2O	Total
ORA_2A_016	HSR	76.04	0.13	14.42	0.09	0.74	0.13	0.57	5.91	1.97	100
ORA_2A_016	HSR	76.07	0	14.42	0.2	0.69	0.29	2.01	4.49	1.82	100
ORA_2A_016	HSR	76.09	0.09	14.21	0.17	1.06	0.04	1.81	4.68	1.86	100
ORA_2A_016	HSR	76.09	0.12	13.43	0.18	0.43	0.13	0.72	5.4	1.92	100
ORA_2A_016	HSR	76.12	0.08	13.68	0.11	0.73	0.17	0.68	6.26	2.18	100
ORA_2A_016	HSR	76.19	0.17	13.68	0.06	0.88	0.35	0.71	6.01	1.95	100
ORA_2A_016	HSR	76.21	0.17	14.09	0.19	0.81	0	0.55	6.04	1.94	100
ORA_2A_016	HSR	76.25	0	14.02	0.11	0.78	0.05	1.21	5.53	2.05	100
ORA_2A_016	HSR	76.27	0.13	13.95	0.14	0.95	0.02	0.67	5.89	1.97	100
ORA_2A_016	HSR	76.29	0.21	13.86	0.06	1.19	0	0.95	5.44	2.01	100
ORA_2A_016	HSR	76.3	0.12	14.08	0.39	0.86	0	1.91	4.49	1.85	100
ORA_2A_016	HSR	76.34	0.03	13.49	0.04	0.96	0.13	1.09	5.86	2.07	100
ORA_2A_016	HSR	76.35	0	14.29	0.29	1.29	0	1.39	4.7	1.69	100
ORA_2A_016	HSR	76.38	0	14.08	0.08	0.99	0	1.91	4.75	1.81	100
ORA_2A_016	HSR	76.4	0	14.45	0.04	0.46	0.11	0.87	6.04	1.62	100
ORA_2A_016	HSR	76.41	0.12	13.97	0.11	0.6	0.15	0.73	6.03	1.88	100
ORA_2A_016	HSR	76.46	0	13.87	0.15	1.13	0	0.75	5.49	2.16	100
ORA_2A_016	HSR	76.47	0	13.97	0	1.08	0	0.64	5.55	2.28	100
ORA_2A_016	HSR	76.48	0	13.91	0.19	0.7	0.12	0.81	5.79	1.99	100
ORA_2A_016	HSR	76.52	0.06	13.86	0.08	0.78	0.06	1.45	5.04	2.14	100
ORA_2A_016	HSR	76.55	0	13.99	0.01	0.65	0.21	0.56	6.06	1.97	100
ORA_2A_016	HSR	76.57	0	13.58	0.02	0.89	0.22	0.59	5.85	2.27	100
ORA_2A_016	HSR	76.57	0.24	13.56	0	0.73	0.15	0.56	5.8	2.39	100
ORA_2A_016	HSR	76.57	0.06	13.83	0	1.18	0	0.6	5.68	2.08	100
ORA_2A_016	HSR	76.58	0	14.02	0	0.31	0.17	0.79	5.96	2.16	100

ORA_2A_016	HSR	76.59	0.09	13.52	0.09	0.98	0.15	0.93	5.46	2.19	100
ORA_2A_016	HSR	76.6	0.14	13.9	0.34	1.09	0	1.21	4.93	1.79	100
ORA_2A_016	HSR	76.6	0.01	14.01	0.11	1.09	0	1.36	5.13	1.69	100
ORA_2A_016	HSR	76.63	0	13.89	0.13	0.92	0.07	1.46	4.94	1.95	100
ORA_2A_016	HSR	76.64	0.09	14.11	0.04	0.27	0.08	1.19	5.37	2.2	100
ORA_2A_016	HSR	76.66	0.27	13.66	0	0.65	0	0.41	6.19	2.16	100
ORA_2A_016	HSR	76.7	0.26	13.67	0.02	0.98	0.05	0.58	5.69	2.05	100
ORA_2A_016	HSR	76.71	0	13.39	0.08	1.32	0.09	0.74	5.76	1.91	100
ORA_2A_016	HSR	76.73	0	13.54	0.11	0.81	0.24	1.13	5.38	2.06	100
ORA_2A_016	HSR	76.74	0.17	13.52	0.06	0.93	0.08	0.63	5.76	2.11	100
ORA_2A_016	HSR	76.75	0	14.03	0.12	0.45	0	0.61	5.76	2.28	100
ORA_2A_016	HSR	76.75	0.18	13.57	0.01	1.16	0	0.54	5.48	2.32	100
ORA_2A_016	HSR	76.78	0.24	13.84	0.18	0.72	0	1.38	4.98	1.88	100
ORA_2A_016	HSR	76.82	0.15	13.92	0	0.43	0	0.57	5.99	2.13	100
ORA_2A_016	HSR	76.82	0.04	13.84	0.16	0.58	0	0.51	5.93	2.11	100
ORA_2A_016	HSR	76.86	0.15	13.58	0.02	0.87	0	0.92	5.47	2.15	100
ORA_2A_016	HSR	76.86	0.23	13.3	0	1.29	0.02	1.06	5.23	2.01	100
ORA_2A_016	HSR	76.87	0	13.37	0.04	1.19	0.01	1.16	5.42	1.93	100
ORA_2A_016	HSR	76.88	0.08	14.06	0.06	0.3	0.1	1.34	5.17	2.01	100
ORA_2A_016	HSR	76.89	0.01	13.86	0	0.43	0.19	0.7	5.88	2.04	100
ORA_2A_016	HSR	76.9	0.01	13.86	0.14	0.61	0.04	0.73	5.71	2	100
ORA_2A_016	HSR	76.9	0	13.86	0.24	0.32	0	0.74	5.75	2.19	100
ORA_2A_016	HSR	76.91	0	13.82	0.01	0.78	0	0.65	5.62	2.21	100
ORA_2A_016	HSR	76.99	0.02	13.43	0.08	0.98	0.04	0.57	5.7	2.03	99.85
ORA_2A_016	HSR	77.04	0.01	13.87	0.13	0.65	0	0.83	5.44	2.02	100
ORA_2A_016	HSR	77.04	0.01	13.53	0.06	0.98	0	0.4	5.79	2.19	100
ORA_2A_016	HSR	77.05	0.14	13.34	0.03	1.09	0	0.56	5.71	2.07	100
ORA_2A_016	HSR	77.06	0.04	12.85	0.06	1.28	0.18	0.97	5.4	2.16	100
ORA_2A_016	HSR	77.12	0.03	13.31	0.13	0.74	0	0.96	5.46	2.25	100
ORA_2A_016	HSR	77.14	0	13.76	0.05	0.95	0	1.06	4.98	2.05	100
ORA_2A_016	HSR	77.15	0.14	13.41	0.11	0.7	0	0.54	5.8	2.15	100
ORA_2A_016	HSR	77.19	0	13.38	0.02	0.63	0	0.92	5.84	2.03	100
ORA_2A_016	HSR	77.19	0.18	12.8	0.18	1.19	0.08	1.63	4.84	1.91	100
ORA_2A_016	HSR	77.2	0.02	13.43	0.1	0.42	0.14	1.08	5.51	2.1	100
ORA_2A_016	HSR	77.22	0.08	13.47	0	0.89	0	0.43	5.86	2.06	100
ORA_2A_016	HSR	77.22	0.18	13.4	0.1	1.11	0.02	1.06	5.07	1.83	100
ORA_2A_016	HSR	77.23	0	13.65	0.08	0.62	0	0.83	5.43	2.16	100
ORA_2A_016	HSR	77.24	0.03	13.67	0	0.78	0.26	1.17	5.05	1.81	100
ORA_2A_016	HSR	77.25	0	13.48	0.2	0.75	0.09	0.89	5.34	2	100
ORA_2A_016	HSR	77.26	0.12	13.74	0.02	0.67	0	1.08	5.2	1.91	100
ORA_2A_016	HSR	77.27	0	13.2	0.15	1.04	0.07	0.38	5.64	2.24	100
ORA_2A_016	HSR	77.28	0	13.35	0.16	0.77	0	0.54	5.77	2.14	100
ORA_2A_016	HSR	77.31	0	13.44	0.04	0.81	0	0.58	5.63	2.18	100

ORA_2A_016	HSR	77.31	0.21	13.53	0.06	0.66	0	0.53	5.61	2.07	100
ORA_2A_016	HSR	77.33	0	13.57	0.02	1	0.01	0.96	5.35	1.76	100
ORA_2A_016	HSR	77.35	0.01	13.51	0	0.6	0.25	0.44	5.74	2.09	100
ORA_2A_016	HSR	77.36	0	13.55	0.01	0.39	0	0.7	5.86	2.12	100
ORA_2A_016	HSR	77.38	0	13.15	0	0.96	0.22	0.59	5.62	2.07	100
ORA_2A_016	HSR	77.42	0.08	13.18	0.05	0.74	0	0.56	5.75	2.23	100
ORA_2A_016	HSR	77.51	0.05	13.49	0.02	0.71	0	0.68	5.5	2.04	100
ORA_2A_016	HSR	77.52	0.05	13.32	0.16	0.51	0.02	0.73	5.51	2.19	100
ORA_2A_016	HSR	77.53	0	13.21	0.04	0.89	0.03	0.37	5.91	2.03	100
ORA_2A_016	HSR	77.55	0.01	13.43	0.04	0.7	0	0.67	5.56	2.04	100
ORA_2A_016	HSR	77.67	0.06	13.16	0	0.87	0.08	0.48	5.67	2.01	100
ORA_2A_016	HSR	77.69	0.17	13.27	0.04	0.68	0	0.43	5.68	2.04	100
ORA_2A_016	HSR	77.69	0	13.12	0.11	0.54	0.24	0.92	5.38	2	100
ORA_2A_016	HSR	77.7	0	12.95	0	1.18	0.09	0.41	5.89	1.78	100
ORA_2A_016	HSR	77.74	0.09	12.77	0.41	0.89	0.13	1.31	4.65	2.01	100
ORA_2A_016	HSR	77.75	0.03	13.26	0.05	0.64	0.06	0.3	5.87	2.06	100
ORA_2A_016	HSR	77.89	0.07	13.21	0.06	0.38	0.09	0.62	5.55	2.13	100
ORA_2A_016	HSR	78.01	0.21	12.94	0	0.64	0	0.46	5.59	2.14	100
ORA_2A_016	HSR	78.13	0	13.07	0	0.46	0	1.15	5.2	1.98	100
ORA_2A_016	HSR	78.91	0	12.36	0.02	0.99	0.24	1.32	4.33	1.82	100

ORA-2A-023:

Sample	Type	SiO ₂	TiO ₂	Al ₂ O ₃	MgO	FeO	MnO	CaO	Na ₂ O	K ₂ O	Total
ORA_2A_023	Glass (LSR)	73.95	0.16	14.44	0.38	1.43	0	0.9	5.44	3.19	99.89
ORA_2A_023	HSR (Fine Gr)	75.22	0.01	14.33	0.04	0.78	0	0.68	5.49	3.31	99.86
ORA_2A_023	HSR (Fine Gr)	75.44	0	14.1	0	1.15	0.05	0.84	5.26	3.16	100
ORA_2A_023	HSR (Fine Gr)	75.46	0.13	14.12	0.04	0.73	0.08	0.61	5.6	3.23	100
ORA_2A_023	HSR (Fine Gr)	75.47	0.05	14.36	0.02	0.62	0.11	0.68	5.53	3.15	100
ORA_2A_023	HSR (Fine Gr)	75.59	0.11	14.04	0.07	0.83	0	0.61	5.54	3.21	100
ORA_2A_023	HSR (Fine Gr)	75.6	0	13.82	0.02	1.08	0.02	0.78	5.48	3.2	100
ORA_2A_023	HSR (Fine Gr)	75.61	0.1	13.77	0.06	1.3	0	0.69	5.24	3.12	99.88
ORA_2A_023	HSR (Fine Gr)	75.64	0.07	14.02	0.05	0.68	0.13	0.67	5.47	3.14	99.86
ORA_2A_023	HSR (Fine Gr)	75.64	0.02	13.79	0.07	1	0.14	0.82	5.15	3.26	99.9
ORA_2A_023	HSR (Fine Gr)	75.66	0.08	14.03	0.1	0.65	0.01	1.21	4.92	3.34	100
ORA_2A_023	HSR (Fine Gr)	75.67	0.08	13.68	0.02	1.07	0.09	0.85	5.34	3.05	99.86
ORA_2A_023	HSR (Fine Gr)	75.7	0	13.91	0.07	0.82	0.04	0.66	5.67	3.02	99.89
ORA_2A_023	HSR (Fine Gr)	75.77	0.11	13.87	0	0.92	0	0.64	5.33	3.2	99.84
ORA_2A_023	HSR (Fine Gr)	75.83	0.2	13.82	0.05	0.76	0	0.53	5.5	3.21	99.89
ORA_2A_023	HSR (Fine Gr)	75.87	0.1	13.95	0.02	0.67	0.06	0.42	5.54	3.25	99.88
ORA_2A_023	HSR (Fine Gr)	75.88	0.09	13.73	0.07	0.76	0.19	0.53	5.16	3.47	99.89
ORA_2A_023	HSR (Fine Gr)	75.95	0	13.76	0.06	0.85	0	0.67	5.21	3.5	100
ORA_2A_023	HSR (Fine Gr)	75.96	0.16	13.76	0	0.95	0.08	0.67	5.18	3.24	100
ORA_2A_023	HSR (Fine Gr)	75.98	0.32	13.7	0.12	0.52	0.19	0.58	5.52	3.08	100
ORA_2A_023	HSR (Fine Gr)	76.03	0.06	13.93	0.04	1.05	0.09	0.93	4.59	3.28	100
ORA_2A_023	HSR (Fine Gr)	76.11	0.07	13.97	0.06	0.53	0.08	0.51	5.43	3.24	100
ORA_2A_023	HSR (Fine Gr)	76.12	0	13.55	0.01	1.05	0	0.7	5.71	2.86	100
ORA_2A_023	HSR (Fine Gr)	76.13	0	13.91	0	0.61	0.12	0.89	5.13	3.21	100
ORA_2A_023	HSR (Fine Gr)	76.2	0.02	13.77	0.03	0.73	0	0.76	5.41	2.96	99.88
ORA_2A_023	HSR (Fine Gr)	76.24	0.02	13.69	0.06	0.81	0.06	0.58	5.18	3.35	100
ORA_2A_023	HSR (Fine Gr)	76.25	0	13.38	0.02	1.18	0	1.02	5.08	3.06	100
ORA_2A_023	HSR (Fine Gr)	76.26	0.03	13.85	0.01	0.77	0	0.61	5.59	2.87	100
ORA_2A_023	HSR (Fine Gr)	76.27	0.02	13.63	0	0.96	0.07	0.6	5.33	3.12	100
ORA_2A_023	HSR (Fine Gr)	76.29	0.05	13.84	0.03	0.47	0.24	0.64	5.42	3.02	100
ORA_2A_023	HSR (Fine Gr)	76.32	0.03	13.65	0.06	0.86	0.09	0.74	5.03	3.1	99.89
ORA_2A_023	HSR (Fine Gr)	76.38	0	13.79	0.01	0.7	0	0.55	5.32	3.23	100
ORA_2A_023	HSR (Fine Gr)	76.39	0	13.78	0.07	0.72	0.1	0.68	5.15	3.1	100
ORA_2A_023	HSR (Fine Gr)	76.43	0	13.43	0.01	0.98	0.27	0.61	5.13	3.15	100
ORA_2A_023	HSR (Fine Gr)	76.52	0	13.33	0	1.13	0.06	0.42	5.35	3.19	100
ORA_2A_023	HSR (Fine Gr)	76.73	0.1	13.5	0.01	0.81	0	0.59	5.05	3.2	100
ORA_2A_023	HSR (Fine Gr)	76.74	0	13.43	0.07	0.93	0	0.5	5.26	3.07	100
ORA_2A_023	HSR (Fine Gr)	76.76	0	13.88	0.07	0.61	0	0.45	5.21	3.02	100
ORA_2A_023	HSR (Fine Gr)	76.89	0	13.56	0.06	0.72	0	0.42	5.12	3.23	100
ORA_2A_023	HSR (Fine Gr)	76.96	0.12	13.66	0.05	0.4	0	0.45	5.34	3.02	100

ORA_2A_023	HSR (Fine Gr)	76.99	0	13.06	0.01	1.06	0.1	0.63	5.04	3.11	100
ORA_2A_023	HSR (Fine Gr)	77.05	0	13.55	0	0.76	0.11	0.34	5.19	3.01	100
ORA_2A_023	HSR (Fine Gr)	77.08	0.07	13.15	0.03	0.85	0	0.61	5.18	3.04	100
ORA_2A_023	HSR (Fine Gr)	77.13	0.05	13.16	0.06	0.79	0	0.68	5.03	2.97	99.88
ORA_2A_023	HSR (Fine Gr)	77.18	0.09	13.04	0	0.8	0	0.61	5.38	2.92	100
ORA_2A_023	HSR (Fine Gr)	77.22	0	13.4	0.1	0.41	0	0.48	5.34	3.04	100
ORA_2A_023	HSR (Fine Gr)	77.51	0	13.34	0.08	0.64	0	0.41	4.93	3.1	100
ORA_2A_023	HSR Boundary	75.74	0.02	13.92	0.02	1.23	0.08	0.76	5.12	3.12	100
ORA_2A_023	HSR Boundary	75.96	0	13.91	0	0.94	0.03	0.48	5.36	3.33	100
ORA_2A_023	HSR Boundary	76.04	0	13.9	0	0.8	0.1	0.62	5.3	3.23	100
ORA_2A_023	HSR Boundary	76.39	0.09	13.58	0.05	0.75	0.02	0.61	5.33	3.19	100
ORA_2A_023	HSR Boundary	76.81	0.07	13.3	0.04	0.85	0.06	0.42	5.29	3.17	100
ORA_2A_023	HSR Boundary	77.03	0	13.33	0	0.8	0	0.41	5.27	3.15	100
ORA_2A_023	HSR Boundary	77.07	0	13.1	0	0.86	0.07	0.58	5.16	3.02	99.86

ORA-2A-024:

Sample	Type	SiO ₂	TiO ₂	Al ₂ O ₃	MgO	FeO	MnO	CaO	Na ₂ O	K ₂ O	Total
ORA_2A_024	Glass	72.57	0.33	15.37	0.38	2.02	0.02	1.58	5.24	2.49	100
ORA_2A_024	Glass	72.76	0.27	15.02	0.44	2.25	0	1.61	5.1	2.56	100
ORA_2A_024	Glass	72.85	0.27	15.08	0.47	1.99	0.1	1.43	5.46	2.35	100
ORA_2A_024	Glass	72.93	0.19	15.16	0.45	1.85	0	1.37	5.49	2.55	100
ORA_2A_024	Glass	72.96	0.19	14.98	0.49	2	0.09	1.21	5.44	2.5	99.86
ORA_2A_024	Glass	73.29	0.22	14.92	0.32	1.98	0.02	1.3	5.41	2.41	99.88
ORA_2A_024	Glass	73.29	0.26	15.16	0.41	1.46	0.15	1.59	5.26	2.39	100
ORA_2A_024	Glass	73.29	0.1	15.11	0.46	1.96	0.04	1.66	5.02	2.38	100
ORA_2A_024	Glass	73.3	0.15	15.26	0.36	2.65	0.1	1.28	4.46	2.45	100
ORA_2A_024	Glass	73.32	0.14	15.03	0.38	1.73	0.13	1.48	5.27	2.41	99.89
ORA_2A_024	Glass	73.32	0.27	14.94	0.4	1.9	0.09	1.2	5.4	2.48	100
ORA_2A_024	Glass	73.38	0.12	15.3	0.39	1.59	0.06	1.71	5.1	2.35	100
ORA_2A_024	Glass	73.4	0.16	14.79	0.46	2.22	0	1.31	5.35	2.31	100
ORA_2A_024	Glass	73.4	0.24	14.81	0.27	2.09	0.02	1.25	5.38	2.42	99.88
ORA_2A_024	Glass	73.42	0.23	15.14	0.32	1.81	0.02	1.3	5.53	2.23	100
ORA_2A_024	Glass	73.43	0.1	14.98	0.41	1.71	0.11	1.71	5.27	2.28	100
ORA_2A_024	Glass	73.45	0.23	15.33	0.41	1.2	0	1.4	5.49	2.5	100
ORA_2A_024	Glass	73.45	0.23	14.9	0.46	1.63	0.08	1.42	5.39	2.44	100
ORA_2A_024	Glass	73.48	0.22	14.77	0.38	1.72	0	1.27	5.53	2.46	99.83
ORA_2A_024	Glass	73.54	0.15	15.12	0.25	1.7	0.03	1.16	5.43	2.42	99.81
ORA_2A_024	Glass	73.56	0.23	14.9	0.37	1.72	0.08	1.27	5.47	2.4	100
ORA_2A_024	Glass	73.57	0.08	14.71	0.48	1.86	0.07	1.88	5.02	2.33	100
ORA_2A_024	Glass	73.6	0.26	14.96	0.48	1.78	0	1.59	5.05	2.29	100
ORA_2A_024	Glass	73.62	0.24	14.91	0.34	1.86	0.02	1.34	5.41	2.25	100
ORA_2A_024	Glass	73.63	0.1	15.06	0.38	1.61	0.01	1.02	5.69	2.51	100
ORA_2A_024	Glass	73.63	0.14	14.93	0.31	1.8	0.07	1.58	5.19	2.35	100
ORA_2A_024	Glass	73.8	0.3	14.65	0.41	1.81	0	1.19	5.41	2.43	100
ORA_2A_024	Glass	73.82	0.2	14.91	0.42	1.57	0	1.49	5.17	2.42	100
ORA_2A_024	Glass	73.85	0.1	14.63	0.43	1.85	0.1	1.19	5.47	2.37	100
ORA_2A_024	Glass	73.9	0.09	14.72	0.36	1.66	0.12	1.31	5.4	2.43	100
ORA_2A_024	Glass	73.92	0.18	14.61	0.45	1.76	0.04	1.81	4.96	2.26	100
ORA_2A_024	Glass	74.01	0.07	14.32	0.45	2.33	0.11	1.5	4.98	2.23	100
ORA_2A_024	Glass	74.09	0.36	14.64	0.31	1.66	0.09	1.29	5.31	2.25	100
ORA_2A_024	Glass	74.09	0.16	14.77	0.49	1.41	0.1	1.23	5.41	2.35	100
ORA_2A_024	Glass	74.1	0.09	14.77	0.35	1.64	0	1.14	5.59	2.33	100
ORA_2A_024	Glass	74.16	0.08	14.66	0.3	1.67	0.05	1.25	5.53	2.3	100
ORA_2A_024	Glass	74.17	0.05	14.8	0.36	1.57	0.1	1.37	5.34	2.24	100
ORA_2A_024	Glass	74.18	0.05	14.72	0.28	1.76	0.06	1.29	5.32	2.34	100
ORA_2A_024	Glass	74.32	0.16	14.58	0.3	1.66	0	1.28	5.35	2.35	100
ORA_2A_024	Glass	74.33	0.14	14.73	0.28	1.45	0	1.04	5.5	2.53	100
ORA_2A_024	Glass	74.48	0.22	14.28	0.31	1.73	0.14	1.37	5.15	2.34	100
ORA_2A_024	Glass	74.54	0.22	14.44	0.41	1.57	0.13	1.25	5.18	2.27	100
ORA_2A_024	Glass	74.56	0.03	14.2	0.4	1.9	0.17	1.45	4.96	2.33	100
ORA_2A_024	Glass	74.59	0.25	14.28	0.24	1.67	0.04	2.2	4.71	2.01	100
ORA_2A_024	Glass	74.72	0.19	14.13	0.39	1.68	0.15	1.46	4.99	2.3	100
ORA_2A_024	Glass	74.83	0.07	14.61	0.22	1.38	0.03	1.06	5.5	2.31	100

ORA_2A_024	Glass	75.26	0.21	13.92	0.36	1.66	0	1.16	5.15	2.27	100
ORA_2A_024	Glass	75.5	0.18	14	0.18	1.2	0.23	1.21	5.2	2.32	100
ORA_2A_024	Glass	75.88	0.12	13.87	0.15	1.42	0.13	1.13	5.03	2.28	100
ORA_2A_024	Glass	75.31	0.22	13.92	0.3	1.61	0.06	1.45	4.92	2.21	100

Sample	Type	SiO ₂	TiO ₂	Al ₂ O ₃	MgO	FeO	MnO	CaO	Na ₂ O	K ₂ O	Total
ORA_2A_024	Glass (HSR)	76.33	0.07	13.85	0.05	1.06	0.08	0.88	5.71	1.98	100
ORA_2A_024	Glass (HSR)	76.35	0	13.67	0.01	1.44	0.03	1.02	5.64	1.84	100
ORA_2A_024	Glass (HSR)	76.44	0.03	13.78	0.04	0.86	0.03	0.84	5.76	2.09	99.88
ORA_2A_024	Glass (HSR)	76.51	0.06	13.86	0.02	0.93	0.09	0.6	5.72	2.22	100
ORA_2A_024	Glass (HSR)	76.52	0.1	13.59	0.03	1.1	0	0.77	5.86	1.92	99.89
ORA_2A_024	Glass (HSR)	76.53	0.15	13.64	0	1.1	0	0.46	5.83	2.15	99.86
ORA_2A_024	Glass (HSR)	76.57	0.14	13.77	0.22	1.24	0	1.26	4.79	2.01	100
ORA_2A_024	Glass (HSR)	76.57	0	13.83	0.1	0.83	0.04	0.73	5.77	2.14	100
ORA_2A_024	Glass (HSR)	76.59	0.14	13.75	0.04	1	0.02	0.96	5.42	2.09	100
ORA_2A_024	Glass (HSR)	76.61	0.04	13.61	0	1.1	0	0.57	6.07	2.01	100
ORA_2A_024	Glass (HSR)	76.64	0.1	13.5	0.12	1.26	0.08	0.78	5.48	2.04	100
ORA_2A_024	Glass (HSR)	76.67	0.06	13.79	0.07	0.83	0	0.61	5.82	2.14	100
ORA_2A_024	Glass (HSR)	76.74	0	13.6	0.2	1.17	0.09	1.19	4.99	2.02	100
ORA_2A_024	Glass (HSR)	76.76	0	13.44	0.05	1.5	0	0.54	5.54	2.17	100
ORA_2A_024	Glass (HSR)	76.79	0.01	13.69	0	0.9	0	0.5	5.95	2.16	100
ORA_2A_024	Glass (HSR)	76.8	0	13.4	0.03	0.76	0.04	0.9	5.45	2.03	100
ORA_2A_024	Glass (HSR)	76.82	0.1	13.37	0.01	1.18	0	0.68	5.82	2.03	100
ORA_2A_024	Glass (HSR)	76.84	0	13.77	0.02	0.81	0.01	0.87	5.5	2.18	100
ORA_2A_024	Glass (HSR)	76.86	0	13.74	0	0.84	0	0.78	5.87	1.91	100
ORA_2A_024	Glass (HSR)	76.86	0.18	13.42	0.01	1.03	0.17	0.55	5.71	2.06	100
ORA_2A_024	Glass (HSR)	76.86	0.17	13.57	0.03	1.03	0.07	0.62	5.47	2.19	100
ORA_2A_024	Glass (HSR)	76.88	0.07	13.47	0	1.16	0.06	0.5	5.79	2.07	100
ORA_2A_024	Glass (HSR)	76.89	0.06	13.35	0.01	1.01	0.13	0.66	5.71	2.17	100
ORA_2A_024	Glass (HSR)	76.89	0.12	13.32	0.16	1.13	0	1.08	5.13	2.17	100
ORA_2A_024	Glass (HSR)	76.92	0.07	13.54	0.01	0.9	0.07	0.45	5.79	2.26	100
ORA_2A_024	Glass (HSR)	76.93	0	13.53	0.03	1.11	0.01	0.8	5.55	2.04	100
ORA_2A_024	Glass (HSR)	76.93	0.09	13.6	0.05	0.84	0	0.59	5.84	2.06	100
ORA_2A_024	Glass (HSR)	76.94	0.1	13.33	0.08	1.23	0.04	0.87	5.51	1.9	100
ORA_2A_024	Glass (HSR)	76.98	0.11	13.44	0.04	0.97	0	0.65	5.78	2.04	100
ORA_2A_024	Glass (HSR)	76.98	0	13.57	0	0.72	0	0.5	5.96	2.13	99.86
ORA_2A_024	Glass (HSR)	76.98	0	13.5	0.07	0.81	0	0.72	5.61	2.16	99.86
ORA_2A_024	Glass (HSR)	76.99	0.08	13.44	0	0.94	0.19	0.42	5.77	2.16	100
ORA_2A_024	Glass (HSR)	76.99	0.04	13.71	0	0.74	0.1	0.62	5.78	2.03	100
ORA_2A_024	Glass (HSR)	77.03	0	13.78	0.07	0.73	0.01	0.54	5.54	2.14	99.86
ORA_2A_024	Glass (HSR)	77.03	0.03	13.27	0.01	0.89	0.19	0.51	5.72	2.22	99.86
ORA_2A_024	Glass (HSR)	77.04	0	13.77	0.05	0.75	0.01	0.71	5.6	2.07	100
ORA_2A_024	Glass (HSR)	77.06	0.19	13.34	0.04	0.91	0.11	0.65	5.6	2.1	100
ORA_2A_024	Glass (HSR)	77.06	0.05	13.43	0	1.11	0	0.49	5.62	2.1	99.87
ORA_2A_024	Glass (HSR)	77.07	0.06	13.35	0.02	1.12	0.04	0.75	5.66	1.93	100
ORA_2A_024	Glass (HSR)	77.07	0	13.59	0	0.71	0.02	0.54	5.83	2.11	99.86
ORA_2A_024	Glass (HSR)	77.08	0.03	13.48	0.08	0.89	0	0.72	5.54	2.19	100
ORA_2A_024	Glass (HSR)	77.08	0.05	13.45	0	0.95	0.04	0.6	5.65	2.04	99.85
ORA_2A_024	Glass (HSR)	77.1	0.12	13.49	0.06	0.9	0.06	0.65	5.46	2.03	99.87
ORA_2A_024	Glass (HSR)	77.12	0.08	13.44	0.06	0.86	0.01	0.74	5.55	2.14	100
ORA_2A_024	Glass (HSR)	77.15	0.03	13.51	0.06	0.85	0.05	0.72	5.59	2.04	100
ORA_2A_024	Glass (HSR)	77.17	0.05	13.37	0.06	0.79	0.11	0.53	5.69	2.23	100

ORA_2A_024	Glass (HSR)	77.18	0.05	13.4	0.03	0.72	0.15	0.84	5.35	2.15	99.87
ORA_2A_024	Glass (HSR)	77.19	0.09	13.66	0.03	0.67	0.05	0.83	5.44	2.03	100
ORA_2A_024	Glass (HSR)	77.24	0.07	13.43	0	0.97	0	0.48	5.7	2.1	100
ORA_2A_024	Glass (HSR)	77.24	0.03	13.5	0.05	0.95	0	0.93	5.31	1.99	100
ORA_2A_024	Glass (HSR)	77.25	0	13.59	0	0.73	0.02	0.85	5.44	2.11	100
ORA_2A_024	Glass (HSR)	77.25	0.08	13.26	0.11	0.92	0.09	0.67	5.42	2.08	99.88
ORA_2A_024	Glass (HSR)	77.27	0	13.48	0.04	0.88	0.01	0.69	5.48	2.15	100
ORA_2A_024	Glass (HSR)	77.27	0.03	13.23	0.04	1.03	0	0.76	5.5	2.13	100
ORA_2A_024	Glass (HSR)	77.28	0	13.36	0.02	0.98	0.02	0.78	5.6	1.96	100
ORA_2A_024	Glass (HSR)	77.29	0	13.37	0	0.76	0.1	0.78	5.54	2.04	99.88
ORA_2A_024	Glass (HSR)	77.29	0	13.44	0.14	0.6	0.14	0.96	5.29	2.02	99.87
ORA_2A_024	Glass (HSR)	77.29	0.06	13.33	0.06	1.03	0	0.72	5.46	2.06	100
ORA_2A_024	Glass (HSR)	77.32	0	13.38	0	0.67	0.03	0.72	5.56	2.15	99.83
ORA_2A_024	Glass (HSR)	77.35	0	13.33	0.05	0.96	0.09	0.38	5.62	2.22	100
ORA_2A_024	Glass (HSR)	77.36	0.01	13.44	0	0.87	0.01	0.55	5.69	2.07	100
ORA_2A_024	Glass (HSR)	77.36	0.06	13.37	0.01	0.96	0	0.46	5.56	2.21	100
ORA_2A_024	Glass (HSR)	77.36	0.11	13.35	0.08	0.68	0	0.63	5.59	2.2	100
ORA_2A_024	Glass (HSR)	77.36	0.05	13.49	0.11	0.68	0	0.76	5.39	2.16	100
ORA_2A_024	Glass (HSR)	77.36	0	13.3	0.13	0.78	0	0.97	5.35	2.1	100
ORA_2A_024	Glass (HSR)	77.38	0	13.37	0	1.07	0	0.56	5.49	2.12	100
ORA_2A_024	Glass (HSR)	77.4	0.04	13.25	0.01	0.82	0.04	0.79	5.38	2.16	99.88
ORA_2A_024	Glass (HSR)	77.41	0.15	13.28	0.06	0.57	0.15	0.72	5.58	2.07	100
ORA_2A_024	Glass (HSR)	77.45	0.1	13.52	0	0.6	0.01	0.79	5.39	2.15	100
ORA_2A_024	Glass (HSR)	77.48	0	13.24	0.01	0.99	0	0.46	5.65	2.17	100
ORA_2A_024	Glass (HSR)	77.48	0.05	13.43	0	0.69	0.09	0.74	5.37	2.17	100
ORA_2A_024	Glass (HSR)	77.48	0.06	13.37	0	0.85	0.02	0.67	5.52	2.04	100
ORA_2A_024	Glass (HSR)	77.5	0	13.26	0	1.1	0.01	0.63	5.41	2.08	100
ORA_2A_024	Glass (HSR)	77.54	0	13.19	0	1.08	0	0.95	5.32	1.91	100
ORA_2A_024	Glass (HSR)	77.54	0.08	13.13	0.05	0.71	0.11	0.72	5.6	2.05	100
ORA_2A_024	Glass (HSR)	77.56	0	13.23	0.07	0.59	0.07	0.62	5.46	2.26	99.87
ORA_2A_024	Glass (HSR)	77.57	0	12.99	0.08	1.18	0.05	1.24	5.12	1.78	100
ORA_2A_024	Glass (HSR)	77.57	0.02	13.41	0.1	0.87	0.01	0.6	5.26	2.15	100
ORA_2A_024	Glass (HSR)	77.58	0.06	13.09	0.03	1.01	0.03	0.34	5.7	2.16	100
ORA_2A_024	Glass (HSR)	77.59	0	13.22	0.01	0.66	0.02	0.62	5.63	2.1	99.84
ORA_2A_024	Glass (HSR)	77.62	0.06	13.09	0	0.92	0	0.71	5.52	2.09	100
ORA_2A_024	Glass (HSR)	77.65	0	13.46	0	0.6	0.02	0.75	5.45	2.07	100
ORA_2A_024	Glass (HSR)	77.69	0	13.52	0	0.41	0	0.82	5.42	2.13	100
ORA_2A_024	Glass (HSR)	77.78	0.08	13.2	0	0.68	0.01	0.84	5.37	2.03	100
ORA_2A_024	Glass (HSR)	77.78	0	13.35	0.01	0.56	0	0.69	5.33	2.15	99.87
ORA_2A_024	Glass (HSR)	77.92	0.06	13.21	0.07	0.44	0.05	0.67	5.27	2.18	99.87
ORA_2A_024	Glass (HSR)	78	0	13	0	0.85	0	0.57	5.59	1.99	100

ORA-2A-031:

Sample	Type	SiO ₂	TiO ₂	Al ₂ O ₃	MgO	FeO	MnO	CaO	Na ₂ O	K ₂ O	Total
ORA_2A_031	HSR	77.57	0.19	13	0.03	1.14	0.06	0.92	4.7	2.38	100
ORA_2A_031	HSR	77.19	0.03	13.2	0	0.88	0.07	0.41	5.55	2.55	99.88
ORA_2A_031	HSR	77.54	0.02	13.23	0.04	0.93	0	0.48	5.38	2.38	100
ORA_2A_031	HSR	77.95	0.05	13.27	0.04	0.37	0.01	1.6	4.52	2.06	99.87
ORA_2A_031	HSR	77.2	0.04	13.25	0	0.84	0.08	0.43	5.73	2.33	99.89
ORA_2A_031	HSR	77.23	0	13.4	0	0.82	0.03	0.41	5.58	2.37	99.85
ORA_2A_031	HSR	77.25	0.04	13.27	0.1	0.83	0.06	0.62	5.61	2.21	100
ORA_2A_031	HSR	77.34	0	13.5	0	0.75	0	0.27	5.8	2.34	100
ORA_2A_031	HSR	77.01	0.18	13.45	0.06	0.93	0.18	0.31	5.62	2.26	100
ORA_2A_031	HSR	77.4	0	13.46	0	0.86	0	0.33	5.62	2.32	100
ORA_2A_031	HSR	77.83	0	13.33	0	0.45	0.01	0.45	5.53	2.4	100
ORA_2A_031	HSR	77.6	0	13.12	0	0.93	0	0.41	5.52	2.42	100
ORA_2A_031	HSR	77.62	0.1	13.14	0	1.02	0	0.31	5.6	2.21	100
ORA_2A_031	HSR	77.44	0.14	13.18	0.05	0.73	0.18	0.33	5.63	2.3	100
ORA_2A_031	HSR	77.1	0	13.38	0	1.08	0	0.43	5.64	2.36	100
ORA_2A_031	HSR	76.72	0.39	13.38	0	1.06	0	0.29	5.73	2.42	100
ORA_2A_031	HSR	77.26	0.08	13.3	0	0.79	0.09	0.35	5.77	2.37	100
ORA_2A_031	HSR	77.19	0.09	13.22	0	1.09	0.13	0.37	5.43	2.47	100
ORA_2A_031	HSR	77.4	0.09	12.81	0.18	1.04	0.09	0.36	5.64	2.38	100
ORA_2A_031	HSR	77.04	0.19	13.31	0.1	1.12	0	0.32	5.62	2.29	100
ORA_2A_031	HSR	77.38	0.15	13.41	0	0.53	0	0.56	5.5	2.46	100
ORA_2A_031	HSR	77.85	0.21	13.13	0.1	0.74	0	0.24	5.51	2.22	100
ORA_2A_031	HSR	77.49	0	13.13	0.02	0.88	0	0.44	5.64	2.39	100
ORA_2A_031	HSR	77.6	0	13.33	0.09	0.68	0	0.29	5.59	2.42	100
ORA_2A_031	HSR	77.03	0.05	13.46	0.07	1.06	0.12	0.43	5.57	2.2	100
ORA_2A_031	HSR	76.75	0.01	13.59	0	1.23	0.11	0.52	5.56	2.23	100
ORA_2A_031	HSR	77.66	0	13.09	0.12	0.74	0.11	0.31	5.69	2.29	100
ORA_2A_031	HSR	77.36	0	13.24	0	1.01	0.08	0.43	5.7	2.19	100
ORA_2A_031	HSR	77.1	0.17	13.65	0	0.75	0	0.33	5.71	2.3	100
ORA_2A_031	HSR	77.3	0	13.28	0	0.9	0.25	0.34	5.63	2.3	100
ORA_2A_031	HSR	78.02	0	12.87	0	0.89	0	0.54	5.41	2.28	100
ORA_2A_031	HSR	77.57	0.03	13.43	0	0.96	0	0.31	5.47	2.23	100
ORA_2A_031	HSR	77.38	0.04	13.37	0.19	0.85	0	0.22	5.76	2.19	100
ORA_2A_031	HSR	77.12	0.01	13.35	0.19	1.01	0.14	0.7	5.07	2.43	100
ORA_2A_031	HSR	76.84	0.12	13.18	0.02	1.01	0.26	0.49	5.63	2.34	99.88
ORA_2A_031	HSR	77.32	0	13.37	0	0.72	0.07	0.4	5.59	2.39	99.85
ORA_2A_031	HSR	77.22	0.04	13.32	0.01	0.8	0.05	0.4	5.56	2.46	99.86
ORA_2A_031	HSR	76.64	0.18	13.61	0.34	1.37	0.12	0.68	4.84	2.23	100
ORA_2A_031	HSR	77.31	0.02	13.2	0	1.09	0.06	0.61	5.3	2.41	100

ORA-2A-032:

Sample	Type	SiO ₂	TiO ₂	Al ₂ O ₃	MgO	FeO	MnO	CaO	Na ₂ O	K ₂ O	Total
ORA_2A_032	HSR	76.87	0.14	13.34	0	1.09	0	0.72	5.25	2.59	100
ORA_2A_032	HSR	77.2	0	13.11	0.02	1.14	0.04	0.52	5.28	2.53	99.83
ORA_2A_032	HSR	77.24	0.11	13.1	0.13	1.2	0.16	0.85	4.85	2.35	100
ORA_2A_032	HSR	77.24	0.03	13.45	0.06	0.97	0	0.46	5.27	2.38	99.87
ORA_2A_032	HSR	77.27	0.19	13.04	0.03	1.08	0.12	0.41	5.3	2.35	99.81
ORA_2A_032	HSR	77.27	0.25	13.05	0.03	1.09	0	0.52	5.4	2.39	100
ORA_2A_032	HSR	77.29	0.14	13.21	0.08	0.94	0	0.5	5.26	2.58	100
ORA_2A_032	HSR	77.3	0.1	12.99	0.04	1	0.03	0.65	5.46	2.43	100
ORA_2A_032	HSR	77.33	0.13	13.08	0.02	1.04	0	0.54	5.41	2.44	100
ORA_2A_032	HSR	77.34	0.17	13.11	0.07	0.89	0.04	0.6	5.36	2.42	100
ORA_2A_032	HSR	77.34	0.03	13.15	0	1.03	0.1	0.47	5.35	2.43	99.88
ORA_2A_032	HSR	77.36	0.07	13	0.15	1.34	0.13	0.74	4.73	2.38	99.89
ORA_2A_032	HSR	77.36	0.07	13.19	0.03	0.93	0	0.6	5.3	2.52	100
ORA_2A_032	HSR	77.4	0.03	13.19	0	0.87	0.07	0.55	5.46	2.42	100
ORA_2A_032	HSR	77.45	0	13.22	0	1.08	0.02	0.51	5.28	2.43	100
ORA_2A_032	HSR	77.45	0.02	13.08	0.01	0.85	0.17	0.51	5.25	2.53	99.87
ORA_2A_032	HSR	77.45	0	13.06	0.07	1.07	0.03	0.52	5.36	2.44	100
ORA_2A_032	HSR	77.47	0.12	13.17	0.03	0.95	0.01	0.45	5.37	2.44	100
ORA_2A_032	HSR	77.48	0.05	13.19	0.01	1.07	0.03	0.44	5.44	2.27	100
ORA_2A_032	HSR	77.48	0.2	12.93	0.03	1.09	0.12	0.57	5.15	2.43	100
ORA_2A_032	HSR	77.49	0.1	13.2	0.03	0.84	0.04	0.48	5.31	2.52	100
ORA_2A_032	HSR	77.5	0.02	13.15	0.02	0.92	0.04	0.5	5.38	2.46	100
ORA_2A_032	HSR	77.5	0.08	13.06	0	0.95	0.05	0.56	5.17	2.48	99.84
ORA_2A_032	HSR	77.5	0.07	13.07	0.01	0.95	0.05	0.57	5.23	2.4	99.84
ORA_2A_032	HSR	77.51	0.05	13.1	0	1.1	0.02	0.51	5.24	2.47	100
ORA_2A_032	HSR	77.52	0	13.04	0.09	1.08	0.14	0.65	5.1	2.38	100
ORA_2A_032	HSR	77.53	0.13	13.02	0.08	0.9	0.07	0.52	5.46	2.3	100
ORA_2A_032	HSR	77.54	0.03	13.08	0	0.99	0	0.44	5.49	2.42	100
ORA_2A_032	HSR	77.56	0	12.93	0	1.02	0.03	0.49	5.32	2.51	99.87
ORA_2A_032	HSR	77.57	0.09	12.95	0.06	0.85	0.07	0.49	5.37	2.42	99.87
ORA_2A_032	HSR	77.58	0.05	13.19	0	0.74	0.01	0.5	5.29	2.52	99.87
ORA_2A_032	HSR	77.61	0.01	12.82	0.09	1.19	0	0.97	4.77	2.36	99.83
ORA_2A_032	HSR	77.61	0.08	13.23	0.02	0.7	0.02	0.44	5.24	2.53	99.88
ORA_2A_032	HSR	77.62	0.01	12.93	0.03	1.19	0.02	0.53	5.2	2.45	100
ORA_2A_032	HSR	77.66	0.09	12.94	0.14	0.9	0	0.71	5.19	2.37	100
ORA_2A_032	HSR	77.68	0.01	12.87	0.05	1	0	0.5	5.38	2.5	100
ORA_2A_032	HSR	77.71	0.11	13.09	0.05	0.65	0.12	0.52	5.34	2.4	100
ORA_2A_032	HSR	77.73	0.04	13.15	0.01	0.72	0.03	0.5	5.32	2.5	100
ORA_2A_032	HSR	77.75	0.04	12.99	0.09	1.15	0	0.9	4.78	2.3	100
ORA_2A_032	HSR	77.76	0.06	13.23	0.03	0.79	0	0.46	5.29	2.38	100

ORA_2A_032	HSR	77.85	0.02	13.03	0.07	0.85	0.06	0.59	5.22	2.32	100
ORA_2A_032	HSR	77.88	0	12.94	0.04	0.94	0	0.49	5.37	2.34	100
ORA_2A_032	HSR	77.9	0.05	13.16	0	0.65	0.1	0.56	5.36	2.21	100

ORA-2A-035:

Sample	Type	SiO2	TiO2	Al2O3	MgO	FeO	MnO	CaO	Na2O	K2O	Total
ORA_2A_035	HSR	76.51	0.17	13.49	0	1.1	0	0.55	5.34	2.84	100
ORA_2A_035	HSR	76.68	0	13.38	0	1.17	0	1.12	4.95	2.7	100
ORA_2A_035	HSR	76.71	0.07	13.16	0.06	1.16	0.04	0.54	5.25	3.02	100
ORA_2A_035	HSR	76.78	0.07	13.13	0.06	0.99	0	0.63	5.58	2.76	100
ORA_2A_035	HSR	76.93	0	13.23	0	1.1	0	0.43	5.46	2.86	100
ORA_2A_035	HSR	76.96	0	13.11	0.06	0.63	0.33	0.63	5.07	3.21	100
ORA_2A_035	HSR	76.96	0.15	13.18	0.01	1.04	0.09	0.5	5.35	2.72	100
ORA_2A_035	HSR	77.01	0.13	13.05	0	1.01	0	0.48	5.33	3	100
ORA_2A_035	HSR	77.02	0.11	13.41	0	1.03	0	0.39	5.24	2.8	100
ORA_2A_035	HSR	77.03	0.13	13.16	0.01	1.01	0	0.49	5.11	2.92	99.87
ORA_2A_035	HSR	77.03	0.16	13.1	0.1	0.82	0.01	0.68	5.38	2.73	100
ORA_2A_035	HSR	77.07	0.02	13.14	0	0.91	0.32	0.52	5.21	2.8	100
ORA_2A_035	HSR	77.08	0.08	13.27	0	0.86	0	0.53	5.2	2.99	100
ORA_2A_035	HSR	77.14	0	13.44	0	0.73	0	0.47	5.25	2.97	100
ORA_2A_035	HSR	77.17	0.09	12.92	0	1.05	0.1	0.6	5.16	2.93	100
ORA_2A_035	HSR	77.18	0.03	13.12	0.02	1.06	0	0.65	5.15	2.78	100
ORA_2A_035	HSR	77.18	0.02	13.01	0.02	1	0.11	0.54	5.06	2.95	99.88
ORA_2A_035	HSR	77.19	0.03	12.92	0.09	0.92	0.13	0.47	5.14	2.97	99.84
ORA_2A_035	HSR	77.19	0.07	13.17	0	0.88	0.06	0.44	5.25	2.81	99.87
ORA_2A_035	HSR	77.2	0.01	13.54	0.11	0.71	0.02	0.39	5.06	2.97	100
ORA_2A_035	HSR	77.21	0.01	13.03	0.02	1.06	0	0.48	5.23	2.84	99.87
ORA_2A_035	HSR	77.21	0	13.15	0	1.09	0	0.51	5.15	2.89	100
ORA_2A_035	HSR	77.23	0.16	13.16	0.01	0.85	0	0.45	5.07	2.92	99.84
ORA_2A_035	HSR	77.26	0.04	13.21	0	0.78	0.1	0.3	5.31	3.01	100
ORA_2A_035	HSR	77.28	0.07	13.19	0.09	0.91	0.04	0.56	5.07	2.78	100
ORA_2A_035	HSR	77.29	0.06	13.19	0	0.91	0.01	0.54	5.08	2.92	100
ORA_2A_035	HSR	77.29	0.03	13.2	0	1	0.02	0.43	5.24	2.79	100
ORA_2A_035	HSR	77.3	0.03	13.23	0	0.84	0	0.45	5.19	2.95	100
ORA_2A_035	HSR	77.3	0	13.12	0.06	0.95	0	0.51	5.21	2.86	100
ORA_2A_035	HSR	77.3	0.04	13.03	0.02	0.79	0.16	0.52	5.23	2.91	100
ORA_2A_035	HSR	77.33	0.03	13.34	0	0.69	0.12	0.47	5.19	2.83	100
ORA_2A_035	HSR	77.37	0.02	13.11	0	0.85	0.01	0.52	5.25	2.87	100
ORA_2A_035	HSR	77.38	0.07	13.01	0.22	0.66	0.1	0.44	5.21	2.91	100
ORA_2A_035	HSR	77.41	0.07	13.05	0	0.95	0.04	0.46	5.18	2.84	100
ORA_2A_035	HSR	77.41	0.07	13.1	0	1.06	0.2	0.37	5.07	2.71	100

ORA_2A_035	HSR	77.42	0.04	13.1	0.02	0.88	0.04	0.43	5.07	2.89	99.88
ORA_2A_035	HSR	77.42	0	13.45	0.03	0.41	0.1	0.49	5.27	2.83	100
ORA_2A_035	HSR	77.43	0.1	13.13	0	0.66	0.01	0.37	5.37	2.93	100
ORA_2A_035	HSR	77.46	0.06	13.28	0.02	0.7	0	0.32	5.19	2.98	100
ORA_2A_035	HSR	77.47	0.08	13.24	0.04	0.98	0	0.38	5.21	2.61	100
ORA_2A_035	HSR	77.48	0.09	12.77	0.05	1.14	0.1	0.91	4.71	2.74	100
ORA_2A_035	HSR	77.57	0	13.18	0	0.87	0.06	0.42	5.12	2.77	100
ORA_2A_035	HSR	77.58	0	12.8	0	1.08	0.08	1.1	4.53	2.71	99.89
ORA_2A_035	HSR	77.62	0.08	12.85	0.03	0.92	0	0.49	4.91	2.93	99.83
ORA_2A_035	HSR	77.62	0.14	13.14	0	0.6	0	0.43	5.34	2.73	100
ORA_2A_035	HSR	77.64	0	12.9	0	1.07	0	0.53	5.12	2.75	100
ORA_2A_035	HSR	77.72	0	13.03	0	1.1	0.07	0.51	4.88	2.67	100
ORA_2A_035	HSR	77.77	0.06	13.13	0.09	0.49	0	0.44	5.13	2.9	100
ORA_2A_035	HSR	77.78	0	13.01	0	0.84	0.27	0.32	4.92	2.86	100

ORA-2A-040:

Sample	Type	SiO2	TiO2	Al2O3	MgO	FeO	MnO	CaO	Na2O	K2O	Total
ORA_2A_040	HSR	76.09	0.09	13.59	0.09	1.15	0.41	0.5	5.41	2.67	100
ORA_2A_040	HSR	76.21	0.3	13.53	0.23	1.07	0.15	0.42	5.4	2.69	100
ORA_2A_040	HSR	76.35	0	13.27	0.02	1.11	0.23	0.54	5.73	2.74	100
ORA_2A_040	HSR	76.36	0.02	13.75	0.13	1.13	0.02	0.42	5.66	2.51	100
ORA_2A_040	HSR	76.42	0.3	13.46	0.13	0.89	0.31	0.54	5.39	2.56	100
ORA_2A_040	HSR	76.43	0	13.58	0.03	0.88	0.22	0.63	5.44	2.8	100
ORA_2A_040	HSR	76.48	0	13.6	0.04	1.15	0.1	0.56	5.47	2.61	100
ORA_2A_040	HSR	76.48	0.21	13.45	0	1.03	0.16	0.51	5.5	2.65	100
ORA_2A_040	HSR	76.48	0	13.31	0	0.98	0.25	0.56	5.74	2.69	100
ORA_2A_040	HSR	76.52	0	13.35	0	1.28	0	0.48	5.73	2.64	100
ORA_2A_040	HSR	76.52	0.16	13.39	0.21	1.16	0	0.54	5.47	2.55	100
ORA_2A_040	HSR	76.53	0.13	13.49	0.1	1.2	0.02	0.66	5.25	2.62	100
ORA_2A_040	HSR	76.6	0	13.05	0.12	1.27	0.36	0.43	5.55	2.62	100
ORA_2A_040	HSR	76.61	0.07	13.61	0	1.02	0.05	0.37	5.49	2.77	100
ORA_2A_040	HSR	76.72	0.2	13.24	0.1	0.94	0.13	0.37	5.52	2.79	100
ORA_2A_040	HSR	76.72	0.13	13.05	0	1.06	0.38	0.4	5.64	2.62	100
ORA_2A_040	HSR	76.73	0.08	13.32	0	0.99	0.22	0.55	5.54	2.57	100
ORA_2A_040	HSR	76.75	0.18	13.5	0	0.46	0.35	0.5	5.55	2.71	100
ORA_2A_040	HSR	76.77	0	13.07	0.15	1.53	0.02	0.41	5.64	2.42	100
ORA_2A_040	HSR	76.79	0.07	13.14	0	1.04	0.13	0.43	5.54	2.86	100
ORA_2A_040	HSR	76.79	0.18	13.37	0	1.29	0	0.21	5.53	2.62	100
ORA_2A_040	HSR	76.79	0	13.02	0.1	1.13	0.3	0.49	5.52	2.66	100
ORA_2A_040	HSR	76.8	0.38	13	0	1.13	0.26	0.5	5.5	2.44	100
ORA_2A_040	HSR	76.8	0	13.47	0	1.08	0.06	0.49	5.35	2.5	99.74

ORA_2A_040	HSR	76.81	0	13.25	0.13	0.85	0.14	0.61	5.46	2.74	100
ORA_2A_040	HSR	76.83	0.08	13.46	0.07	0.83	0.29	0.4	5.47	2.57	100
ORA_2A_040	HSR	76.84	0	13.4	0.02	1.33	0	0.22	5.59	2.6	100
ORA_2A_040	HSR	76.84	0.06	13.4	0.12	0.71	0.2	0.86	5.24	2.56	100
ORA_2A_040	HSR	76.85	0.18	13.32	0.15	0.74	0.04	0.34	5.44	2.92	100
ORA_2A_040	HSR	76.87	0.06	13.4	0	0.9	0.13	0.43	5.54	2.65	100
ORA_2A_040	HSR	76.87	0	13.61	0	0.98	0	0.55	5.41	2.59	100
ORA_2A_040	HSR	76.87	0	13.64	0.14	0.69	0.17	0.69	5.27	2.54	100
ORA_2A_040	HSR	76.89	0	13.11	0.21	1.21	0.09	0.4	5.09	3	100
ORA_2A_040	HSR	76.9	0.03	13.18	0	0.94	0.35	0.3	5.54	2.75	100
ORA_2A_040	HSR	76.91	0	13.07	0.16	0.9	0	0.47	5.89	2.59	100
ORA_2A_040	HSR	76.93	0.07	13.16	0.06	1.11	0.11	0.43	5.54	2.58	100
ORA_2A_040	HSR	76.94	0.15	13.42	0.05	1.04	0.04	0.42	5.36	2.57	100
ORA_2A_040	HSR	76.95	0	13.4	0	0.88	0.14	0.4	5.48	2.6	99.85
ORA_2A_040	HSR	76.96	0.07	13.14	0	1.13	0.15	0.39	5.59	2.58	100
ORA_2A_040	HSR	76.96	0	13.57	0.03	0.84	0.21	0.28	5.54	2.58	100
ORA_2A_040	HSR	76.97	0	13.58	0.23	0.74	0.19	0.36	5.26	2.68	100
ORA_2A_040	HSR	76.98	0.12	13.35	0.09	1.24	0.14	0.75	4.96	2.38	100
ORA_2A_040	HSR	77	0.04	13.08	0	1.16	0	0.56	5.55	2.6	100
ORA_2A_040	HSR	77	0.02	13.22	0	1.02	0	0.4	5.6	2.74	100
ORA_2A_040	HSR	77	0	13.23	0.09	0.93	0.2	0.77	5.22	2.57	100
ORA_2A_040	HSR	77.02	0.1	12.99	0.06	0.96	0.18	0.43	5.5	2.75	100
ORA_2A_040	HSR	77.03	0.04	13.28	0.04	0.94	0.03	0.4	5.53	2.6	99.89
ORA_2A_040	HSR	77.04	0	13.53	0	1.12	0.11	0.37	5.4	2.42	100
ORA_2A_040	HSR	77.06	0	13.34	0	0.91	0.05	0.44	5.51	2.58	99.9
ORA_2A_040	HSR	77.08	0	13.7	0	0.71	0	0.5	5.52	2.49	100
ORA_2A_040	HSR	77.1	0	13.27	0	1.14	0.3	0.43	5.18	2.58	100
ORA_2A_040	HSR	77.1	0	13.16	0.11	0.82	0.25	0.32	5.64	2.61	100
ORA_2A_040	HSR	77.11	0.19	12.99	0	1.28	0	0.68	5.52	2.23	100
ORA_2A_040	HSR	77.12	0	13.42	0	0.99	0.01	0.32	5.35	2.79	100
ORA_2A_040	HSR	77.13	0.01	13.66	0	0.61	0.13	0.49	5.19	2.78	100
ORA_2A_040	HSR	77.14	0	13.03	0.06	1.06	0	0.47	5.53	2.71	100
ORA_2A_040	HSR	77.15	0	13.37	0	0.84	0.04	0.4	5.58	2.49	99.87
ORA_2A_040	HSR	77.17	0	13.17	0	1.05	0.24	0.32	5.62	2.42	100
ORA_2A_040	HSR	77.18	0.06	13.33	0	0.71	0.25	0.38	5.45	2.64	100
ORA_2A_040	HSR	77.18	0	13.23	0.12	0.79	0.14	0.52	5.43	2.57	100
ORA_2A_040	HSR	77.2	0	13.23	0.04	1.19	0.09	0.74	5.01	2.51	100
ORA_2A_040	HSR	77.21	0.12	13.24	0.1	0.84	0	0.55	5.4	2.54	100
ORA_2A_040	HSR	77.23	0	13.28	0.07	1.25	0	0.81	4.92	2.43	100
ORA_2A_040	HSR	77.23	0.04	13.4	0	0.81	0.02	0.47	5.43	2.61	100
ORA_2A_040	HSR	77.23	0	13.34	0.03	0.81	0.05	0.45	5.45	2.54	99.9
ORA_2A_040	HSR	77.23	0	13.35	0.15	1.06	0	0.39	5.1	2.72	100
ORA_2A_040	HSR	77.24	0.12	13.17	0.04	0.9	0	0.46	5.5	2.45	99.88

ORA_2A_040	HSR	77.24	0.08	13.54	0	0.4	0	0.6	5.62	2.53	100
ORA_2A_040	HSR	77.26	0.02	13.28	0.06	0.87	0.01	0.48	5.53	2.5	100
ORA_2A_040	HSR	77.29	0.03	13.17	0.16	1.09	0.04	0.96	4.86	2.39	100
ORA_2A_040	HSR	77.31	0.15	13.24	0	0.8	0.08	0.51	5.34	2.57	100
ORA_2A_040	HSR	77.36	0	13.14	0.08	0.94	0.15	1.13	4.8	2.27	99.88
ORA_2A_040	HSR	77.37	0.21	13.36	0	0.69	0.1	0.39	5.3	2.57	100
ORA_2A_040	HSR	77.38	0	12.95	0.07	0.88	0	0.53	5.51	2.68	100
ORA_2A_040	HSR	77.39	0.03	13.14	0.08	1.13	0.01	0.64	5.12	2.47	100
ORA_2A_040	HSR	77.41	0	13.4	0.02	0.64	0	0.23	5.55	2.74	100
ORA_2A_040	HSR	77.42	0.03	12.84	0.1	0.76	0.18	0.58	5.51	2.58	100
ORA_2A_040	HSR	77.42	0.22	12.97	0	0.93	0.09	0.27	5.49	2.61	100
ORA_2A_040	HSR	77.42	0	12.94	0.06	1.1	0	0.53	5.41	2.54	100
ORA_2A_040	HSR	77.43	0	13.26	0.01	1.16	0	1.02	4.91	2.22	100
ORA_2A_040	HSR	77.46	0	13.27	0	0.77	0.09	0.29	5.44	2.67	100
ORA_2A_040	HSR	77.49	0	12.73	0.05	0.84	0	0.32	5.95	2.62	100
ORA_2A_040	HSR	77.5	0.3	13.08	0.05	0.85	0	0.33	5.44	2.45	100
ORA_2A_040	HSR	77.52	0.05	13.14	0.01	0.71	0	0.32	5.61	2.64	100
ORA_2A_040	HSR	77.52	0	13.11	0.05	0.51	0	0.59	5.51	2.71	100
ORA_2A_040	HSR	77.53	0.04	12.85	0	0.92	0.19	0.78	5.43	2.26	100
ORA_2A_040	HSR	77.54	0.08	13.03	0.01	0.87	0	0.52	5.47	2.49	100
ORA_2A_040	HSR	77.55	0.1	13.25	0	0.75	0	0.19	5.55	2.61	100
ORA_2A_040	HSR	77.57	0.2	13.19	0.08	0.43	0.27	0.43	5.13	2.7	100
ORA_2A_040	HSR	77.57	0	13.12	0	0.81	0.18	0.41	5.4	2.51	100
ORA_2A_040	HSR	77.58	0.01	13.36	0	0.61	0.13	0.3	5.48	2.52	100
ORA_2A_040	HSR	77.59	0.08	12.81	0.04	0.85	0	0.64	5.42	2.57	100
ORA_2A_040	HSR	77.6	0.02	13.43	0	0.59	0	0.38	5.44	2.54	100
ORA_2A_040	HSR	77.61	0.03	12.91	0.13	0.58	0.08	0.52	5.49	2.64	100
ORA_2A_040	HSR	77.65	0.05	12.75	0	1	0.18	0.44	5.39	2.54	100
ORA_2A_040	HSR	77.8	0	13.08	0.14	1.08	0.05	1.36	4.35	2.02	99.88
ORA_2A_040	HSR	77.91	0	13.01	0.01	0.65	0	0.38	5.62	2.42	100
ORA_2A_040	HSR	77.96	0.16	13.09	0	0.55	0	0.37	5.34	2.52	100
ORA_2A_040	HSR	77.96	0.1	12.9	0	0.71	0.11	0.26	5.37	2.59	100

ORA-5B-402:

Sample	Type	SiO2	TiO2	Al2O3	MgO	FeO	MnO	CaO	Na2O	K2O	Total
ORA_5B_402	HSR	76.76	0.11	13.29	0.08	1.18	0.04	0.53	4.87	3.14	100
ORA_5B_402	HSR	76.83	0.07	13.43	0.01	0.92	0.05	0.6	4.93	3.18	100
ORA_5B_402	HSR	76.85	0.01	13.14	0	1.13	0	0.68	4.88	3.29	100
ORA_5B_402	HSR	76.92	0.04	13.11	0.09	1.23	0.04	0.55	4.74	3.27	100
ORA_5B_402	HSR	77.05	0	13.19	0.05	1.17	0.16	0.82	4.39	3.18	100
ORA_5B_402	HSR	77.05	0.12	13.01	0.23	1.4	0.01	0.94	4.11	3.13	100

ORA_5B_402	HSR	77.09	0	13.24	0.08	1.2	0.02	0.72	4.44	3.2	100
ORA_5B_402	HSR	77.11	0.12	13.16	0.15	1.17	0.03	0.89	4.23	3.15	100
ORA_5B_402	HSR	77.14	0.14	13.03	0.07	0.91	0.12	0.48	4.92	3.18	100
ORA_5B_402	HSR	77.15	0.1	13.12	0.11	1.12	0.02	0.77	4.29	3.32	100
ORA_5B_402	HSR	77.16	0.19	13.15	0.23	1.17	0.03	0.99	3.79	3.29	100
ORA_5B_402	HSR	77.18	0.02	13.3	0.22	1.04	0	0.7	4.31	3.24	100
ORA_5B_402	HSR	77.19	0.08	13.27	0	0.73	0.16	0.55	4.87	3.14	100
ORA_5B_402	HSR	77.22	0.13	13.34	0.09	0.99	0.05	0.9	4.1	3.19	100
ORA_5B_402	HSR	77.23	0.06	13.26	0.14	0.9	0	0.64	4.6	3.18	100
ORA_5B_402	HSR	77.28	0.09	13.21	0.12	1.01	0.03	0.65	4.48	3.12	100
ORA_5B_402	HSR	77.38	0.05	13.16	0.18	1.18	0	1.01	3.96	3.09	100
ORA_5B_402	HSR	77.46	0.09	13.12	0.11	0.91	0	0.87	4.3	3.14	100

ORA-5B-404A:

Sample	Type	SiO2	TiO2	Al2O3	MgO	FeO	MnO	CaO	Na2O	K2O	Total
ORA_5B_404A	HSR	76.41	0.18	13.26	0.06	1.15	0.18	0.57	5.06	3.12	100
ORA_5B_404A	HSR	76.62	0.03	13.35	0	1.17	0.18	0.46	4.93	3.26	100
ORA_5B_404A	HSR	76.66	0	13.3	0.05	1.18	0.1	0.52	5.12	3.07	100
ORA_5B_404A	HSR	76.73	0.09	13.39	0.03	1.1	0.15	0.49	4.8	3.2	100
ORA_5B_404A	HSR	76.75	0.06	13.13	0.07	1	0.2	0.55	5.04	3.19	100
ORA_5B_404A	HSR	76.76	0.11	13.17	0.04	1.2	0.08	0.64	4.9	3.1	100
ORA_5B_404A	HSR	76.77	0.09	13.41	0.05	0.88	0.08	0.57	4.84	3.31	100
ORA_5B_404A	HSR	76.8	0.06	13.09	0.1	1.06	0.05	0.62	4.97	3.26	100
ORA_5B_404A	HSR	76.82	0.06	13.33	0.01	1.03	0.14	0.44	4.99	3.18	100
ORA_5B_404A	HSR	76.82	0.04	13.31	0.04	0.96	0.18	0.52	4.98	3.16	100
ORA_5B_404A	HSR	76.82	0.11	13.23	0.03	1.1	0	0.48	4.89	3.21	99.86
ORA_5B_404A	HSR	76.83	0	13.39	0	1.16	0.05	0.51	5.1	2.97	100
ORA_5B_404A	HSR	76.83	0.16	13.09	0.07	1.13	0	0.63	5.07	3.04	100
ORA_5B_404A	HSR	76.86	0.11	13.28	0	0.97	0.06	0.55	5.07	3.09	100
ORA_5B_404A	HSR	76.86	0.1	13.29	0.03	1.01	0	0.5	4.89	3.19	99.86
ORA_5B_404A	HSR	76.87	0.19	13.19	0.02	1.06	0.01	0.48	4.98	3.19	100
ORA_5B_404A	HSR	76.87	0	13.28	0.03	1	0.12	0.55	4.89	3.26	100
ORA_5B_404A	HSR	76.87	0.07	13.16	0	1.02	0.01	0.52	5.1	3.24	100
ORA_5B_404A	HSR	76.9	0.1	12.93	0.11	1.01	0.07	0.53	5.03	3.19	99.88
ORA_5B_404A	HSR	76.91	0.02	13.23	0.08	0.89	0.03	0.55	5.06	3.23	100
ORA_5B_404A	HSR	76.92	0	13.3	0.06	1.04	0	0.44	5.14	3.1	100
ORA_5B_404A	HSR	76.92	0.11	13.32	0	0.96	0.06	0.56	4.79	3.13	99.84
ORA_5B_404A	HSR	76.95	0.06	13.12	0.07	1	0	0.47	4.96	3.25	99.86
ORA_5B_404A	HSR	76.97	0.06	13.19	0.06	1.11	0.05	0.64	4.77	3.15	100
ORA_5B_404A	HSR	76.98	0.14	13.25	0.12	1.08	0.21	0.68	4.47	3.07	100
ORA_5B_404A	HSR	76.99	0.1	13.28	0.07	1	0	0.53	4.88	3.14	100

ORA_5B_404A	HSR	77	0.12	13.24	0.02	0.91	0.05	0.52	4.92	3.21	100
ORA_5B_404A	HSR	77	0.03	13.24	0.07	1.05	0	0.51	4.9	3.19	100
ORA_5B_404A	HSR	77.02	0.16	13.2	0.02	0.91	0.14	0.55	4.97	3.02	100
ORA_5B_404A	HSR	77.03	0.09	13.25	0.04	1.1	0	0.63	4.75	3.11	100
ORA_5B_404A	HSR	77.03	0	13.23	0.04	0.94	0.19	0.52	4.89	3.16	100
ORA_5B_404A	HSR	77.03	0.01	13.11	0.06	1.12	0	0.54	5.05	3.08	100
ORA_5B_404A	HSR	77.03	0.07	13.25	0.03	0.78	0.16	0.51	4.97	3.19	100
ORA_5B_404A	HSR	77.04	0.03	13.4	0.11	0.88	0	0.47	5.08	2.99	100
ORA_5B_404A	HSR	77.07	0.12	13.09	0.07	0.81	0.05	0.52	4.96	3.31	100
ORA_5B_404A	HSR	77.08	0	13.31	0	0.98	0.04	0.51	4.97	3.12	100
ORA_5B_404A	HSR	77.12	0.09	13.25	0	0.88	0.01	0.48	4.88	3.3	100
ORA_5B_404A	HSR	77.13	0.07	13.33	0.04	0.92	0.13	0.52	4.75	3.12	100
ORA_5B_404A	HSR	77.14	0.01	13.41	0.04	0.84	0	0.52	4.94	3.1	100
ORA_5B_404A	HSR	77.18	0.07	13.12	0	0.95	0	0.51	4.86	3.17	99.87
ORA_5B_404A	HSR	77.18	0.18	13.08	0.15	0.91	0	0.5	4.88	3.12	100
ORA_5B_404A	HSR	77.22	0	13.23	0.04	0.9	0.02	0.47	4.88	3.1	99.87
ORA_5B_404A	HSR	77.22	0.02	13.06	0	0.88	0.04	0.5	5.04	3.22	100
ORA_5B_404A	HSR	77.23	0.01	13.19	0	0.87	0.05	0.59	4.97	3.08	100
ORA_5B_404A	HSR	77.27	0	13.12	0.13	1.26	0.03	0.8	4.31	3.09	100
ORA_5B_404A	HSR	77.29	0	13.16	0.02	0.98	0	0.48	4.9	3.17	100
ORA_5B_404A	HSR	77.35	0.11	13.09	0.07	0.76	0.11	0.67	4.45	3.38	100
ORA_5B_404A	HSR	77.36	0	13.19	0.02	0.79	0	0.65	4.8	3.19	100
ORA_5B_404A	HSR	77.37	0	13.16	0.01	0.78	0	0.5	4.95	3.23	100
ORA_5B_404A	HSR	77.45	0	13.11	0.05	0.73	0	0.51	4.9	3.26	100
ORA_5B_404A	HSR	77.46	0.1	13.23	0.09	0.52	0.11	0.48	4.96	3.05	100
ORA_5B_404A	HSR	77.47	0	13.1	0.06	0.83	0	0.52	4.92	3.1	100
ORA_5B_404A	HSR	77.67	0.03	13.28	0	0.59	0	0.52	4.77	3.14	100

ORA-5B-404B:

Sample	Type	SiO2	TiO2	Al2O3	MgO	FeO	MnO	CaO	Na2O	K2O	Total
ORA_5B_404B	HSR	76.51	0	13.48	0.16	1.3	0	0.57	4.69	3.3	100
ORA_5B_404B	HSR	76.6	0.08	13.33	0.05	1.12	0	0.6	5.1	3.13	100
ORA_5B_404B	HSR	76.62	0.06	13.32	0.03	1.31	0.04	0.56	4.95	3.11	100
ORA_5B_404B	HSR	76.69	0	13.22	0.13	1.16	0.06	0.61	4.93	3.07	99.87
ORA_5B_404B	HSR	76.72	0.14	13.25	0.11	1.09	0	0.5	4.81	3.26	99.89
ORA_5B_404B	HSR	76.74	0.03	13.06	0.06	1.41	0.03	0.6	4.85	3.22	100
ORA_5B_404B	HSR	76.75	0.18	13.04	0.02	1.14	0.07	0.58	4.84	3.26	99.88
ORA_5B_404B	HSR	76.76	0.07	13.17	0.09	1.05	0	0.64	4.86	3.24	99.89
ORA_5B_404B	HSR	76.76	0.06	13.22	0.08	1.02	0.03	0.57	4.86	3.25	99.85
ORA_5B_404B	HSR	76.78	0.08	13.26	0.09	1.09	0.18	0.58	4.76	3.18	100
ORA_5B_404B	HSR	76.78	0.07	13.29	0.09	1.04	0.11	0.61	4.72	3.28	100

ORA_5B_404B	HSR	76.78	0.08	13.24	0.04	1	0.02	0.7	4.81	3.18	99.86
ORA_5B_404B	HSR	76.83	0.1	13.27	0.1	1.1	0	0.54	4.79	3.29	100
ORA_5B_404B	HSR	76.83	0.06	13.3	0	1.03	0.28	0.5	4.81	3.19	100
ORA_5B_404B	HSR	76.83	0.19	13.22	0.05	1	0.04	0.63	4.83	3.2	100
ORA_5B_404B	HSR	76.84	0.1	13.3	0.04	1.09	0.06	0.52	4.9	3.16	100
ORA_5B_404B	HSR	76.87	0.14	13.37	0.03	0.93	0	0.52	4.88	3.25	100
ORA_5B_404B	HSR	76.87	0	13.02	0.17	1.14	0.4	0.7	4.21	3.47	100
ORA_5B_404B	HSR	76.89	0.03	13.17	0.11	1.01	0.11	0.6	4.78	3.29	100
ORA_5B_404B	HSR	76.89	0.06	13.28	0	1	0.03	0.59	4.92	3.23	100
ORA_5B_404B	HSR	76.9	0.16	13.37	0.12	0.94	0.13	0.47	4.8	3.11	100
ORA_5B_404B	HSR	76.91	0.21	13.24	0.07	0.9	0.03	0.61	4.77	3.14	99.88
ORA_5B_404B	HSR	76.92	0.13	13.1	0.06	1.08	0.07	0.55	4.9	3.19	100
ORA_5B_404B	HSR	76.97	0.02	13.17	0.05	0.89	0	0.6	4.94	3.23	99.89
ORA_5B_404B	HSR	76.97	0.14	13.13	0.1	1.17	0	0.65	4.68	3.14	100
ORA_5B_404B	HSR	76.98	0	13.16	0.07	1.19	0.05	0.55	4.84	3.16	100
ORA_5B_404B	HSR	76.99	0	13.37	0.04	0.76	0	0.67	4.92	3.24	100
ORA_5B_404B	HSR	77.01	0.05	13.26	0.07	0.95	0	0.49	4.87	3.3	100
ORA_5B_404B	HSR	77.02	0.08	13.2	0.03	1.03	0	0.56	4.96	3.13	100
ORA_5B_404B	HSR	77.02	0.06	13.29	0.02	0.98	0	0.58	4.73	3.31	100
ORA_5B_404B	HSR	77.03	0.07	13.2	0.03	0.98	0.02	0.61	4.95	3.1	100
ORA_5B_404B	HSR	77.05	0.11	13.1	0	1.02	0.08	0.6	4.82	3.22	100
ORA_5B_404B	HSR	77.06	0.12	13.18	0	0.82	0.03	0.54	5.02	3.24	100
ORA_5B_404B	HSR	77.07	0.03	13.18	0.06	0.9	0	0.63	4.84	3.16	99.87
ORA_5B_404B	HSR	77.08	0.06	13.18	0.04	0.95	0.02	0.62	4.88	3.16	100
ORA_5B_404B	HSR	77.09	0.21	12.89	0.03	1.17	0	0.53	4.87	3.23	100
ORA_5B_404B	HSR	77.09	0.09	13.24	0.04	0.86	0.08	0.57	4.95	3.07	100
ORA_5B_404B	HSR	77.09	0	13.1	0.07	1.14	0	0.55	4.89	3.15	100
ORA_5B_404B	HSR	77.1	0	13.24	0.01	1.15	0.13	0.48	4.86	3.03	100
ORA_5B_404B	HSR	77.16	0.01	13.23	0	0.92	0	0.51	4.93	3.24	100
ORA_5B_404B	HSR	77.16	0.07	13.08	0.03	1.07	0	0.58	4.86	3.15	100
ORA_5B_404B	HSR	77.2	0.15	13.03	0.03	0.88	0.05	0.55	4.8	3.31	100
ORA_5B_404B	HSR	77.23	0.08	13.24	0.01	0.82	0.14	0.51	4.82	3.15	100
ORA_5B_404B	HSR	77.23	0.02	13.17	0.13	1.04	0	0.64	4.63	3.15	100
ORA_5B_404B	HSR	77.25	0	13.29	0.01	0.88	0.03	0.66	4.74	3.13	100
ORA_5B_404B	HSR	77.29	0	13.01	0.01	0.92	0.16	0.62	4.85	3.14	100

ORA-5B-412A:

Sample	Type	SiO2	TiO2	Al2O3	MgO	FeO	MnO	CaO	Na2O	K2O	Total
ORA_5B_412A	Glass	74.8	0.23	14.29	0.18	1.29	0.06	0.37	5.45	3.34	100
ORA_5B_412A	Glass	74.97	0.21	14.09	0.15	1.45	0.07	0.68	5.07	3.3	100
ORA_5B_412A	Glass	74.99	0.1	14.37	0.15	0.96	0	0.67	5.1	3.67	100

ORA_5B_412A	Glass	75.03	0.12	14.02	0.18	1.68	0.08	0.69	5.07	3.13	100
ORA_5B_412A	Glass	75.1	0.25	13.92	0.27	1.54	0.08	0.77	5.01	3.07	100
ORA_5B_412A	Glass	75.18	0.15	14.18	0.09	1.32	0.12	0.68	4.87	3.41	100
ORA_5B_412A	Glass	75.23	0.19	13.81	0.29	1.7	0.03	0.71	5.06	2.98	100
ORA_5B_412A	Glass	75.3	0.22	13.98	0.18	1.43	0	0.67	5.03	3.2	100
ORA_5B_412A	Glass	75.3	0.15	13.94	0.06	1.37	0.12	0.75	4.98	3.34	100
ORA_5B_412A	Glass	75.33	0.12	14.02	0.17	1.31	0.1	0.77	5.1	3.09	100
ORA_5B_412A	Glass	75.34	0.21	13.82	0.15	1.5	0.04	0.69	5.09	3.15	100
ORA_5B_412A	Glass	75.35	0.11	14.23	0.13	1.15	0.03	0.72	5.14	3.14	100
ORA_5B_412A	Glass	75.35	0.19	14.08	0.17	1.21	0.1	0.63	5.15	3.13	100
ORA_5B_412A	Glass	75.36	0.2	14.14	0.12	1.28	0.01	0.72	5.14	3.04	100
ORA_5B_412A	Glass	75.36	0.08	13.92	0.13	1.43	0.02	0.78	5.16	3.12	100
ORA_5B_412A	Glass	75.38	0.16	13.88	0.25	1.55	0.03	0.65	5.03	3.06	100
ORA_5B_412A	Glass	75.39	0.17	13.81	0.18	1.4	0.03	0.7	4.98	3.33	100
ORA_5B_412A	Glass	75.41	0.15	14.08	0.15	1.23	0	0.7	4.98	3.29	100
ORA_5B_412A	Glass	75.42	0	14.11	0.1	1.17	0.03	0.33	4.82	4.01	100
ORA_5B_412A	Glass	75.42	0.11	13.8	0.22	1.4	0.09	0.76	5.1	3.1	100
ORA_5B_412A	Glass	75.44	0.2	13.97	0.21	1.14	0.1	0.65	5.09	3.21	100
ORA_5B_412A	Glass	75.45	0.23	14.01	0.15	1.29	0	0.56	5.22	3.11	100
ORA_5B_412A	Glass	75.48	0.14	14.1	0.12	1.15	0.07	0.8	5.05	3.09	100
ORA_5B_412A	Glass	75.48	0.1	13.82	0.17	1.29	0.08	0.71	5.03	3.32	100
ORA_5B_412A	Glass	75.5	0.21	14.09	0.2	1.05	0	0.7	5.12	3.12	100
ORA_5B_412A	Glass	75.5	0.17	14.04	0.22	1.21	0.01	0.69	4.99	3.17	100
ORA_5B_412A	Glass	75.56	0.12	13.7	0.22	1.48	0.09	0.69	5.05	3.09	100
ORA_5B_412A	Glass	75.67	0.13	13.82	0.13	1.42	0.02	0.67	5.01	3.15	100
ORA_5B_412A	Glass	75.73	0.11	13.71	0.22	1.62	0	0.65	4.91	3.04	100
ORA_5B_412A	Glass	75.74	0.13	13.94	0.12	1.06	0	0.69	5.21	3.12	100
ORA_5B_412A	Glass	75.78	0.09	13.76	0.2	1.23	0	0.77	5.11	3.06	100
ORA_5B_412A	Glass	75.81	0.09	13.79	0.11	1.29	0.05	0.68	5.06	3.11	100
ORA_5B_412A	HSR	76.03	0.15	13.75	0.1	1.08	0.04	0.74	5.05	3.05	100
ORA_5B_412A	HSR	76.03	0.15	13.84	0.05	1.07	0.02	0.71	4.92	3.21	100
ORA_5B_412A	HSR	76.08	0.17	13.56	0.09	1.31	0.09	0.76	4.91	3.04	100
ORA_5B_412A	HSR	76.18	0.24	13.56	0.2	1.22	0	0.58	4.93	3.08	100
ORA_5B_412A	HSR	76.33	0	13.74	0.12	1.05	0.01	0.59	4.76	3.39	100
ORA_5B_412A	HSR	76.4	0.17	13.36	0.08	1.16	0.11	0.67	4.96	3.09	100
ORA_5B_412A	HSR	76.51	0.12	13.67	0.02	1	0.03	0.64	4.87	3.13	100
ORA_5B_412A	HSR	76.56	0.16	13.41	0	0.93	0.08	0.67	4.86	3.31	100
ORA_5B_412A	HSR	76.97	0.07	13.36	0.03	0.94	0.02	0.59	5.03	3	100
ORA_5B_412A	HSR	77.03	0.1	12.83	0.01	1.61	0	0.53	4.82	3.08	100
ORA_5B_412A	HSR	77.07	0.03	12.91	0.04	1.4	0.06	0.54	4.84	3.11	100
ORA_5B_412A	HSR	77.14	0.19	13.03	0.06	0.93	0.09	0.56	4.93	3.06	100
ORA_5B_412A	HSR	77.17	0	13.23	0.07	1.01	0	0.58	4.82	3.12	100
ORA_5B_412A	HSR	77.21	0.09	12.77	0.03	1.43	0	0.51	4.81	3.15	100

ORA_5B_412A	HSR	77.23	0.07	12.91	0.02	1.11	0.14	0.54	4.84	3.13	100
ORA_5B_412A	HSR	77.3	0.13	12.98	0.06	1.13	0	0.48	4.83	3.09	100
ORA_5B_412A	HSR	77.42	0	12.91	0.09	1.07	0.02	0.54	4.78	3.18	100
ORA_5B_412A	HSR	77.55	0.08	12.95	0.03	0.93	0	0.57	4.72	3.17	100
ORA_5B_412A	HSR	77.57	0.05	13.02	0.09	0.73	0.05	0.54	4.84	3.12	100
ORA_5B_412A	HSR	77.69	0	12.8	0.01	1.18	0	0.55	4.73	3.04	100
ORA_5B_412A	HSR	77.71	0.03	12.83	0.05	0.8	0.12	0.62	4.77	3.08	100
ORA_5B_412A	HSR	77.72	0.18	12.87	0.03	0.71	0	0.53	4.86	3.1	100
ORA_5B_412A	HSR	77.73	0.05	12.72	0.09	0.92	0	0.56	4.67	3.25	100
ORA_5B_412A	HSR	77.73	0	12.92	0.03	0.85	0.03	0.56	4.79	3.1	100
ORA_5B_412A	HSR	77.8	0.09	12.85	0.06	0.7	0.03	0.61	4.74	3.12	100
ORA_5B_412A	HSR	77.31	0	13.11	0.08	0.86	0.1	0.57	4.82	3.17	100

ORA-5B-412B:

Sample	Type	SiO2	TiO2	Al2O3	MgO	FeO	MnO	CaO	Na2O	K2O	Total
ORA_5B_412B	Glass	73.53	0.14	15.27	0.1	1.43	0.05	1.25	5.26	2.96	100
ORA_5B_412B	Glass	74.23	0.12	14.77	0.13	1.12	0.12	1.3	5.23	2.98	100
ORA_5B_412B	Glass	74.35	0.15	14.62	0.22	1.35	0.03	0.84	4.92	3.51	100
ORA_5B_412B	Glass	74.48	0.12	14.62	0.21	1.09	0.12	1.06	5.28	2.88	99.87
ORA_5B_412B	Glass	74.72	0.13	14.75	0.02	0.9	0.09	1.34	4.36	3.69	100
ORA_5B_412B	Glass	74.91	0.15	14.31	0.13	1.14	0	0.88	4.91	3.56	100
ORA_5B_412B	Glass	74.93	0.08	13.97	0.28	1.61	0.12	0.76	5.12	3.12	100
ORA_5B_412B	Glass	74.94	0.23	13.98	0.18	1.48	0.05	0.74	5.14	3.14	99.89
ORA_5B_412B	Glass	74.96	0.11	13.95	0.23	1.51	0.09	0.68	4.87	3.24	100
ORA_5B_412B	Glass	74.96	0.16	14.17	0.28	1.53	0.05	0.66	5.11	3.07	100
ORA_5B_412B	Glass	74.96	0.23	14.18	0.24	1.43	0.11	0.47	4.8	3.56	100
ORA_5B_412B	Glass	75.03	0.24	13.97	0.23	1.67	0.01	0.74	4.99	3.12	100
ORA_5B_412B	Glass	75.04	0.18	14.09	0.08	1.2	0.09	0.64	5	3.55	99.87
ORA_5B_412B	Glass	75.04	0.13	14.1	0.15	1.39	0.01	0.75	5.16	3.16	99.88
ORA_5B_412B	Glass	75.06	0.22	13.88	0.26	1.86	0.07	0.66	4.96	3.02	100
ORA_5B_412B	Glass	75.14	0.15	13.8	0.18	1.87	0.02	0.72	4.93	3.09	99.9
ORA_5B_412B	Glass	75.17	0.1	14.06	0.19	1.43	0.04	0.67	5.21	3.12	100
ORA_5B_412B	Glass	75.2	0.06	13.84	0.26	1.56	0.09	0.75	4.95	3.17	99.89
ORA_5B_412B	Glass	75.2	0.21	14.06	0.18	1.37	0.09	0.75	4.92	3.21	100
ORA_5B_412B	Glass	75.22	0.08	14.24	0.12	1.25	0	1.1	4.95	3.04	100
ORA_5B_412B	Glass	75.23	0.22	14.11	0.19	1.38	0.02	0.65	5.03	3.17	100
ORA_5B_412B	Glass	75.25	0.09	13.95	0.15	1.53	0	0.67	4.75	3.6	100
ORA_5B_412B	Glass	75.27	0.19	13.84	0.17	1.58	0.1	0.72	5.07	3.06	100
ORA_5B_412B	Glass	75.31	0.17	13.67	0.22	1.54	0.1	0.78	5.05	3.03	99.88
ORA_5B_412B	Glass	75.31	0.23	14.01	0.09	1.19	0.02	0.8	4.9	3.32	99.87
ORA_5B_412B	Glass	75.31	0.22	14.14	0.14	1.21	0.05	0.74	5.03	3.16	100

ORA_5B_412B	Glass	75.31	0.17	13.85	0.12	1.48	0	0.8	4.94	3.33	100
ORA_5B_412B	Glass	75.34	0.2	13.92	0.07	1.35	0.08	0.73	5.13	3.08	99.9
ORA_5B_412B	Glass	75.34	0.17	14.26	0.21	1.05	0.1	0.68	4.73	3.35	99.9
ORA_5B_412B	Glass	75.36	0.23	13.83	0.22	1.59	0.08	0.71	4.97	3.02	100
ORA_5B_412B	Glass	75.36	0.1	13.98	0.12	1.34	0.14	0.68	5.1	3.18	100
ORA_5B_412B	Glass	75.36	0.04	14.36	0.1	1.04	0	0.89	5.06	3.15	100
ORA_5B_412B	Glass	75.37	0.1	14.07	0.27	1.3	0.07	0.67	4.9	3.15	99.9
ORA_5B_412B	Glass	75.38	0.17	13.95	0.19	1.42	0	0.71	5.03	3.16	100
ORA_5B_412B	Glass	75.4	0.14	14.09	0.19	1.33	0	0.74	5.12	2.99	100
ORA_5B_412B	Glass	75.4	0.19	13.91	0.15	1.25	0.07	0.68	5.09	3.13	99.88
ORA_5B_412B	Glass	75.41	0.21	13.84	0.17	1.4	0.02	0.73	5	3.21	100
ORA_5B_412B	Glass	75.43	0.04	13.85	0.26	1.41	0	0.74	5.09	3.17	100
ORA_5B_412B	Glass	75.44	0.14	14	0.13	1.28	0	0.75	5.07	3.09	99.9
ORA_5B_412B	Glass	75.45	0.07	13.88	0.18	1.34	0.12	0.65	5.09	3.21	100
ORA_5B_412B	Glass	75.45	0.12	14.09	0.2	1.31	0	0.67	5.04	3.12	100
ORA_5B_412B	Glass	75.51	0.16	13.67	0.18	1.6	0.06	0.72	4.97	3.13	100
ORA_5B_412B	Glass	75.52	0.13	14.18	0.1	0.95	0.13	0.76	5.01	3.1	99.88
ORA_5B_412B	Glass	75.52	0.06	14.09	0.25	1.25	0.07	0.7	4.95	3.11	100
ORA_5B_412B	Glass	75.52	0.13	13.7	0.16	1.34	0.08	0.66	5.08	3.21	99.88
ORA_5B_412B	Glass	75.53	0.15	13.94	0.23	1.12	0.05	0.73	5.09	3.05	99.89
ORA_5B_412B	Glass	75.55	0.16	13.87	0.15	1.27	0	0.72	5.04	3.25	100
ORA_5B_412B	Glass	75.56	0.1	13.62	0.1	1.76	0.02	0.65	4.95	3.22	100
ORA_5B_412B	Glass	75.57	0.15	13.8	0.18	1.59	0.04	0.75	4.96	2.98	100
ORA_5B_412B	Glass	75.57	0.13	13.85	0.14	1.38	0.11	0.74	5.07	3.02	100
ORA_5B_412B	Glass	75.57	0.13	13.97	0.16	1.18	0.06	0.76	4.86	3.3	100
ORA_5B_412B	Glass	75.59	0.16	14.01	0.18	1.13	0.05	0.64	4.94	3.3	100
ORA_5B_412B	Glass	75.61	0.17	13.67	0.17	1.37	0.11	0.85	4.81	3.23	100
ORA_5B_412B	Glass	75.61	0.19	13.85	0.08	1.26	0.1	0.84	4.98	3.09	100
ORA_5B_412B	Glass	75.64	0.2	13.99	0.09	0.93	0.08	0.72	5.14	3.22	100
ORA_5B_412B	Glass	75.64	0.05	13.84	0.09	1.29	0.05	0.74	5.07	3.22	100
ORA_5B_412B	Glass	75.66	0.29	13.66	0.15	1.33	0.05	0.63	4.9	3.23	99.89
ORA_5B_412B	Glass	75.73	0.09	13.76	0.17	1.24	0.08	0.65	5.06	3.22	100
ORA_5B_412B	Glass	75.74	0.23	13.79	0.22	1.08	0.14	0.72	4.96	3.13	100
ORA_5B_412B	Glass	75.75	0.14	13.56	0.16	1.52	0	0.72	5.05	3.12	100
ORA_5B_412B	Glass	75.76	0.11	13.91	0.04	1.14	0.11	0.8	5.03	3.09	100
ORA_5B_412B	Glass	75.76	0.11	13.69	0.15	1.46	0	0.63	5.04	3.15	100
ORA_5B_412B	Glass	75.79	0.22	13.62	0.18	1.37	0	0.62	5.13	2.94	99.88
ORA_5B_412B	Glass	75.8	0.26	13.87	0.17	0.98	0	0.67	5.11	3.13	100
ORA_5B_412B	Glass	75.81	0.16	14.01	0.11	0.92	0.06	0.76	5.05	3.11	100
ORA_5B_412B	Glass	75.84	0.15	13.51	0.23	1.67	0.09	0.65	4.8	3.05	100
ORA_5B_412B	Glass	75.86	0.08	13.67	0.2	1.34	0.01	0.74	4.88	3.22	100
ORA_5B_412B	Glass	75.86	0.12	13.76	0.19	1.25	0.01	0.69	5.03	3.11	100
ORA_5B_412B	Glass	75.89	0.2	13.91	0.07	1.02	0	0.74	4.84	3.33	100

ORA_5B_412B	Glass	75.9	0.1	13.96	0.11	0.71	0.03	0.73	5.04	3.25	99.82
ORA_5B_412B	Glass	75.93	0.22	13.81	0.16	1.19	0	0.57	4.94	3.18	100
ORA_5B_412B	Glass	75.94	0.21	13.45	0.17	1.39	0.04	0.71	5.03	3.07	100
ORA_5B_412B	Glass	75.94	0.14	14.01	0.09	0.95	0	0.53	4.86	3.48	100
ORA_5B_412B	HSR	75.96	0.17	13.81	0.08	1.06	0.04	0.63	5.09	3.15	100
ORA_5B_412B	HSR	75.96	0.12	13.91	0.13	0.99	0	0.59	5.05	3.26	100
ORA_5B_412B	HSR	76.01	0.05	13.59	0.04	1.43	0	0.84	4.92	3.13	100
ORA_5B_412B	HSR	76.04	0.15	13.84	0.08	0.76	0.08	0.64	5.13	3.17	99.89
ORA_5B_412B	HSR	76.04	0.1	13.53	0.2	1.2	0.08	0.63	5.02	3.19	100
ORA_5B_412B	HSR	76.13	0	13.9	0.04	0.87	0.02	0.9	5.21	2.82	99.9
ORA_5B_412B	HSR	76.22	0.21	13.73	0.11	0.99	0.07	0.69	4.82	3.16	100
ORA_5B_412B	HSR	76.35	0.16	13.31	0.2	1.56	0.05	0.57	4.68	3.12	100
ORA_5B_412B	HSR	76.47	0.11	13.61	0.01	1.01	0	0.53	4.94	3.33	100
ORA_5B_412B	HSR	76.47	0.16	13.32	0.08	1.16	0.1	0.59	4.8	3.22	99.89
ORA_5B_412B	HSR	76.54	0	13.58	0	1.05	0.06	0.7	4.94	3.13	100
ORA_5B_412B	HSR	76.66	0.21	13.21	0.12	1.35	0.1	0.64	4.8	2.92	100
ORA_5B_412B	HSR	76.74	0.2	13.4	0.06	0.89	0.09	0.65	4.73	3.24	100
ORA_5B_412B	HSR	76.86	0.02	13.39	0.04	0.85	0	0.65	5.06	3.03	99.89
ORA_5B_412B	HSR	76.89	0.06	13.2	0.07	1.17	0.13	0.62	4.8	3.05	100
ORA_5B_412B	HSR	76.93	0.14	13.33	0	1	0	0.58	4.84	3.18	100
ORA_5B_412B	HSR	76.96	0.03	13.43	0	0.83	0.02	0.54	4.79	3.4	100
ORA_5B_412B	HSR	76.98	0.16	13.14	0.08	1.05	0	0.54	4.72	3.35	100
ORA_5B_412B	HSR	77.03	0.15	12.86	0.03	1.22	0.08	0.58	4.72	3.33	100
ORA_5B_412B	HSR	77.08	0	13.22	0.05	1.01	0.01	0.8	4.75	3.07	100
ORA_5B_412B	HSR	77.17	0.13	13.27	0.05	0.8	0.01	0.59	4.91	3.09	100
ORA_5B_412B	HSR	77.25	0.2	12.79	0.06	1.19	0.01	0.51	4.86	3.02	99.89
ORA_5B_412B	HSR	77.26	0.08	12.96	0.11	1.16	0.1	0.53	4.8	3	100
ORA_5B_412B	HSR	77.26	0.07	13.04	0.05	1.25	0	0.53	4.75	3.05	100
ORA_5B_412B	HSR	77.27	0.06	12.97	0.02	1.09	0	0.6	4.94	3.05	100
ORA_5B_412B	HSR	77.36	0	13.21	0.03	0.86	0	0.56	4.83	3.13	100
ORA_5B_412B	HSR	77.39	0.06	12.94	0.02	0.92	0.13	0.58	4.94	3.02	100
ORA_5B_412B	HSR	77.46	0.08	13.08	0	0.99	0	0.5	4.77	3.12	100
ORA_5B_412B	HSR	77.5	0.03	13.08	0.02	0.86	0.02	0.48	4.74	3.26	100
ORA_5B_412B	HSR	77.5	0.07	12.98	0	0.94	0.11	0.49	4.82	3.09	100
ORA_5B_412B	HSR	77.5	0.04	13.17	0.05	0.75	0	0.59	4.87	3.03	100
ORA_5B_412B	HSR	77.51	0.04	12.87	0.04	0.76	0.12	0.63	4.85	3.17	100
ORA_5B_412B	HSR	77.51	0.04	13.16	0	0.73	0	0.57	4.96	3.03	100
ORA_5B_412B	HSR	77.51	0.02	13.02	0.05	0.88	0.03	0.59	4.76	3.13	100
ORA_5B_412B	HSR	77.53	0.11	13.09	0.04	0.54	0.08	0.49	4.53	3.59	100
ORA_5B_412B	HSR	77.55	0.11	12.84	0	1	0.05	0.5	4.88	3.07	100
ORA_5B_412B	HSR	77.59	0.04	12.91	0	1.02	0.13	0.5	4.66	3.16	100
ORA_5B_412B	HSR	77.6	0	13.26	0.07	0.77	0	0.59	4.51	3.2	100
ORA_5B_412B	HSR	77.6	0.19	12.92	0	0.85	0	0.49	4.72	3.23	100

ORA_5B_412B	HSR	77.61	0.11	12.73	0	1.06	0	0.5	4.77	3.21	100
ORA_5B_412B	HSR	77.61	0.05	12.87	0.02	1.07	0.01	0.59	4.65	3.14	100
ORA_5B_412B	HSR	77.64	0.07	13.16	0.05	0.49	0.03	0.54	4.86	3.15	100
ORA_5B_412B	HSR	77.64	0.02	12.91	0.02	0.96	0	0.59	4.75	3.13	100
ORA_5B_412B	HSR	77.65	0.14	12.73	0.04	0.92	0.1	0.48	4.85	3.07	100
ORA_5B_412B	HSR	77.65	0.04	13.11	0.05	0.61	0.1	0.42	4.84	3.06	99.88
ORA_5B_412B	HSR	77.71	0.1	13.03	0.1	0.65	0	0.53	4.56	3.21	99.88
ORA_5B_412B	HSR	77.72	0.14	12.98	0.05	0.62	0.07	0.5	4.8	3.12	100
ORA_5B_412B	HSR	77.73	0.1	12.96	0.11	0.9	0	0.39	4.74	3.06	100
ORA_5B_412B	HSR	77.74	0.13	12.68	0.09	1.26	0	0.48	4.37	3.25	100
ORA_5B_412B	HSR	77.74	0.09	12.86	0.09	0.78	0	0.63	4.79	3.03	100
ORA_5B_412B	HSR	77.74	0	12.7	0.04	1.06	0	0.52	4.85	3.08	100
ORA_5B_412B	HSR	77.74	0.1	12.78	0.01	0.93	0.08	0.54	4.76	3.06	100
ORA_5B_412B	HSR	77.78	0.1	12.92	0.13	0.56	0.14	0.56	4.71	3.09	100
ORA_5B_412B	HSR	77.8	0.07	12.79	0	0.83	0.02	0.54	4.83	3.13	100
ORA_5B_412B	HSR	77.82	0.01	12.62	0	1.24	0	0.56	4.49	3.15	99.88
ORA_5B_412B	HSR	77.82	0.08	13.02	0.07	0.6	0	0.42	4.82	3.16	100
ORA_5B_412B	HSR	77.86	0.1	12.61	0.02	0.97	0.08	0.56	4.45	3.36	100
ORA_5B_412B	HSR	77.91	0	12.98	0	0.77	0	0.56	4.73	3.06	100
ORA_5B_412B	HSR	77.92	0.04	12.76	0	0.85	0	0.56	4.69	3.17	100
ORA_5B_412B	HSR	77.97	0	12.73	0.06	0.82	0.07	0.51	4.69	3.16	100
ORA_5B_412B	HSR	77.98	0	12.76	0	0.74	0	0.6	4.63	3.28	100
ORA_5B_412B	HSR	78.04	0.09	12.65	0.07	0.77	0.05	0.49	4.67	3.17	100
ORA_5B_412B	HSR	78.39	0.05	12.52	0.04	0.95	0	0.61	4.32	3.11	100
ORA_5B_412B	HSR	78.97	0	12.17	0.06	0.84	0.08	0.5	4.36	3.02	100

ORA-5B-414:

Sample	Type	SiO2	TiO2	Al2O3	MgO	FeO	MnO	CaO	Na2O	K2O	Total
ORA_5B_414	Glass	71.05	0.08	16.64	0.13	1.54	0.04	1.51	5	4.01	100
ORA_5B_414	Glass	71.93	0.2	15.8	0.37	1.83	0.09	0.9	5.15	3.73	100
ORA_5B_414	Glass	72.21	0.24	15.38	0.23	1.85	0.2	0.62	4.82	4.45	100
ORA_5B_414	Glass	72.26	0.14	15.87	0.28	1.61	0	1.04	4.53	4.28	100
ORA_5B_414	Glass	72.34	0.22	15.9	0.25	1.65	0.18	0.73	4.18	4.56	100
ORA_5B_414	Glass	72.57	0.16	15.56	0.19	1.52	0.04	1.32	4.66	3.99	100
ORA_5B_414	Glass	72.75	0.19	15.4	0.15	1.41	0.06	0.67	5.22	4.01	99.87
ORA_5B_414	Glass	72.79	0.17	15.33	0.24	1.72	0.13	0.65	4.87	4.11	100
ORA_5B_414	Glass	73.15	0.19	15.3	0.21	1.67	0.08	0.75	4.55	4.11	100
ORA_5B_414	Glass	73.39	0.17	15.21	0.19	1.5	0.12	0.65	4.6	4.03	99.86
ORA_5B_414	Glass	73.47	0.19	15.11	0.15	1.39	0.09	0.71	5.28	3.61	100
ORA_5B_414	Glass	73.52	0.13	15.14	0.13	1.26	0	0.89	5.05	3.87	100
ORA_5B_414	Glass	73.54	0.13	14.74	0.21	1.9	0.22	0.8	4.04	4.41	100

ORA_5B_414	Glass	73.63	0.17	15.02	0.21	1.64	0	0.69	5.26	3.36	100
ORA_5B_414	Glass	73.84	0.24	14.82	0.25	1.55	0.12	0.8	4.21	4.16	100
ORA_5B_414	Glass	73.87	0.1	15.05	0.13	1.12	0.04	0.79	5.37	3.53	100
ORA_5B_414	Glass	73.96	0.14	14.92	0.14	1.21	0.1	0.71	4.89	3.92	100
ORA_5B_414	Glass	73.99	0.1	14.56	0.24	1.74	0.02	0.56	4.73	3.93	99.87
ORA_5B_414	Glass	73.99	0.09	14.78	0.14	1.41	0.11	0.6	4.75	4.13	100
ORA_5B_414	Glass	74.02	0.15	14.52	0.18	1.6	0.08	0.7	4.81	3.82	99.88
ORA_5B_414	Glass	74.12	0.13	14.64	0.17	1.47	0	0.71	5.15	3.61	100
ORA_5B_414	Glass	74.16	0.12	14.8	0.04	1.45	0.03	0.65	5.29	3.46	100
ORA_5B_414	Glass	74.18	0.08	14.65	0.07	1.52	0.13	0.69	5.27	3.4	100
ORA_5B_414	Glass	74.19	0.05	14.86	0	1.05	0.02	0.68	5.14	3.9	99.89
ORA_5B_414	Glass	74.22	0.06	14.58	0.25	1.37	0.26	0.76	5.22	3.28	100
ORA_5B_414	Glass	74.27	0.12	14.61	0.08	1.15	0.17	0.61	4.97	3.87	99.85
ORA_5B_414	Glass	74.37	0.08	14.64	0.12	1.25	0.08	0.7	5.21	3.55	100
ORA_5B_414	Glass	74.37	0.09	14.65	0.16	1.39	0	0.69	4.91	3.74	100
ORA_5B_414	Glass	74.38	0.08	14.69	0.17	1.17	0.06	0.72	4.78	3.83	99.88
ORA_5B_414	Glass	74.42	0.18	14.4	0.16	1.54	0	0.66	4.93	3.7	100
ORA_5B_414	Glass	74.43	0.18	14.66	0.21	1.23	0.05	0.85	5.13	3.27	100
ORA_5B_414	Glass	74.6	0.03	14.65	0.08	0.89	0.07	0.85	5.15	3.68	100
ORA_5B_414	Glass	74.62	0.08	14.2	0.14	1.41	0.13	0.59	4.95	3.89	100
ORA_5B_414	Glass	74.66	0	14.86	0.11	0.54	0.06	0.89	5.18	3.7	100
ORA_5B_414	Glass	74.7	0.13	14.36	0.14	1.16	0.05	0.67	4.98	3.79	100
ORA_5B_414	Glass	74.83	0.02	14.12	0.14	1.45	0.07	0.51	4.67	4.06	99.88
ORA_5B_414	Glass	74.89	0.02	14.41	0.17	1.15	0.08	0.68	4.5	4.11	100
ORA_5B_414	Glass	75	0.07	14.1	0.13	1.45	0.06	0.61	4.77	3.68	99.86
ORA_5B_414	Glass	75.03	0.03	14.38	0.04	1.07	0	0.73	5.39	3.33	100
ORA_5B_414	Glass	75.04	0.07	14.44	0.04	1.16	0.08	0.63	5	3.54	100
ORA_5B_414	Glass	75.04	0.12	14.4	0	1.12	0.1	0.59	5.2	3.43	100
ORA_5B_414	Glass	75.05	0.12	14.16	0.13	1.35	0.04	0.6	4.76	3.8	100
ORA_5B_414	Glass	75.09	0.1	14.35	0	1.13	0.02	0.67	5.2	3.43	100
ORA_5B_414	Glass	75.1	0.02	14.22	0.08	1.34	0.04	0.66	4.8	3.63	100
ORA_5B_414	Glass	75.12	0.17	14.42	0.03	1.09	0	0.82	5.27	3.08	100
ORA_5B_414	Glass	75.13	0.03	14.03	0.1	1.38	0.02	0.77	5.15	3.26	99.88
ORA_5B_414	Glass	75.14	0.19	14.08	0.05	1.32	0.01	0.62	5.01	3.58	100
ORA_5B_414	Glass	75.14	0.13	14.11	0.08	1.27	0	0.67	5.24	3.26	99.9
ORA_5B_414	Glass	75.22	0.08	14.16	0.03	1.26	0.06	0.61	5.13	3.44	100
ORA_5B_414	Glass	75.24	0.04	13.76	0.08	1.71	0.14	0.66	5.04	3.34	100
ORA_5B_414	Glass	75.24	0	14.24	0.04	1.13	0	0.78	5.2	3.37	100
ORA_5B_414	Glass	75.25	0.04	14.46	0.06	0.93	0	0.61	4.97	3.69	100
ORA_5B_414	Glass	75.26	0	14.04	0.11	1.33	0	0.71	5.23	3.18	99.87
ORA_5B_414	Glass	75.3	0.02	14.08	0.04	1.25	0	0.67	5.21	3.43	100
ORA_5B_414	Glass	75.34	0	14.14	0.08	1.05	0	0.61	5.08	3.71	100
ORA_5B_414	Glass	75.39	0.08	13.99	0.04	1.29	0.03	0.83	4.82	3.53	100

ORA_5B_414	Glass	75.44	0.05	14.13	0.11	1.04	0.07	0.56	5.01	3.58	100
ORA_5B_414	Glass	75.53	0.13	14.04	0.04	1.1	0	0.62	5.1	3.44	100
ORA_5B_414	Glass	75.54	0.14	14.23	0.07	0.91	0.02	0.66	5.15	3.28	100
ORA_5B_414	Glass	75.55	0.1	13.77	0.11	1.39	0.05	0.48	5.04	3.52	100
ORA_5B_414	Glass	75.58	0.12	13.85	0.09	1.23	0.09	0.63	5.11	3.21	99.89
ORA_5B_414	Glass	75.58	0.04	13.96	0.1	1.41	0	0.57	4.85	3.49	100
ORA_5B_414	Glass	75.66	0.01	14.22	0.05	0.8	0.01	0.63	5.17	3.44	100
ORA_5B_414	Glass	75.67	0.06	13.97	0.11	1.09	0.05	0.63	4.88	3.54	100
ORA_5B_414	Glass	75.68	0	13.75	0.02	1.49	0.08	0.61	5.1	3.27	100
ORA_5B_414	Glass	75.69	0.13	13.99	0.17	1.14	0.02	0.56	4.55	3.75	100
ORA_5B_414	Glass	75.74	0.04	13.98	0.04	1.16	0.04	0.66	4.96	3.37	100
ORA_5B_414	Glass	75.77	0	14.34	0.05	0.61	0	0.48	5.08	3.66	100
ORA_5B_414	Glass	75.78	0.09	13.79	0.12	1.13	0.09	0.53	4.73	3.74	100
ORA_5B_414	Glass	75.84	0.05	13.75	0.11	0.97	0.13	0.51	4.95	3.59	99.9
ORA_5B_414	Glass	75.85	0.15	13.82	0.05	1.1	0.05	0.49	4.86	3.62	100
ORA_5B_414	Glass	75.87	0.04	13.82	0.07	1.13	0.08	0.64	5.17	3.04	99.86
ORA_5B_414	Glass	75.9	0.05	13.93	0.06	0.91	0.08	0.59	5.11	3.37	100
ORA_5B_414	HSR	76.05	0.09	13.9	0.07	0.72	0	0.53	5.03	3.48	99.88
ORA_5B_414	HSR	76.05	0.13	13.65	0.15	1.16	0.06	0.61	4.83	3.35	100
ORA_5B_414	HSR	76.06	0.05	13.78	0.08	1.11	0.08	0.53	5.1	3.21	100
ORA_5B_414	HSR	76.08	0.15	13.65	0.03	1.19	0.06	0.45	5.02	3.37	100
ORA_5B_414	HSR	76.22	0.1	13.7	0.11	1.08	0.05	0.49	4.67	3.57	100
ORA_5B_414	HSR	76.23	0.05	13.85	0.07	0.68	0.19	0.58	4.99	3.37	100
ORA_5B_414	HSR	76.35	0.07	13.7	0.01	1.05	0.04	0.49	4.91	3.38	100
ORA_5B_414	HSR	76.36	0.14	13.74	0	0.56	0.08	0.72	4.68	3.72	100
ORA_5B_414	HSR	76.37	0	13.65	0.02	1.21	0.03	0.43	4.88	3.41	100
ORA_5B_414	HSR	76.38	0.01	13.63	0.05	0.86	0.13	0.57	5.06	3.32	100
ORA_5B_414	HSR	76.44	0.09	13.72	0.03	0.95	0	0.68	5.07	3.03	100
ORA_5B_414	HSR	76.59	0.12	13.43	0	0.96	0.15	0.6	4.6	3.55	100
ORA_5B_414	HSR	76.61	0.03	13.39	0.05	1.21	0.01	0.45	4.65	3.6	100
ORA_5B_414	HSR	76.83	0.1	13.36	0.04	1.16	0	0.71	4.87	2.93	100
ORA_5B_414	HSR	77.04	0.06	13.4	0.04	0.92	0.02	0.55	4.98	2.98	100
ORA_5B_414	HSR	77.19	0	13.01	0.03	1.15	0.04	0.56	4.78	3.23	100
ORA_5B_414	HSR	77.27	0	13.14	0.22	1.11	0.11	0.72	4.24	3.2	100
ORA_5B_414	HSR	77.39	0.13	13.15	0	0.69	0	0.46	4.85	3.33	100
ORA_5B_414	HSR	77.44	0.13	13.02	0.07	0.87	0.11	0.48	4.83	3.05	100
ORA_5B_414	HSR	77.49	0.07	12.97	0	0.78	0.12	0.52	4.91	3.13	100
ORA_5B_414	HSR	77.57	0.12	12.78	0.06	0.91	0.01	0.55	4.9	3.11	100
ORA_5B_414	HSR	77.61	0.04	12.82	0	0.96	0.13	0.4	4.82	3.11	99.89
ORA_5B_414	HSR	77.62	0.01	12.93	0	0.91	0.06	0.44	4.82	3.21	100
ORA_5B_414	HSR	77.75	0.12	13.02	0.11	0.71	0	0.45	4.82	3.01	100

E. Normalized Alkali Feldspar Compositions

Sample	K	Na	Ca
ORA_2A_001	61.000	38.000	1.000
ORA_2A_001	61.386	37.624	0.990
ORA_2A_001	62.000	37.000	1.000
ORA_2A_001	61.000	38.000	1.000
ORA_2A_002	58.586	40.404	1.010
ORA_2A_002	57.732	41.237	1.031
ORA_2A_002	58.000	41.000	1.000
ORA_2A_002	59.804	39.216	0.980
ORA_2A_002	59.375	39.583	1.042
ORA_2A_002	65.306	33.673	1.020
ORA_2A_002	55.446	41.584	2.970
ORA_2A_002	62.376	36.634	0.990
ORA_2A_002	62.245	36.735	1.020
ORA_2A_002	63.000	36.000	1.000
ORA_2A_002	61.616	37.374	1.010
ORA_2A_002	60.606	37.374	2.020
ORA_2A_002	58.000	40.000	2.000
ORA_2A_002	61.616	37.374	1.010
ORA_2A_003	65.625	33.333	1.042
ORA_2A_003	63.265	34.694	2.041
ORA_2A_003	63.265	35.714	1.020
ORA_2A_016	62.376	36.634	0.990
ORA_2A_016	55.556	43.434	1.010
ORA_2A_016	60.396	37.624	1.980
ORA_2A_016	59.184	38.776	2.041
ORA_2A_016	59.794	37.113	3.093
ORA_2A_023	62.000	37.000	1.000
ORA_2A_023	63.000	36.000	1.000
ORA_2A_023	61.000	37.000	2.000
ORA_2A_023	59.596	39.394	1.010
ORA_2A_023	59.406	38.614	1.980
ORA_2A_023	59.000	39.000	2.000
ORA_2A_023	61.765	36.275	1.961
ORA_2A_023	56.701	41.237	2.062
ORA_2A_023	60.396	38.614	0.990

ORA_2A_023	62.000	37.000	1.000
ORA_2A_023	56.566	41.414	2.020
ORA_2A_023	59.596	39.394	1.010
ORA_2A_023	61.000	38.000	1.000
ORA_2A_023	61.000	38.000	1.000
ORA_2A_023	56.000	43.000	1.000
ORA_2A_023	61.000	38.000	1.000
ORA_2A_023	65.000	34.000	1.000
ORA_2A_023	62.000	36.000	2.000
ORA_2A_023	57.000	40.000	3.000
ORA_2A_023	62.245	36.735	1.020
ORA_2A_023	58.586	40.404	1.010
ORA_2A_023	61.616	37.374	1.010
ORA_2A_023	63.000	36.000	1.000
ORA_2A_023	62.245	37.755	0.000
ORA_2A_023	60.784	37.255	1.961
ORA_2A_023	62.000	37.000	1.000
ORA_2A_023	62.626	36.364	1.010
ORA_2A_024	61.386	37.624	0.990
ORA_2A_024	61.224	37.755	1.020
ORA_2A_024	57.576	41.414	1.010
ORA_2A_024	54.000	44.000	2.000
ORA_2A_024	61.616	37.374	1.010
ORA_2A_031	61.000	38.000	1.000
ORA_2A_031	63.636	35.354	1.010
ORA_2A_031	62.000	37.000	1.000
ORA_2A_031	62.626	36.364	1.010
ORA_2A_031	61.000	38.000	1.000
ORA_2A_031	63.000	36.000	1.000
ORA_2A_031	61.000	38.000	1.000
ORA_2A_031	62.245	36.735	1.020
ORA_2A_031	61.224	37.755	1.020
ORA_2A_031	62.000	37.000	1.000
ORA_2A_031	62.000	37.000	1.000
ORA_2A_032	68.000	31.000	1.000
ORA_2A_032	66.667	32.292	1.042
ORA_2A_032	67.677	31.313	1.010
ORA_2A_035	65.306	33.673	1.020
ORA_2A_035	64.356	34.653	0.990

ORA_2A_035	64.000	34.000	2.000
ORA_2A_035	64.646	34.343	1.010
ORA_2A_035	64.646	34.343	1.010
ORA_2A_035	64.000	35.000	1.000
ORA_2A_035	59.596	39.394	1.010
ORA_2A_035	63.636	35.354	1.010
ORA_2A_035	64.000	35.000	1.000
ORA_2A_035	66.000	33.000	1.000
ORA_2A_035	66.327	32.653	1.020
ORA_2A_035	64.646	34.343	1.010
ORA_2A_035	61.616	37.374	1.010
ORA_2A_035	56.566	42.424	1.010
ORA_2A_035	64.646	34.343	1.010
ORA_2A_035	62.245	36.735	1.020
ORA_2A_035	63.366	34.653	1.980
ORA_2A_035	59.596	38.384	2.020
ORA_2A_035	58.163	40.816	1.020
ORA_2A_035	64.646	34.343	1.010
ORA_2A_035	65.306	33.673	1.020
ORA_2A_035	64.646	34.343	1.010
ORA_2A_035	65.000	34.000	1.000
ORA_2A_035	65.306	33.673	1.020
ORA_2A_035	65.000	34.000	1.000
ORA_2A_035	65.000	34.000	1.000
ORA_2A_035	64.646	34.343	1.010
ORA_2A_035	64.646	34.343	1.010
ORA_2A_035	64.646	34.343	1.010
ORA_2A_035	64.646	34.343	1.010
ORA_2A_035	63.265	35.714	1.020
ORA_2A_035	65.000	34.000	1.000
ORA_2A_035	64.000	35.000	1.000
ORA_2A_040	62.000	37.000	1.000
ORA_2A_040	62.245	36.735	1.020
ORA_2A_040	62.245	36.735	1.020
ORA_2A_040	62.626	36.364	1.010
ORA_2A_040	64.286	34.694	1.020
ORA_2A_040	62.000	37.000	1.000
ORA_2A_040	62.245	36.735	1.020
ORA_2A_040	62.376	36.634	0.990
ORA_5B_402	71.000	28.000	1.000
ORA_5B_402	69.000	30.000	1.000
ORA_5B_402	70.000	29.000	1.000

ORA_5B_402	70.000	28.000	2.000
ORA_5B_402	63.636	35.354	1.010
ORA_5B_402	69.000	29.000	2.000
ORA_5B_402	70.707	28.283	1.010
ORA_5B_402	68.000	31.000	1.000
ORA_5B_402	71.429	27.551	1.020
ORA_5B_402	71.429	27.551	1.020
ORA_5B_402	70.000	29.000	1.000
<hr/>			
ORA_5B_404A	66.327	32.653	1.020
ORA_5B_404A	51.515	46.465	2.020
ORA_5B_404A	66.000	33.000	1.000
ORA_5B_404A	69.000	30.000	1.000
ORA_5B_404A	52.041	45.918	2.041
ORA_5B_404A	68.687	29.293	2.020
ORA_5B_404A	63.265	35.714	1.020
<hr/>			
ORA_5B_404B	63.636	35.354	1.010
ORA_5B_404B	71.000	28.000	1.000
ORA_5B_404B	67.010	30.928	2.062
ORA_5B_404B	64.948	32.990	2.062
ORA_5B_404B	72.727	26.263	1.010
<hr/>			
ORA_5B_412A	52.632	45.263	2.105
ORA_5B_412A	54.639	43.299	2.062
ORA_5B_412A	58.163	39.796	2.041
ORA_5B_412A	62.500	36.458	1.042
ORA_5B_412A	65.306	32.653	2.041
<hr/>			
ORA_5B_414	52.632	45.263	2.105

F. Normalized Plagioclase Compositions

Sample	Or	Ab	An
ORA_2A_002	3.030	53.535	43.434
ORA_2A_002	1.031	9.278	89.691
ORA_2A_002	2.000	56.000	42.000
ORA_2A_002	2.000	61.000	37.000
ORA_2A_002	5.051	63.636	31.313
ORA_2A_002	8.000	80.000	12.000
ORA_2A_002	7.527	65.591	26.882

ORA_2A_002	4.082	59.184	36.735
ORA_2A_002	9.901	79.208	10.891
ORA_2A_002	8.000	80.000	12.000
ORA_2A_002	8.000	80.000	12.000
ORA_2A_002	8.911	69.307	21.782
ORA_2A_002	3.093	56.701	40.206
ORA_2A_002	2.020	55.556	42.424
ORA_2A_002	1.010	42.424	56.566
ORA_2A_002	7.921	79.208	12.871
ORA_2A_002	5.051	61.616	33.333
ORA_2A_002	2.970	75.248	21.782
ORA_2A_002	8.000	80.000	12.000
ORA_2A_002	5.102	60.204	34.694
ORA_2A_002	4.000	62.000	34.000
ORA_2A_002	2.041	47.959	50.000
ORA_2A_002	7.071	78.788	14.141
ORA_2A_002	4.167	61.458	34.375
ORA_2A_002	4.301	65.591	30.108
ORA_2A_003	7.216	75.258	17.526
ORA_2A_016	7.143	72.449	20.408
ORA_2A_016	7.921	80.198	11.881
ORA_2A_016	3.030	52.525	44.444
ORA_2A_016	8.602	80.645	10.753
ORA_2A_016	8.911	78.218	12.871
ORA_2A_016	6.667	65.556	27.778
ORA_2A_016	6.250	71.875	21.875
ORA_2A_016	3.191	71.277	25.532
ORA_2A_016	5.263	58.947	35.789
ORA_2A_016	6.863	79.412	13.725
ORA_2A_023	7.071	70.707	22.222
ORA_2A_023	10.000	78.000	12.000
ORA_2A_023	8.081	79.798	12.121
ORA_2A_023	8.000	79.000	13.000
ORA_2A_023	9.091	78.788	12.121
ORA_2A_024	8.000	80.000	12.000
ORA_2A_024	7.000	80.000	13.000
ORA_2A_024	7.143	80.612	12.245
ORA_2A_031	9.000	80.000	11.000

ORA_2A_031	8.081	79.798	12.121
ORA_2A_031	9.184	78.571	12.245
ORA_2A_031	3.093	41.237	55.670
ORA_2A_031	6.931	78.218	14.851
ORA_2A_031	2.020	33.333	64.646
ORA_2A_031	1.010	30.303	68.687
ORA_2A_031	7.000	80.000	13.000
ORA_2A_031	8.081	79.798	12.121
ORA_2A_031	9.091	79.798	11.111
ORA_2A_031	8.333	80.208	11.458
ORA_2A_031	4.040	73.737	22.222
ORA_2A_032	8.247	74.227	17.526
ORA_2A_032	8.163	71.429	20.408
ORA_2A_032	7.000	72.000	21.000
ORA_2A_032	2.000	50.000	48.000
ORA_2A_035	1.010	22.222	76.768
ORA_2A_035	1.010	20.202	78.788
ORA_2A_035	3.000	61.000	36.000
ORA_2A_035	10.101	77.778	12.121
ORA_2A_035	11.111	77.778	11.111
ORA_2A_035	8.911	77.228	13.861
ORA_2A_035	10.101	76.768	13.131
ORA_2A_035	8.000	77.000	15.000
ORA_2A_035	12.245	75.510	12.245
ORA_2A_035	8.163	75.510	16.327
ORA_2A_035	7.000	78.000	15.000
ORA_2A_035	8.081	78.788	13.131
ORA_2A_035	8.000	77.000	15.000
ORA_2A_035	9.474	74.737	15.789
ORA_2A_035	8.000	76.000	16.000
ORA_2A_035	9.901	76.238	13.861
ORA_2A_035	9.091	76.768	14.141
ORA_2A_035	11.000	74.000	15.000
ORA_2A_035	11.000	76.000	13.000
ORA_2A_035	8.247	78.351	13.402
ORA_2A_035	9.677	76.344	13.978
ORA_2A_035	8.000	75.000	17.000
ORA_2A_040	8.081	80.808	11.111

ORA_2A_040	10.101	78.788	11.111
ORA_2A_040	8.000	80.000	12.000
ORA_2A_040	9.000	79.000	12.000
ORA_2A_040	9.000	79.000	12.000
ORA_2A_040	7.843	79.412	12.745
ORA_2A_040	8.081	79.798	12.121
ORA_2A_040	8.333	80.208	11.458
ORA_2A_040	9.091	79.798	11.111
ORA_2A_040	9.000	81.000	10.000
ORA_2A_040	14.286	75.510	10.204
ORA_2A_040	9.091	77.778	13.131
ORA_2A_040	10.101	78.788	11.111
ORA_2A_040	11.111	75.758	13.131
ORA_2A_040	6.061	81.818	12.121
ORA_2A_040	3.000	63.000	34.000
ORA_2A_040	3.000	62.000	35.000
ORA_5B_402	5.000	65.000	30.000
ORA_5B_402	7.071	66.667	26.263
ORA_5B_402	8.081	66.667	25.253
ORA_5B_402	4.082	62.245	33.673
ORA_5B_402	9.184	65.306	25.510
ORA_5B_402	7.071	68.687	24.242
ORA_5B_402	7.071	68.687	24.242
ORA_5B_402	7.071	64.646	28.283
ORA_5B_402	8.081	67.677	24.242
ORA_5B_402	8.081	64.646	27.273
ORA_5B_402	7.071	67.677	25.253
ORA_5B_404A	8.081	71.717	20.202
ORA_5B_404A	7.143	71.429	21.429
ORA_5B_404A	7.143	72.449	20.408
ORA_5B_404A	10.309	70.103	19.588
ORA_5B_404A	8.081	71.717	20.202
ORA_5B_404A	6.061	70.707	23.232
ORA_5B_404A	10.309	68.041	21.649
ORA_5B_404A	6.000	72.000	22.000
ORA_5B_404A	10.101	67.677	22.222
ORA_5B_404A	5.155	73.196	21.649
ORA_5B_404A	5.051	63.636	31.313
ORA_5B_404A	6.000	67.000	27.000
ORA_5B_404A	6.122	62.245	31.633
ORA_5B_404A	6.122	64.286	29.592

ORA_5B_404A	6.122	64.286	29.592
ORA_5B_404A	5.941	64.356	29.703
ORA_5B_404A	9.091	61.616	29.293
ORA_5B_404A	6.061	66.667	27.273
<hr/>			
ORA_5B_404B	6.061	67.677	26.263
ORA_5B_404B	8.163	65.306	26.531
ORA_5B_404B	6.122	66.327	27.551
ORA_5B_404B	4.040	58.586	37.374
ORA_5B_404B	6.931	66.337	26.733
ORA_5B_404B	5.051	58.586	36.364
ORA_5B_404B	9.000	65.000	26.000
ORA_5B_404B	12.371	65.979	21.649
ORA_5B_404B	5.051	72.727	22.222
ORA_5B_404B	9.091	64.646	26.263
<hr/>			
ORA_5B_412A	3.125	61.458	35.417
ORA_5B_412A	6.316	70.526	23.158
ORA_5B_412A	6.122	72.449	21.429
<hr/>			
ORA_5B_412B	9.375	63.542	27.083
<hr/>			
ORA_5B_414	8.163	66.327	25.510
ORA_5B_414	9.474	76.842	13.684
ORA_5B_414	7.292	77.083	15.625
ORA_5B_414	7.292	78.125	14.583
ORA_5B_414	7.368	74.737	17.895

G. Biotite Compositions (TiO2 and Mg#)

Sample	TiO2	MgO# (As Fe2O3)
ORA_2A_003	5.11	0.228
ORA_2A_003	3.89	0.212
ORA_2A_003	4.75	0.233
<hr/>		
ORA_2A_023	3.1	0.159
ORA_2A_023	3.38	0.179
<hr/>		
ORA_2A_031	3.23	0.160
ORA_2A_031	3.35	0.178
ORA_2A_031	3.49	0.183

ORA_2A_031	2.97	0.169
ORA_2A_031	3.29	0.168
ORA_2A_031	3.38	0.164
ORA_2A_031	3.43	0.167
ORA_2A_031	3.66	0.164
ORA_2A_031	4.11	0.191
<hr/>		
ORA_2A_032	4.8	0.231
ORA_2A_032	5.32	0.234
ORA_2A_032	5.15	0.240
ORA_2A_032	5.58	0.230
ORA_2A_032	5.08	0.236
ORA_2A_032	5.37	0.233
<hr/>		
ORA_2A_035	3.9	0.213
ORA_2A_035	3.96	0.202
<hr/>		
ORA_2A_040	3.3	0.175
ORA_2A_040	2.95	0.162
ORA_2A_040	3.16	0.169
ORA_2A_040	2.69	0.172
ORA_2A_040	3.12	0.180
ORA_2A_040	3.3	0.174
<hr/>		
ORA_5B_402	5.73	0.289
ORA_5B_402	5.04	0.298
ORA_5B_402	5.41	0.291
ORA_5B_402	5.32	0.282
ORA_5B_402	5.82	0.292
ORA_5B_402	7.67	0.287
ORA_5B_402	5.29	0.280
ORA_5B_402	5.59	0.295
ORA_5B_402	5.36	0.279
ORA_5B_402	4.84	0.287
ORA_5B_402	5.58	0.289
ORA_5B_402	4.97	0.297
ORA_5B_402	5.21	0.291
ORA_5B_402	5.31	0.287
ORA_5B_402	5.31	0.280
ORA_5B_402	5.36	0.292
<hr/>		
ORA_5B_404A	4.53	0.247
ORA_5B_404A	4.87	0.251

ORA_5B_404A	4.01	0.282
ORA_5B_404A	4.29	0.240
ORA_5B_404A	4.63	0.254
ORA_5B_404B	5.49	0.294
ORA_5B_404B	5.64	0.281
ORA_5B_404B	5.22	0.285
ORA_5B_404B	5.65	0.287
ORA_5B_404B	5.88	0.306
ORA_5B_404B	5.91	0.283
ORA_5B_404B	5.45	0.278
ORA_5B_414	5.04	0.255
ORA_5B_414	4.58	0.257

H. Normalized Fayalite Compositions

Sample	Ca	Mg	Fe
ORA_2A_003	0.66	1.64	97.70
ORA_2A_003	0.26	10.65	89.09
ORA_2A_003	0.26	10.47	89.27
ORA_2A_003	0.27	11.08	88.65
ORA_2A_003	0.28	5.31	94.41
ORA_2A_024	0.26	4.39	95.35
ORA_2A_024	0.00	4.72	95.28
ORA_2A_024	0.00	4.28	95.72
ORA_2A_024	0.26	4.71	95.03
ORA_2A_024	0.00	4.51	95.49

I. Normalized OPX Compositions

Sample	Ca	Mg	Fe
ORA_2A_003	0.12	4.74	94.07
ORA_2A_003	1.61	4.42	93.98
ORA_2A_003	2.30	3.23	94.47
ORA_2A_024	0.79	3.97	95.24
ORA_2A_024	2.13	3.40	94.47
ORA_2A_024	1.65	4.53	93.83
ORA_2A_024	1.66	3.73	94.61

ORA_2A_024	2.17	3.91	93.91
-------------------	------	------	-------

REFERENCES

- Bachmann, O., and Bergantz, G., 2008, The magma reservoirs that feed supereruptions: Elements, v. 4, p. 17–21, doi:10.2113/GSELEMENTS.4.1.17.
- Bégué, F., Deering, C.D., Gravley, D.M., Kennedy, B.M., Chambefort, I., Gualda, G.A.R., and Bachmann, O., 2014, Extraction, storage and eruption of multiple isolated magma batches in the paired Mamaku and Ohakuri eruption, Taupo volcanic zone, New Zealand: Journal of Petrology, doi:10.1093/petrology/egu038.
- Best, M.G., Christiansen, E.H., de Silva, S., and Lipman, P.W., 2016, Slab-rollback ignimbrite flareups in the southern Great Basin and other Cenozoic American arcs: A distinct style of arc volcanism: Geosphere, v. 12, p. 1097–1135, doi:10.1130/GES01285.1.
- Cashman, K. V., and Giordano, G., 2014, Calderas and magma reservoirs: Journal of Volcanology and Geothermal Research, v. 288, p. 28–45, doi:10.1016/j.jvolgeores.2014.09.007.
- Cassinis, G., Perotti, C.R., and Ronchi, A., 2012, Permian continental basins in the Southern Alps (Italy) and peri-mediterranean correlations: International Journal of Earth Sciences, doi:10.1007/s00531-011-0642-6.
- De Rita, D., and Giordano, G., 1996, Volcanological and structural evolution of Roccamonfina volcano (Italy): origin of the summit caldera: Geological Society, London, Special Publications, v. 110, p. 209–224, doi:10.1144/GSL.SP.1996.110.01.16.

Gualda, G.A.R., and Ghiorso, M.S., 2013, The Bishop Tuff giant magma body: An alternative to the Standard Model: Contributions to Mineralogy and Petrology, doi:10.1007/s00410-013-0901-6.

Hildreth, W., 2004, Volcanological perspectives on Long Valley, Mammoth Mountain, and Mono Craters: Several contiguous but discrete systems: Journal of Volcanology and Geothermal Research, v. 136, p. 169–198, doi:10.1016/j.jvolgeores.2004.05.019.

Hildreth, W., 1981, Gradients in silicic magma chambers: Implications for lithospheric magmatism: v. 86, 10153–10192 p., doi:10.1029/JB086iB11p10153.

Lipman, P.W., 2007, Incremental assembly and prolonged consolidation of Cordilleran magma chambers: Evidence from the Southern Rocky Mountain volcanic field: Geosphere, v. 3, p. 42, doi:10.1130/GES00061.1.

Lipman, P.W., 1965, Chemical comparison of glassy and crystalline volcanic rocks: Contributions to General Geology, p. 24.

Marocchi, M., Morelli, C., Mair, V., Klötzli, U., and Bargossi, G.M., 2008, Evolution of Large Silicic Magma Systems: New U-Pb Zircon Data on the NW Permian Athesian Volcanic Group (Southern Alps, Italy): The Journal of Geology, v. 116, p. 480–498, doi:10.1086/590135.

Miller, C.F., Furbish, D.J., Walker, B.A., Claiborne, L.L., Koteas, G.C., Bleick, H.A., and Miller, J.S., 2011, Growth of plutons by incremental emplacement of sheets in crystal-rich

host: Evidence from Miocene intrusions of the Colorado River region, Nevada, USA: Tectonophysics, doi:10.1016/j.tecto.2009.07.011.

Miller, C.F., and Wark, D.A., 2008, Supervolcanoes and their explosive supereruptions: Elements, v. 4, p. 11–15, doi:10.2113/GSELEMENTS.4.1.11.

Pamukcu, A.S., Gualda, G.A.R., Ghiorso, M.S., Miller, C.F., and McCracken, R.G., 2015, Phase-equilibrium geobarometers for silicic rocks based on rhyolite-MELTS—Part 3: Application to the Peach Spring Tuff (Arizona–California–Nevada, USA): Contributions to Mineralogy and Petrology, v. 169, p. 33, doi:10.1007/s00410-015-1122-y.

Ring, U., and Richter, C., 1994, The Variscan structural and metamorphic evolution of the eastern Southalpine basement: Journal of the Geological Society, v. 151, p. 755–766, doi:10.1144/gsjgs.151.5.0755.

Scott, R.B., 1971, Alkali Exchange during Devitrification and Hydration of Glasses in Ignimbrite Cooling Units: The Journal of Geology, v. 79, p. 100–110.

Sparks RSJ, Self S, Grattan JP, O., and C, Pyle DM, R.H., 2005, Supereruptions: global effects and future threats.:

Willcock, M.A.W., Bargossi, G.M., Weinberg, R.F., Gasparotto, G., Cas, R.A.F., Giordano, G., and Marocchi, M., 2015, A complex magma reservoir system for a large volume intra- to extra-caldera ignimbrite: Mineralogical and chemical architecture of the VEI8, Permian Ora ignimbrite (Italy): Journal of Volcanology and Geothermal Research, v. 306, p. 17–40, doi:10.1016/j.jvolgeores.2015.09.015.

Willcock, M.A.W., and Cas, R.A.F., 2014, Primary welding and crystallisation textures preserved in the intra-caldera ignimbrites of the Permian Ora Formation, northern Italy: Implications for deposit thermal state and cooling history: Bulletin of Volcanology, v. 76, p. 1–16, doi:10.1007/s00445-014-0819-5.

Willcock, M.A.W., Cas, R.A.F., Giordano, G., and Morelli, C., 2013, The eruption, pyroclastic flow behaviour, and caldera in-filling processes of the extremely large volume (>1290km³), intra- to extra-caldera, Permian Ora (Ignimbrite) Formation, Southern Alps, Italy: Journal of Volcanology and Geothermal Research, v. 265, p. 102–126, doi:10.1016/j.jvolgeores.2013.08.012.